Bryanne M. Gordon

The generation of geochemical gradients in the pre-caldera Glass Mountain high-SiO_2 rhyolites of Long Valley, CA: clues to the origin and preservation of Rb-Sr isochrons

submitted in partial fulfillment of the requirements for the degree of
Master of Science in Earth and Environmental Sciences
Department of Earth and Environmental Sciences
The University of Michigan

Rebecca Lange — Signature

Accepted by:

Name	Date
Rebecca Lange	8/12/2022

Adam C. Simon — Signature

Name	Date
Adam C. Simon	17August2022

Department Chair Signature

Name	Date
Marin K. Clark	8/21/2022

Earth and Environmental Sciences
UNIVERSITY OF MICHIGAN

Abstract

The high-SiO_2 rhyolites of Glass Mountain (GM), which preceded eruption of the Bishop Tuff, have exceptionally low contents of Sr (~4 to ~0.1 ppm). They also display ~2-fold variation in several trace-element contents, including Rb. This produced highly variable and large Rb/Sr ratios among the Older GM units, which enabled Davies et al. (1994) to document two Rb/Sr isochrons, interpreted as distinct differentiation events at 2.047 ± 0.013 and 1.894 ± 0.014 Ma, respectively. Only one Older GM unit (OC) has an eruption age (2.045 ± 0.020; Simon et al., 2014) that is indistinguishable from its isochron age; all other Older GM units erupted later, up to ~360 kyr after their isochron age (Davies et al., 1994). Two outstanding questions emerge: (1) What differentiation mechanism produced the wide range in Rb/Sr ratios? (2) What allowed the differentiation results (i.e., range of Rb/Sr ratios) to be undisturbed for up to 360 kyr prior to eruption? In this study, new whole-rock analyses on 18 GM units were combined with new, high-resolution Fe-Ti oxide thermometry to test the hypothesis that differentiation of the Older GM units occurred through segregation of variable melt fractions from a parental granitic mush, which contained the same nine mineral phases found as phenocrysts in the GM units (and Bishop Tuff). Because element concentrations in the interstitial melt of the parental mush were controlled by their bulk partition coefficients, mineral-melt partition coefficients from the literature could be used to infer the average stoichiometry of the crystallizing/melting reaction in the mush. The deduced proportions for allanite, zircon and apatite are ~0.044, ~0.013, and ~0.015%, respectively. The proportion of titanomagnetite exceeded that of ilmenite in the reaction, and temperatures in the parental mush were too cool (<725 °C) to involve biotite. It is further shown that the first eruptive unit (OC) segregated at ~660°C under H_2O-rich fluid-saturated conditions at a pressure of ~385 MPa (Wilke et al.,

2017). It is proposed that the remaining Older GM units, which segregated at higher melt fractions and temperatures (680-720°C), were held in cold storage as dikes, similar to the rhyolite dike swarms that formed in the Miocene bimodal granitic plutons that formed in the Colorado River extensional corridor (e.g., Miller et al., 2011; Hodge et al., 2006). Over the ensuing 360 kyr, episodic remelting of GM high-SiO_2 rhyolite dikes that exceeded critical widths (>5 m; based on critical width calculations using equation from Petford et al., (1993) would have led to their rapid ascent and eruption.

Introduction

The high-SiO_2 rhyolites (77-78 wt%) of Glass Mountain (GM), California, are among the most evolved silicate magmas on Earth. In addition to their near-eutectic compositions, they contain exceptionally low concentrations of Sr (~4 to ~0.1 ppm; Halliday et al., 1989), an indication of extreme magmatic differentiation. They are also the precursors to the supervolcano eruption of the Bishop Tuff (>600 km^3), a compositionally zoned rhyolite (74-77 wt% SiO_2) (Hildreth, 1979), which formed the Long Valley caldera at ~765 ka (Andersen et al., 2017). The Glass Mountain rhyolites (~100 km^3; Hildreth, 2004) outcrop along the northeastern margin of the caldera (**Fig. 1**) and are divided into two groups (**Fig. 2**) based on eruption age. The Older GM flow units (~25 km^3) erupted between 2.1 and 1.4 Ma, whereas the Younger GM units (~75 km^3) erupted between 1.2 and 0.79 Ma (Metz and Mahood, 1985; Davies et al., 1994; Hildreth, 2004; Simon et al., 2014).

One of the most remarkable features of the Glass Mountain rhyolites, which display minimal change in their major element concentrations (i.e., near eutectic compositions), is their ~2-fold variation in the concentrations of several trace elements, including Rb, Sr, U, Nb, Hf, Cs,

Y and Ta (**Fig. 3**; data from the data of Metz and Mahood, 1991 and Halliday et al., 1989). Note that the concentration gradients are largest in the Older GM units. The ~2-fold change in Rb concentration among the Glass Mountain samples, combined with their remarkably low Sr concentrations, has produced highly variable Rb/Sr ratios among the different eruptive units (**Fig. 3**). Moreover, the Rb/Sr ratios in the Glass Mountain samples are among the highest documented for granitic rocks globally, leading to significant growth of their $^{87}Sr/^{86}Sr$ ratios over the ~2.1 Myr history of the Long Valley volcanic field. This, in turn, led Halliday et al. (1989) to discover that the Older GM eruptive units had whole-rock $^{87}Sr/^{86}Sr$ values that were linearly correlated with their Rb/Sr ratios, thus defining two isochrons (~2.1 and ~1.9 Ma, respectively). Davies et al. (1994) re-analyzed these units and improved the precision ($\pm 2\sigma$) of the isochrons (2.047 ± 0.013 Ma; 1.894 ± 0.014 Ma). The results indicate that there were two distinct and relatively short-lived (≤ 14 kyrs) differentiation events that produced the range in Rb/Sr ratios in the Older GM rhyolites, which were then preserved (i.e., not disturbed) under storage conditions prior to the episodic eruption of the Older GM units over the ensuing 360 kyrs. A similar result was obtained for the Younger GM units, where two isochrons were obtained (1.151 ± 0.010 and 1.091 ± 0.034 Ma; Davies and Halliday, 1998). Once again, two distinct and short-lived differentiation events (≤34 kyr) produced a range of Rb/Sr ratios in the Younger GM rhyolites, which were then preserved prior to their episodic eruptions over the next ~300 kyrs.

Two outstanding questions emerge from these results on the Glass Mountain high-SiO_2 rhyolites. First, what is the differentiation mechanism that produced the wide range in Rb/Sr ratios among the Older and Younger GM units? Whatever the process, it must have occurred at least four different times and each was short-lived (≤ 14-34 kyrs). Second, what allowed the differentiation results (i.e., spread in Rb/Sr ratios) to be preserved prior to eruption? Both

questions have been debated and discussed at length in the literature, as discussed below. In this study, we re-examine these two unresolved questions.

(1) What differentiation mechanisms produced the large variations in trace-element concentrations in the Glass Mountain rhyolites?

The 2-fold variations in trace element concentrations seen in the Glass Mountain rhyolites are also found in the high-SiO_2 rhyolite portion of Bishop Tuff (Fig. 3). In the latter case, they were shown to be strongly correlated with temperature (Hildreth, 1979; Jolles and Lange, 2019). Moreover, it has been clearly established that the geochemical gradient with temperature in the Bishop magma preceded phenocryst growth (e.g., Hildreth and Wilson, 2007; Jolles and Lange, 2019). Several researchers have proposed that these large trace element variations in concentration, often observed in high-SiO_2 rhyolites, may be the result of variable melt segregation from a granitic mush (Metz and Mahood, 1991; Hildreth, 2004, 2017; Hildreth and Wilson, 2007). Wolff et al. (2015) showed that these trace element variations have patterns consistent with mineral-melt partition coefficients that involve the observed phenocryst phases.

These insights led Jolles and Lange (2021a) to propose that the geochemical gradients with temperature in the Bishop Tuff rhyolitic magma developed as a result of mineral-melt partitioning between interstitial melt and surrounding crystals in the parental mush from which variable melt fractions were segregated. To further quantify and test this hypothesis, they used the linear trends of increasing vs decreasing element concentration with temperature (used as a proxy for melt fraction) to infer relative degrees of incompatibility vs compatibility for various elements *i* (relative compatibility values; RCV_i) between crystals and melt in the parental mush. The relative compatibility values (RCV_i) were shown to be linearly correlated with their

respective bulk partition coefficients (bulk D_i). Mineral-melt partition coefficients from the literature were then used to infer the average stoichiometry of the crystallization/melting reaction in the parental mush: 32% quartz + 34% plagioclase + 31% K-feldspar + 1.60% biotite + 0.42% titanomagnetite + 0.34% ilmenite + 0.093% allanite + 0.025% zircon + 0.024% apatite. The tectosilicate proportions constrain the location of the eutectic in the Quartz (Qz)-Plagioclase (Pl) K-feldspar (Kfs) system, which reflects the pressure (350-500 MPa) and activity of water (~0.4-0.6) during segregation of the high-SiO_2 rhyolite portion of the Bishop Tuff from its parental mush.

One of the primary goals of this study is to perform a similar analysis on the Glass Mountain high-SiO_2 rhyolites. In other words, does segregation of variable melt fractions from a granitic parental mush explain the ~2-fold variations in various trace element concentrations in the Glass Mountain rhyolites, and what stoichiometry for the melting/crystallization reaction is required? Can the temperature, pressure, and activity of water in the parental mush during melt segregation be constrained? To undertake this analysis, it is necessary to obtain high-resolution Fe-Ti oxide temperatures on as many Glass Mountain eruptive units as possible. High-precision analyses of major-, minor- and trace-element concentrations on these eruptive units are also required.

(2) What storage conditions enabled the preservation of the Rb-Sr isochrons in the Glass Mountain rhyolites?

The second outstanding question concerns the preservation of the Rb/Sr isochrons in the Glass Mountain rhyolites during storage between the differentiation events (isochron ages) and eruption. Proposed models to address this question have spawned the most controversy and

debate in the literature. Halliday et al. (1989) favor a model where the differentiated Glass Mountain melts, spanning a range of Rb/Sr ratios, are held in a fully molten state in the upper parts of a magmatic reservoir over surprisingly long-time spans (≤360 kyrs), namely the time interval between the isochron ages (differentiation events) and the eruptive ages. Sparks et al. (1990) challenge this idea on the basis that it is difficult to maintain a fully molten magma body in the cool upper crust without loss of heat and thus partial crystallization, which would disturb the Rb/Sr isochrons. They proposed that the differentiation processes more likely occur by partial melting of granitic parents.

Halliday (1990) and Mahood (1990) present separate responses to Sparks et al. (1990). Halliday (1990) points out how easy it would be to disturb the Rb/Sr isochrons due to the exceptionally low Sr concentrations in the Glass Mountain rhyolites, and that the mechanism proposed by Sparks et al. (1990) cannot explain the remarkable preservation of the Rb/Sr isochrons during storage intervals >100's of kyrs. Mahood (1990) offers a model where the Glass Mountain high-SiO_2 rhyolites are stored in the roofzone of a large magma chamber, sometimes fully liquid and sometimes fully crystallized. Because of the near-eutectic nature of these melts (i.e., they fully melt and crystallize over a small temperature interval) they rapidly solidify and remelt with minimal crystal fractionation effects. Mahood (1990) thus proposes that the Glass Mountain rhyolites represent a roofzone rind that fully "freezes" and "thaws", without disturbing the Rb/Sr ratios, over the time interval between the differentiation events (isochron ages) and eruptive episodes. In a more recent study, Simon and Reid (2005) propose that the Glass Mountain rhyolites, after differentiation, may have been stored as co-existing but separate magmas, possibly within a non-convecting mush.

In this study, we draw upon insights derived from this prior debate as well as newer field studies that reveal the architecture of plutonic bimodal (granite-diorite) systems that produced high-SiO_2 rhyolite in an extensional tectonic setting, namely the Miocene intrusions exposed in the Colorado River extensional corridor in southern Nevada (e.g., Miller et al., 2011). For example, in the Searchlight pluton (Bachl et al., 2001; Eddy et al., 2022) and Spirit Mountain batholith (Walker et al., 2007), an accumulation of sills form >1 and >2 km thick bodies of leucogranite (>76 wt% SiO_2) at the top of these two intrusions, which is rare to non-existent in subduction-related granitoid plutons. Moreover, both intrusions contain swarms of late-stage rhyolite dikes with individual widths of 5-20 m. In the case of the Searchlight pluton, they are comprised of high-SiO_2 rhyolite (Bachl et al., 2001; Hodge et al., 2006). In this study, we explore the hypothesis that the Glass Mountain rhyolites were held in cold storage under near- to sub-solidus conditions (after differentiation created the spread in Rb/Sr ratios) in a similar dike swarm, which enabled preservation of the Rb/Sr isochrons until these near-eutectic dikes were remelted due to the arrival of heat and H_2O-rich fluid from recently emplaced basaltic sills.

Tectonic and Geological Setting

Glass Mountain is part of the Long Valley volcanic field, which produced the Bishop Tuff and associated caldera. It is located in eastern California, along the western edge of the Basin and Range extensional province (**Fig. 1**). Between 2.2 and 0.8 Ma, ~100 km^3 of rhyolite erupted to form the Glass Mountain complex (Metz and Mahood, 1985; 1991; Hildreth, 2004), which was followed by the climactic eruption of the >600 km^3 Bishop Tuff within six days (Wilson and Hildreth, 1997) to form the Long Valley caldera at ~765 ka (Andersen et al., 2017).

In close association with the rhyolitic volcanism, a significant volume of basalt erupted adjacent to the Long Valley caldera over the last 4.5 Myr, following a volcanic hiatus in the region from 8-4.5 Ma (Bailey, 1989; Du Bray et al., 2016). Seismic studies indicate a mid-crustal (~10 to ~20-km depth) low-velocity zone underneath Long Valley caldera (Flinders et al., 2018; Frasseto et al., 2011; Thurber et al., 2009), which indicates the presence of melt and/or fluid. The Long Valley basalts were formed by partial melting of subduction-modified lithosphere (Cousins, 1996), which was triggered by upwelling asthenosphere due to lithosphere delamination beneath the eastern Sierra Nevada (e.g., Manley et al., 2000; Saleeby et al., 2003; Zandt et al., 2004).

The crustal column into which the basalts were emplaced is ~32 km thick and largely composed of Mesozoic granitoid (down to ~30 km depth; Fleidner et al., 2000). The granitoid in the immediate vicinity of Long Valley caldera is predominantly the Triassic Scheelite Intrusive Suite (Barth et al., 2011), a granodiorite and granite (62-77 wt% SiO_2) that is compositionally similar to the Cretaceous intrusive suites of the Sierra Nevada batholith.

Previous Work

Metz and Mahood (1985) present K-Ar eruption ages for 30 Glass Mountain eruptive units and divided them into two groups based on age (pre and post 1.2 Ma), which also corresponds to a shift in Nd isotopic composition (Halliday et al., 1989). Subsequent $^{40}Ar/^{39}Ar$ ages on sanidine separates in a subset of samples (three in Davies et al., 1994 and five in Simon et al., 2014) have an improved accuracy and precision. For example, the oldest eruptive unit OC has an $^{40}Ar/^{39}Ar$ eruption age of 1.999 ± 0.015 Ma (Davies et al., 1994) and 2.045 ± .020 Ma (Simon et al., 2014); the two ages overlap within 2σ analytical error. The recent $^{40}Ar/^{39}Ar$

eruption age for OC (2.045 ± .020) matches its Rb-Sr isochron (differentiation) age (2.047 ± 0.013 Ma; Davies et al., 1994).

Rb and Sr concentrations (the latter by isotope dilution) and Sr and Nd isotopic compositions of the Glass Mountain rhyolites were analyzed by Halliday et al., 1989, Davies et al., 1994 and Davies and Halliday 1998. Collectively, these studies reveal two distinct Rb-Sr isochrons for both the Older GM and Younger GM units, respectively. Moreover, the eruptive units that form each of the two isochrons for both age groups line up spatially into an inner (along NE rim of Long Valley caldera) and outer (parallel) alignment of vents. The initial $^{87/86}Sr$ isotopic composition of both the Older and Younger GM isochrons range from 0.7060 to 0.7063 and thus overlap with coeval basaltic eruptions in the region (0.7060-0.7067; Cousens, 1996). Nd isotopic compositions of the Older GM units have a larger crustal component (epsilon Nd = -3 to -4) compared to those of the Younger GM units (epsilon Nd = -1) (Halliday et al., 1989; Davies et al., 1994; Davies and Halliday, 1998; Simon et al., 2014). Pb isotopic analyses also demonstrate the greater crustal contribution to the Older versus Younger GM rhyolites (Simon et al., 2007).

Zircon crystallization ages in three Older and two Younger GM units (OC, OD, OL, YA, YG) are reported in Simon and Reid (2005) and Simon et al. (2007). In general, zircon ages in each eruptive unit span the interval between their isochron and eruption ages, including the 360 ky interval for unit OD. In some samples (e.g., unit OC), zircon ages slightly predate the isochron age, which may reflect the presence of zircon antecrysts. In other samples (e.g., unit OL), zircon ages predate the eruption age by ≤160 ky. A similar record of feldspar crystallization ages in GM units is based on Sr-model ages on select feldspar cores (Davies et al., 1994; Davies and Halliday, 1998), but in this case they largely cluster close to the isochron age in each sample.

Metz and Mahood (1991) present a comprehensive study of whole-rock and phenocryst compositions for the Glass Mountain high-SiO_2 rhyolite suite. Over 30 samples were analyzed for major and trace element compositions using x-ray fluorescence (XRF) and instrumental neutron activation analyses (INAA). In addition, phenocryst abundances were determined, and microprobe analyses of key mineral phases were obtained. Metz and Mahood (1991) show that most of the Glass Mountain rhyolites are crystal-poor, with the vast majority containing <5% (mostly ≤2%). One anomalous Older GM unit (OD) contains 20% crystals, whereas six Older GM units (OC, OE, OF, OG, OW, OX) and two Younger GM units (YG and YP) contain between 6-8%. Most samples contain nine mineral phases (quartz, sanidine, plagioclase, titanomagnetite, ilmenite, biotite, allanite, zircon and apatite), the exact same assemblage that is found in the high-SiO_2 rhyolite portion of the Bishop Tuff (Hildreth, 1979; Hildreth and Wilson, 2007; Jolles and Lange, 2019). Metz and Mahood (1991) applied Fe-Ti oxide thermometry to four Older GM units (OL, ON, OT, OX) and three Younger GM units (YG, YJ and YK). Reported temperatures, based on the model of Buddington and Lindsey (1964), range from 695 to 720°C, with no systematic difference between the Older and Younger GM units.

Waters and Andrews (2016) performed phase-equilibrium and decompression crystallization experiments on a representative Glass Mountain rhyolite under H_2O-saturated conditions between 75-225 MPa and 700-850 °C. Their results demonstrate that GM rhyolites with temperatures of ~700-720°C must have contained >6 wt% H_2O at their liquidus. In addition, their study demonstrates that intergrowths of quartz and sanidine (i.e., granophyric texture) form rapidly (within ≤ 4 hours) during H_2O-saturated decompression experiments (i.e., conditions that mimic H_2O degassing during rhyolite ascent).

Whole-Rock Geochemistry

Methods

Eighteen samples from 10 eruptive units were collected in this study (locations are shown in Table 1). Seven samples are from six of the Older GM units (OB, OC, OD, OL, OT and OZ); two samples from flow unit OL were taken. Eleven samples are from five of the Younger GM units (YA, YB, YE, YG and YO); two samples from YE and YG and five samples from YO were collected. All samples are glassy black obsidians; interior portions of blocks were crushed in a tungsten carbide shatter box and sent for analysis at Activation Laboratories, Ltd., Ontario, Canada. Inductively coupled plasma-mass spectrometry (ICP-MS) was used for determination of major and trace elements.

Results

Major and trace elemental analyses for all 18 samples are shown in Tables 1 and 2. All samples are high-SiO_2 (76.9-78.1 wt%) rhyolites with low MgO contents ranging from 0.03-0.06 wt%, consistent with data from Metz and Mahood (1991). CaO contents and K_2O/Na_2O ratios are systematically lower in the Older GM units (0.33-0.44 wt%; 1.00-1.15) compared to the Younger GM units (0.46-0.50 wt%; 1.17-1.27), again consistent with results from Metz and Mahood (1991). All Older GM samples have Sr contents below detection limit (< 2 ppm), whereas Younger GM samples have Sr contents that range from 3-4 ppm. The one exception is the Older GM sample OD, which contains an elevated Sr content of 4 ppm (Table 2), consistent with isotope dilution measurements made by Halliday et al. (1989) and Davies et al. (1994). Ba concentrations in all 18 samples are low (2-12 ppm), which is inconsistent with Metz and Mahood (1991) where much higher values (31-79 ppm) are reported. Another systematic

difference is found in Zr concentrations. In this study, values range from 71-85 ppm, whereas Metz and Mahood (1991) report values from 90-117 ppm. All other element concentrations are broadly similar between this study and those reported in Metz and Mahood (1991). We attribute the differences in Ba and Zr concentration analyses to the difference in analytical approach, XRF by Metz and Mahood (1991) and ICP-MS in this study.

Using Ta as an index of differentiation (following Metz and Mahood, 1991), plots of the major, minor and trace element concentrations of the Older and Younger GM units are compared to those in the high-SiO_2 rhyolite portion of the Bishop Tuff from Jolles and Lange (2021a) in **Figures 4-8**.

Major-element concentration gradients with Ta

The Younger GM samples have SiO_2, Al_2O_3, Na_2O and K_2O concentrations that overlap those of the Bishop Tuff, whereas the Older GM samples extend to higher Ta contents and show systematic differences in their Na_2O and K_2O contents (**Fig. 4**). The Na_2O contents of the Older GM units increase with Ta and are shifted to higher concentrations relative to the Younger GM and Bishop Tuff samples (**Fig. 4c**). In contrast, the K_2O contents of the Older GM samples are unchanging with Ta content but are shifted to slightly lower values relative to the Younger GM and Bishop Tuff samples (**Fig. 4d**).

Minor-element concentration gradients with Ta

Whole rock minor-element (TiO_2, MgO, CaO and $Fe_2O_3^T$) concentrations of the Younger GM units largely overlap with those of the Early-type Bishop Tuff samples (**Fig. 5**). In contrast, the Older GM samples are shifted to lower TiO_2, MgO and CaO contents and higher $Fe_2O_3^T$

contents. As a function of increasing Ta content, the Older GM units have TiO_2 and MgO contents that are unchanging (**Fig. 5a,b**), whereas both CaO and $Fe_2O_3^T$ contents in the Older GM units systematically decrease (**Fig. 5c,d**).

Trace-element concentration gradients with Ta

The rare earth element (REE) concentrations (the lanthanides and yttrium) of the Younger GM samples largely overlap those from the Bishop Tuff (**Fig. 6**). In contrast, the Older GM samples extend to higher Ta contents and often to higher REE contents. Concentrations of La and Ce in the Older GM units slightly decrease with Ta, whereas the concentration of Pr is largely unchanged (slightly increases) with Ta content. For all other REEs (Sm, Gd, Tb, Dy, Yb, Lu, Y), their respective concentrations in the Older GM units display strong, linear correlations (R^2 = 0.90-0.97) with Ta content.

In a separate plot (**Fig. 7**), an additional six trace elements (Rb, Cs, U, Th, Mn and Hf) are plotted with Ta content. Once again, the trace element contents of the Younger GM samples largely overlap those found in the high-SiO_2 rhyolite portion of the Bishop Tuff. In contrast, trace elements in the Older GM units extend to higher concentrations and display strong linear correlations (R^2 = 0.95-0.98 for all except Th).

In another plot (**Fig. 8**), Ba and Sr concentrations are plotted with Ta and a different pattern emerges. In this case, Ba and Sr are inversely correlated with Ta in the Bishop Tuff samples and extend over a relatively wide range of concentration (>factor of six) over a narrow range in Ta content. Conversely, the Glass Mountain samples are characterized by low concentrations of Sr and Ba, with the Younger GM units overlapping the lowest of the Bishop

Tuff samples. The Older GM units have the lowest concentrations of Ba and Sr of all three suites, and both Sr and Ba are relatively unchanging with Ta content.

Mineral Analyses of Titanomagnetite and Ilmenite

Methods

Fe-Ti oxides were analyzed with a Cameca SX-100 Electron Microprobe in the Robert Mitchell Laboratory at the University of Michigan. Samples were crushed and oxide separates were mounted in epoxy for microprobe analysis. Fe-Ti oxides were then examined with BSE imaging to determine if there was any alteration and/or exsolution. Altered grains (i.e., those with exsolution lamellae) were readily observed and avoided. Among the ten flow units sampled in this study, three (OD, OZ, and YG) contained oxides with extensive alteration and could not be analyzed, whereas another two (YA, YB) did not contain ilmenite. Therefore, only five flow units (OB, OC, OL, YE and YO) contained two Fe-Ti oxides for which analyses of both could be analyzed.

Analyses were made with a focused (i.e., spot) beam, an acceleration voltage of 15 kV and a beam current of 20nA. Elements analyzed were Si, Ti, Al, Fe, V, Zn, Mn, Mg, and Ca at a peak and background counting time of 20 s for each element. A compilation of all microprobe standards used for each element is presented in **Table S1 (Appendix 1).** Uncertainties (±1s) based on counting statistics for titanomagnetite and ilmenite, respectively, are ±0.20 wt% and 0.64 wt% TiO_2, ±0.07 and 0.04 wt% Al_2O_3, ±0.81 and 0.53 wt% FeO^T, ±0.08 and 0.12 wt% MnO, and ±0.03 and 0.04 wt% MgO. On the basis of stoichiometry, FeO and Fe_2O_3 contents were calculated in titanomagnetite and ilmenite. Only those analyses with recalculated totals between 98 and 101 wt% were used for this study.

In addition to calculating uncertainties due to counting statistics, another assessment of microprobe uncertainty was made by evaluating analytical results on the standards used for TiO_2 (Ilmenite, NMNH 96189) and FeO^T (Magnetite, NMNH 114887). A histogram of all analyses (n=100) of wt%TiO_2 on the ilmenite standard is shown in **Figure 9a**. The average TiO_2 content (45.72 wt%) is close to that reported for the standard (45.70 wt%; Jarosewich et al., 1980), and the 2σ variation among all analyses is ± 0.93 wt%. A similar histogram of all analyses (n=99) is shown in **Figure 9b** for wt% FeO^T in the magnetite standard. The average FeO^T content (92.89 wt%) is close to that reported for the standard (92.55 wt%; Jarosewich et al., 1980), and the 2σ variation among all analyses is ± 0.99 wt%. Since the 1s counting statistic for TiO_2 (± 0.61 wt%) and FeO^T (± 0.94 wt%) is ≤ the 2σ variation in the analyses of the ilmenite and magnetite standards, respectively, any analytical variations in the oxide TiO_2 and FeO^T concentrations that are less than their respective 1s counting errors are considered unresolved from analytical uncertainty. Following Jolles and Lange (2019), this applies to all element analyses and was used to determine whether there was more than one population of titanomagnetite and/or ilmenite in each sample.

Jolles and Lange (2019) performed a statistical evaluation of analytical uncertainty to constrain the minimum number of analyses of ilmenite and titanomagnetite in a rhyolite sample (assuming a single population of each phase of the same composition) so that the uncertainties of temperatures determined from Fe-Ti oxide thermometry (e.g., Ghiorso and Evans, 2008) are ≤10 °C. Their results showed that ≥21 ilmenite and ≥56 titanomagnetite are required, which was sought in this study as well.

Results

Individual analyses of ilmenite and titanomagnetite obtained on each Glass Mountain sample are reported in **Table S2 and S3 (Appendix 1**). To test whether more than one compositionally distinct population of ilmenite and/or titanomagnetite is present in each obsidian sample, scatter plots of wt% MgO vs. TiO_2 for all ilmenite (**Fig. 10**) and titanomagnetite **(Fig. 11**) analyses in each sample were created. The average composition and 2σ error bar (based on counting statistics) is shown for each sample. The results show, on the basis of MgO analyses, that only a single population of ilmenite and titanomagnetite is found in each sample. For ilmenite, the range in wt% TiO_2 is also less than analytical uncertainty (consistent with single population), but for titanomagnetite, the range in wt% TiO_2 exceeds analytical uncertainty for some samples (importantly, not for flow unit OC; only a single population of both ilmenite and titanomagnetite is clearly established in this sample). This spread in wt% TiO_2 in titanomagnetite may reflect real changes in temperature during crystallization, which is discussed later in the paper. A similar set of scatter plots were made for ilmenite (**Fig. 12**) and titanomagnetite (**Fig. 13**), but with wt% MgO plotted vs wt% FeO^T. In all cases, the range in analyses is within 2σ analytical uncertainty and, therefore, only a single population of ilmenite and titanomagnetite, respectively, is detected in each sample. Thus, the average of all titanomagnetite and ilmenite analyses in each sample accurately represents the composition of each oxide phase, respectively, and is reported in **Table 3**. Also shown in **Table 3** are the number of discrete ilmenite and titanomagnetite grains analyzed in each sample (N), as well as the total number of analyses (n).

Fe-Ti Two-Oxide Thermometry and Oxybarometry

Test of equilibrium and method

The Bacon and Hirschmann (1988) Mg/Mn equilibrium test, which is based on plots of molar $\log(Mg/Mn)^{titanomagnetite}$ versus molar $\log(Mg/Mn)^{ilmenite}$, was applied to the average ilmenite and titanomagnetite compositions reported for each Glass Mountain sample in this study (**Table 3**). The results are shown in **Figure 14** together with those obtained from the average analyses reported in Metz and Mahood (1991); all Fe-Ti oxide analyses pass the Bacon and Hirschmann (1988) test.

Since the Fe-Ti oxides in all Glass Mountain samples pass this equilibrium test, they were considered suitable for application of the Ghiorso and Evans (2008) Fe-Ti two-oxide thermometer and oxybarometer. The thermometer is based on the following exchange reaction between ilmenite (ilm) and titanomagnetite (tmte):

$$\underset{\text{ilm}}{FeTiO_3} + \underset{\text{tmte}}{Fe_3O_4} = \underset{\text{ilm}}{Fe_2O_3} + \underset{\text{tmte}}{Fe_2TiO_4} \qquad (1)$$

In Eq. 1, temperature favors the right side of the reaction. Therefore, an increase in the TiO_2 content of titanomagnetite and a decrease in the TiO_2 content of ilmenite each correlates with a higher calculated temperature.

The equilibrium between the two oxides also permits the oxygen fugacity in the coexisting fluid and/or melt phase to be calculated, based on the following reaction:

$$\underset{\text{tmte}}{4Fe_3O_4} + \underset{\text{fluid/melt}}{O_2} = \underset{\text{ilm}}{6Fe_2O_3} \qquad (2)$$

The oxybarometer of Ghiorso and Evans (2008) reports oxygen fugacity (fO_2) results (derived from Eq. 2) in ΔNNO units (i.e, relative to those for the Ni-NiO buffer; O'Neil and Pownceby, 1993), where $\Delta NNO = \log fO_2(\text{sample}) - \log fO_2(\text{Ni-NiO buffer})$ and is calculated at the same

temperature obtained from the exchange reaction in Eq. 2. The advantage of reporting results in ΔNNO log units is that the resulting oxidation state values are largely independent of temperature. For example, Kress and Carmichael (1988) found that equilibration of individual natural melts along the Ni-NiO buffer over a range of temperatures (and thus a range of fO_2 values) at 1 bar led to nearly constant melt ferric-ferrous ratios in each melt composition. The same was true if natural melts were equilibrated at +1 or -1 log units relative to the Ni-NiO buffer over a range of temperatures (and thus a range of fO_2 values).

Results and Uncertainties

For all titanomagnetite and ilmenite pairs reported in **Table 3**, temperature and ΔNNO were calculated using the Fe-Ti two-oxide model of Ghiorso and Evans (2008). The results are tabulated in **Table 3** and plotted (ΔNNO vs temperature) in **Figure 15**. Uncertainties in the calculated temperatures are based on the statistical model presented by Jolles and Lange (2019), which showed how many analyses of each oxide were required (assuming a single population in each sample and given the determined microprobe analytical uncertainty) to obtain an average TiO_2 and FeO^T concentration in each phase that is within ± 0.2 wt% of its true value. Uncertainties in these two oxide components contribute the largest uncertainty to calculated temperatures from the Fe-Ti two-oxide exchange reaction in Eq. 1. These analytical uncertainties (≤ 0.2 wt%) in TiO_2 and FeO^T, in turn, lead to uncertainties in calculated temperatures from the Ghiorso and Evans (2008) thermometer of ≤2 and ≤4 °C, respectively. Uncertainties in ΔNNO values are only based on FeO^T analyses and are ≤ 0.02 log units.

Based on the number of ilmenite (n=18 to 117) and titanomagnetite (n= 21 to 441) analyses obtained in this study, propagated uncertainties in calculated temperature range from ±

3 to ± 9 °C. However, this assumes a single population of ilmenite and titanomagnetite in each sample. This is demonstrably the case for ilmenite in all samples (**Figs. 10 and 12**), but for samples from OB and OL, it is possible that the larger range in TiO_2 content in the titanomagnetite analyses (**Fig. 11**) reflect a real variation in crystallization temperature. When these variations in the TiO_2 content of titanomagnetite are incorporated into the Ghiorso and Evans (2008) two-oxide thermometer, calculated temperatures deviate from the average by ≤ ± 10°C. Thus, the effect is relatively minor. It is noteworthy that variations in the FeO^T analyses, which control ΔNNO values, are less than the analytical error (**Fig. 13**). Thus, no variation in ΔNNO is detected within each sample.

Plots of ΔNNO vs Fe-Ti oxide temperature

The ΔNNO and temperature results for the samples from this study are compared to those obtained from Jolles and Lange (2019) on the high-SiO_2 rhyolite portion of the Bishop Tuff (Early- and Transitional-type only) in **Figure 15a**. The results from sample OC (this study) and those from the Bishop Tuff fall along a linear trend, with an R^2 value of 0.96. Sample OC has the lowest temperature (660 °C) and the lowest ΔNNO value (-0.7). The remaining Glass Mountain samples from this study (OB, OL, YE, YO) all have similar temperatures (690-703°C), but a wide range of ΔNNO values (-0.6 to +0.1) over such a narrow temperature interval compared to the Bishop Tuff samples. There is no systematic difference in temperature between the Older and Younger GM units, but there is a difference in ΔNNO values, with the Older GM units systematically lower (**Fig. 15a**). For comparison, the Bishop samples with the lowest temperature have the lowest ΔNNO values; temperatures range from 698-752°C and ΔNNO values range from -0.4 to +0.1 (Jolles and Lange, 2019).

When the Ghiorso and Evans (2008) thermometer and oxybarometer is applied to the Fe-Ti oxide analyses reported in Metz and Mahood (1991) on a different set of eruptive flow units from those analyzed in this study (except for flow unit OL), the results (**Fig. 15b)** also lead to a relatively narrow range in temperature (698-724) and a wide range in ΔNNO values (-0.5 to +0.4). Notably, the ΔNNO results extend to higher values than measured for the GM units in this study and for the high-SiO_2 rhyolite portion of the Bishop Tuff (Jolles and Lange, 2019). For the Metz and Mahood (1991) results, there are no systematic differences between the Older and Younger GM units in either temperature or ΔNNO values.

Only one flow unit was analyzed for two Fe-Ti oxides in both this study and Metz and Mahood (1991), namely OL. The temperatures obtained from each study are similar (703 vs 698 °C), but the ΔNNO values are distinctly different (-0.6 and -0.2). Thus, good reproducibility between the two studies is found with temperature, but not with ΔNNO values. Metz and Mahood (1991) do not report details regarding their Fe-Ti oxide microprobe analyses, but they report analyzing more than one grain for each oxide phase and that their results are based on an average of analyses (the number for each phase is not known). As noted earlier, their results pass the Bacon and Hirschmann (1988) Mg/Mn equilibrium test (**Fig. 14b**).

Plots of Ta (ppm) vs Fe-Ti oxide temperature

Since Ta is a useful index of differentiation, it is of interest to see how it plots as a function of Fe-Ti oxide temperature. The results for the Older and Younger GM units from this study reveals a poor correlation (**Fig. 15c**), in sharp contrast to the strong linear correlation (R^2 = 0.91) observed for the high-SiO_2 rhyolite portion of the Bishop Tuff (Jolles and Lange, 2021). For the eruptive units studies by Metz and Mahood (1991), a similar poor correlation is found

(**Fig. 15d**). These poor correlations are not surprising if the Ta concentrations in the Glass Mountain rhyolites were attained during the differentiation events (e.g., segregation of variable melt fractions from a granitic, crystal-rich mush) dated by the Rb-Sr isochrons of Halliday et al. (1989), Davies et al. (1994) and Davies and Halliday (1998), whereas the Fe-Ti oxide phenocrysts record melt temperature immediately prior to eruption. Because the GM eruption ages are often younger (by 100's of kyrs) than the differentiation (isochron) ages, a storage interval is implicated. If storage occurred as sub-solidus dikes, similar to those observed in the Searchlight pluton in southern Nevada (e.g., Hodge et al., 2006), subsequent remelting of these dikes is expected to lead to melt temperatures that differ from those at the time of initial melt segregation from a plutonic granitic mush.

Origin of Trace Element Concentration Variations in the Glass Mountain Rhyolites

Segregation of variable interstitial melt fractions from granitic crystal-rich mush

In this study, we quantitatively evaluate whether the element concentration variations in the Glass Mountain rhyolites (**Figs. 4-8**) can be explained by segregation of different interstitial melt fractions from a granitic, crystal-rich mush that contains the same nine phenocryst phases found in the Older and Younger GM eruptive units (quartz, sanidine, plagioclase, biotite, titanomagnetite, ilmenite, zircon, allanite, apatite). We follow the same methodology employed by Jolles and Lange (2021a) to examine whether an average stoichiometry of the crystallization/melting reaction in the parental mush can be deduced. As noted in that study, there are two endmember processes by which interstitial melts can develop in a crystal-rich mush (1) extensive crystallization of a parental liquid or (2) partial melting of a parental solidified body. In the case of crystallization, fluid dynamic studies have shown that segregation via

compaction is optimized after 50-70% crystallization (e.g., Dufek and Bachmann, 2010). Such crystal-rich conditions favor geochemical models based on closed-system equilibrium crystallization rather than open-system Rayleigh fractional crystallization, and the former model has the additional advantage of applying equally to equilibrium partial melting conditions. The equilibrium crystallization/melting equation is

$$\frac{C_i^{liq}}{C_i^{parent}} = \frac{1}{F + D_i^{bulk} - FD_i^{bulk}} \quad (3)$$

where C_i^{liq} is the concentration of element i in the interstitial liquid, C_i^{parent} is the initial concentration of element *i* in the bulk parent, *F* is the melt fraction, and D_i^{bulk} is the bulk partition coefficient for element *i* between the interstitial melt and the crystallizing/melting mineral assemblage.

As seen from Eq. 3, under equilibrium crystallization/melting conditions, the concentration of an element in the interstitial melt (within a crystal-rich mush) will vary as a function of its bulk partition coefficient (D_i^{bulk}) and its melt fraction (*F*), which is schematically illustrated in **Figure 16**. For elements that have concentrations that strongly increase with melt fraction, it can be inferred that they are strongly compatible and have bulk partition coefficients that are >1. Conversely, for elements that have concentrations that strongly decrease with melt fraction, it can be inferred that they are strongly incompatible and bulk partition coefficients that are <1. For elements that have concentrations that are relatively flat and unchanging with melt fraction, they may have bulk partition coefficients that are close to 1.

If a proxy for melt fraction can be identified in the Glass Mountain rhyolites, trace-element concentration gradients with melt fraction can be used to infer not only which elements are compatible and incompatible, but also how the elements rank, relative to one another in degree of compatibility and incompatibility. By constraining the relative degrees of

compatibility/incompatibility for key elements, tight constraints on the stoichiometry of the crystallization/melting reaction in the parental, granitic mush to the Glass Mountain rhyolites can be obtained. Following Jolles and Lange (2021a), this can be obtained from: (1) slopes of element concentration with melt fraction in the Glass Mountain rhyolites, and (2) element partition coefficients between high-SiO_2 rhyolite melt and the nine mineral phases in the Glass Mountain rhyolites. The latter are well known from the literature (previously reported in Jolles and Lange, 2021) and shown in **Table 4**.

Ta as an effective proxy for melt fraction (and temperature) for the Bishop Tuff samples

The strong linear correlation between Ta and Fe-Ti oxide temperature for the high-SiO_2 rhyolite portion of the Bishop Tuff samples (**Fig. 15c**) suggests that Ta (as well as temperature) can be used as a proxy for melt fraction in the development of relative compatibility values (RCV_i) for each element *i*. To test this hypothesis on the Bishop Tuff samples previously examined by Jolles and Lange (2021a), Ta-RCV_i values were constructed for each element *i* and are defined as the slope of its concentration with Ta divided by its average concentration. Because Ta values are expected to decrease as melt fraction (and temperature) increases (**Fig. 16**), a negative sign is added to be consistent with the original temperature based RCV_i values from Jolles and Lange (2021a). Ta-RCV_i values were calculated for the 11 trace elements (seven lanthanides, Y, Hf, Th and U) that are entirely controlled by only three accessory phases (allanite, zircon and apatite) in the parental mush. These Ta-RCV_i values for the Bishop Tuff samples are reported in **Table 5** and **Figures 6 and 7**. Note that they have different values compared to the original RCV_i values from Jolles and Lange (2021a), which were based on Fe-

Ti oxide temperature, rather than Ta, as the proxy for melt fraction. However, the two sets of RCVi values are strongly and linearly correlated (R^2=0.9967; **Fig. 17a**).

Jolles and Lange (2021a) used the original RCV_i values to constrain the % abundance of allanite, zircon and apatite in the melting/crystallization reaction (between the interstitial melt and surrounding crystals in the parental mush) so that resulting bulk D_i values were linearly correlated with their RCV_i values. In that study the proportion of the three accessory phases (X_{Aln}, X_{Zrn}, X_{Ap}) were determined through an iterative approach using the following reaction:

$$bulk\ D_i = [D_i^{Aln} X_{Aln} + D_i^{Zrn} X_{Zrn} + D_i^{Ap} X_{Ap}] \ . \qquad (4)$$

In Eq. 4, D_i^{Aln}, D_i^{Zrn}, and D_i^{Ap} are the partition coefficients for element *i* between allanite, zircon and apatite, respectively, and high-SiO_2 rhyolite melt; these values are known from the literature and reported in Table 4. Jolles and Lange (2021a) showed that the strongest linear correlation between bulk D_i and RCV_i occurs when the proportions of each phase (in the crystallizing/melting reaction in the parental mush during segregation) are 0.093% allanite, 0.024% zircon and 0.025% apatite (R^2=0.9976; **Fig. 17b**). In this study, it is shown that a similarly strong linear correlation occurs for these same phase abundances when bulk D_i is plotted against the Ta-RCV_i values (R^2=0.9981; **Fig. 17c**). Thus, the same stoichiometry of the melting/crystallization reaction is found for these three accessory phases, irrespective of whether temperature or Ta content is used as a proxy for melt fraction in constructing RCV_i values to deduce the bulk D_i values. This result raises the prospect that Ta concentration can be used, not only as an index of differentiation, but also as a quantitative proxy for melt fraction (and temperature) for the Glass Mountain rhyolites during their segregation as interstitial melts from a parental mush.

Ta as a proxy for melt fraction (and temperature) for the GM rhyolites

An assessment of whether Ta can be used as a proxy for melt fraction (and temperature) for the Glass Mountain rhyolites is made by plotting Ta vs Fe-Ti oxide temperature obtained from the Bishop Tuff samples, together with those Glass Mountain samples that have eruption ages indistinguishable from isochron (i.e., differentiation) ages (**Fig. 18a**). Here, the hypothesis that is being tested is that the time of Fe-Ti oxide crystallization in the rhyolite samples closely followed the time of melt segregation from the parental mush. Only one sample from the Glass Mountain rhyolites, for which Fe-Ti oxide temperatures were obtained, satisfies this constraint, namely unit OC. In other words, only unit OC has an eruption age (2.045 ± 0.020 Ma; Simon et al., 2014) that is indistinguishable from its isochron (differentiation) age (2.047 ± 0.015; Davies et al., 1994). This is also the sample with the highest Ta content (5.7 ppm) and lowest Fe-Ti oxide temperature (660 ± 6 °C), which is consistent with segregation of a relatively low melt fraction (**Figure 16**) from a granitic mush. Note that the combined data in **Figure 18a** display curvature, which is exactly what is expected for such a highly incompatible element such as Ta. According to **Figure 16**, highly incompatible elements will display high concentrations in the liquid phase at low melt fractions (i.e., low temperatures) and show strong curvature as their concentrations decrease with increasing melt fraction (i.e., increasing temperature). Thus, the pattern in **Figure 18a** is exactly what is expected if Ta is an effective proxy for melt fraction (and temperature) in a parental mush.

When a polynomial is fit to the curved data in **Figure 18a**, the result allows temperature at the time of melt segregation (i.e., differentiation) to be calculated for all the Glass Mountain samples analyzed in this study (Table 2) and in Metz and Mahood (1991). The results show that the Older and Younger GM units from this study have Ta-temperatures that range from 660-

714°C and 701-743°C, respectively (**Fig. 18b**). For the Metz and Mahood (1991) data, the Older and Younger GM Ta-temperatures range from 660-703°C and 702-717°C, respectively (**Fig. 18c**). The lowest Ta-temperatures from both studies agree (similar Ta concentrations were obtained on units OC, OD and OL), but the highest temperatures differ because our Ta analyses extend to lower values than those reported in Metz and Mahood (1991) for other units (e.g., OT and YG). Overall, the results are petrologically reasonable (i.e., 660°C is close to the water-saturated solidus of granitic bodies at ~300-400 MPa; Tuttle and Bowen, 1958; Piwinksi and Wyllie, 1968; Johannes, 1984; Johannes and Holtz, 1996). The results also provide a clear explanation for why the Older GM units have incompatible trace elements that extend to such high concentrations, which exceed those in the Younger GM and Bishop Tuff samples (**Figs. 3, 6, 7**). In addition, because the Older GM samples span only half the temperature range (660-720°C) of the combined data in **Figure 18a**, when these samples are plotted by themselves (**Fig. 18d**) the relationship between Ta and temperature are well described by a linear fit (R^2=0.98). This result shows that Ta can be used a linear proxy for melt fraction in the construction of relative compatibility values for elements in the Older GM units.

Construction of Ta-RCV$_i$ values for the Older Glass Mountain rhyolites

In this study, we focus attention on the Older GM units since they display such a wide range of trace element concentrations, which lends itself to an analysis of the stoichiometry of the melting/crystallization reaction in their parental granitic mush prior to melt segregation, following the methods of Jolles and Lange (2021a). For each major, minor and trace-element component, the Ta-RCV$_i$ is constructed from the negative slope of its concentration with Ta divided by its average concentration (**Figs 4-8**; **Table 4**).

Major element Ta-RCV$_i$ values

Of the four anhydrous major element components in the Older Glass Mountain rhyolites, the Ta-RCV$_i$ values for SiO_2, Al_2O_3, and K_2O are all close to zero (**Fig. 4**). This is consistent with invariant behavior at the eutectic in the Quartz (Qz)-Plagioclase (Pl) K-feldspar (Kfs) system. The exception is found with the Na_2O component, which decreases with increasing Ta content (decreasing melt fraction), leading to a negative Ta-RCV$_i$ value of -0.3 (**Fig. 4c**). This result is consistent with a migration of the location of the eutectic within the Qz-Pl-Kfs system (e.g., Johannes and Holtz, 1996), away from the Na-rich plagioclase endmember, with increasing melt fraction during segregation of the Older GM rhyolite from their parental mush. The significance of this finding is discussed later in the paper.

Minor element Ta-RCV$_i$ values

Of the four minor element components, Ta-RCV$_i$ values for TiO_2 and MgO are both close to zero, whereas those for CaO and $Fe_2O_3^T$ are both 0.6 and reflect compatible behavior (**Fig. 5**). For the CaO component, this likely reflects its compatible behavior in plagioclase relative to the interstitial melt. For the total iron component, this likely reflects compatible behavior in the two Fe-Ti oxide phases relative to the interstitial melt. Concentrations of Fe_2O_3 and FeO can be plotted separately, based on ferric-ferrous ratios calculated for each sample for which ΔNNO and temperatures were obtained from two Fe-Ti oxides. Fe^{3+}/Fe^T ratios were calculated (and reported in Table 1) using the Kress and Carmichael (1991) experimentally calibrated model, which allows the ferric-ferrous ratio in natural melts to be calculated as a function of temperature, oxygen fugacity and melt composition. Because the GM rhyolites have major

element compositions that are so similar, their differences in ΔNNO values only reflect differences in their Fe^{3+}/Fe^{T} ratios.

Because only three data points are available for Fe_2O_3 and FeO for the Older GM units, Ta-RCV_i values were calculated for two cases: (1) Older GM units only, and (2) both Older and Younger GM units. In both cases, the Ta-RCV_i for Fe_2O_3 is greater than that for FeO, which was also found by Jolles and Lange (2021a) for the high-SiO_2 rhyolite portion of the Bishop Tuff.

Trace element Ta-RCV_i values

The Ta-RCV_i values for the REEs (**Table 4**) show that the order of their incompatibility broadly follows their order in the periodic table with La > Ce > Pr > Nd > Sm > Gd > Tb ~ Dy ~ Yb ~ Lu ~ Y (**Fig. 6**). (Europium is not included here because it occurs in two valences (2+ and 3+), unlike the other REEs that all have 3+ valance.). To first order, this is the same overall pattern obtained from the Bishop Tuff samples (Jolles and Lange, 2021; **Table 5**). In the Bishop case, Sm contents have a flat slope with Ta (and Fe-Ti oxide temperature), whereas for the Older GM units, it is Pr contents that are relatively flat with Ta. In both cases (Bishop Tuff and Older GM), the Ta-RCV_i values of 0.0 and -0.1 are consistent with bulk partition coefficients for Sm and Pr, respectively, between interstitial melt and crystalline phases in the parental mush that are close to ~1. The heavy rare earth elements (Tb, Dy, Yb, Ly, Y) have the largest negative Ta-RCV_i values (-2.1, -2.2) and are thus the most incompatible of the REEs.

Among the trace elements plotted in **Figure 7**, the order of compatibility is Hf > Rb > Th > U ~ Mn > Cs, ranging from -1.2 to -2.5. Of all the trace elements, Cs has the highest negative Ta-RCV_i value and is thus the most incompatible. For Sr and Ba, which are plotted in **Figure 8**, the flat patterns with Ta do not necessarily reflect a bulk partition coefficient of ~1, but instead

could reflect exceptionally large bulk partition coefficients, which is explained and discussed later in this paper.

Constraints on Mineral-Melt Reactions in the Parental Mush of the Older GM Rhyolites

One of the primary objectives of this study was to determine whether the stoichiometry of the crystallizing/melting reaction in the parental mush (from which the interstitial melt was extracted at different melt fractions to form the Older GM units) can be constrained from the Ta-RCV_i values tabulated in Table 4, along with available mineral-melt partition coefficients between high-SiO_2 rhyolite melt and the nine mineral phases observed as phenocrysts in the Glass Mountain rhyolites. Following Jolles and Lange (2021a), the following eutectic reaction is proposed:

$$\%X_1 Qz + \%X_2 Pl + \%X_3 Kfs + \%X_4 Bt + \%X_5 Mag + \%X_6 Ilm + \%X_7 Zrn + \%X_8 Ap + \%X_9 Aln = 100\% liquid \quad (5)$$

The goal is to constrain the values of X_1 to X_9 (relative proportions of each phase in the melting/crystallizing reaction) through an iterative set of linear fits to evaluate if a single, average stoichiometry can be obtained that leads to bulk partition coefficients for each element that are linearly correlated with their respective relative compatibility values (i.e., Ta-RCV_i values; Table 4). An additional constraint is that bulk D_i is ~1 in the case of Ta-RCV_i = ~0, and bulk Di <1 for negative Ta-RCV_i (element *i* is incompatible in the parental mush) and bulk D_i >1 for positive Ta-RCV_i (element *i* is compatible in the parental mush).

Constraints on % allanite, % zircon and % apatite in reaction

The hypothesis evaluated for the Older GM units is that the Ta-RCV$_i$ for the trace elements are linearly related with their bulk partition coefficients (bulk D$_i$). A test of this hypothesis is made by examining the relationship between bulk D$_i$ and Ta-RCV$_i$ for 11 trace elements (seven lanthanides, Y, Hf, Th and Y), which are entirely controlled by only three accessory phases: allanite, apatite and zircon. Allanite is notable for its exceptionally large partition coefficients for the REEs, which progressively decrease in magnitude from the light to middle to heavy REEs (Table 4); thus, allanite is the primary control on the REEs. Zircon primarily controls Hf and U, apatite is the main control on Y, and both allanite and zircon control the behavior of Th (Table 4).

Ideally, Eq. 4 would be used in a multiple linear regression to constrain the abundances of allanite, zircon and apatite (i.e., X_{Aln}, X_{Zrn}, X_{Ap}, respectively), since the partition coefficients are known for each of the 11 trace elements between these three phases and high-SiO_2 rhyolite melt (i.e., D_i^{Aln}, D_i^{Zrn}, and D_i^{Ap}; Table 4). However, since the bulk Di for each element in the parental mush is not known in advance, a multiple linear regression cannot be performed. Instead, following Jolles and Lange (2021a), a series of iterative steps (outlined below) allow bulk D$_i$ values to be calculated using Eq. 4 (by estimating the % abundances of allanite, zircon and apatite) and then plotted against the Ta-RCV$_i$ to test for a linear relationship (**Fig. 19**).

The first step in testing for a linear correlation between Ta-RCV$_i$ and bulk D$_i$ is to assign Pr a bulk D_i value of ~1 because it has a Ta-RCV$_i$ value close to 0 (-0.1; **Fig. 6c**). Next, an iterative approach was taken, where the proportions of zircon and apatite were first assumed to be zero, which allowed the proportion of allanite required to generate a bulk D_{Pr} of 1 to be calculated. For an allanite–liquid Pr partition coefficient of ~2167 (between that for Ce and Nd;

Table 4), the proportion of allanite is 1/2167 (or 0.046%). When these proportions (0.046% allanite, 0% zircon, 0% apatite) were input into Eq. 4, the bulk D_i for all 11 trace elements were calculated and plotted against their respective Ta-RCV$_i$ values. The results are shown in **Figure 19a** and illustrate a strong linear correlation ($R^2 = 0.910$). This is a notable result, since the Ta-RCV_i values are obtained entirely from whole-rock analyses of the Older GM units (Table 1), whereas the bulk D_i values are based entirely on the Mahood & Hildreth (1983) partition coefficient results for allanite (Table 4). This initial result strongly supports the hypothesis that Ta-RCV_i and bulk D_i values are linearly correlated.

The results in **Figure 19a** show that the largest outlier from the linear trend is Hf, which reflects the need to include zircon (Hf is strongly compatible in zircon; **Table 4**). Through a set of iterative steps, increments of zircon were added to Eq. 4 in increments of 0.001%, while adjusting the proportion of allanite to ensure that the bulk D_i is 1 when the Ta-RCV$_i$ is zero. The best linear fit ($R^2 = 0.992$) occurs with 0.044% allanite and 0.012% zircon (**Fig. 19b**).

The final iterative step was to add apatite to Eq. 4 in increments of 0.001% (and the proportion of allanite adjusted each time to ensure that bulk $D_i = 1$ when Ta-RCV$_i$ =0) until the best linear fit between bulk D_i and RCV_i was found (**Fig. 19c**). The addition of apatite improves the fit for Y. The result ($R^2 = 0.993$) leads to 0.044% allanite, 0.012% zircon, and 0.015% apatite in the crystallization/melting reaction in Eq. 4. These proportions are approximately half those deduced by Jolles and Lange (2021a) for the Bishop Tuff parental mush (**Fig. 17b,c**), which is consistent with the lower melt fractions (and temperatures; 660-714°C) inferred for the Older GM melts compared to those for the high-SiO_2 rhyolite portion of the Bishop Tuff (698-752°C; Jolles and Lange, 2019).

Effect of uncertainties in mineral-melt partition coefficients

Uncertainties in the mineral–melt partition coefficients for the 11 trace elements will impact the results in two different ways, depending on whether the errors are systematic or random. If there is a systematic error, and all D_i are too low (or too high) by a factor of two, then the deduced stoichiometry for the three mineral phases will also be too high (or too low) by a factor of two. If there are large, random errors among all D_i, moving them in different directions, then the R^2 values on the linear fits in **Figure 19** will degrade. The fact the R^2 values are >0.99 in **Figures 19b and 19c** strongly supports the validity of the mineral–melt partition coefficients from the literature that were used (Table 4). In either case, the key conclusion that these three mineral phases (allanite, zircon, apatite) in the crystallization/melting reaction in the parental mush controlled the concentration gradients of these 11 trace elements remains robust.

Constraints on % biotite, % titanomagnetite and % ilmenite in reaction

In the reaction in Eq. 5, the bulk partition coefficients for the minor elements, namely Ti, Fe^T (Fe^{3+}, Fe^{2+}) and Mg, are primarily controlled by biotite (Bt), titanomagnetite (Mag), and ilmenite (Ilm). Therefore, the following model equation can be used to calculate the bulk D_i for these minor elements:

$$\text{bulk } D_i = [D_i^{Ilm} * X_{Ilm} + D_i^{Mag} * X_{Mag} + D_i^{Bt} * X_{Bt}] \quad (6)$$

Because the bulk D_i values for these elements are not known, a test of a linear relationship with their respective Ta-RCV_i values is required. For Ti and Mg, their unchanging concentrations with temperature (**Fig. 5a,b**) either reflect a bulk partition coefficient of 1, or the lack of involvement of their controlling mineral phases in the crystallizing/melting reaction in the parental mush. Jolles and Lange (2021a) showed there was evidence for minimal involvement of

biotite in the crystallizing/melting reaction for Bishop melts segregated at low temperatures (≤720°C). A similar conclusion can be drawn here, supported by the low temperatures (660-714 °C) inferred during segregation of the Older GM units (**Fig. 18b**). Moreover, there is independent experimental evidence (e.g., Piwinskii and Wyllie, 1968) that biotite is relatively refractory (i.e., does not melt or break down below 720°C) relative to the water saturated, low-temperature eutectic melting temperatures (~650-680°C) at ~200-400 MPa in the the Qz–Pl–Kfs system (e.g., Johannes and Holtz, 1996).

To infer the relative abundance of titanomagnetite and ilmenite, it is necessary to revisit plots of ΔNNO vs. temperature. In **Figure 15**, these plots were derived from the Fe-Ti oxide phases in the Glass Mountain eruptive unit. However, since there is evidence that most of the GM units were erupted up to 360 kyrs after differentiation (i.e, melt segregation from a parental mush), the Fe-Ti oxide temperatures in **Figure 15** record conditions in the melt immediately prior to eruption and not those during melt segregation. For the latter, the Ta-temperatures are most relevant, and in **Figure 20a**, the ΔNNO values obtained in this study for the Older and Younger GM units are replotted against Ta-temperature. There is a remarkable overlap with the ΔNNO vs temperature data for the high-SiO_2 rhyolite portion of the Bishop Tuff (which was obtained entirely from the Fe-Ti oxides).

Note that the ΔNNO values are largely insensitive to temperature and thus primarily reflect the Fe^{3+}/Fe^{T} ratios in the samples, which were likely attained during differentiation (i.e., segregation of variable melt fractions from the parental mush). In a plot of Fe^{3+}/Fe^{T} vs. Ta-temperature (**Fig. 20b**), the GM units once again overlap with those for the high-SiO_2 rhyolite portion of the Bishop Tuff. Both data sets define a linear increase in melt Fe^{3+}/Fe^{T} ratio with increasing temperature (i.e., melt fraction during segregation).

The cause for the increase in Bishop Tuff oxidation state with temperature has long interested researchers (e.g., Hildreth, 1977; Ghiorso & Sack, 1991; Carmichael, 1991; Hildreth & Wilson, 2007; Ghiorso & Evans, 2008). Jolles and Lange (2021a) showed that the increase in Fe^{3+}/Fe^{T} with temperature simply reflects the larger bulk partition coefficient for Fe^{3+} (bulk $D_{Fe^{3+}}$ = 1.90) relative to that for Fe^{2+} (bulk $D_{Fe^{2+}}$=1.02) during crystallization/melting in the parental mush. The larger bulk Di for Fe^{3+} relative to that for Fe^{2+} is due to a higher proportion of titanomagnetite ($D_{Fe^{3+}} > D_{Fe^{2+}}$;Table 4) relative to ilmenite ($D_{Fe^{3+}} < D_{Fe^{2+}}$; Table 4) in the crystallizing/melting reaction in the parental mush.

A similar inference can be deduced for the Older (and Younger) GM units, namely the % abundance of titanomagnetite exceeded that of ilmenite, given the close overlap between the Older and Younger GM and Bishop Tuff data in **Fig. 20b**). Because only three Fe^{3+}/Fe^{T} data points are available for the Older GM samples, only these broad constraints can be made at this time on the relative abundances of titanomagnetite and ilmenite in the melting/crystallizing reaction in the parental mush

Constraints on % quartz, %plagioclase, %K-feldspar (location of eutectic)

The next objective is to constrain the relative proportions of quartz, plagioclase, and K-feldspar in the crystallizing/melting reaction in Eq. 5. This goal is equivalent to finding the location of the eutectic in the Qz–Pl–Kfs ternary, which is a strong function of pressure (P_{total}) and activity of water (Johannes & Holtz, 1996) during crystallization/melting in the parental mush. Because Sr and Ba contents are so low (and relatively unchanging with Ta content) in the Older GM samples (Fig. 8), they cannot be utilized to constrain the relative abundance of plagioclase and K-feldspar in the mineral-melt reaction during melt segregation. Note also that

their pattern in **Figure 8**, namely their low concentrations that vary little with melt fraction, is expected for elements with exceptionally large bulk partition coefficients, which is predicted for both Sr and Ba (e.g., Blundy and Wood, 1991) under three conditions: (1) low temperatures (660-700°C), (2) low An contents in plagioclase in the parental mush (consistent with low CaO contents in the Older GM units; Fig. 5;), and (3) the high-SiO_2 character of the interstitial melts.

Fortunately, the systematic increase in the K_2O/Na_2O ratio analyzed in the Older and Younger GM samples as a function of Ta-temperature (a proxy for increasing melt fraction in the parental mush) allows constraints to be placed on the changing activity of water during melt segregation. It is well established from the experimental literature (e.g., Johannes and Holtz, 1996) that the location of the minimum/eutectic in the Qz–Pl–Kfs ternary systematically shifts away from plagioclase with decreasing activity of H_2O (a_{H2O}). Thus, the interstitial melt (eutectic composition) in a granitic crystalline mush at a relatively high a_{H2O} will have a lower K_2O/Na_2O ratio than a melt that forms and segregates at a lower a_{H2O}. The results in **Figure 21** clearly reveal the effect of decreasing activity of water with increasing melt fraction (Ta-temperature as a proxy) during segregation from the parental mush.

An overview of phase-equilibrium experiments in the Qz-Pl-Kfs-H2O system (e.g., Johannes and Holtz, 1996) clearly show that unit OC, with a relative low Fe-Ti oxide (and Ta-based) temperature of ~660°C, must have segregated from its parental granitic mush under conditions that closely approached water saturation ($a_{H2O} > 0.9$) and depths of ~300-400 MPa. These conditions require dissolved water concentrations ≥ 7 wt% in the interstitial high-SiO_2 rhyolite melt, consistent with phase-equilibrium experiments on a representative GM sample (Waters and Andrews, 2016). Moreover, the primary source of the water in the parental mush must have been derived from the degassing of basaltic sills or dikes emplaced into the crust

beneath Glass Mountain since the pre-existing granitoid crust only contains ≤ 0.6 wt% H_2O (in the form of modal biotite and hornblende; Bateman and Chappell, 1979); the latter is insufficient to provide the required water in the Long Valley rhyolites, as previously discussed by Jolles and Lange (2021a).

Average water contents of Plio-Quaternary Long Valley basalts, which erupted in close association with the Long Valley caldera, are ~4 wt% (Jolles and Lange, 2021b). An estimate of the average CO_2 contents in these basalts, based on comparison with similar basalts, is ~4000 ppm CO_2 (e.g., Wallace, 2005). If these basalts are representative of those emplaced into the crust beneath the Long Valley volcanic field during formation of the Glass Mountain rhyolites, then their exsolved fluid phase would have a composition of $X_{H_2O}^{fluid}$ = ~0.95. The presence of such an H_2O-rich fluid would strongly lower the solidus temperature of granitoids and thus lead to the formation of interstitial melts at temperatures as low as ~660 °C, similar to that of unit OC. Moreover, Jolles and Lange (2021a) showed that for a fixed mass of H_2O-rich fluid present at the onset of partial melting of a granitoid, it is expected that H_2O concentrations in the interstitial melt will progressively decrease as melt fraction increases. This will result in interstitial melts with progressively lower activities of H_2O, and thus higher K_2O/Na_2O ratios, with increasing melt fraction, which is the pattern found for the Older and Younger GM sample (**Fig. 21)**.

In summary, the broad conclusion that can be drawn is that the onset of melt segregation of the Older GM units from its parental mush began at a temperature of ~660°C, at an activity of H_2O that was initially close to ~0.95, and at depths corresponding to 300-400 MPa. This pressure interval is consistent with the calculated pressure of ~385 MPa for unit OC (assuming ~7 wt% H_2O) from the rhyolite barometer of Wilke et al. (2017), which is based on an extensive set of phase-equilibrium experiments in the Qz-Pl-Kfs-H_2O system from the literature. The

stoichiometry of the melting reaction in the parental granitic mush at a pressure of ~385 MPa, an activity of H_2O of ~0.95, and a temperature of ~660°C can be deduced from the experimental results from Holtz et al. (1992), namely ~33.5% quartz + ~25.5 % K-feldspar + ~41 % plagioclase. However, this stoichiometry would have changed (i.e., less plagioclase and relatively more quartz and K-feldspar) as melt fraction increased and a_{H2O} decreased (i.e., dissolved water in the interstitial melt decreased), leading to higher K_2O/Na_2O ratios in the melt.

Preservation of Glass Mountain Rb-Sr Isochrons (Nature of Storage Conditions)

The second major objective of this paper is to revisit the preservation of the Rb/Sr isochrons between the time of differentiation (i.e., formation of spread in Rb/Sr ratios among the different Older and Younger GM rhyolites) and subsequent eruption, which spanned up to ~360 ky (e.g., Davies et al., 1994; Davies and Halliday, 1998; Simon and Reid, 2005). Given the exceptionally low Sr contents in the Glass Mountain rhyolites, relative to their relatively high Rb contents, their Rb/Sr ratios would be easily disturbed during any process that involved crystal fractionation, partial melting, crustal contamination and/or mixing with an unrelated magma. As previously discussed in the introduction, this has spawned a broad debate in the literature about the nature of the storage of the GM melts during the time interval between differentiation and eruption. Moreover, the evidence from zircon ages (Simon and Reid, 2005; Simon et al., 2007), shows that intermittent crystallization occurred in the different Glass Mountain eruptive units during their respective storage intervals.

Here, it is proposed that the Glass Mountain rhyolites were held in cold storage in a series of dikes, which initially, immediately after the isochron differentiation events, may have been relatively thin (e.g., on the scale of tens of cm). Dikes made of eutectic, high-SiO_2 rhyolite, such

as the GM units, will readily undergo nearly complete melting when heated to temperatures (660-720°C; Table 3) and a_{H2O} conditions (i.e., ~5-7 wt% H_2O in the melt phase; Waters and Andrews, 2016) documented for the Glass Mountain rhyolites. It is possible that the wide span of zircon crystallization ages in individual GM units (Simon and Reid, 2005; Simon et al., 2007) may reflect episodes where initially formed, thin dikes were remelted and remobilized (due to periodic emplacement of basaltic sills/dikes, which crystallized and degassed, allowing a fluid phase to transfer the required heat and H_2O to the high-SiO_2 rhyolite dikes), leading to their coalescence into progressively wider dikes. Over time, dikes of >5 m width may have formed, similar to those found in the Miocene bimodal granitic intrusions in southern Nevada (e.g., Bachl et al., 2001; Walker et al., 2007; Hodge et al., 2006). At this point, subsequent remelting of dikes, which exceed critical widths for km-scale transport through the upper crust (e.g., Petford et al., 1993), would enable their immediate ascent to the surface and thus eruption.

Evidence to support this hypothesis is found in the textures of phenocrysts found in the Glass Mountain rhyolites. For example, photomicrographs of quartz phenocrysts in unit OD (Fig. 22a-b) display diffusion-limited (i.e., rapid growth) textures, including hopper textures. Moreover, large (~1000 micron) granophyric intergrowths of sanidine and quartz are also found (**Fig. 22c-d**), which were experimentally demonstrated by Waters and Andrews (2016) to reflect rapid growth over time scales of < 1 day. Work is currently underway to study in more detail the compositions and textures of the phenocryst assemblage in the GM rhyolites. The goal is to further test whether the GM phenocrysts grew rapidly during ascent, driven by H_2O-degassing crystallization (e.g., Waters and Lange, 2017). In the meantime, the occurrence of high-SiO_2 rhyolite dike swarms in extensional bimodal intrusions (e.g., Hodge et al., 2006; Miller et al.,

2011) suggests that cold storage of the Glass Mountain rhyolites in a similar dike swarm is a viable hypothesis that merits further evaluation.

Conclusions

Several key conclusions were drawn in this study, which focused on understanding the origin of the large 2-fold variations of trace element concentrations in the Older Glass Mountain rhyolites. It was shown that the geochemical gradients could be explained by the segregation of variable melt fractions from a parental, granitic mush, which contained the same nine mineral phases found as phenocrysts in the erupted lavas (quartz + sanidine + plagioclase + biotite + titanomagnetite + ilmenite + allanite + zircon + apatite). More specifically, the 2-fold variations in the REEs, as well as in Th, U and Hf, can entirely be attributed to the relative proportion of the three accessory phases (0.044% allanite, 0.014% zircon, 0.015% apatite) in the crystallizing/melting reaction in the parental mush. Temperatures at the time of melt segregation (660-714°C) were too cool for the involvement of biotite, whereas the % of titanomagnetite must have exceeded that of ilmenite in the crystallizing/melting reaction in the parental mush. This is required so that the bulk partition coefficient of Fe^{3+} exceeds that of Fe^{2+}, which explains the increase in the Glass Mountain rhyolite Fe^{3+}/Fe^{T} ratio with temperature at the time of melt segregation. The relative proportions of the tectosilicate phases in the mineral-melt reaction in the parental mush reflects the location of the eutectic in the Qz-Pl-Kfs system, which in turn is determined by the pressure (depth) and activity of water in the granitic mush. The high-resolution Fe-Ti oxide temperature obtained on Older GM unit OC, which is the only unit to have an eruption age that is indistinguishable from its isochron (i.e., differentiation) age, is 660 ± 6 °C. This low temperature constrains the location of eutectic to be close to the pure water-

saturated solidus of a granitic parent at ~350 MPa. The source of heat and water was most likely H_2O-rich fluids derived from the degassing of basaltic sills and dikes emplaced into the crust beneath the Long Valley volcanic field.

Another key conclusion of this study concerns the preservation of the Rb/Sr isochrons, even though their ages, which date the melt segregation process outlined above, predate the eruption ages by up to 360 ky. Here, it is shown that cold storage of the Glass Mountain rhyolites as dikes (similar to the rhyolite dike swarms found in extensional bimodal intrusions) is a viable hypothesis since it explains the preservation of Rb/Sr isochrons, as well as the ease with which remobilization can occur due to the influx of heat and water through degassing of recently emplaced basaltic sills. Evidence from the literature of episodic zircon crystallization in the Glass Mountain rhyolites during their storage may reflect discrete remelting events that led to the coalescence of initially thin dikes into wider ones, until critical widths (>5 m) were reached, enabling the successful transport of the GM rhyolites to the surface.

References

Andersen NL, Jicha BR, Singer BS, Hildreth W (2017) Incremental heating of Bishop Tuff sanidine reveals preeruptive radiogenic Ar and rapid remobilization from cold storage. Proceedings of the National Academy of Science of the USA 114(47):12407–12412

Bachl CA, Miller CF, Miller JS, Faulds JE (2001) Construction of a pluton: Evidence from an exposed cross section of the Searchlight pluton, Eldorado Mountains, Nevada. Geological Society of America Bulletin 113(9):1213-1228

Bacon CR, Hirschmann MM (1988) Mg/Mn partitioning as a test for equilibrium between coexisting Fe–Ti oxides. American Mineralogist 73:57–61

Bailey RA (1989) Geologic map of the Long Valley caldera, Mono-Inyo Craters volcanic chain, and vicinity, eastern California. United States Geological Survey Map I-1933, scale 1:62,500; pamphlet

Barbee O, Chesner C, Deering C (2020) Quartz crystals in Toba rhyolite show textures symptomatic of rapid crystallization. American Mineralogist 105:194-226

Barth AP, Walker JD, Wooden JL, Riggs NR, Schweickert RA (2011) Birth of the Sierra Nevada magmatic arc: Early Mesozoic plutonism and volcanism in the east-central Sierra Nevada of California. Geosphere 7 (4): 877–897

Blundy JD, Wood BJ (1991) Crystal-chemical controls on the partitioning of Sr and Ba between plagioclase feldspar, silicate melts, and hydrothermal solutions. Geochim Cosmochim Acta 55:193–209

Buddington AF, Lindsley DH (1964) Iron-titanium oxide minerals and synthetic equivalents. Journal of Petrology 5(2):310–357

Carmichael, ISE (1991) The redox states of basic and silicic magmas: a reflection of their source regions? Contributions to Minerology and Petrology 106: 129-141

Cousens, BL (1996) Magmatic evolution of Quaternary mafic magmas at Long Valley Caldera and the Devils Postpile, California: Effects of crustal contamination on lithospheric mantle-derived magmas. Journal of Geophysical Research 101: 27673–27689

Davies GR, Halliday AN (1998) Development of the Long Valley rhyolitic magma system: strontium and neodymium isotope evidence from glasses and individual phenocrysts. Geochimica et Cosmochimica Acta 62:3561-3574

Davies GR, Halliday AN, Mahood GA, Hall CM, (1994). Isotopic constraints on the production rates, crystallization histories and residence times of pre-caldera silicic magmas, Long Valley, California. Earth and Planetary Science Letters 125: 17–37

Du Bray EA, John DA, Cousens BL, Hayden LA, Vikre PG (2016). Geochemistry, petrologic evolution, and ore deposits of the Miocene Bodie Hills volcanic field, California and Nevada. American Mineralogist 101(3):644–677

Dufek J, Bachmann O (2010) Quantum magmatism: Magmatic compositional gaps generated by melt-crystal dynamics. Geology 38(8): 687-790

Eddy MP, Pamukcu A, Schoene B, Steiner-Leach T, Bell EA (2022) Constraints on the timescales and processes that led to high-SiO_2 rhyolite production in the Searchlight pluton, Nevada, USA. Geosphere 18:1000-1019

Fliedner MM, Klemperer SL, Christensen NI (2000) Three-dimensional seismic model of the Sierra Nevada arc, California, and implications for crustal and mantle composition. Journal of Geophysical Research 105(B5): 10899–10922

Flinders AF, Shelly DR, Dawson PB, Hill DP, Tripoli B, Shen Y (2018) Seismic evidence for significant melt beneath the Long Valley Caldera, California, USA. Geology 46(9):799-802

Frassetto AM, Zandt G, Gilbert H, Owens TJ, Jones CH (2011). Structure of the Sierra Nevada from receiver functions and implications for lithospheric foundering. Geosphere 7(4): 898–921

Ghiorso M, Evans BW (2008) Thermodynamics of rhombohedral oxide solutions and revision of the Fe–Ti two-oxide geothermometer and oxygen barometer. American Journal of Science 308:957–1039

Halliday AN (1990) Reply to comment of R.S.J. Sparks, H.E. Huppert, and C.J.N. Wilson on "Evidence for long residence times of rhyolitic magma in the Long Valley magmatic system: the isotopic record in precaldera lavas of Glass Mountain". Earth and Planetary Science Letters 99: 390-394

Halliday AN, Mahood GA, Holden P, Metz JM, Dempster TJ, Davidson JP (1989) Evidence for long residence times of rhyolitic magma in the Long Valley magmatic system: the isotopic record in precaldera lavas of Glass Mountain. Earth and Planetary Science Letters 94:274-290

Hildreth W (1977) The magma chamber of the Bishop Tuff: gradients in temperature, pressure, and composition, Ph.D. thesis., Berkeley University of California

Hildreth W (1979) The Bishop Tuff: evidence for the origin of compositional zonation in silicic magma chambers. In: Chapin CE, Elston WE (eds) Ash-flow tuffs. Geological Society of America Special Papers 180: 43–75

Hildreth W (2004) Volcanological perspectives on Long Valley, Mammoth Mountain, and Mono Craters: several contiguous but discrete systems. Journal of Volcanology and Geothermal Research 136:169-198

Hildreth W (2017) A refreshing overview of the Bishop Tuff. In: Hildreth W, Fierstein J (eds) Geologic field-trip guide to Long Valley Caldera, California. U.S. Geological Survey Scientific Investigations Report 2017-5022-L

Hildreth W, Wilson CJN (2007) Compositional zoning of the Bishop Tuff. Journal of Petrology 48:934–952

Hodge K, Miller CF, Miller JS, Faulds J (2006) Dike emplacement at the Searchlight, NV, volcano-plutonic complex. GSA.

Holtz F, Behrens H, Dingwell DB, Taylor RP (1992) Water solubility in aluminosilicate melts of haplogranite compositions at 2 kbar. Chemical Geology 96:289-302

Jarosewich E, Nelen JA, Norberg JA (1980) Reference samples for electron microprobe analysis. Geo Stand News Letters 4:43–47

Johannes W (1984). Beginning of melting in the granite system Qz–Or–Ab–An–H_2O. Contributions to Mineralogy and Petrology 86: 264–273.

Johannes W, Holtz F (1996) Petrogenesis and Experimental Petrology of Granitic Rocks Minerals and Rocks. Minerals 22:115-275.

Jolles JSR, Lange RA (2019) High-resolution Fe–Ti oxide thermometry applied to single-clast pumices from the Bishop Tuff: a re-examination of compositional variations in phenocryst phases with temperature. Contributions to Minerology and Petrology 174:70

Jolles JSR, Lange RA (2021a) Origin of compositional gradients with temperature in the high-SiO_2 rhyolite portion of the Bishop Tuff: constraints on mineral–melt–fluid reactions in the parental mush. Journal of Petrology 62:1-25

Jolles JSR, Lange RA (2021b) Temperatures and water contents of Long Valley, CA basalts: application of olivine-melt thermometry and hygrometry at the liquidus. Journal of Volcanology and Geothermal Research 417: 107298

Kress VC, Carmichael ISE (1991) The compressibility of silicate liquids containing Fe_2O_3 and the effect of composition, temperature, oxygen fugacity and pressure on their redox states. Contributions to Minerology and Petrology 108:82-92

Mahood GA (1990) Second reply to comment of R.S.J. Sparks, H.E. Huppert and C.J.N. Wilson on "Evidence for long residence times of rhyolitic magma in the Long Valley magmatic system: the isotopic record in the precaldera lavas of Glass Mountain". Earth and Planetary Science Letters 99 (4): 395-399

Mahood GA, Hildreth EW (1983) Large partition coefficients for trace elements in high-silica rhyolites. Geochimica et Cosmochimica Acta 47:11-30

Manley CR, Glazner AF, Farmer GL (2000) Timing of volcanism in the Sierra Nevada of California: Evidence for Pliocene delamination of the basaltic root? Geology 28(9): 811–814

Metz JM, Bailey RA (1993) Geologic map of Glass Mountain, Mono County, California: Geological Survey, Miscellaneous Investigations Series Map I-1995, scale 1:24,00

Metz JM, Mahood GA (1985) Precursors to the Bishop Tuff Eruption: Glass Mountain, Long Valley, California. Journal of Geophysical Research 90: 121-126

Metz JM, Mahood GA (1991) Development of the Long Valley, California, magma chamber recorded in precaldera rhyolite lavas of Glass Mountain. Contributions to Minerology and Petrology 106:379-397

Miller CF, Furbish DJ, Walker BA, Claiborne LI, Koteas GC, Bleick HA, Miller JS (2011) Growth of plutons by incremental emplacement of sheets in crystal-rich host: Evidence from Miocene intrusions of the Colorado River region, Nevada, USA. Tectonophysics 500:65-77

Petford N, Kerr RC, Lister JR (1993) Dike transport of granitoid magmas. Geology 21(9): 845-848

Piwinskii AJ, Wyllie PJ (1968) Experimental studies of igneous rock series: A zoned pluton in the Wallowa Batholith, Oregon. The Journal of Geology 76: 205–234

O'Neill HSC, Pownceby MI (1993) Thermodynamic data from redox reactions at high temperatures. I. An experimental and theoretical assessment of the electrochemical method using stabilized zirconia electrolytes, with revised values for the Fe-"FeO", Co-CoO, Ni-NiO and Cu-Cu_2O oxygen buffers, and new data for the W-WO_2 buffer. Contributions to Mineralogy and Petrology 114:296-314

Sack RO, Ghiorso MS (1991) Chromian spinels as petrogenetic indicators: thermodynamics and petrological applications. American Mineralogist 76: 827-847

Saleeby J, Ducea M, Clemens-Knott D (2003) Production and loss of high-density batholitic root, southern Sierra Nevada, California. Tectonics 22(6):1064

Simon JI, Reid MR (2005) The pace of rhyolite differentiation and storage in an 'archetypical' silicic magma system, Long Valley, California. Earth and Planetary Science Letters 235:123-140

Simon JI, Reid MR, Young ED (2007) Lead isotopes by LA-MC-ICPMS: Tracking the emergence of mantle signatures in an evolving silicic magma system. Geochimica et Cosmochimica Acta 71: 2014-2035

Simon JI, Weis D, DePaolo DJ, Renne PR, Mundil R, Schmitt AK (2014) Assimilation of preexisting Pleistocene intrusions at Long Valley by periodic magma recharge accelerates rhyolite generation: rethinking the remelting model. Contributions to Mineralogy and Petrology 167: 955

Sparks SJ, Huppert HE, Wilson CJN (1990) Comment on "Evidence for long residence times of rhyolitic magma in the Long Valley magmatic system: the isotopic record in precaldera lavas of Glass Mountain" by A.N. Halliday, G.A. Mahood, P. Holden, J.M. Metz, T.J. Dempster and J.P. Davidson. Earth and Planetary Science Letters 99: 387-389

Thurber C, Zhang H, Brocher T, Langenheim V (2009) Regional three-dimensional seismic velocity model of the crust and uppermost mantle of northern California. Journal of Geophysical Research 114 (B1)

Tuttle OF, Bowen NL (1958) Origin of Granite in the Light of Experimental Studies in the System $NaAlSi_3O_8$–$KAlSi_3O_8$–SiO_2–H_2O. Geological Society of America 74: 1-153

Walker BA, Miller CF, Claiborne LL, Wooden JL, Miller JS, (2007) Geology and geochronology of the Spirit Mountain batholith, southern Nevada: Implications for timescales and physical processes of batholith construction. Journal of Volcanology and Geothermal Research 167:239-262

Wallace PJ (2005) Volatiles in subduction-zone magmas: concentrations based on melt inclusion and volcanic gas data. Journal of Volcanology and Geothermal Research 140:217-240

Waters LE, Andrews BJ (2016) The role of superheating in the formation of Glass Mountain obsidians (Long Valley, CA) inferred through crystallization of sanidine. Contributions to Mineralogy and Petrology 179:79

Waters LE, Lange RA (2017) Why aplites freeze and rhyolites erupt: controls on the accumulation and eruption of high-SiO_2 (eutectic) melts. Geology 45: 1019-1022.

Wilke S, Holtz F, Neave DA, Almeev R (2017) The effect of anorthite content and water on the quartz-feldspar cotectic compositions in the rhyolitic system and implications for geobarometry. Journal of Petrology, 58:789-818

Wilson CJN, Hildreth W (1997) The Bishop Tuff: new insights from eruptive stratigraphy. The Journal of Geology 105(407):439

Wolff JA, Ellis BS, Ramos FC, Starkel WA, Boroughs S, Olin PH, Bachmann O (2015). Remelting of cumulates as a process for producing chemical zoning in silicic tuffs: A comparison of cool, wet and hot, dry rhyolitic magma systems. Lithos 236–237, 275–286

Zandt G, Hersh G, Owens TJ, Ducea M, Saleeby J, Jones CH (2004) Active foundering of a continental arc root beneath the southern Sierra Nevada in California. Nature 431(7004): 41–46

Figures:

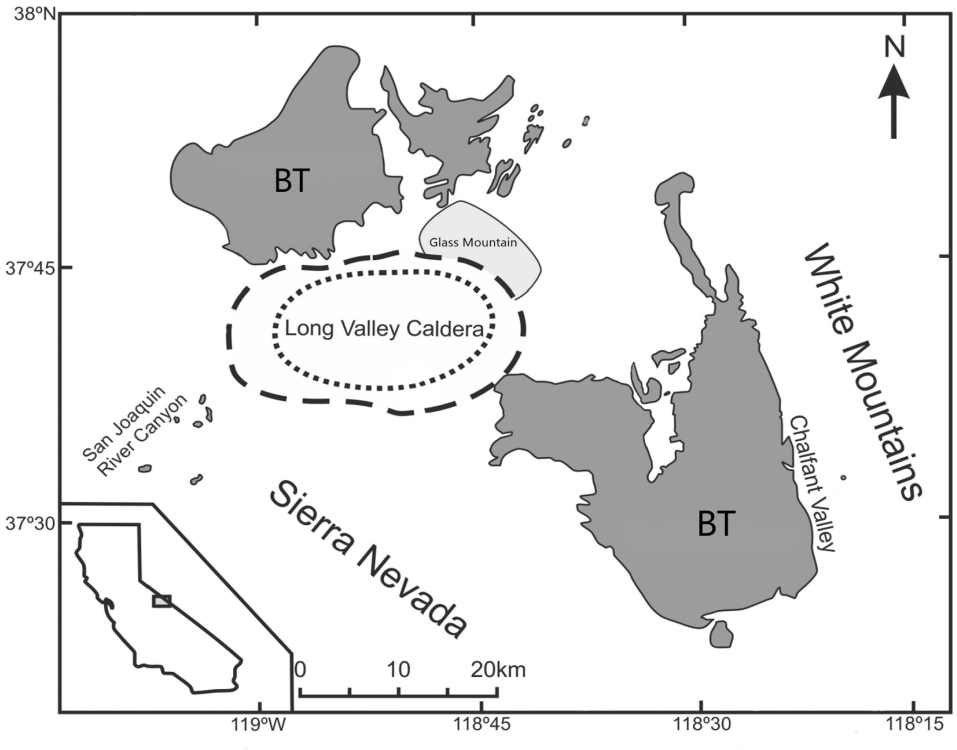

Figure 1: Map of Glass Mountain and Long Valley Caldera, California. Map modified from Chamberlin et al. (2015). Caldera rim is shown by the dashed line, Glass Mountain is the light gray and the Bishop Tuff (BT) is the dark gray.

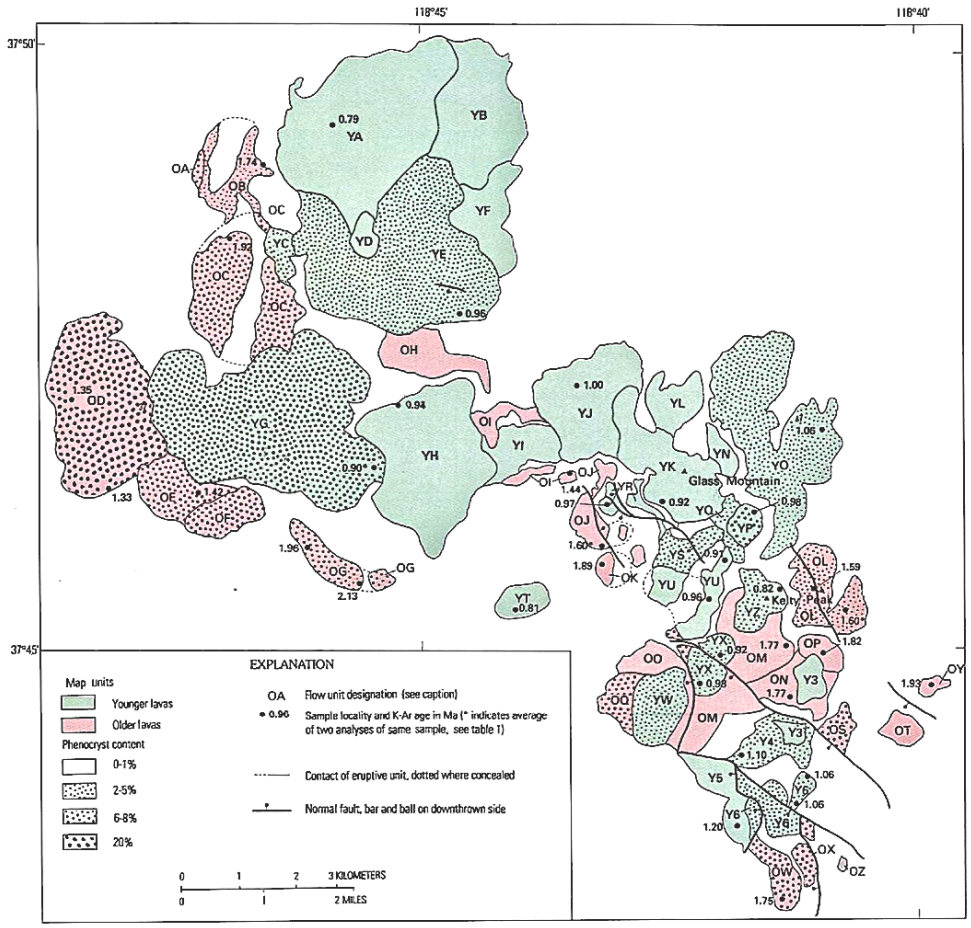

Figure 2: Geologic map of the Glass Mountain (GM) eruptive units modified from Metz and Bailey (1993). Older GM units are shown in pink and Younger GM units are shown in green. K-Ar ages in Ma are from Metz and Mahood (1985) and are the average of two analyses of the same sample.

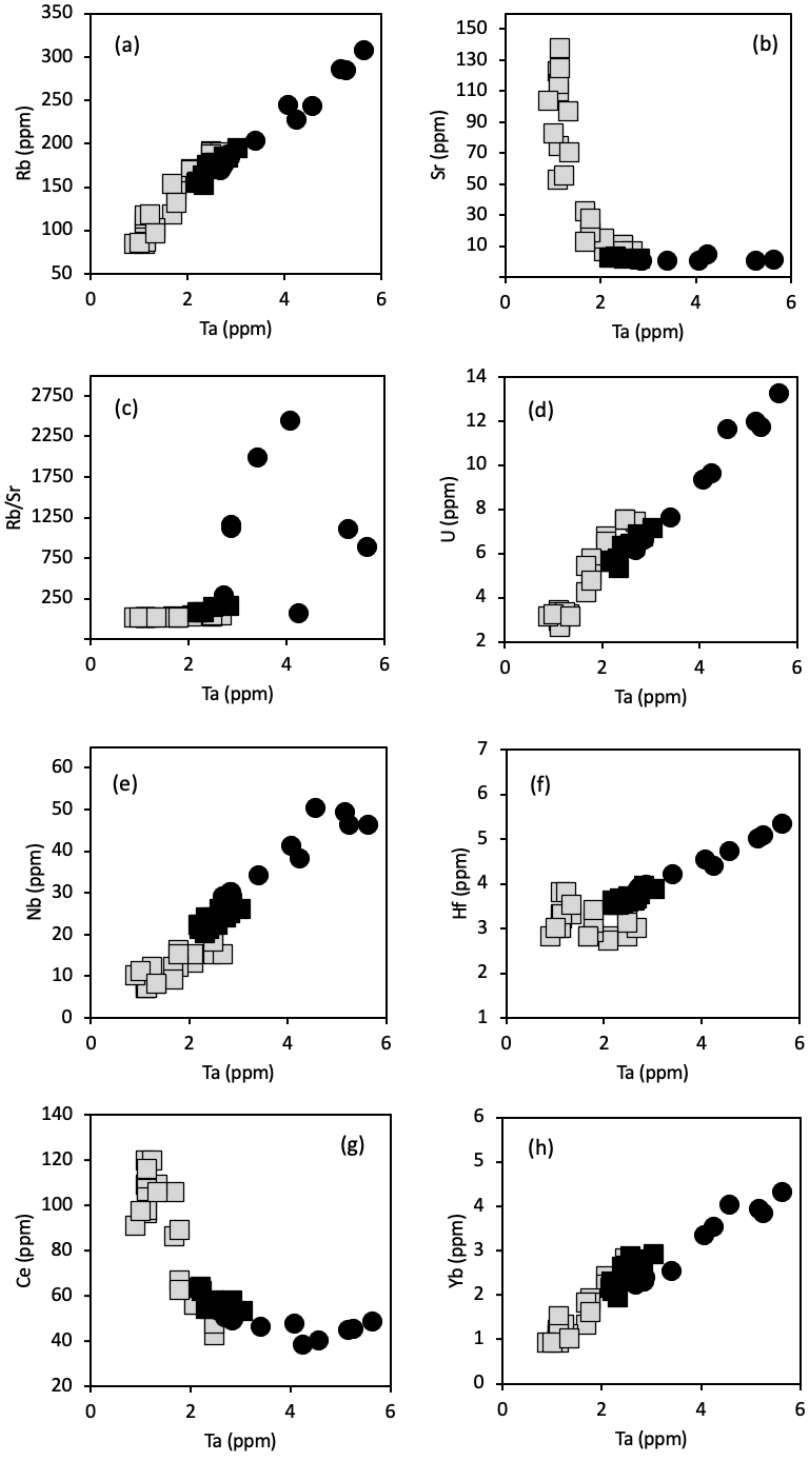

Figure 3: Select whole-rock trace-element concentrations (ppm) vs. Ta (ppm) for the Glass Mountain samples from Metz and Mahood (1991). Older and Younger GM samples shown by black circles and black boxes, respectively. Also show for comparison are the Bishop Tuff data (grey boxes) from Jolles and Lange (2019) and Note that the Glass Mountain Sr analyses are from Halliday et al. (1989).

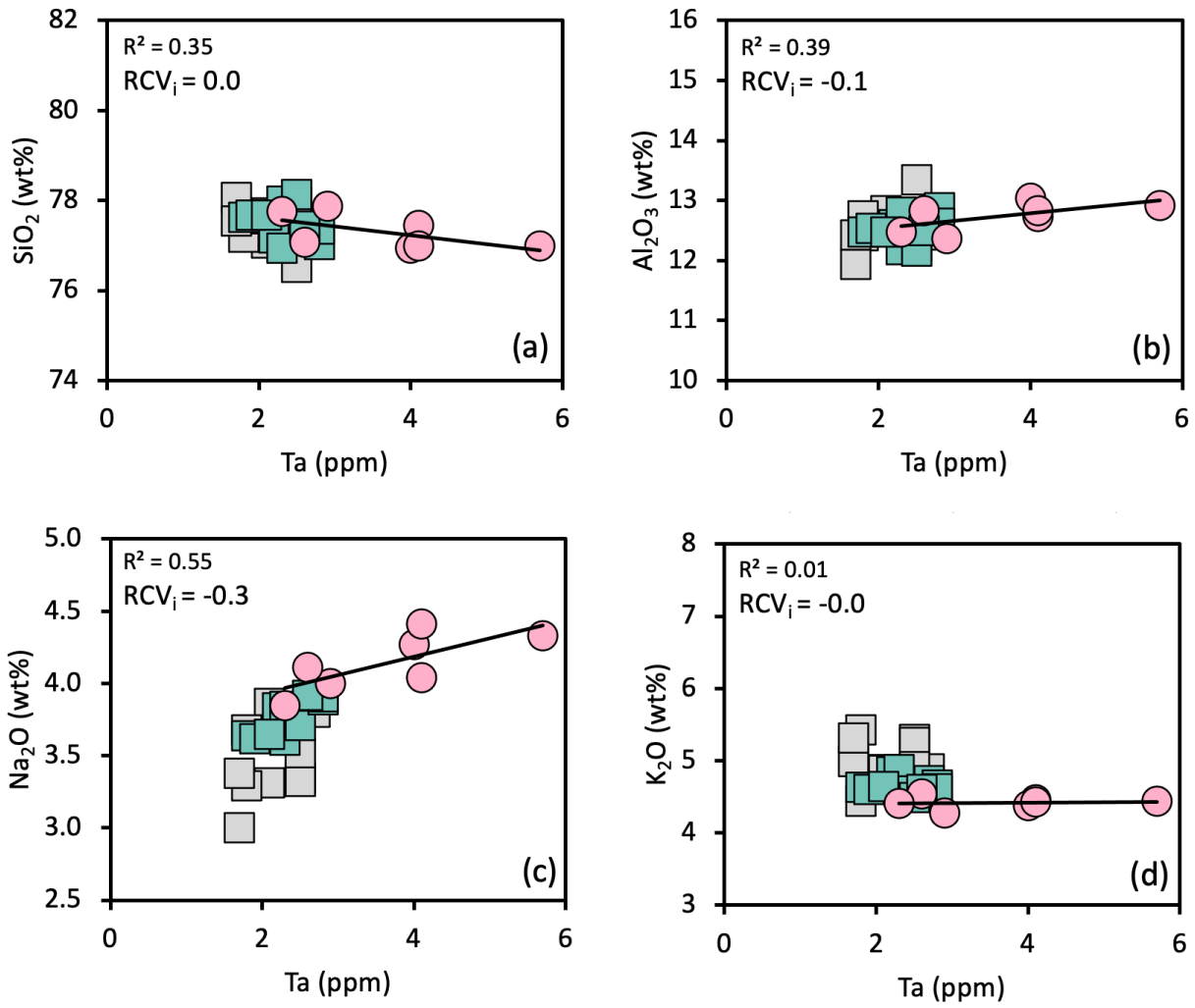

Figure 4: Major-element concentration (wt%) variations with Ta (ppm) content. Older (pink) and Younger (green) Glass Mountain data are from this study, whereas and Early- and Transitional-type Bishop Tuff samples (grey) are from Jolles and Lange (2021a). The R^2 values on linear fits to the Older GM samples are shown, as well as Ta-RCV$_i$ values (see text for definition of Ta-based relative compatibility values).

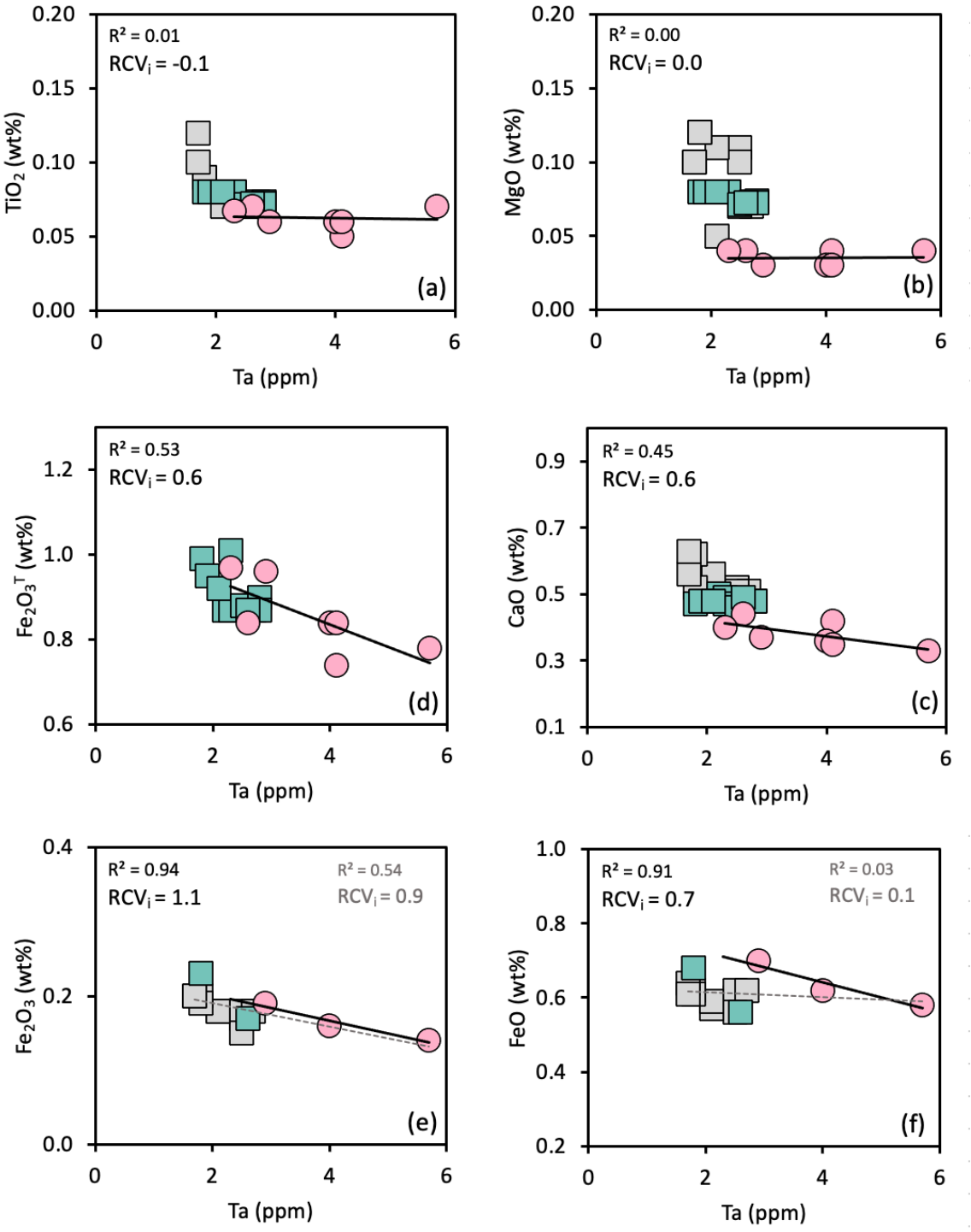

Figure 5: Minor-element concentration (wt%) gradients with Ta (ppm) concentration. Symbols are the same as Figure 4. The R^2 values on linear fits to the Older GM samples are shown, as well as Ta-RCV_i values (see text for definition of Ta-based relative compatibility values). For the Fe_2O_3 and FeO components, linear fits to both Younger and Older GM samples are also shown (see text).

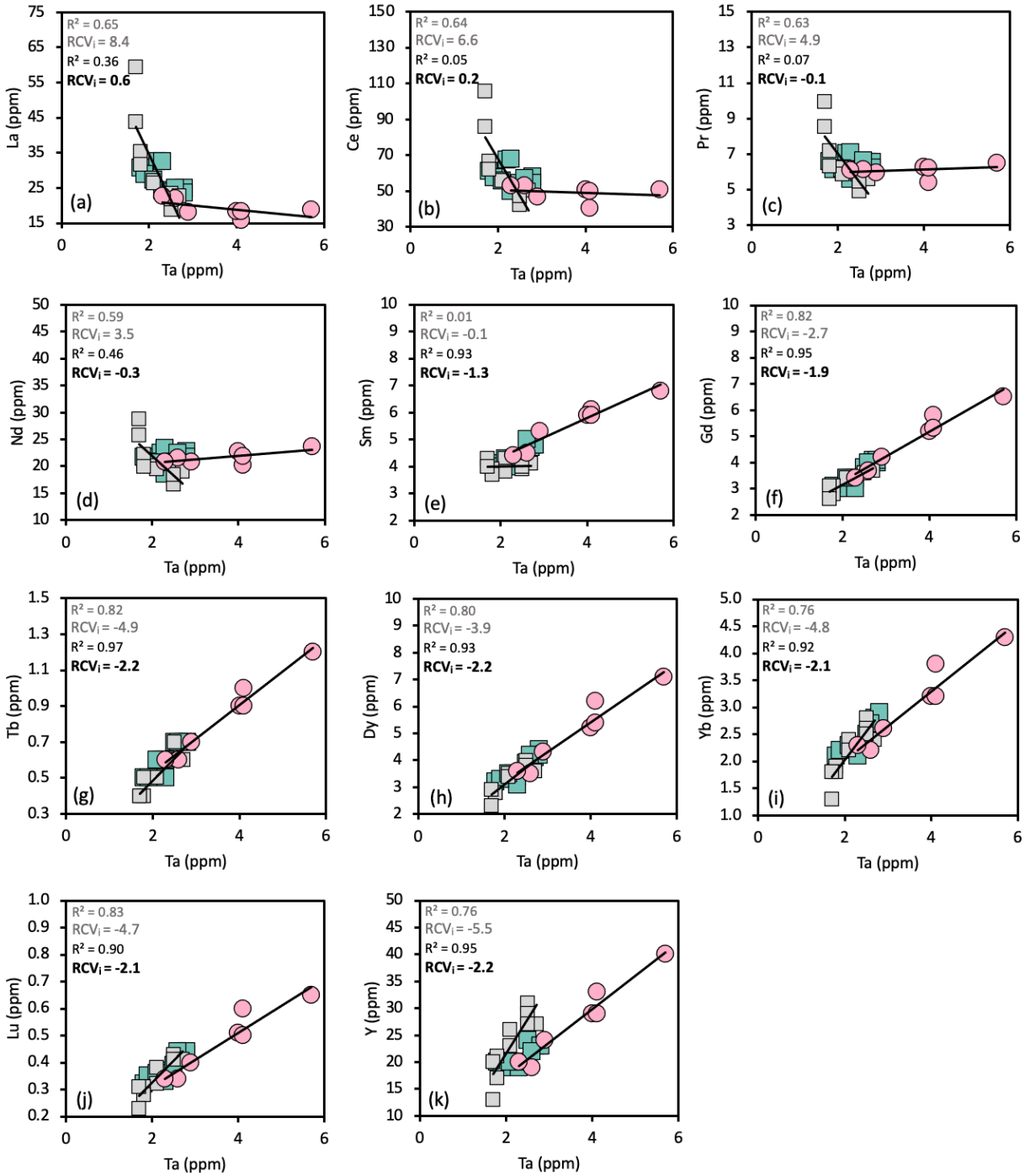

Figure 6: Rare earth element (REE) concentration (ppm) gradients with Ta (ppm) concentration. Symbols are the same as Figure 4. The R^2 values on linear fits to the Older GM samples are shown, as well as Ta-RCV_i values (see text for definition of Ta-based relative compatibility values). Also shown are R^2 and Ta-RCV_i values for the high-SiO_2 rhyolite portion of the Bishop Tuff from Jolles and Lange (2021a).

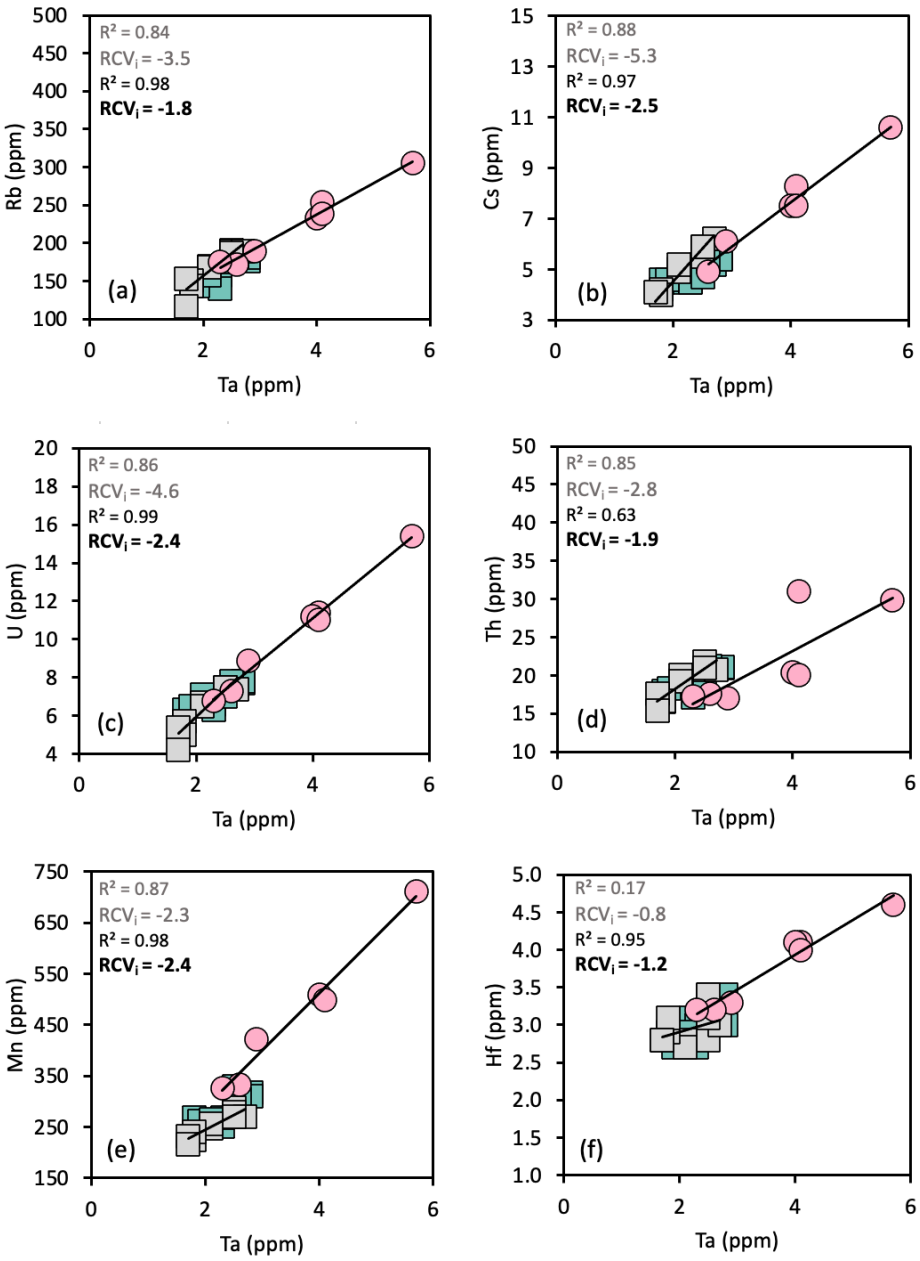

Figure 7: Select trace element concentration (ppm) gradients with Ta (ppm) concentration. Symbols are the same as Figure 4. The R^2 values on linear fits to the Older GM samples are shown, as well as Ta-RCV_i values (see text for definition of Ta-based relative compatibility values). Also shown are R^2 and Ta-RCV_i values for the high-SiO_2 rhyolite portion of the Bishop Tuff from Jolles and Lange (2021a).

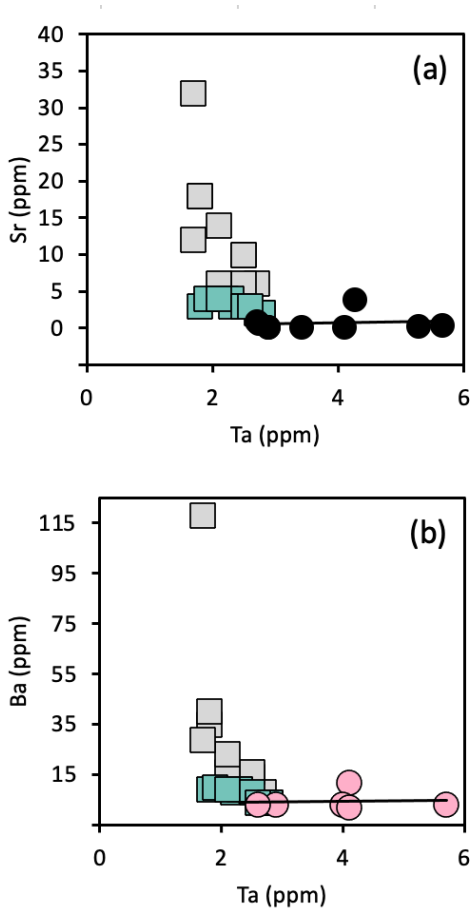

Figure 8: (a) Sr (ppm) and (b) Ba concentration (ppm) gradients with Ta (ppm) concentration. Symbols are the same as Figure 4. Data for Sr are from Halliday et al. (1989) on samples studied by Metz and Mahood (1991). Data for Ba are from this study. Also shown are data from the Bishop Tuff (grey) from Jolles and Lange (2021a).

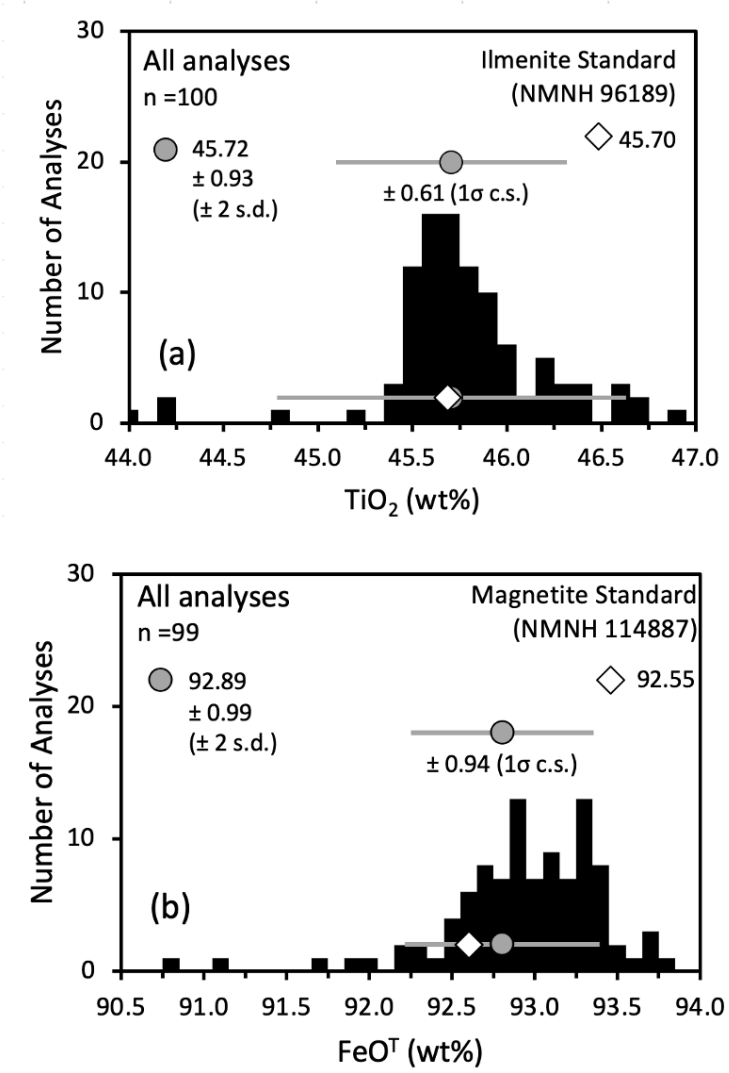

Figure 9: Histogram of all microprobe analyses of (a) wt% TiO_2 in the ilmenite standard (NMNH 96189) and (b) wt% FeO^T in the magnetite standard (NMNH 114887) when analyzed as unknowns. A total of 100 and 99 analyses were made on each standard, respectively. The reported wt% TiO_2 and wt% FeO^T in the ilmenite and magnetite standards are 45.70 and 92.55, respectively (Jarosewich et al., 1980), which are close to the averages (±2σ) of all analyses of 47.72 (±0.61) wt% TiO_2 and 92.89 (±0.99) wt% FeO^T, respectively. These averages match the reported values within the 1σ uncertainty based on microprobe counting statistics of ± 0.61 wt% TiO_2 and ± 0.94 wt% FeO^T.

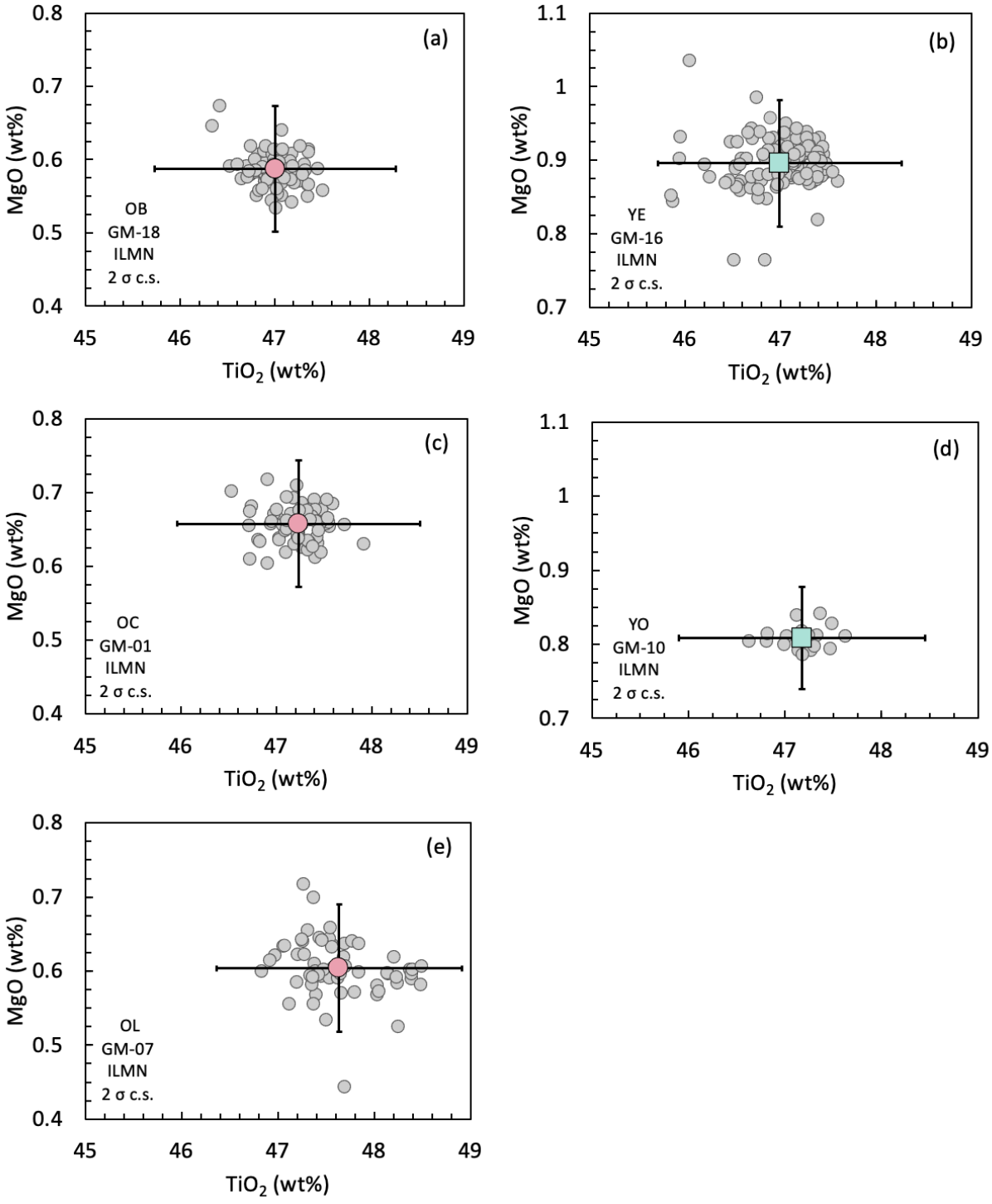

Figure 10: Plots of MgO (wt%) vs. TiO_2 (wt%) for all ilmenite analyses (grey) in each GM sample (OB, OC, OL, YE and YO)., with microprobe analyzed ilmenite. The average of these analyses is shown (pink for Older GM samples; green for Younger GM samples) with error bars that reflect the 2σ counting statistic uncertainty from the microprobe analyses.

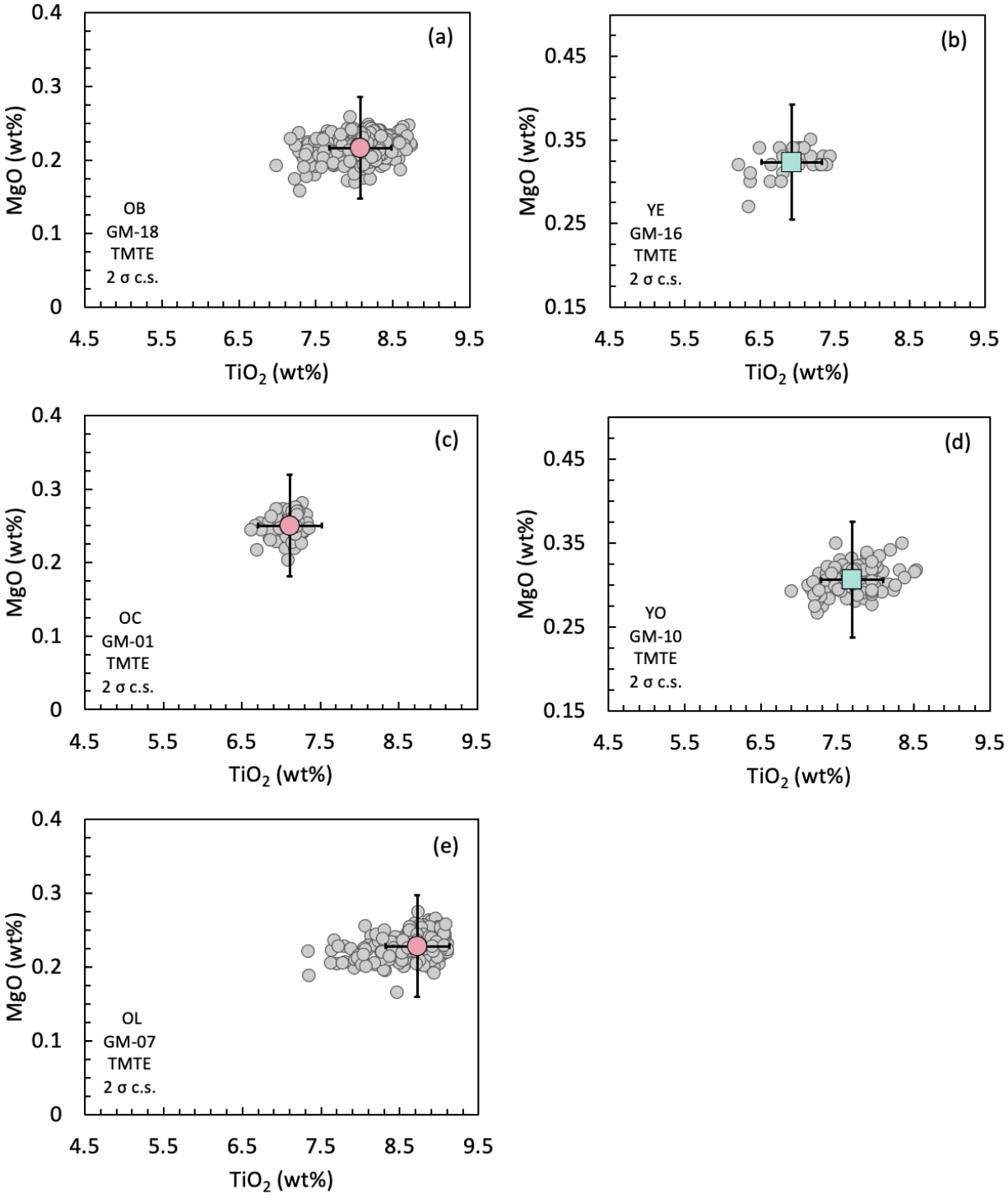

Figure 11: Plots of MgO (wt%) vs. TiO_2 (wt%) for all titanomagnetite analyses (grey) in each GM sample (OB, OC, OL, YE and YO). Symbols are the same as Figure 10.

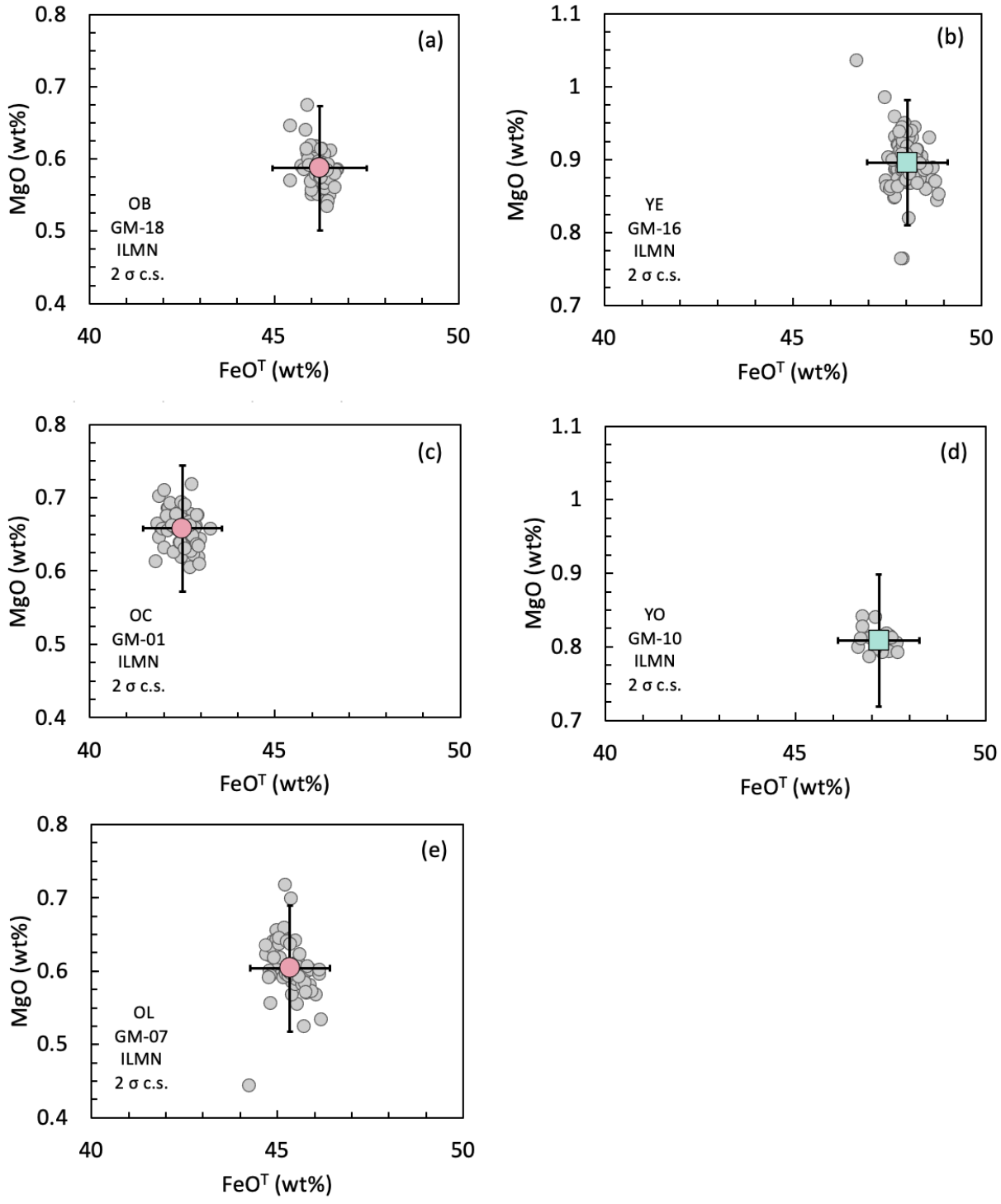

Figure 12: Plots of MgO (wt%) vs. FeO^T (wt%) for all ilmenite analyses (grey) in each GM sample (OB, OC, OL, YE and YO). Symbols are the same as Figure 10.

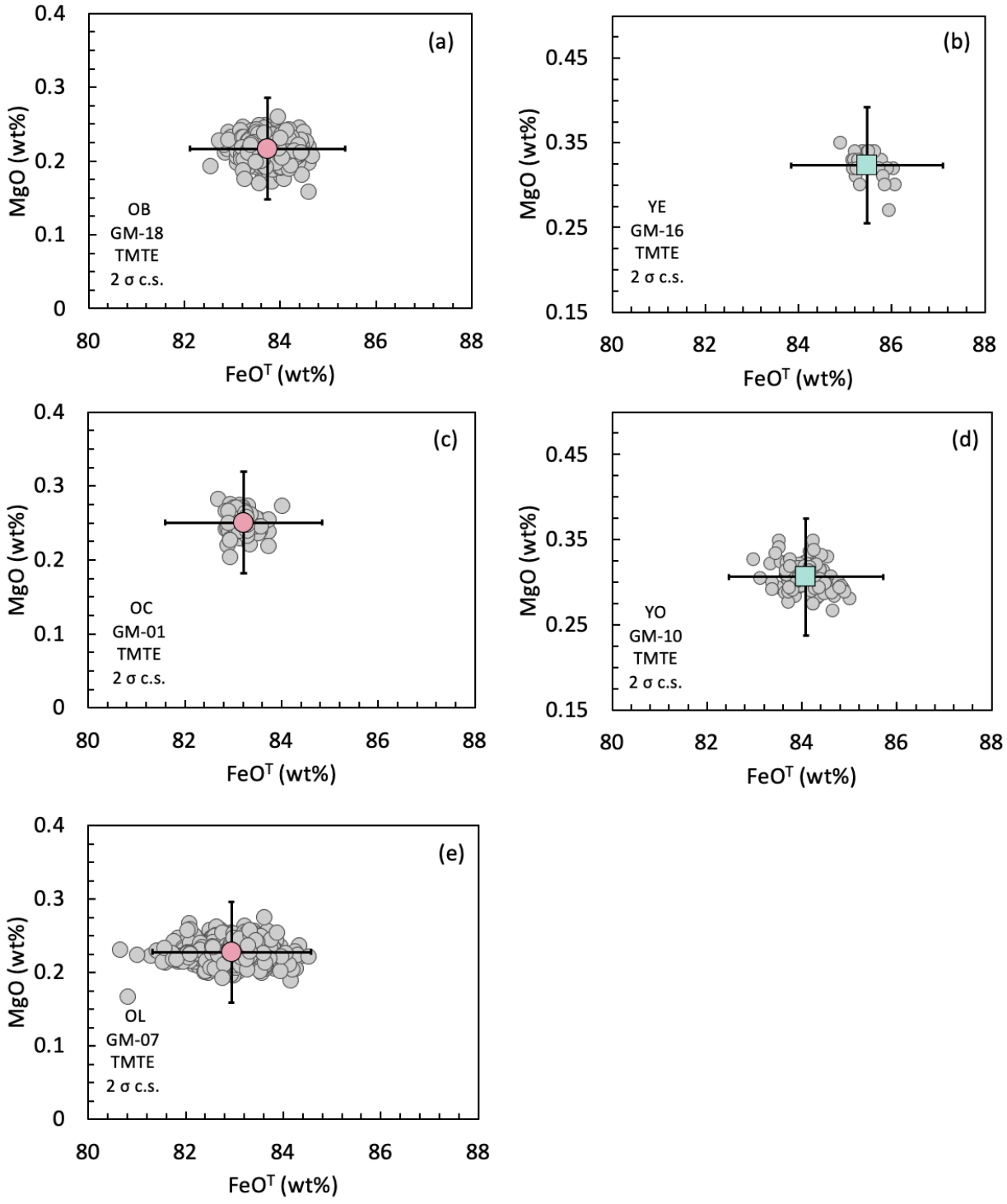

Figure 13: Plots of MgO (wt%) vs. FeO^T (wt%) for all titanomagnetite analyses (grey) in each GM sample (OB, OC, OL, YE and YO). Symbols are the same as Figure 10.

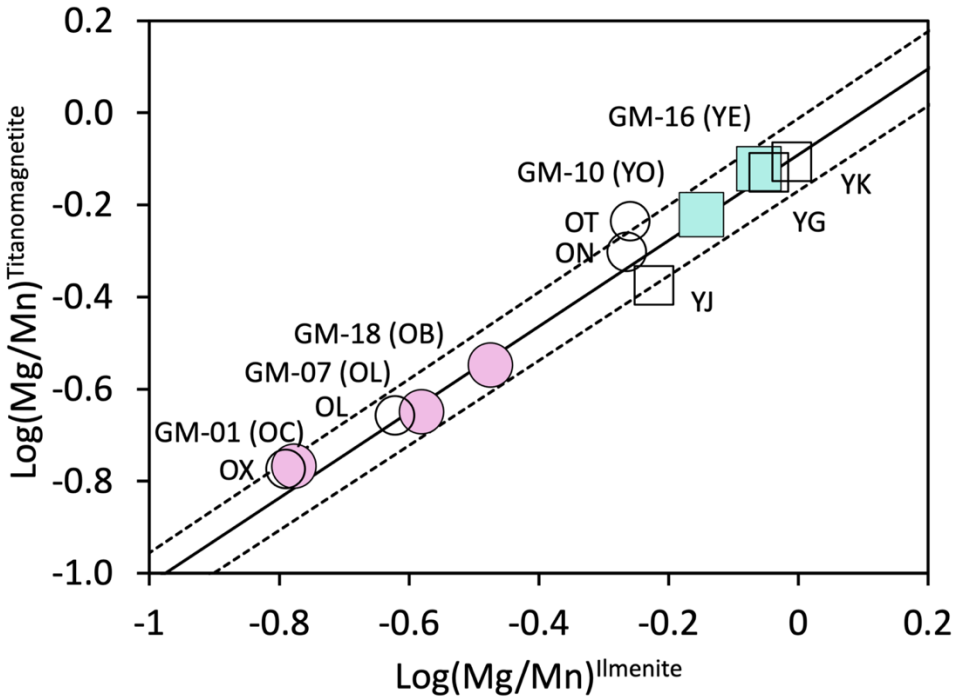

Figure 14: Plot of average $\log(Mg/Mn)^{titanomagnetite}$ versus $\log(Mg/Mn)^{ilmenite}$ obtained from Fe-Ti oxide analyses. Data from this study are shown in pink circles (Older GM) and green squares (Younger GM). Also shown are data from Metz and Mahood (1991) as open circles (Older GM) and open squares (Younger GM). The solid line is the Bacon and Hirshmann (1988) equilibrium relationship, and the dashed lines show the $\pm 2\sigma$ error envelope.

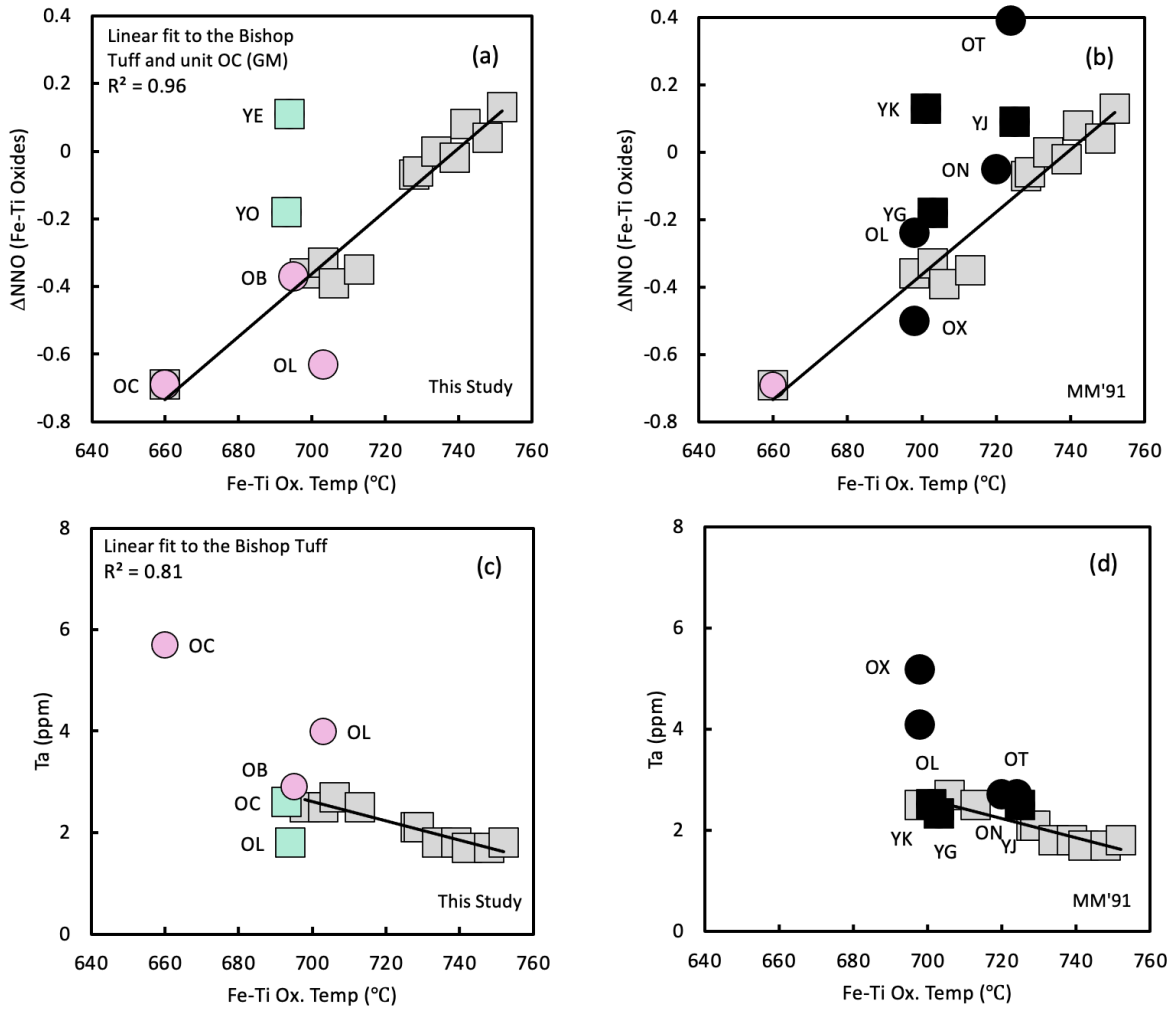

Figure 15: (a-b) Plots of ΔNNO vs. Fe-Ti oxide temperature (obtained from the Ghiorso and Evans, 2008, thermometer/oxybarometer) for the Glass Mountain samples from (a) this study (Older GM are pink circles; Younger GM are green squares) and (b) Metz and Mahood (1991) (Older GM are black circles; Younger GM are black squares). Also shown are results obtained for the high-SiO_2 rhyolite portion of the Bishop Tuff (grey) from Jolles and Lange (2019). The linear fit in (a) and (b) is to the data from the Bishop Tuff and sample OC (this study) only; these are the only samples shown that plausibly crystallized Fe-Ti oxide immediately after melt segregation from a parental mush and immediately prior to eruption. Note the strong linear correlation (R^2=.96) to those data, and the scatter about that line of most GM data (this study and Metz and Mahood, 1991). (c-d) Plots of Ta (ppm) vs Fe-Ti oxide temperature. Symbols the same as in (a-b). The linear fit in (c-d) is to the Bishop data only (R^2=0.91); the GM data (this study and Metz and Mahood, 1991) scatter around this line.

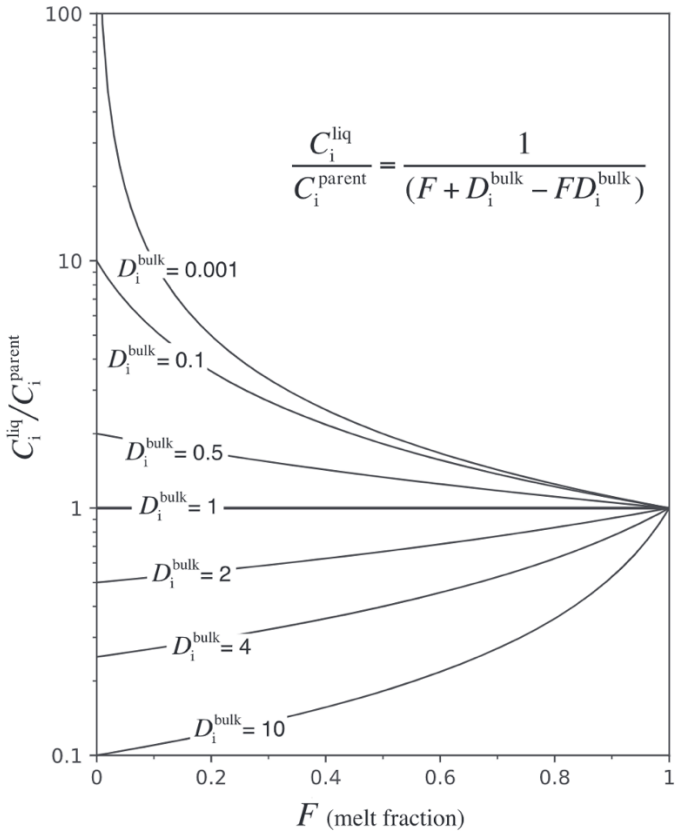

Figure 16: Equilibrium melting/crystallization diagram for different melt fractions (F) and bulk partition coefficients (D_i), following the equation shown. The concentration of an element in the liquid is (C_i^{liq}) and the concentration of an element in the parental source is (C_i^{parent}). For elements with bulk $D_i < 1$, their concentration in the liquid will decrease with increasing melt fraction, whereas for elements with bulk $Di > 1$, their concentration in the liquid will increase with increasing melt. For elements with bulk $D_i = 1$, concentrations will remain flat with melt fraction.

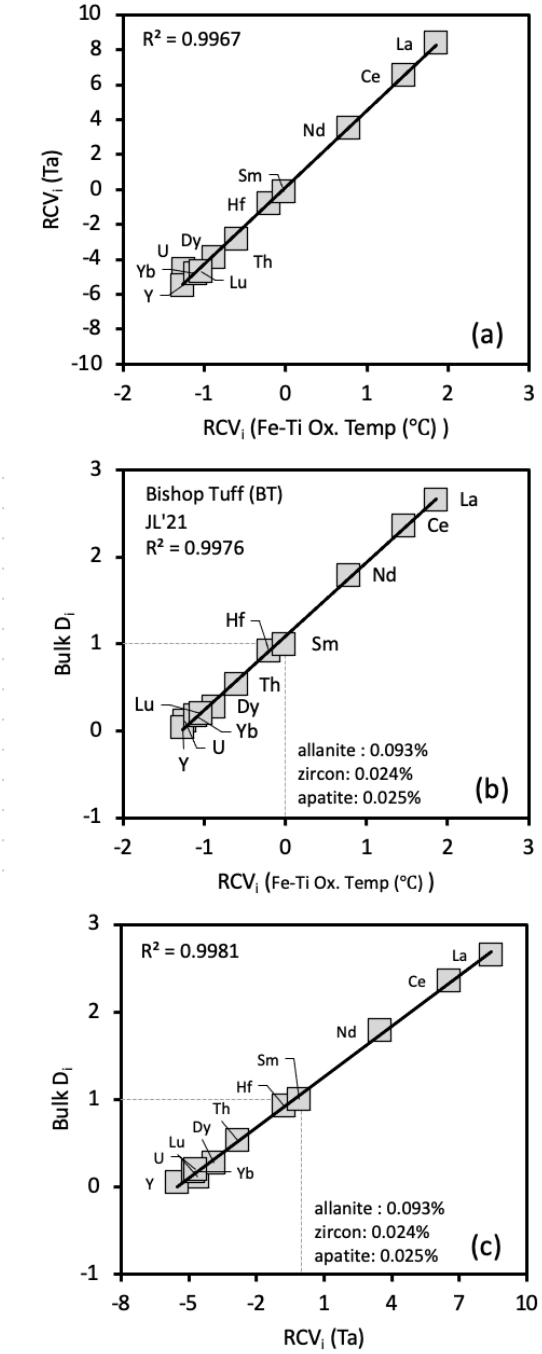

Figure 17: (a) Plot of Ta-RCV_i vs RCV_i derived from Fe-Ti oxide temperatures for the high-SiO_2 rhyolite portion of the Bishop Tuff from the data of Jolles and Lange (2021a). The two sets of RCV_i differ (Table 5) but are strongly correlated (R^2=0.9967). (b) Plot of bulk Di vs RCVi (based on Fe-Ti oxide temperatures) reported by Jolles and Lange (2021a) for the 11 elements controlled by allanite, zircon and apatite in the crystallizing/melting reaction in the parental mush, based on the reported abundances (0.93% allanite, 0.024% zircon, 0.025% apatite). (c) Same as (b), except the y-axis shows Ta-RCV_i values. The similarity of results between (c) and (b) shows that Ta-RCV_i values work equally well to constrain the stoichiometry of the crystallizing/melting reaction in the parental mush.

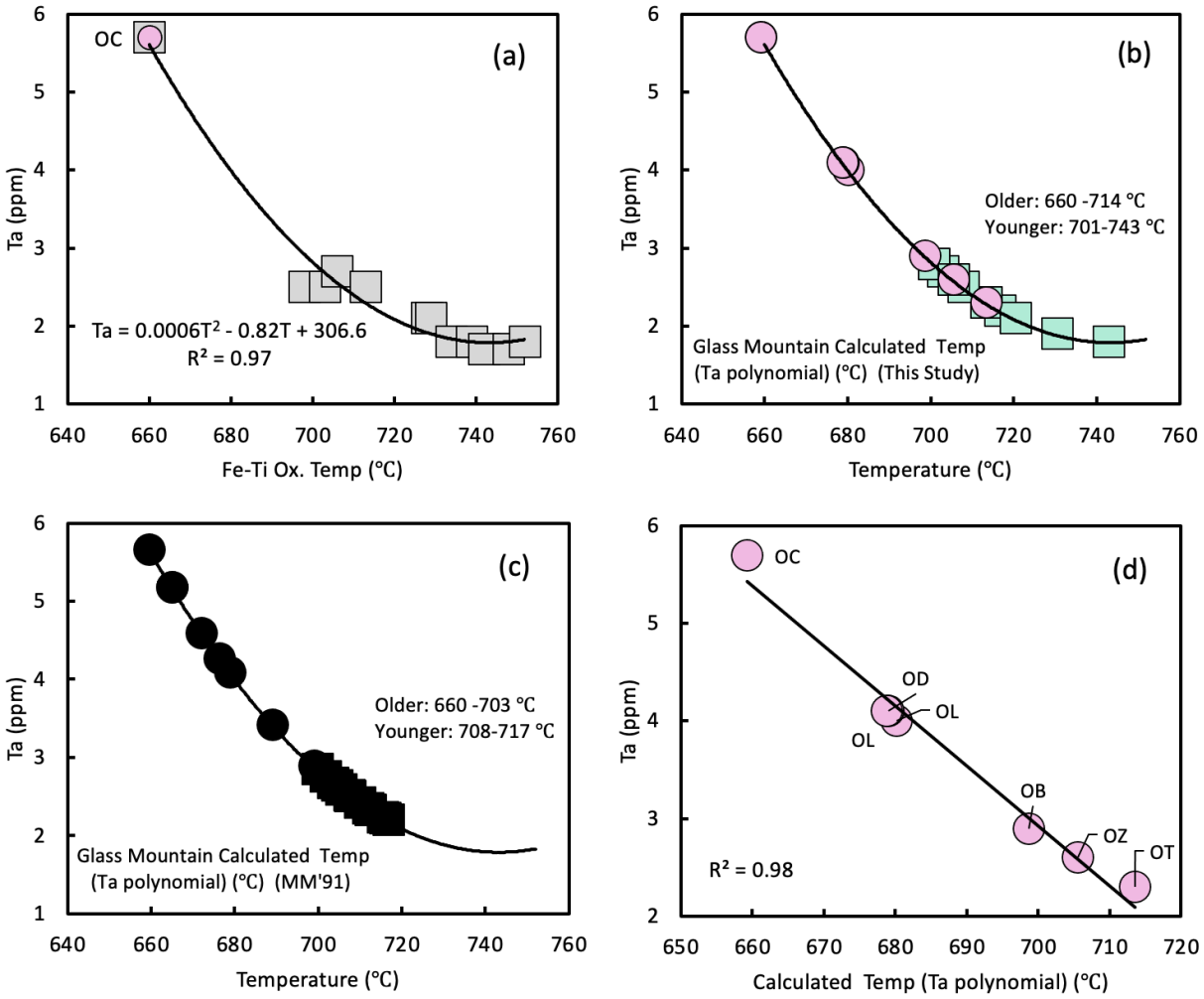

Figure 18: (a) Plot of Ta (ppm) versus Fe-Ti oxide temperature for the high-SiO_2 rhyolite portion of the Bishop Tuff (Jolles and Lange, 2021) together with that for Older GM unit OC, which has an eruption age indistinguishable from its isochron (i.e., differentiation) age. All samples shown in this plot plausibly crystallized Fe-Ti oxide immediately after melt segregation from a parental mush and immediately prior to eruption. A fitted polynomial to the curved data is shown. (b) The fitted polynomial from (a) with calculated position of Older (pink circles) and Younger (green squares) GM samples from this study. The results allow the temperature of the Older (660-714 °C) and Younger (701-743°C) GM samples at the time of melt segregation to be estimated. (c) Same as in (b) but data from Metz and Mahood (1991). (d) Ta (ppm) vs. calculated temperature from the Ta polynomial in (a) for the Older GM samples from this study only. For this subset of data, a strong linear relationship is found (R^2=0.98), which means that Ta can be used as a linear proxy of melt fraction (and temperature) in the construction of Ta-RCV_i values for the Older GM samples.

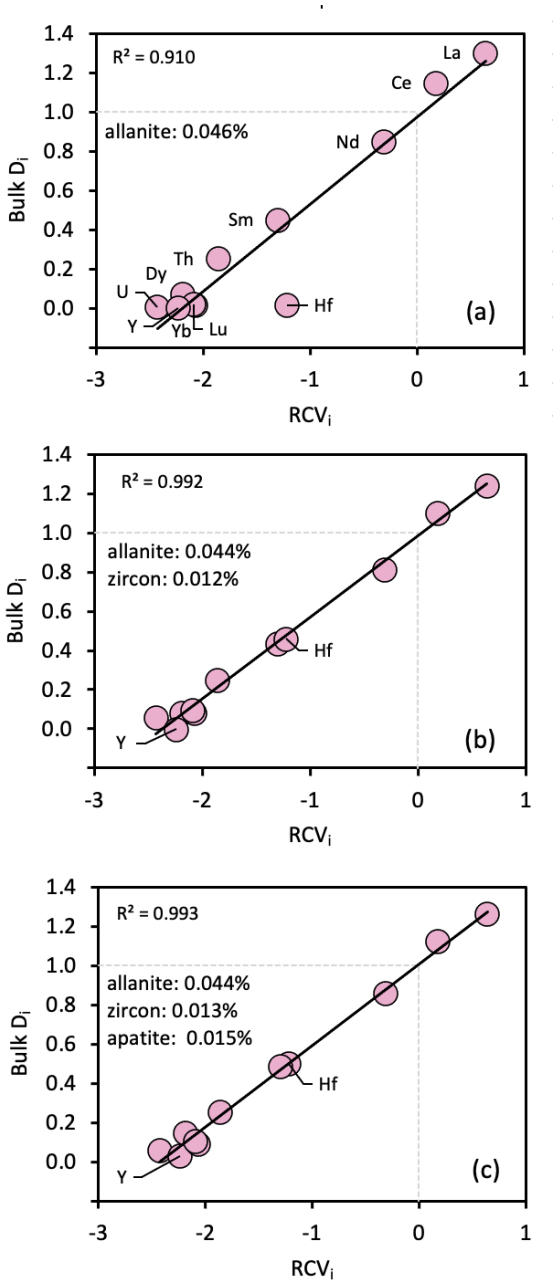

Figure 19: (a-c) Plot of bulk D_i calculated from Eq. 4 and literature partition coefficients (Table 4) vs Ta-RCV_i for each of 11 elements that depend only on proportion of allanite, zircon, and apatite in the crystallizing/melting reaction in the parental mush (see text). Data are from Older GM samples from this study only (pink circles). In all cases, phase abundances lead to predicted bulk D_i of ~1 when Ta-RCV_i is zero (dashed lines). (a) Linear correlation between bulk D_i and Ta-RCV_i for all elements, based only on allanite (see text). The main outlier is Hf, which strongly partitions into zircon. (b) Optimized abundance of both allanite (0.044%) and zircon (0.013%) that gives best fit (R^2=0.992) to trace-element line (see text). (c) Optimized abundance of all three accessory phases (0.044% allanite, 0.013% zircon, 0.012% apatite) that gives best fit (R^2=0.993) to trace-element line (see text).

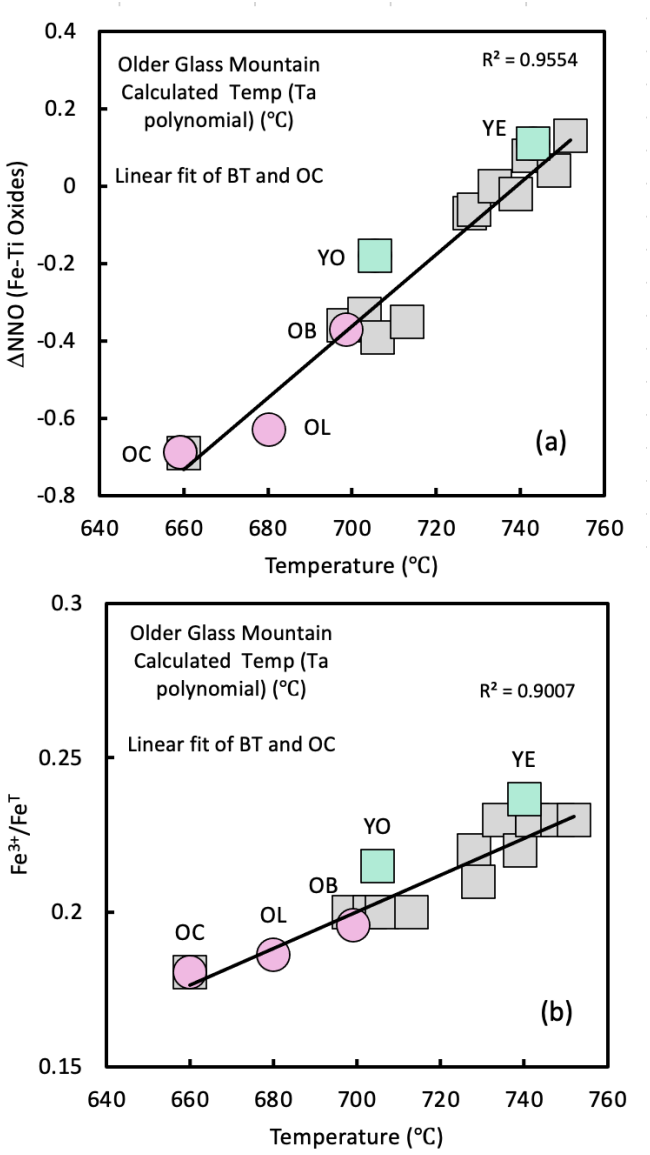

Figure 20: (a) Plot of ΔNNO vs. calculated temperature (for Older and Younger GM samples from this study) from Ta polynomial in Fig. 18a. The results from this study based on Ta-temperatures now plot together with data for the Bishop Tuff samples from Jolles and Lange (2019). (b) Calculated Fe^{3+}/Fe^{T} values (see text) vs calculated temperatures from Ta polynomial in Fig. 18a. The recalculated data from this study (Older and Younger GM samples) display the same linear relationship shown by the Bishop Tuff data.

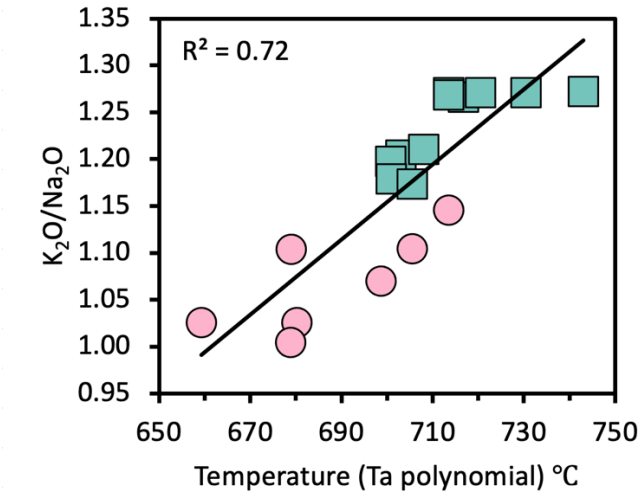

Figure 21: Plot of K_2O/Na_2O (wt%) of the Older (pink circles) and Younger (green squares) GM rhyolites from this study versus temperature calculated from the Ta-polynomial in Fig. 18a, which is a proxy for melt fraction during segregation from a parental mush. The trend of increasing K_2O/Na_2O with temperature (proxy for melt fraction) of the interstitial melt reflects migration of the eutectic toward the K-feldspar component in the Qz-Pl-Kfs ternary as a function of decreasing activity of H_2O (Holtz et al., 1992).

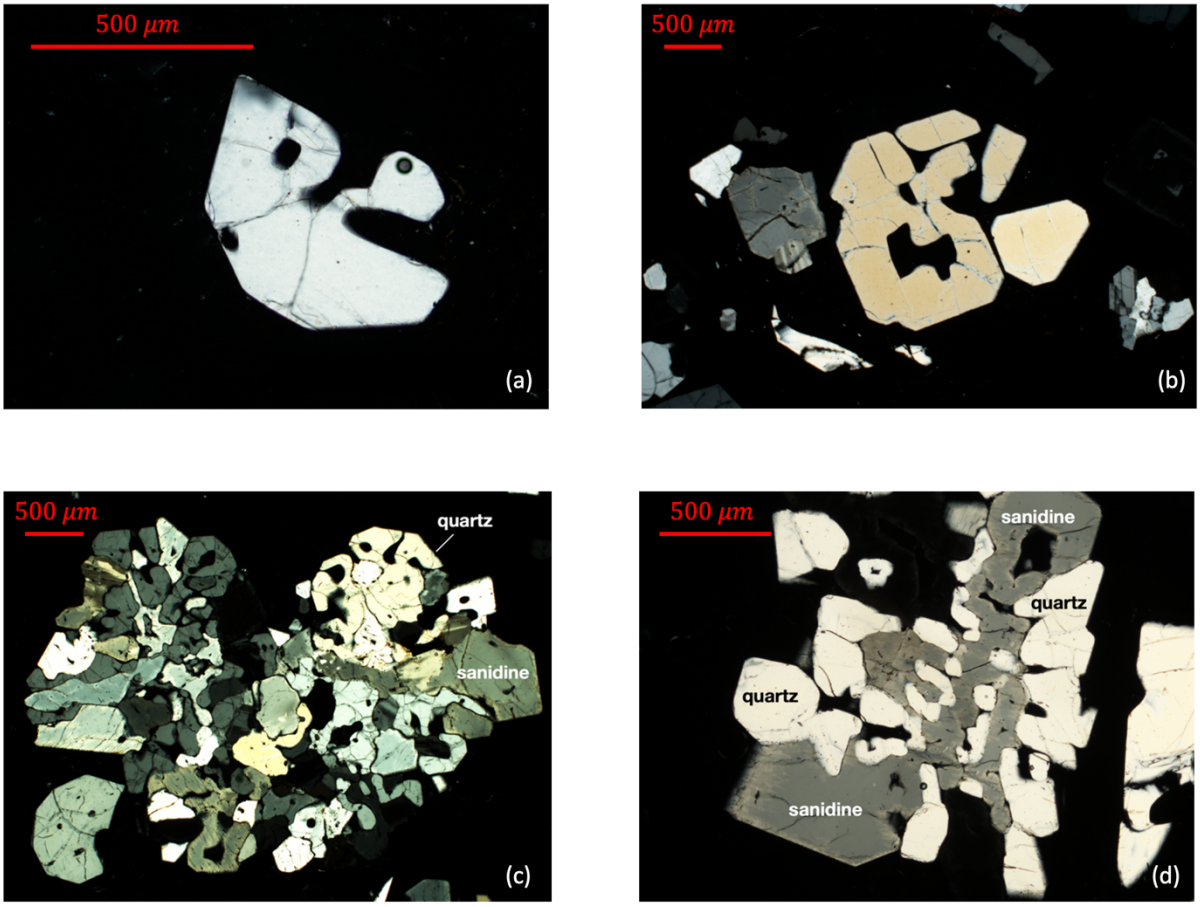

Figure 22: Photomicrographs of crystals in Older GM unit OD, including (a) quartz with diffusion-limited protuberances and growth embayment, (b) quartz with hopper texture, (c-d) granophyric intergrowths of quartz and sanidine; both phases display skeletal polyhedral textures consistent with rapid growth (e.g., Barbee et al., 2020).

Tables:

Table 1 Whole-rock major and minor element (wt%) concentrations for Younger and Older Glass Mountain samples

Sample	GM-18	GM-01	GM-JJ-10	GM-07	GM-11	GM-20	GM-08	GM-02	GM-03	GM-15a	GM-16
Eruptive Unit	OB	OC	OD	OL	OL	OT	OZ	YA	YB	YE	YE
Age (Ma)	1.74	2.00/2.05[1]	1.69/1.69[1]	1.87/1.93[1]	1.60					0.96	0.96
Lat. (N 37°)	.81381°	.80224°	.78450°	.76461°	.76500°	0.74133°	.71102°	.82868°	.82991°	.79483°	.79483°
Long. (W 118°)	.78604°	.79119°	.81683°	.68333°	.67694°	0.67166°	.68978°	.77610°	.74023°	.74294°	.74294°
SiO_2	77.87	76.99	77.45	76.94	76.99	77.75	77.07	77.17	76.94	77.98	77.62
TiO_2	0.06	0.07	0.05	0.06	0.06	0.07	0.07	0.08	0.08	0.08	0.08
Al_2O_3	12.37	12.92	12.73	13.04	12.83	12.48	12.83	12.60	12.80	12.18	12.48
$^{1}Fe_2O_3^T$	0.96	0.78	0.74	0.84	0.84	0.97	0.84	0.87	0.87	1.01	0.99
MnO	0.06	0.09	0.06	0.07	0.07	0.04	0.04	0.03	0.03	0.04	0.04
MgO	0.03	0.04	0.04	0.03	0.03	0.04	0.04	0.05	0.06	0.05	0.04
CaO	0.37	0.33	0.42	0.36	0.35	0.40	0.44	0.50	0.49	0.47	0.47
Na_2O	4.00	4.33	4.04	4.27	4.41	3.85	4.11	3.83	3.84	3.61	3.64
K_2O	4.28	4.44	4.46	4.38	4.43	4.41	4.54	4.85	4.88	4.58	4.63
P_2O_5	0.00	0.01	0.00	0.01	0.00	1.04	0.02	0.00	0.00	0.01	0.01
LOI	0.28	0.44	2.68	0.38	0.42	0.46	0.40	0.35	0.33	0.29	0.26
Total	99.2	99.8	99.2	98.7	99.6	100.6	98.6	99.5	100.2	99.1	99.4
$^{1}Fe^{3+}/Fe^T$	0.201	0.202	0.200	0.201	0.222	0.213	0.228	0.220	0.231	0.228	0.229
K_2O/Na_2O	1.07	1.03	1.10	1.03	1.00	1.15	1.10	1.27	1.27	1.27	1.27
^{3}Ta-Temp (°C)	699	660	679	680	679	714	706	717	714	743	714

Major element analyses normalized to 100%. LOI and original totals also shown.
K-Ar ages from Metz and Mahood (1985)
[1] $^{40}Ar/^{39}Ar$ ages from Davies et al. (1994)/Simon et al, (2014)
[2] Fe^{3+}/Fe^T calculated from Kress and Carmichael (1991) based on temperature and oxygen fugacity from two Fe-Ti oxides (see Table 3)
[3] Temperature determined from Ta polynomial in Fig. 18a

Table 1 (continued)

Sample	GM-12	GM-13	GM-04	GM-05	GM-06	GM-09	GM-10
Eruptive Unit	YG	YG	YO	YO	YO	YO	YO
Age (Ma)	0.90	0.90	1.06	1.06	1.06	1.06	1.06
Lat. (N 37°)	.79146°	.78945°	.79658°	.79232°	.77329°	.76460°	.76472°
Long. (W 118°)	.79421°	.79164°	.69234°	.68111°	.68336°	.69012°	.68970°
SiO_2	77.68	77.68	77.20	78.13	77.02	77.36	77.43
TiO_2	0.08	0.08	0.07	0.07	0.07	0.07	0.07
Al_2O_3	12.53	12.47	12.65	12.16	12.88	12.62	12.50
[1]$Fe_2O_3^T$	0.95	0.92	0.87	0.88	0.90	0.87	0.87
MnO	0.03	0.03	0.04	0.04	0.04	0.04	0.04
MgO	0.04	0.04	0.05	0.05	0.05	0.04	0.06
CaO	0.48	0.48	0.48	0.46	0.48	0.48	0.49
Na_2O	3.62	3.65	3.92	3.71	3.89	3.91	3.92
K_2O	4.60	4.64	4.72	4.49	4.66	4.61	4.60
P_2O_5	0.00	0.01	0.00	0.01	0.00	0.00	0.00
LOI	0.37	0.27	0.37	0.49	0.48	0.32	0.38
Total	99.1	100.7	98.7	99.8	98.5	98.5	99.9
[1]Fe^{3+}/Fe^T							0.22
K_2O/Na_2O	1.27	1.27	1.20	1.21	1.20	1.18	1.17
[3]Ta-Temp (°C)	731	721	703	708	701	701	706

Major element analyses normalized to 100%. LOI and original totals also shown.
K-Ar ages from Metz and Mahood (1985)
[1] $^{40}Ar/^{39}Ar$ ages from Davies et al. (1994)/Simon et al, (2014)
[2] Fe^{3+}/Fe^T calculated from Kress and Carmichael (1991) based on temperature and oxygen fugacity from two Fe-Ti oxides (see Table 3)
[3] Temperature determined from Ta polynomial in Fig. 18a

Table 2 Whole-rock trace element (ppm) concentrations for Older and Younger Glass Mountain

Sample	GM-18	GM-01	GM-JJ-10	GM-07	GM-11	GM-20	GM-08	GM-02	GM-03	GM-15a	GM-16
Eruptive Unit	OB	OC	OD	OL	OL	OT	OZ	YA	YB	YE	YE
Ba	3	3	12	3	2	<2	3	8	9	9	9
Sr	< 2	< 2	2	< 2	< 2	<2	< 2	4	4	3	3
Sr[1]	0.11	0.35	3.92	0.10	0.10			2.32		2.31	2.31
Rb	207	305	254	233	239	175	172	157	157	140	143
Rb[1]	207	308	232	245	245			159		158	158
Zr	79	85	77	83	84	84	76	75	78	72	75
Nb	25	41	36	30	32	20	19	14	15	15	15
Hf	3.3	4.6	4.1	4.1	4.0	3.2	3.2	3.1	3.0	2.7	2.8
Ta	2.9	5.7	4.1	4.0	4.1	2.3	2.6	2.2	2.3	2.3	1.8
Cs	6.1	10.6	8.3	7.5	7.5	5.0	4.9	4.5	4.5	4.5	4.6
Th	17.0	29.9	31.0	20.4	20.0	17.3	17.6	19.2	18.9	17.1	18.0
U	8.9	15.4	11.4	11.2	11.0	6.8	7.3	6.7	6.6	6.3	6.3
Mn	423	712	473	510	499	327	333	253	251	268	268
Y	24	40	33	29	29	20	19	20	19	20	20
La	18.2	18.7	15.8	18.4	18.3	22.6	22.0	32.6	32.5	24.3	30.8
Ce	46.8	50.9	40.4	50.7	49.9	53.2	53.0	67.5	67.8	49.8	60.9
Pr	5.98	6.49	5.40	6.29	6.24	6.10	6.15	7.04	7.10	5.61	6.57
Nd	20.9	23.6	20.3	22.7	21.8	20.9	21.6	22.5	23.4	18.6	21.7
Sm	5.3	6.8	6.1	5.9	5.9	4.4	4.5	4.1	4.3	4.0	4.1
Eu	< 0.05	< 0.05	<0.05	< 0.05	< 0.05	<0.05	< 0.05	< 0.05	< 0.05	0.06	< 0.05
Gd	4.2	6.5	5.8	5.2	5.3	3.4	3.7	3.4	3.4	3.0	3.1
Tb	0.7	1.2	1.0	0.9	0.9	0.6	0.6	0.6	0.6	0.5	0.5
Dy	4.3	7.1	6.2	5.2	5.4	3.6	3.5	3.5	3.4	3.1	3.2
Ho	0.8	1.4	1.1	1.0	1.0	0.7	0.7	0.7	0.7	0.6	0.6
Er	2.5	4.0	3.5	3.0	3.1	2.1	2.2	2.1	2.1	1.9	2.0
Tm	0.39	0.61	0.55	0.49	0.46	0.33	0.33	0.32	0.33	0.30	0.31
Yb	2.6	4.3	3.8	3.2	3.2	2.3	2.2	2.3	2.3	2.1	2.1
Lu	0.40	0.65	0.60	0.51	0.50	0.34	0.34	0.37	0.36	0.33	0.32

[1] Analyses from Halliday et al. (1989) on samples collected by Metz and Mahood (1991)

Table 2 (continued)

Sample	GM-12	GM-13	GM-04	GM-05	GM-06	GM-09	GM-10
Eruptive Unit	YG	YG	YO	YO	YO	YO	YO
Ba	10	9	4	8	4	4	4
Sr	4	4	2	3	2	2	3
Sr[1]	2.49	2.49	1.20	1.20	1.20	1.20	1.20
Rb	143	157	180	175	176	181	182
Rb[1]	162	162	182	182	182	182	182
Zr	72	78	75	85	71	76	77
Nb	14	17	18	21	17	19	19
Hf	2.7	2.9	3.2	3.4	3.0	3.4	3.2
Ta	1.9	2.1	2.7	2.5	2.8	2.8	2.6
Cs	4.6	5.0	5.2	4.7	5.4	5.4	5.3
Th	18.3	19.3	20.9	19.4	21.0	21.1	21.2
U	6.5	7.1	7.6	7.0	7.7	7.8	7.8
Mn	262	265	309	329	318	310	306
Y	19	20	23	24	23	23	22
La	28.9	27.3	24.8	23.8	25.0	23.5	25.0
Ce	57.6	55.5	56.5	54.2	57.8	54.4	57.1
Pr	6.13	6.18	6.56	5.98	6.55	6.22	6.63
Nd	20.8	20.7	21.8	20.9	22.8	21.7	22.4
Sm	4.0	4.3	4.7	4.3	4.8	4.8	5.0
Eu	< 0.05	0.06	< 0.05	< 0.05	< 0.05	< 0.05	< 0.05
Gd	3.0	3.4	4.1	3.8	4.0	4.1	4.0
Tb	0.5	0.6	0.7	0.7	0.7	0.7	0.7
Dy	3.3	3.5	4.1	3.9	4.4	4.2	4.2
Ho	0.7	0.7	0.8	0.8	0.9	0.9	0.8
Er	2.0	2.3	2.6	2.5	2.6	2.6	2.4
Tm	0.33	0.34	0.37	0.37	0.37	0.41	0.40
Yb	2.2	2.3	2.8	2.5	2.8	2.9	2.7
Lu	0.35	0.36	0.43	0.39	0.43	0.44	0.44

[1] Analyses from Halliday et al. (1989) on samples collected by Metz and Mahood (1991)

Table 3 Average composition (wt%) of titanomagnetite and ilmenite in younger and older Glass Mountain samples

Sample	GM-18	GM-01	GM-07	GM-16	GM-10
Eruptive Unit	OB	OC	OL	YE	YO
Study	This Study	This Study	This Study	This Study	This Study
TMTE, *N; n*	30;444	71;71	55;540	1;21	14;87
SiO_2	0.11	0.11	0.11	0.18	0.15
TiO_2	8.08	7.11	8.82	6.93	7.67
Al_2O_3	0.79	0.70	0.78	1.02	0.99
Fe_2O_3	52.14	55.32	50.78	54.13	52.51
V_2O_3	0.04	0.03	0.04	0.04	0.05
Cr_2O_3	0.00	0.00	0.00	0.00	0.00
FeO	36.82	33.41	37.05	36.66	36.84
MnO	1.37	2.69	1.81	0.77	0.91
MgO	0.22	0.25	0.23	0.33	0.31
CaO	0.00	0.00	0.00	0.00	0.00
Total	99.80	99.99	99.92	100.17	99.42
$\ln(X_{Mg}/X_{Mn})$	-0.55	-0.77	-0.65	-0.12	-0.22
ILMN, *N;n*	5;111	25;65	5;62	4;117	3;18
SiO_2	0.05	0.05	0.10	0.08	0.14
TiO_2	47.01	47.21	47.64	46.99	47.18
Al_2O_3	0.13	0.04	0.07	0.10	0.26
Fe_2O_3	10.40	12.35	9.72	11.47	10.99
V_2O_3	0.23	0.22	0.23	0.24	0.24
Cr_2O_3	0.00	0.00	0.00	0.00	0.00
FeO	36.97	31.35	36.63	37.76	37.31
MnO	3.09	6.95	4.08	1.82	2.01
MgO	0.59	0.66	0.61	0.90	0.81
CaO	0.03	0.00	0.02	0.01	0.03
Total	98.77	100.07	99.18	99.35	98.95
$\ln(X_{Mg}/X_{Mn})$	-0.47	-0.78	-0.58	-0.06	-0.15
Fe-Ti T (°C)[2]	698	660	703	690	695
Prop. Err. (°C)	±3	± 6	± 4	±9	± 10
ΔNNO[2]	-0.4	-0.7	-0.6	0.1	-0.2
[2]TiO_2 (rutile)	0.5	0.4	0.4	0.6	0.5

[1] MM'91 = (Metz and Mahood, 1991)
[2] Determined with two-oxide geothermometer/oxybarometer of Ghiorso and Evans (2008)

Table 3 (continued)

Sample	165	215	161	220	147	147	004
Eruptive Unit	OL	ON	OT	OX	[3]YG	YJ	YK
Study	[1]MM'91	[1]MM'91	[1]MM'91	[1]MM'91	[1]MM'91	[1]MM'91	[1]MM'91
TMTE, *N; n*							
SiO_2	0.20	0.27	0.28	0.12	0.15	0.10	0.13
TiO_2	7.67	8.06	7.02	7.90	7.52	7.98	7.25
Al_2O_3	0.91	0.99	1.02	0.77	1.07	0.94	1.08
Fe_2O_3	53.50	52.60	54.20	53.00	53.03	54.40	54.40
V_2O_3							
Cr_2O_3							
FeO	36.70	37.30	36.40	35.70	36.75	37.50	36.80
MnO	1.84	1.13	1.09	2.51	0.83	1.21	0.72
MgO	0.23	0.32	0.36	0.24	0.35	0.29	0.32
CaO							
Total	101.03	101.23	100.70	100.20	100.19	103.20	101.22
$\ln(X_{Mg}/X_{Mn})$	-0.66	-0.30	-0.24	-0.77	-0.13	-0.37	-0.11
ILMN, *N;n*							
SiO_2	0.09	0.11	0.02	0.06	0.02	0.02	0.06
TiO_2	47.00	47.30	45.90	47.10	47.18	47.20	47.00
Al_2O_3	0.05	0.09	0.06	0.05	0.04	0.06	0.04
Fe_2O_3	10.10	10.60	13.10	10.00	10.33	11.30	10.60
V_2O_3							
Cr_2O_3							
FeO	36.90	38.50	37.19	35.10	38.80	38.60	38.90
MnO	4.27	2.49	2.46	6.18	1.72	2.35	1.62
MgO	0.58	0.77	0.77	0.57	0.88	0.80	0.90
CaO							
Total	99.08	100.10	99.73	98.98	99.03	100.30	99.30
$\ln(X_{Mg}/X_{Mn})$	-0.62	-0.26	-0.26	-0.79	-0.05	-0.22	-0.01
Fe-Ti T (°C)[2]	698	720	724	698	703	725	701
Prop. Err. (°C)							
ΔNNO[2]	-0.2	0.0	0.4	-0.5	0.0	0.1	0.1
[2]TiO_2 (rutile)	0.5	0.5	0.6	0.4	0.6	0.6	0.6

[1] MM'91 = (Metz and Mahood, 1991)
[2] Determined with two-oxide geothermometer/oxybarometer of Ghiorso and Evans (2008)
[3] Averaged YG from MM'91

Table 4 Mineral-melt element partition coefficients; RCVi and bulk Di constraints for the Older Glass Mountain rhyolites

Element	Quartz	Plagioclase[1]	K-spar[1]	Biotite[2,3]	Titano-magnetite[2,3]	Ilmenite[2,3]	Allanite[2]	Zircon[2]	Apatite[2]	Ta-RCV$_i$	Bulk D$_i$
Ti				60.9	122	676	32.4			-0.1	
Fe^{3+}				32	282	56.9	20.5			1.1	
Mg				117	3.6	9.38	13.4			0.0	
Ca				0.12			18.8		83	0.6	
Fe^{2+}		5.99	0.264	32	65.1	64.5	21.5			0.7	
Ba		1.6	13	7							
Sr		6.1	3.5								
Rb		0.011	0.66	4.3						-8.0	
Hf				0.65		0.65	28	3742		-1.2	0.50
Th				0.511	1.63	0.427	548	91.2		-1.9	0.25
U				0.131		0.063	17	383		-2.4	0.06
Mn				11	27.7	60.3	15.3			-2.4	
Y									177	-2.2	0.03
La		0.3	0.048	3.4	11	1.31	2827	7.2	108	0.6	1.26
Ce		0.171	0.019	2.77	9.7	1.19	2494	10	163	0.2	1.12
Nd		0.075	0.005	2.2	6.9	0.96	1840	2.6	308	-0.3	0.86
Sm		0.043	0.008	1.28	3.77	0.684	977	11.1	351	-1.3	0.48
Eu		4.67	3	0.73	0.9	0.4	100	20			
Dy				0.5		0.37	150	108	438	-2.2	0.15
Yb				0.32		0.55	37	564		-2.1	0.09
Lu				0.39		0.74	44	648		-2.1	0.10

[1] Chamberlain et al. (2015) proportions based on P_{total} = 500 MPa and X_{H2O} = 0.5
[2] Mahood and Hildreth (1983)
[3] Jolles and Lange (2021a)

Table 5 RCV_i and Bulk D_i for select trace elements from the Bishop Tuff controlled by allanite, zircon, and apatite

Element	[1]RCV_i	[1]Bulk D_i	[2]Ta-RCV_i
Hf	-0.2	0.92	-0.78
Th	-0.6	0.53	-2.84
U	-1	0.11	-4.59
Y	-1.3	0.04	-5.5
La	1.9	2.66	8.41
Ce	1.5	2.36	6.56
Nd	0.8	1.79	3.49
Sm	0	1.00	-0.11
Dy	-0.9	0.27	-3.89
Yb	-1.1	0.17	-4.81
Lu	-1	0.20	-4.68

[1] Calculated in Jolles and Lange (2021a); Fe-Ti oxide temperature as proxy for melt fraction
[2] This study; Ta (ppm) used as a proxy for melt fraction

Supplementary Tables:

Table S1 Electron Microprobe Analyses - Conditions

Instrument

Cameca SX100, EMAL/University of Michigan

Phase	Intensity correction	Accelerating Voltage (kV)	Beam Current (nA)	Beam Size (µm)	Peak Counting Time (s)
Fe-Ti oxides	X-PHI	15	20	0	20

Standard	Elements Calibrated
Wollastonite	Si, Ca
Ilmenite (NMNH-Ilmen Mountains)	Ti
Gahnite, Harvard	Al, Zn
V2O5	V
Magnetite (NMNH-Minas Gerais, Brazil)	Fe
Geikelite	Mg
Rhodonite (Broken Hill)	Mn

Table S2 Ilmenite analyses

Sample	Eruptive Unit	Analysis	SiO_2	TiO_2	Al_2O_3	Fe_2O_3	V_2O_3	Cr_2O_3	FeO	MnO	MgO	CaO	Total	FeO^T
GM_18	OB	GM_18_2_ILMN_1_1	0.03	46.70	0.11	10.89	0.23	0.00	36.69	3.11	0.59	0.00	98.43	46.49
GM_18	OB	GM_18_2_ILMN_1_2	0.03	47.08	0.08	10.34	0.25	0.00	36.99	3.24	0.58	0.02	98.72	46.30
GM_18	OB	GM_18_2_ILMN_1_3	0.02	46.74	0.06	10.53	0.27	0.00	36.79	3.16	0.58	0.01	98.29	46.26
GM_18	OB	GM_18_2_ILMN_1_5	0.04	47.15	0.08	10.00	0.27	0.00	37.10	3.13	0.59	0.02	98.51	46.10
GM_18	OB	GM_18_2_ILMN_1_6	0.02	46.90	0.06	10.30	0.23	0.00	37.09	3.09	0.60	0.02	98.39	46.35
GM_18	OB	GM_18_2_ILMN_1_7	0.14	47.07	0.37	11.18	0.24	0.00	35.97	3.13	0.55	0.10	98.86	46.03
GM_18	OB	GM_18_2_ILMN_1_8	0.05	46.73	0.09	10.64	0.23	0.00	36.72	3.16	0.58	0.07	98.37	46.29
GM_18	OB	GM_18_2_ILMN_1_9	0.11	46.90	1.43	15.61	0.24	0.00	31.40	3.09	0.57	0.03	99.47	45.44
GM_18	OB	GM_18_2_ILMN_1_10	0.09	46.52	0.98	14.48	0.26	0.00	32.71	3.18	0.59	0.05	98.93	45.75
GM_18	OB	GM_18_2_ILMN_1_11	0.04	47.36	0.11	10.22	0.22	0.00	37.11	3.26	0.61	0.02	99.03	46.31
GM_18	OB	GM_18_2_ILMN_1_12	0.05	46.90	0.05	9.80	0.21	0.00	37.26	3.07	0.57	0.01	98.01	46.08
GM_18	OB	GM_18_2_ILMN_1_13	0.02	47.20	0.06	9.65	0.23	0.00	37.33	3.14	0.58	0.01	98.36	46.01
GM_18	OB	GM_18_2_ILMN_1_14	0.06	46.80	0.27	11.07	0.24	0.00	36.12	3.12	0.58	0.02	98.42	46.08
GM_18	OB	GM_18_2_ILMN_1_15	0.02	46.91	0.04	10.07	0.23	0.00	37.19	3.08	0.60	0.01	98.22	46.26
GM_18	OB	GM_18_2_ILMN_1_16	0.04	46.85	0.07	10.17	0.24	0.00	36.96	3.11	0.60	0.01	98.15	46.11
GM_18	OB	GM_18_2_ILMN_1_17	0.04	47.18	0.08	9.63	0.24	0.00	37.23	3.12	0.61	0.00	98.21	45.90
GM_18	OB	GM_18_2_ILMN_1_28	0.06	46.99	0.09	9.90	0.24	0.00	37.06	3.09	0.60	0.01	98.18	45.97
GM_18	OB	GM_18_2_ILMN_1_29	0.04	47.06	0.04	9.82	0.25	0.00	37.29	3.09	0.60	0.00	98.26	46.12
GM_18	OB	GM_18_2_ILMN_1_31	0.03	47.35	0.05	9.90	0.24	0.00	37.50	3.15	0.57	0.01	98.86	46.41
GM_18	OB	GM_18_2_ILMN_1_32	0.04	47.17	0.05	9.78	0.23	0.00	37.30	3.20	0.60	0.01	98.45	46.11
GM_18	OB	GM_18_2_ILMN_1_36	0.07	46.42	0.38	11.90	0.23	0.00	35.19	3.13	0.67	0.01	98.11	45.90
GM_18	OB	GM_18_2_ILMN_1_37	0.10	46.83	0.08	10.22	0.23	0.00	36.98	3.11	0.61	0.00	98.26	46.18
GM_18	OB	GM_18_2_ILMN_1_40	0.06	46.90	0.05	10.07	0.21	0.00	37.23	3.12	0.58	0.01	98.29	46.29
GM_18	OB	GM_18_2_ILMN_1_41	0.06	46.96	0.11	10.53	0.26	0.00	36.86	3.10	0.61	0.02	98.58	46.34
GM_18	OB	GM_18_2_ILMN_1_42	0.05	47.17	0.07	9.95	0.22	0.00	37.23	3.13	0.60	0.05	98.55	46.18
GM_18	OB	GM_18_2_ILMN_1_43	0.05	46.88	0.05	10.30	0.22	0.00	37.03	3.08	0.58	0.14	98.38	46.30
GM_18	OB	GM_18_2_ILMN_1_44	0.10	46.65	0.06	10.46	0.23	0.00	36.85	3.13	0.57	0.11	98.20	46.26
GM_18	OB	GM_18_2_ILMN_1_45	0.07	47.01	0.12	10.49	0.22	0.00	37.05	3.08	0.58	0.02	98.70	46.49
GM_18	OB	GM_18_2_ILMN_1_46	0.02	46.91	0.12	10.39	0.25	0.00	36.74	3.11	0.60	0.03	98.24	46.09
GM_18	OB	GM_18_2_ILMN_1_47	0.04	47.36	0.04	9.71	0.25	0.00	37.43	3.18	0.61	0.03	98.76	46.17
GM_18	OB	GM_18_2_ILMN_1_48	0.02	47.27	0.06	9.92	0.27	0.00	37.19	3.15	0.62	0.02	98.60	46.12
GM_18	OB	GM_18_2_ILMN_1_49	0.05	47.06	0.06	10.13	0.25	0.00	37.15	3.16	0.59	0.00	98.56	46.27
GM_18	OB	GM_18_2_ILMN_1_50	0.05	47.03	0.04	9.95	0.24	0.00	37.25	3.21	0.55	0.00	98.29	46.20

Table S2 (continued)

Sample	Eruptive Unit	Analysis	SiO_2	TiO_2	Al_2O_3	Fe_2O_3	V_2O_3	Cr_2O_3	FeO	MnO	MgO	CaO	Total	FeO^T
GM_18	OB	GM_18_2_ILMN _2_3	0.15	46.94	0.06	9.90	0.23	0.00	37.35	3.03	0.58	0.01	98.34	46.25
GM_18	OB	GM_18_2_ILMN _2_7	0.15	46.79	0.06	10.24	0.25	0.00	37.09	3.08	0.60	0.01	98.35	46.31
GM_18	OB	GM_18_2_ILMN _2_8	0.11	47.07	0.03	9.74	0.24	0.00	37.44	3.06	0.61	0.00	98.37	46.20
GM_18	OB	GM_18_2_ILMN _2_9	0.13	47.02	0.07	9.90	0.23	0.00	37.34	3.06	0.61	0.01	98.46	46.25
GM_18	OB	GM_18_2_ILMN _2_10	0.14	46.89	0.08	10.52	0.23	0.00	37.07	3.13	0.61	0.01	98.80	46.54
GM_18	OB	GM_18_2_ILMN _2_12	0.13	46.81	0.06	9.97	0.24	0.00	37.21	3.07	0.55	0.02	98.17	46.19
GM_18	OB	GM_18_2_ILMN _2_15	0.14	46.97	0.04	9.96	0.22	0.00	37.48	3.11	0.54	0.00	98.54	46.44
GM_18	OB	GM_18_2_ILMN _2_16	0.13	47.08	0.05	9.91	0.25	0.00	37.41	3.07	0.57	0.03	98.55	46.33
GM_18	OB	GM_18_2_ILMN _2_17	0.11	47.28	0.06	9.27	0.22	0.00	37.63	3.06	0.59	0.01	98.25	45.97
GM_18	OB	GM_18_2_ILMN _2_18	0.17	46.80	0.06	10.06	0.27	0.00	37.13	3.06	0.59	0.01	98.16	46.19
GM_18	OB	GM_18_2_ILMN _2_19	0.14	46.83	0.06	9.83	0.25	0.00	37.19	3.09	0.56	0.01	98.03	46.03
GM_18	OB	GM_18_2_ILMN _2_20	0.12	47.23	0.05	9.88	0.24	0.00	37.51	3.12	0.58	0.01	98.76	46.40
GM_18	OB	GM_18_2_ILMN _2_21	0.19	46.98	0.06	10.07	0.25	0.00	37.30	3.07	0.61	0.00	98.59	46.36
GM_18	OB	GM_18_2_ILMN _2_23	0.15	46.61	0.06	10.51	0.23	0.00	36.98	3.10	0.59	0.01	98.36	46.44
GM_18	OB	GM_18_2_ILMN _2_24	0.19	47.25	0.04	9.29	0.20	0.00	37.89	3.02	0.57	0.01	98.56	46.25
GM_18	OB	GM_18_2_ILMN _2_25	0.19	47.03	0.06	9.68	0.20	0.00	37.48	3.08	0.61	0.00	98.34	46.18
GM_18	OB	GM_18_2_ILMN _2_26	0.15	46.92	0.06	9.63	0.23	0.00	37.34	3.06	0.57	0.00	98.03	46.01
GM_18	OB	GM_18_2_ILMN _2_31	0.18	47.23	0.05	9.11	0.23	0.00	37.61	3.13	0.58	0.01	98.21	45.81
GM_18	OB	GM_18_2_ILMN _2_33	0.13	46.94	0.05	9.78	0.22	0.00	37.34	3.11	0.58	0.00	98.20	46.14
GM_18	OB	GM_18_2_ILMN _2_34	0.15	46.87	0.07	10.24	0.25	0.00	37.18	3.05	0.59	0.00	98.48	46.39
GM_18	OB	GM_18_3_ILMN_3_1	0.06	46.34	0.76	13.30	0.24	0.00	33.47	3.21	0.65	0.02	98.10	45.44
GM_18	OB	GM_18_3_ILMN_4_1	0.02	47.51	0.05	9.70	0.23	0.00	37.83	3.03	0.56	0.02	99.02	46.56
GM_18	OB	GM_18_3_ILMN_4_2	0.03	47.35	0.05	9.60	0.18	0.00	37.88	3.01	0.55	0.00	98.69	46.51
GM_18	OB	GM_18_3_ILMN_4_3	0.03	47.18	0.04	9.49	0.14	0.00	37.93	2.98	0.54	0.01	98.36	46.47
GM_18	OB	GM_18_3_ILMN_4_4	0.04	47.02	0.04	9.39	0.09	0.00	37.98	2.96	0.53	0.03	98.04	46.43
GM_18	OB	GM_18_3_ILMN_5_5	0.12	46.99	0.06	10.00	0.27	0.00	36.92	3.27	0.60	0.05	98.39	45.92
GM_18	OB	GM_18_3_ILMN_5_8	0.15	47.05	0.09	10.23	0.27	0.00	36.99	3.22	0.60	0.01	98.67	46.20
GM_18	OB	GM_18_3_ILMN_5_10	0.14	46.75	0.07	10.26	0.25	0.00	36.89	3.15	0.62	0.01	98.19	46.12
GM_18	OB	GM_18_3_ILMN_5_13	0.16	46.91	0.07	10.05	0.25	0.00	36.95	3.27	0.62	0.01	98.33	46.00
GM_18	OB	GM_18_3_ILMN_5_25	0.17	47.08	0.08	9.88	0.24	0.00	36.97	3.28	0.64	0.08	98.43	45.86
GM_18	OB	GM_18_3_ILMN_5_26	0.17	46.99	0.07	9.81	0.22	0.00	37.06	3.29	0.61	0.05	98.39	45.89
GM_18	OB	GM_18_3_ILMN_6_1	0.06	47.19	0.05	10.04	0.19	0.00	37.64	3.03	0.58	0.01	98.86	46.67
GM_18	OB	GM_18_3_ILMN_6_2	0.04	47.08	0.05	9.83	0.20	0.00	37.43	3.03	0.61	0.00	98.33	46.28

Table S2 (continued)

Sample	Eruptive Unit	Analysis	SiO_2	TiO_2	Al_2O_3	Fe_2O_3	V_2O_3	Cr_2O_3	FeO	MnO	MgO	CaO	Total	FeO^T
GM_18	OB	GM_18_3_ILMN_6_3	0.03	47.31	0.06	9.74	0.23	0.00	37.58	3.00	0.59	0.00	98.65	46.34
GM_18	OB	GM_18_3_ILMN_6_4	0.03	46.71	0.04	10.24	0.18	0.00	37.29	2.98	0.58	0.01	98.18	46.50
GM_18	OB	GM_18_3_ILMN_6_5	0.05	47.46	0.05	9.67	0.21	0.00	37.79	3.06	0.59	0.01	99.00	46.50
GM_18	OB	GM_18_3_ILMN_6_6	0.03	47.21	0.04	9.76	0.19	0.00	37.66	3.06	0.57	0.00	98.58	46.45
GM_18	OB	GM_18_3_ILMN_6_8	0.07	47.03	0.05	9.79	0.20	0.00	37.55	3.04	0.56	0.02	98.35	46.36
GM_18	OB	GM_18_3_ILMN_6_9	0.04	47.36	0.05	9.58	0.21	0.00	37.76	3.00	0.57	0.01	98.65	46.38
GM_18	OB	GM_18_3_ILMN_6_10	0.03	46.92	0.04	10.27	0.22	0.00	37.26	3.11	0.57	0.00	98.53	46.50
GM_18	OB	GM_18_3_ILMN_6_11	0.04	47.18	0.04	9.51	0.20	0.00	37.70	3.00	0.57	0.01	98.29	46.25
GM_18	OB	GM_18_3_ILMN_6_12	0.03	47.33	0.05	10.00	0.22	0.00	37.71	2.98	0.59	0.01	98.96	46.71
GM_18	OB	GM_18_3_ILMN_6_13	0.14	47.19	0.12	9.68	0.23	0.00	37.25	3.10	0.59	0.00	98.36	45.95
GM_18	OB	GM_18_3_ILMN_6_14	0.06	46.87	0.04	10.26	0.19	0.00	37.42	3.07	0.56	0.00	98.55	46.65
GM_18	OB	GM_18_3_ILMN_6_16	0.02	46.80	0.06	10.53	0.19	0.00	37.21	3.04	0.58	0.01	98.52	46.69
GM_18	OB	GM_18_3_ILMN_6_17	0.13	47.10	0.05	9.59	0.21	0.00	37.64	2.99	0.57	0.01	98.38	46.27
GM_18	OB	GM_18_3_ILMN_6_18	0.04	46.98	0.06	10.24	0.24	0.00	37.24	3.03	0.59	0.01	98.49	46.46
GM_18	OB	GM_18_3_ILMN_6_19	0.04	47.30	0.05	10.07	0.21	0.00	37.59	3.10	0.58	0.00	99.02	46.65
GM_18	OB	GM_18_3_ILMN_6_20	0.06	46.73	0.05	10.39	0.24	0.00	37.10	3.00	0.58	0.01	98.23	46.45
GM_01	OC	GM-01 Ilmn 1-3	0.08	47.02	0.04	10.13	0.20	0.00	32.99	7.35	0.66	0.00	99.67	42.10
GM_01	OC	GM-01 Ilmn 2-1	0.07	47.56	0.02	9.46	0.22	0.00	33.44	7.41	0.65	0.00	99.85	41.95
GM_01	OC	GM-01 Ilmn 2-2	0.06	47.41	0.02	9.18	0.21	0.00	33.53	7.30	0.61	0.00	99.50	41.79
GM_01	OC	GM-01 Ilmn 2-3	0.04	47.24	0.04	9.77	0.19	0.00	33.08	7.50	0.65	0.00	99.66	41.87
GM_01	OC	GM-01 Ilmn 2-4	0.10	47.43	0.03	9.55	0.22	0.00	33.42	7.40	0.63	0.00	99.85	42.01
GM_01	OC	GM-01 Ilmn 2-5	0.04	47.34	0.08	9.88	0.22	0.00	32.94	7.40	0.66	0.00	99.61	41.83
GM_01	OC	GM-01 Ilmn 3-1	0.04	47.10	0.04	9.76	0.21	0.00	33.70	6.73	0.62	0.00	99.62	42.48
GM_01	OC	GM-01 Ilmn 3-2	0.01	47.03	0.06	9.90	0.17	0.00	33.72	6.61	0.64	0.00	99.50	42.63
GM_01	OC	GM-01 Ilmn 3-3	0.03	47.24	0.07	10.37	0.20	0.00	33.59	6.80	0.68	0.00	100.29	42.92
GM_01	OC	GM-01 Ilmn 3-4	0.02	47.32	0.05	10.17	0.23	0.00	33.70	6.75	0.66	0.00	100.11	42.84
GM_01	OC	GM-01 Ilmn 3-5	0.04	46.91	0.04	10.06	0.19	0.00	33.67	6.70	0.60	0.00	99.52	42.72
GM_01	OC	GM-01 Ilmn 4-1	0.03	47.43	0.03	9.85	0.24	0.00	33.96	6.67	0.64	0.00	99.93	42.82
GM_01	OC	GM-01 Ilmn 4-2	0.02	47.72	0.04	9.64	0.23	0.00	34.04	6.83	0.66	0.00	100.42	42.72
GM_01	OC	GM-01 Ilmn 4-3	0.04	47.03	0.12	10.88	0.25	0.00	33.16	6.75	0.64	0.00	100.04	42.95
GM_01	OC	GM-01 Ilmn 4-4	0.05	47.09	0.05	10.33	0.24	0.00	33.47	6.80	0.65	0.00	99.87	42.77
GM_01	OC	GM-01 Ilmn 4-5	0.02	47.27	0.04	10.64	0.23	0.00	33.69	6.75	0.66	0.00	100.40	43.27
GM_01	OC	GM-01 Ilmn 4-6	0.04	47.47	0.04	9.81	0.20	0.00	34.12	6.69	0.62	0.00	100.18	42.95

Table S2 (continued)

Sample	Eruptive Unit	Analysis	SiO_2	TiO_2	Al_2O_3	Fe_2O_3	V_2O_3	Cr_2O_3	FeO	MnO	MgO	CaO	Total	FeO^T
GM_01	OC	GM-01 Ilmn 5-1	0.07	47.27	0.02	9.78	0.24	0.00	33.47	7.12	0.63	0.00	99.75	42.27
GM_01	OC	GM-01 Ilmn 5-2	0.07	47.23	0.02	10.02	0.22	0.00	33.46	7.14	0.64	0.00	99.98	42.48
GM_01	OC	GM-01 Ilmn 6-1	0.05	47.48	0.04	9.69	0.21	0.00	33.49	7.21	0.68	0.00	99.93	42.21
GM_01	OC	GM-01 Ilmn 7-1	0.07	47.52	0.03	9.38	0.22	0.00	33.53	7.25	0.66	0.00	99.81	41.97
GM_01	OC	GM-01 Ilmn 7-2	0.02	47.59	0.03	9.67	0.24	0.00	33.41	7.28	0.69	0.00	100.09	42.11
GM_01	OC	GM-01 Ilmn 8-1	0.08	46.91	0.03	11.01	0.24	0.00	32.85	7.23	0.72	0.00	100.41	42.75
GM_01	OC	GM-01 Ilmn 9-1	0.09	46.53	0.04	9.97	0.20	0.00	32.92	6.97	0.70	0.00	98.55	41.89
GM_01	OC	GM-01 Ilmn 9-2	0.09	47.21	0.05	9.60	0.22	0.00	33.38	6.98	0.71	0.00	99.35	42.02
GM_01	OC	GM-01 Ilmn 9-3	0.07	46.74	0.05	10.15	0.18	0.00	33.07	7.01	0.68	0.00	99.03	42.21
GM_01	OC	GM-01 Ilmn 10-1	0.13	47.40	0.03	9.78	0.24	0.00	33.63	7.05	0.69	0.00	100.15	42.43
GM_01	OC	GM-01 Ilmn 10 -2	0.11	47.28	0.05	9.77	0.21	0.00	33.60	6.91	0.68	0.00	99.74	42.39
GM_01	OC	GM-01 Ilmn 10-3	0.09	47.38	0.05	9.81	0.23	0.00	33.62	6.96	0.67	0.00	99.84	42.45
GM_01	OC	GM-01 Ilmn 11-1	0.09	47.30	0.06	9.75	0.24	0.00	33.59	6.85	0.66	0.00	99.74	42.37
GM_01	OC	GM-01 Ilmn 11-2	0.09	47.26	0.03	9.42	0.22	0.00	33.65	6.88	0.69	0.00	99.38	42.13
GM_01	OC	GM-01 Ilmn 11-3	0.14	46.98	0.15	10.20	0.25	0.00	33.04	6.75	0.67	0.00	99.41	42.22
GM_01	OC	GM-01 Ilmn 11-4	0.06	47.14	0.05	9.94	0.22	0.00	33.49	6.88	0.66	0.00	99.70	42.43
GM_01	OC	GM-01 Ilmn 12-1	0.09	46.71	0.05	10.09	0.23	0.00	33.05	6.95	0.66	0.00	99.29	42.12
GM_01	OC	GM-01 Ilmn 12-2	0.15	46.72	0.05	9.91	0.23	0.00	33.17	6.90	0.67	0.00	99.53	42.08
GM_01	OC	GM-01 Ilmn 12-3	0.07	47.34	0.04	9.97	0.23	0.00	33.59	6.95	0.68	0.00	100.12	42.57
GM_01	OC	GM-01 Ilmn 13-1	0.13	46.95	0.02	10.12	0.23	0.00	33.24	7.12	0.66	0.00	99.71	42.34
GM_01	OC	GM-01 Ilmn 13-2	0.16	47.18	0.04	9.55	0.21	0.00	33.58	6.94	0.69	0.00	99.63	42.17
GM_01	OC	GM-01 Ilmn 13-3	0.14	47.11	0.05	10.11	0.20	0.00	33.38	7.06	0.69	0.00	100.01	42.49
GM_01	OC	GM-01 Ilmn 14-1	0.02	47.35	0.05	10.09	0.21	0.00	33.66	6.82	0.68	0.00	100.15	42.74
GM_01	OC	GM-01 Ilmn 14-2	0.04	47.07	0.06	10.14	0.20	0.00	33.42	6.88	0.66	0.00	99.71	42.54
GM_01	OC	GM-01 Ilmn 14-3	0.02	47.11	0.03	10.34	0.22	0.00	33.53	6.87	0.65	0.00	100.08	42.84
GM_01	OC	GM-01 Ilmn 15-1	0.00	47.32	0.04	10.20	0.24	0.00	33.45	6.99	0.67	0.00	100.16	42.62
GM_01	OC	GM-01 Ilmn 15-2	0.01	47.41	0.06	10.16	0.20	0.00	33.33	7.18	0.68	0.00	100.18	42.47
GM_01	OC	GM-01 Ilmn 15-3	0.01	47.55	0.03	9.70	0.25	0.00	33.60	7.06	0.66	0.00	100.23	42.33
GM_01	OC	GM-01 Ilmn 15-4	0.02	47.38	0.02	10.01	0.27	0.00	33.50	6.99	0.67	0.00	100.13	42.51
GM_01	OC	GM-01 Ilmn 15-5	0.02	47.53	0.06	10.03	0.24	0.00	33.54	6.96	0.69	0.00	100.21	42.56
GM_01	OC	GM-01 Ilmn 16-1	0.02	47.15	0.06	10.22	0.23	0.00	33.27	6.96	0.67	0.00	99.90	42.47
GM_01	OC	GM-01 Ilmn 16-2	0.01	47.32	0.04	10.04	0.26	0.00	33.32	7.05	0.68	0.00	100.08	42.35
GM_01	OC	GM-01 Ilmn 17-1	0.04	47.26	0.03	9.95	0.22	0.00	33.50	7.07	0.64	0.00	99.84	42.45

Table S2 (continued)

Sample	Eruptive Unit	Analysis	SiO_2	TiO_2	Al_2O_3	Fe_2O_3	V_2O_3	Cr_2O_3	FeO	MnO	MgO	CaO	Total	FeO^T
GM_01	OC	GM-01 Ilmn 19-1	0.00	47.19	0.03	10.24	0.24	0.00	33.57	6.83	0.63	0.00	100.04	42.78
GM_01	OC	GM-01 ilmn 19-2	0.03	47.33	0.03	9.86	0.21	0.00	33.93	6.73	0.62	0.00	100.08	42.81
GM_01	OC	GM-01 ilmn 19-3	0.01	47.47	0.00	9.88	0.21	0.00	33.98	6.86	0.66	0.00	100.39	42.87
GM_01	OC	GM-01 ilmn 20-1	0.12	47.01	0.07	10.46	0.22	0.00	32.93	7.25	0.68	0.00	99.85	42.34
GM_01	OC	GM-01 ilmn 21-1	0.01	47.46	0.04	9.96	0.24	0.00	33.88	6.72	0.66	0.00	100.06	42.84
GM_01	OC	GM-01 ilmn 22-1	0.04	47.42	0.03	9.83	0.19	0.00	33.55	7.17	0.66	0.00	99.87	42.40
GM_01	OC	GM-01 ilmn 23-1	0.00	47.26	0.04	10.05	0.20	0.00	33.68	6.83	0.66	0.00	100.06	42.72
GM_01	OC	GM-01 ilmn 23-2	0.01	47.36	0.04	9.86	0.20	0.00	33.82	6.76	0.66	0.00	100.01	42.69
GM_01	OC	GM-01 ilmn 23-3	0.00	47.34	0.04	10.09	0.22	0.00	33.76	6.80	0.63	0.00	100.20	42.84
GM_01	OC	GM-01 ilmn 23-4	0.01	47.23	0.05	10.42	0.22	0.00	33.61	6.80	0.64	0.00	100.12	42.98
GM_01	OC	GM-01 ilmn 24-1	0.03	46.95	0.02	9.87	0.23	0.00	33.34	6.91	0.66	0.00	99.26	42.22
GM_01	OC	GM-01 ilmn 25-1	0.01	47.54	0.06	9.76	0.19	0.00	33.91	6.80	0.67	0.00	100.16	42.69
GM_01	OC	GM-01 ilmn 25-2	0.02	47.21	0.05	9.87	0.20	0.00	33.69	6.76	0.66	0.00	99.83	42.58
GM_01	OC	GM-01 ilmn 26-1	0.01	47.33	0.03	9.81	0.20	0.00	33.71	6.95	0.64	0.00	100.12	42.54
GM_01	OC	GM-01 ilmn 26-2	0.00	47.24	0.05	9.75	0.19	0.00	33.68	6.84	0.64	0.00	99.77	42.46
GM_01	OC	GM-01 ilmn 26-3	0.02	47.45	0.02	9.80	0.21	0.00	33.96	6.79	0.65	0.00	100.29	42.78
GM_01	OC	GM-01 ilmn 26-4	0.01	47.38	0.05	10.11	0.22	0.00	33.64	6.95	0.63	0.00	100.29	42.74
GM_01	OC	GM-01 ilmn 27-1	0.01	46.82	0.04	10.50	0.20	0.00	33.46	6.71	0.64	0.00	99.78	42.91
GM_01	OC	GM-01 ilmn 27-2	0.02	47.11	0.04	10.03	0.20	0.00	33.69	6.68	0.66	0.00	99.86	42.71
GM_01	OC	GM-01 ilmn 27-3	0.00	46.83	0.03	10.52	0.22	0.00	33.48	6.68	0.63	0.00	99.73	42.94
GM_01	OC	GM-01 ilmn 27-4	0.02	47.24	0.04	10.24	0.23	0.00	33.69	6.70	0.68	0.00	100.17	42.91
GM_01	OC	GM-01 ilmn 27-5	0.02	46.72	0.05	10.62	0.21	0.00	33.41	6.65	0.61	0.00	99.78	42.97
GM_01	OC	GM-01 ilmn 28-1	0.13	47.92	0.03	9.42	0.26	0.00	34.09	7.07	0.63	0.00	100.61	42.57
GM_07a	OL	GM_07a_2_ILMN_1_4	0.14	46.97	0.08	9.56	0.19	0.00	36.24	4.10	0.62	0.02	98.04	44.83
GM_07a	OL	GM_07a_2_ILMN_1_5	0.14	47.08	0.06	9.33	0.21	0.00	36.30	4.12	0.63	0.02	98.02	44.69
GM_07a	OL	GM_07a_2_ILMN_1_6	0.16	47.57	0.08	9.06	0.25	0.00	36.75	4.07	0.60	0.01	98.60	44.91
GM_07a	OL	GM_07a_2_ILMN_1_7	0.15	47.46	0.07	9.02	0.21	0.00	36.68	4.16	0.60	0.00	98.43	44.80
GM_07a	OL	GM_07a_2_ILMN_1_8	0.13	47.38	0.07	9.43	0.23	0.00	36.56	4.15	0.61	0.01	98.62	45.05
GM_07a	OL	GM_07a_2_ILMN_1_9	0.13	47.56	0.10	9.26	0.19	0.00	36.57	4.16	0.64	0.01	98.69	44.91
GM_07a	OL	GM_07a_2_ILMN_1_10	0.13	47.26	0.19	10.06	0.23	0.00	35.84	4.18	0.64	0.01	98.61	44.89
GM_07a	OL	GM_07a_2_ILMN_1_11	0.12	47.53	0.02	9.33	0.22	0.00	36.81	4.15	0.64	0.01	98.94	45.20
GM_07a	OL	GM_07a_2_ILMN_1_12	0.16	47.31	0.10	9.62	0.23	0.00	36.34	4.09	0.65	0.01	98.59	44.99
GM_07a	OL	GM_07a_2_ILMN_1_13	0.17	47.55	0.08	9.46	0.22	0.00	36.69	4.07	0.66	0.01	98.93	45.20

Table S2 (continued)

Sample	Eruptive Unit	Analysis	SiO_2	TiO_2	Al_2O_3	Fe_2O_3	V_2O_3	Cr_2O_3	FeO	MnO	MgO	CaO	Total	FeO^T
GM_07a	OL	GM_07a_2_ILMN_1_14	0.16	47.56	0.05	9.02	0.22	0.00	36.82	4.12	0.63	0.00	98.68	44.94
GM_07a	OL	GM_07a_2_ILMN_1_15	0.19	46.83	0.11	10.33	0.24	0.00	35.94	4.14	0.60	0.01	98.43	45.23
GM_07a	OL	GM_07a_2_ILMN_1_16	0.15	47.20	0.07	9.26	0.22	0.00	36.36	4.17	0.62	0.00	98.19	44.70
GM_07a	OL	GM_07a_2_ILMN_1_17	0.16	46.91	0.08	10.30	0.23	0.00	36.29	3.98	0.61	0.00	98.61	45.55
GM_07a	OL	GM_07a_2_ILMN_1_22	0.19	47.45	0.06	9.03	0.24	0.00	36.69	4.17	0.59	0.02	98.48	44.82
GM_07a	OL	GM_07a_2_ILMN_1_24	0.19	47.06	0.08	9.33	0.18	0.00	36.42	4.10	0.63	0.00	98.13	44.82
GM_07a	OL	GM_07a_2_ILMN_1_25	0.17	47.25	0.06	9.27	0.20	0.00	36.63	4.08	0.64	0.00	98.34	44.98
GM_07a	OL	GM_07a_2_ILMN_1_29	0.18	47.69	0.04	9.06	0.22	0.00	36.90	4.20	0.64	0.01	99.04	45.06
GM_07a	OL	GM_07a_2_ILMN_1_31	0.15	47.44	0.05	9.19	0.20	0.00	36.79	4.07	0.65	0.01	98.61	45.06
GM_07a	OL	GM_07a_2_ILMN_2_31	0.04	47.54	0.04	9.52	0.23	0.00	36.82	4.05	0.59	0.01	98.99	45.39
GM_07a	OL	GM_07a_2_ILMN_2_2	0.03	48.25	0.26	9.98	0.21	0.00	36.73	4.00	0.52	0.01	100.08	45.71
GM_07a	OL	GM_07a_2_ILMN_2_4	0.05	47.68	0.10	9.25	0.23	0.00	36.76	3.94	0.62	0.00	98.73	45.08
GM_07a	OL	GM_07a_2_ILMN_2_6	0.03	48.15	0.03	9.30	0.22	0.00	37.38	4.07	0.60	0.01	99.83	45.75
GM_07a	OL	GM_07a_2_ILMN_2_7	0.06	47.39	0.06	9.82	0.22	0.00	36.62	4.04	0.60	0.02	98.85	45.45
GM_07a	OL	GM_07a_2_ILMN_2_8	0.07	47.48	0.07	10.03	0.28	0.00	36.50	4.01	0.60	0.06	99.13	45.52
GM_07a	OL	GM_07a_2_ILMN_2_9	0.04	47.70	0.06	9.66	0.23	0.00	36.84	4.07	0.61	0.02	99.25	45.53
GM_07a	OL	GM_07a_2_ILMN_2_10	0.04	47.12	0.26	10.99	0.21	0.00	35.64	3.97	0.56	0.06	98.93	45.54
GM_07a	OL	GM_07a_2_ILMN_2_14	0.14	47.42	0.04	9.48	0.21	0.00	36.89	4.00	0.59	0.02	98.90	45.42
GM_07a	OL	GM_07a_2_ILMN_2_15	0.06	47.46	0.09	10.04	0.22	0.00	36.47	4.08	0.64	0.01	99.14	45.50
GM_07a	OL	GM_07a_2_ILMN_2_16	0.02	48.03	0.08	9.90	0.23	0.00	36.98	4.06	0.58	0.05	100.04	45.89
GM_07a	OL	GM_07a_2_ILMN_2_17	0.08	47.40	0.08	9.99	0.25	0.00	36.40	4.11	0.57	0.08	99.06	45.39
GM_07a	OL	GM_07a_2_ILMN_2_19	0.16	47.20	0.10	9.98	0.22	0.00	36.41	4.01	0.59	0.07	98.84	45.39
GM_07a	OL	GM_07a_2_ILMN_2_21	0.04	47.63	0.05	9.44	0.24	0.00	36.68	4.01	0.59	0.16	99.01	45.18
GM_07a	OL	GM_07a_2_ILMN_2_22	0.06	47.77	0.04	9.36	0.23	0.00	36.85	4.07	0.64	0.07	99.22	45.27
GM_07a	OL	GM_07a_2_ILMN_2_23	0.06	47.65	0.40	11.03	0.24	0.00	35.30	4.05	0.60	0.06	99.42	45.23
GM_07a	OL	GM_07a_2_ILMN_2_28	0.05	47.65	0.11	10.30	0.22	0.00	36.53	3.99	0.57	0.19	99.69	45.80
GM_07a	OL	GM_07a_2_ILMN_2_29	0.11	47.35	0.06	9.76	0.19	0.00	36.72	3.97	0.58	0.13	98.92	45.50
GM_07a	OL	GM_07a_2_ILMN_2_30	0.05	47.84	0.06	9.72	0.24	0.00	37.02	3.96	0.60	0.03	99.60	45.76
GM_07a	OL	GM_07a_4_ILMN_1_1	0.07	48.39	0.05	8.91	0.24	0.00	37.51	4.06	0.59	0.01	99.91	45.52
GM_07a	OL	GM_07a_4_ILMN_1_2	0.05	48.37	0.07	9.45	0.25	0.00	37.41	4.02	0.60	0.02	100.33	45.91
GM_07a	OL	GM_07a_4_ILMN_1_4	0.11	48.04	0.05	9.68	0.23	0.00	37.35	4.03	0.57	0.01	100.17	46.06
GM_07a	OL	GM_07a_4_ILMN_1_5	0.11	48.05	0.07	9.60	0.23	0.00	37.30	4.06	0.57	0.01	100.04	45.94
GM_07a	OL	GM_07a_4_ILMN_1_7	0.06	47.50	0.09	10.55	0.23	0.00	36.69	4.05	0.53	0.00	99.86	46.18

Table S2 (continued)

Sample	Eruptive Unit	Analysis	SiO_2	TiO_2	Al_2O_3	Fe_2O_3	V_2O_3	Cr_2O_3	FeO	MnO	MgO	CaO	Total	FeO^T
GM_07a	OL	GM_07a_4_ILMN_1_9	0.06	48.38	0.02	9.56	0.26	0.00	37.54	4.08	0.60	0.02	100.61	46.14
GM_07a	OL	GM_07a_4_ILMN_1_10	0.04	48.40	0.04	9.69	0.26	0.00	37.43	4.08	0.60	0.00	100.64	46.15
GM_07a	OL	GM_07a_4_ILMN_1_11	0.05	48.49	0.03	9.09	0.22	0.00	37.64	4.12	0.61	0.01	100.31	45.82
GM_07a	OL	GM_07a_4_ILMN_1_12	0.08	48.49	0.03	8.95	0.27	0.00	37.63	4.10	0.58	0.01	100.22	45.69
GM_07a	OL	GM_07a_4_ILMN_1_13	0.17	47.69	0.42	9.33	0.22	0.00	35.85	3.98	0.44	0.01	98.23	44.25
GM_07a	OL	GM_07a_4_ILMN_1_16	0.11	47.34	0.13	9.92	0.23	0.00	36.38	4.02	0.59	0.00	98.79	45.31
GM_07a	OL	GM_07a_4_ILMN_1_18	0.08	48.24	0.04	9.12	0.21	0.00	37.55	4.03	0.58	0.01	99.95	45.76
GM_07a	OL	GM_07a_4_ILMN_1_19	0.12	47.80	0.03	9.47	0.21	0.00	37.25	4.08	0.57	0.01	99.59	45.77
GM_07a	OL	GM_07a_4_ILMN_1_20	0.09	48.13	0.06	8.78	0.21	0.00	37.47	3.97	0.60	0.00	99.35	45.36
GM_07a	OL	GM_07a_4_ILMN_1_22	0.18	47.37	1.10	14.53	0.22	0.00	32.30	3.92	0.70	0.02	100.47	45.38
GM_07a	OL	GM_07a_1_ILMN_1_8	0.09	47.37	0.24	9.59	0.20	0.00	36.20	3.84	0.56	0.02	98.20	44.83
GM_07a	OL	GM_07a_1_ILMN_1_12	0.09	47.28	0.04	10.11	0.23	0.00	36.51	4.12	0.62	0.01	99.12	45.61
GM_07a	OL	GM_07a_1_ILMN_1_13	0.09	47.36	0.05	10.11	0.26	0.00	36.49	4.16	0.59	0.01	99.18	45.58
GM_07a	OL	GM_07a_1_ILMN_1_14	0.09	47.26	0.21	10.67	0.23	0.00	35.62	4.10	0.72	0.00	98.93	45.22
GM_07a	OL	GM_07a_1_ILMN_1_15	0.11	48.23	0.11	8.42	0.22	0.00	37.20	4.11	0.59	0.00	99.02	44.77
GM_07a	OL	GM_07a_1_ILMN_1_16	0.07	47.84	0.07	9.53	0.23	0.00	36.77	4.17	0.64	0.02	99.37	45.35
GM_07a	OL	GM_07a_1_ILMN_1_18	0.13	48.21	0.36	9.68	0.20	0.00	36.21	4.08	0.62	0.02	99.53	44.92
GM_16	YE	GM_16_ILMN_1_1	0.09	46.90	0.07	10.92	0.23	0.00	37.86	1.74	0.96	0.01	98.84	47.69
GM_16	YE	GM_16_ILMN_1_3	0.14	46.21	0.11	12.39	0.23	0.00	37.30	1.69	0.89	0.01	98.98	48.44
GM_16	YE	GM_16_ILMN_1_5	0.19	45.95	0.14	12.27	0.22	0.00	36.99	1.65	0.93	0.01	98.45	48.03
GM_16	YE	GM_16_ILMN_1_7	0.17	46.92	0.24	11.53	0.23	0.00	37.34	1.73	0.93	0.01	99.16	47.71
GM_16	YE	GM_16_ILMN_1_8	0.09	47.47	0.08	10.61	0.24	0.00	38.46	1.74	0.88	0.01	99.63	48.00
GM_16	YE	GM_16_ILMN_1_9	0.10	46.71	0.08	11.52	0.20	0.00	37.81	1.73	0.93	0.01	99.18	48.18
GM_16	YE	GM_16_ILMN_1_11	0.19	46.58	0.28	11.64	0.23	0.00	37.00	1.71	0.87	0.00	98.57	47.47
GM_16	YE	GM_16_ILMN_1_12	0.08	46.56	0.06	11.49	0.25	0.00	37.73	1.70	0.87	0.00	98.79	48.08
GM_16	YE	GM_16_ILMN_1_13	0.09	46.26	0.06	12.29	0.23	0.00	37.56	1.68	0.88	0.03	99.12	48.62
GM_16	YE	GM_16_ILMN_1_15	0.19	46.57	0.16	12.16	0.22	0.00	37.58	1.66	0.86	0.00	99.49	48.53
GM_16	YE	GM_16_ILMN_1_16	0.12	46.59	0.09	11.45	0.25	0.00	37.59	1.71	0.90	0.01	98.77	47.89
GM_16	YE	GM_16_ILMN_1_18	0.15	46.86	0.13	11.00	0.24	0.00	37.79	1.75	0.85	0.00	98.83	47.68
GM_16	YE	GM_16_ILMN_1_19	0.18	46.69	0.20	11.26	0.24	0.00	37.35	1.74	0.86	0.01	98.58	47.49
GM_16	YE	GM_16_ILMN_1_20	0.18	46.77	0.15	11.24	0.26	0.00	37.59	1.76	0.85	0.01	98.87	47.70
GM_16	YE	GM_16_ILMN_1_23	0.17	47.41	0.08	10.53	0.24	0.00	38.43	1.74	0.93	0.01	99.51	47.90
GM_16	YE	GM_16_ILMN_2_1	0.16	46.70	0.05	11.55	0.23	0.00	37.84	1.77	0.94	0.00	99.37	48.23

Table S2 (continued)

Sample	Eruptive Unit	Analysis	SiO_2	TiO_2	Al_2O_3	Fe_2O_3	V_2O_3	Cr_2O_3	FeO	MnO	MgO	CaO	Total	FeO^T
GM_16	YE	GM_16_ILMN_2_2	0.20	46.88	0.07	11.84	0.24	0.00	37.97	1.74	0.93	0.01	99.94	48.63
GM_16	YE	GM_16_ILMN_2_3	0.16	46.65	0.07	11.82	0.28	0.00	37.72	1.69	0.90	0.01	99.36	48.36
GM_16	YE	GM_16_ILMN_2_5	0.18	46.48	0.02	11.34	0.27	0.00	37.73	1.72	0.92	0.02	98.73	47.94
GM_16	YE	GM_16_ILMN_2_7	0.10	47.20	0.05	10.89	0.23	0.00	38.29	1.78	0.90	0.01	99.49	48.09
GM_16	YE	GM_16_ILMN_2_8	0.19	46.84	0.11	11.27	0.25	0.00	37.82	1.73	0.90	0.01	99.14	47.96
GM_16	YE	GM_16_ILMN_2_11	0.20	47.35	0.06	10.55	0.27	0.00	38.40	1.74	0.93	0.03	99.56	47.89
GM_16	YE	GM_16_ILMN_2_17	0.16	46.79	0.07	11.40	0.25	0.00	37.77	1.75	0.94	0.01	99.22	48.03
GM_16	YE	GM_16_ILMN_2_18	0.20	47.24	0.06	10.76	0.24	0.00	38.41	1.77	0.89	0.01	99.64	48.09
GM_16	YE	GM_16_ILMN_2_19	0.20	47.08	0.07	10.97	0.25	0.00	38.14	1.78	0.92	0.00	99.44	48.02
GM_16	YE	GM_16_ILMN_2_20	0.19	45.94	0.07	11.86	0.27	0.00	37.03	1.78	0.90	0.02	98.13	47.70
GM_16	YE	GM_16_ILMN_2_22	0.18	47.31	0.08	10.52	0.24	0.00	38.31	1.77	0.92	0.01	99.38	47.78
GM_16	YE	GM_16_ILMN_2_23	0.18	47.43	0.06	10.89	0.25	0.00	38.50	1.80	0.88	0.01	100.05	48.30
GM_16	YE	GM_16_ILMN_2_27	0.20	47.12	0.09	10.92	0.24	0.00	38.20	1.76	0.88	0.01	99.41	48.03
GM_16	YE	GM_16_ILMN_3_1	0.05	47.45	0.10	10.95	0.23	0.00	38.14	1.85	0.91	0.01	99.84	47.99
GM_16	YE	GM_16_ILMN_3_2	0.03	47.34	0.07	11.00	0.25	0.00	38.16	1.90	0.87	0.00	99.71	48.06
GM_16	YE	GM_16_ILMN_3_3	0.02	47.38	0.21	11.64	0.24	0.00	37.60	1.89	0.87	0.01	99.92	48.08
GM_16	YE	GM_16_ILMN_3_4	0.05	47.13	0.09	11.41	0.26	0.00	37.85	1.87	0.89	0.00	99.61	48.12
GM_16	YE	GM_16_ILMN_3_5	0.05	46.70	0.35	12.65	0.24	0.00	36.46	1.86	0.88	0.00	99.23	47.84
GM_16	YE	GM_16_ILMN_3_6	0.06	47.42	0.09	11.12	0.25	0.00	38.00	1.91	0.90	0.05	99.88	48.00
GM_16	YE	GM_16_ILMN_3_7	0.06	47.20	0.09	11.15	0.24	0.00	37.94	1.86	0.91	0.02	99.55	47.97
GM_16	YE	GM_16_ILMN_3_8	0.01	47.27	0.08	11.29	0.26	0.00	37.92	1.89	0.91	0.01	99.67	48.07
GM_16	YE	GM_16_ILMN_3_9	0.05	47.41	0.06	10.46	0.22	0.00	38.29	1.90	0.89	0.02	99.36	47.71
GM_16	YE	GM_16_ILMN_3_10	0.03	47.06	0.07	11.07	0.22	0.00	37.90	1.80	0.93	0.04	99.26	47.86
GM_16	YE	GM_16_ILMN_3_11	0.05	46.95	0.06	11.28	0.26	0.00	37.78	1.87	0.90	0.00	99.28	47.93
GM_16	YE	GM_16_ILMN_3_12	0.01	47.08	0.12	11.36	0.21	0.00	37.73	1.86	0.89	0.03	99.38	47.95
GM_16	YE	GM_16_ILMN_3_13	0.06	47.05	0.08	11.19	0.21	0.00	37.90	1.87	0.95	0.01	99.41	47.97
GM_16	YE	GM_16_ILMN_3_14	0.05	47.46	0.08	10.47	0.22	0.00	38.31	1.83	0.89	0.00	99.40	47.73
GM_16	YE	GM_16_ILMN_3_15	0.08	47.44	0.08	10.58	0.22	0.00	38.35	1.80	0.92	0.01	99.58	47.87
GM_16	YE	GM_16_ILMN_3_16	0.03	47.14	0.06	11.08	0.24	0.00	37.97	1.86	0.92	0.02	99.42	47.94
GM_16	YE	GM_16_ILMN_3_17	0.05	47.17	0.06	11.18	0.25	0.00	38.02	1.79	0.93	0.01	99.55	48.08
GM_16	YE	GM_16_ILMN_3_18	0.02	47.35	0.20	11.36	0.25	0.00	37.56	1.88	0.89	0.02	99.60	47.78
GM_16	YE	GM_16_ILMN_3_19	0.05	47.18	0.06	11.18	0.25	0.00	38.05	1.82	0.89	0.01	99.58	48.11
GM_16	YE	GM_16_ILMN_3_20	0.06	47.15	0.06	11.12	0.21	0.00	38.02	1.93	0.90	0.04	99.63	48.03

Table S2 (continued)

Sample	Eruptive Unit	Analysis	SiO_2	TiO_2	Al_2O_3	Fe_2O_3	V_2O_3	Cr_2O_3	FeO	MnO	MgO	CaO	Total	FeO^T
GM_16	YE	GM_16_ILMN_3_21	0.06	47.22	0.10	11.09	0.23	0.00	37.94	1.82	0.91	0.04	99.47	47.92
GM_16	YE	GM_16_ILMN_3_22	0.07	46.80	0.08	11.18	0.22	0.00	37.71	1.84	0.87	0.05	98.92	47.78
GM_16	YE	GM_16_ILMN_3_24	0.01	47.48	0.07	10.71	0.25	0.00	38.20	1.88	0.90	0.01	99.60	47.84
GM_16	YE	GM_16_ILMN_3_25	0.04	47.15	0.14	11.24	0.23	0.00	37.70	1.86	0.90	0.01	99.37	47.82
GM_16	YE	GM_16_ILMN_3_26	0.03	47.27	0.08	11.04	0.23	0.00	37.99	1.89	0.91	0.01	99.53	47.92
GM_16	YE	GM_16_ILMN_3_27	0.06	46.77	0.33	12.15	0.23	0.00	36.66	1.85	0.86	0.00	98.95	47.59
GM_16	YE	GM_16_ILMN_3_28	0.04	47.34	0.09	11.08	0.24	0.00	38.05	1.84	0.89	0.04	99.66	48.02
GM_16	YE	GM_16_ILMN_3_29	0.08	47.28	0.11	11.31	0.23	0.00	37.96	1.83	0.94	0.00	99.82	48.14
GM_16	YE	GM_16_ILMN_3_30	0.03	46.97	0.08	11.62	0.25	0.00	37.72	1.90	0.88	0.01	99.58	48.18
GM_16	YE	GM_16_ILMN_3_31	0.02	47.18	0.12	11.55	0.22	0.00	37.86	1.79	0.90	0.01	99.72	48.25
GM_16	YE	GM_16_ILMN_3_32	0.03	47.60	0.08	10.66	0.22	0.00	38.46	1.84	0.87	0.01	99.81	48.04
GM_16	YE	GM_16_ILMN_3_33	0.04	47.20	0.09	11.21	0.25	0.00	37.96	1.79	0.91	0.00	99.55	48.05
GM_16	YE	GM_16_ILMN_3_34	0.06	47.20	0.08	11.31	0.24	0.00	37.95	1.90	0.91	0.00	99.72	48.12
GM_16	YE	GM_16_ILMN_3_35	0.06	47.13	0.07	11.04	0.24	0.00	38.07	1.82	0.89	0.00	99.36	48.00
GM_16	YE	GM_16_ILMN_3_36	0.05	47.11	0.10	11.49	0.26	0.00	37.79	1.89	0.88	0.00	99.65	48.13
GM_16	YE	GM_16_ILMN_3_37	0.07	47.28	0.05	10.82	0.26	0.00	38.14	1.83	0.93	0.01	99.47	47.87
GM_16	YE	GM_16_ILMN_3_38	0.07	46.96	0.82	14.39	0.28	0.00	34.64	1.84	0.86	0.01	99.98	47.59
GM_16	YE	GM_16_ILMN_3_39	0.01	47.29	0.10	11.04	0.27	0.00	37.86	1.79	0.92	0.02	99.45	47.79
GM_16	YE	GM_16_ILMN_3_40	0.04	47.39	0.06	10.92	0.19	0.00	38.34	1.92	0.91	0.01	99.81	48.17
GM_16	YE	GM_16_ILMN_3_41	0.05	47.40	0.10	10.42	0.23	0.00	38.15	1.80	0.90	0.01	99.17	47.53
GM_16	YE	GM_16_ILMN_3_42	0.04	47.55	0.10	11.06	0.26	0.00	38.20	1.84	0.88	0.02	100.04	48.15
GM_16	YE	GM_16_ILMN_3_43	0.03	47.38	0.09	10.84	0.22	0.00	38.15	1.87	0.88	0.00	99.50	47.90
GM_16	YE	GM_16_ILMN_3_44	0.04	47.20	0.07	10.97	0.24	0.00	37.98	1.80	0.91	0.04	99.33	47.85
GM_16	YE	GM_16_ILMN_3_45	0.03	47.06	0.07	11.40	0.25	0.00	37.90	1.81	0.88	0.02	99.57	48.15
GM_16	YE	GM_16_ILMN_3_46	0.06	46.53	0.06	12.00	0.24	0.00	37.42	1.88	0.89	0.04	99.17	48.21
GM_16	YE	GM_16_ILMN_3_47	0.03	47.01	0.07	11.13	0.22	0.00	37.90	1.82	0.92	0.02	99.22	47.92
GM_16	YE	GM_16_ILMN_3_48	0.06	47.06	0.10	11.15	0.23	0.00	37.84	1.83	0.90	0.00	99.23	47.87
GM_16	YE	GM_16_ILMN_3_49	0.04	46.97	0.06	11.04	0.22	0.00	38.01	1.84	0.89	0.01	99.11	47.94
GM_16	YE	GM_16_ILMN_3_50	0.03	47.03	0.08	11.30	0.28	0.00	37.77	1.85	0.87	0.02	99.31	47.94
GM_16	YE	GM_16_ILMN_3_51	0.05	47.18	0.07	11.10	0.25	0.00	38.04	1.84	0.88	0.01	99.47	48.03
GM_16	YE	GM_16_ILMN_3_52	0.02	46.55	0.07	11.66	0.23	0.00	37.44	1.81	0.93	0.02	98.77	47.92
GM_16	YE	GM_16_ILMN_3_53	0.04	46.54	0.09	11.51	0.25	0.00	37.43	1.76	0.86	0.06	98.60	47.78
GM_16	YE	GM_16_ILMN_3_54	0.05	47.42	0.10	10.58	0.21	0.00	38.11	1.83	0.90	0.09	99.37	47.64

Table S2 (continued)

Sample	Eruptive Unit	Analysis	SiO_2	TiO_2	Al_2O_3	Fe_2O_3	V_2O_3	Cr_2O_3	FeO	MnO	MgO	CaO	Total	FeO^T
GM_16	YE	GM_16_2_ILMN_4_1	0.04	46.77	0.09	11.76	0.23	0.00	37.53	1.92	0.88	0.03	99.35	48.12
GM_16	YE	GM_16_2_ILMN_4_3	0.05	47.09	0.13	11.75	0.19	0.00	37.84	1.83	0.90	0.01	99.87	48.41
GM_16	YE	GM_16_2_ILMN_4_4	0.04	46.94	0.08	11.82	0.24	0.00	37.67	1.89	0.91	0.04	99.67	48.30
GM_16	YE	GM_16_2_ILMN_4_5	0.18	46.05	1.58	18.04	0.22	0.00	30.46	1.94	1.04	0.03	99.56	46.69
GM_16	YE	GM_16_2_ILMN_4_7	0.09	47.31	0.09	11.18	0.23	0.00	38.06	1.94	0.87	0.01	99.87	48.12
GM_16	YE	GM_16_2_ILMN_4_8	0.08	47.08	0.26	12.14	0.23	0.00	37.10	1.93	0.92	0.01	99.82	48.02
GM_16	YE	GM_16_2_ILMN_4_9	0.12	47.39	0.23	11.77	0.21	0.00	37.64	1.95	0.88	0.00	100.26	48.23
GM_16	YE	GM_16_2_ILMN_4_10	0.12	46.51	0.49	13.19	0.18	0.00	36.04	1.93	0.76	0.03	99.38	47.91
GM_16	YE	GM_16_2_ILMN_4_11	0.07	47.28	0.10	11.48	0.22	0.00	38.04	1.90	0.87	0.01	100.09	48.37
GM_16	YE	GM_16_2_ILMN_4_12	0.07	47.40	0.12	11.02	0.21	0.00	38.16	1.96	0.82	0.01	99.87	48.08
GM_16	YE	GM_16_2_ILMN_4_13	0.06	47.19	0.07	11.11	0.22	0.00	38.11	1.87	0.87	0.00	99.62	48.11
GM_16	YE	GM_16_2_ILMN_4_14	0.09	45.87	0.08	13.09	0.21	0.00	37.05	1.81	0.84	0.01	99.11	48.83
GM_16	YE	GM_16_2_ILMN_4_15	0.14	45.86	0.08	13.01	0.21	0.00	37.16	1.76	0.85	0.01	99.12	48.86
GM_16	YE	GM_16_2_ILMN_4_17	0.05	47.04	0.09	11.31	0.21	0.00	37.82	1.90	0.94	0.00	99.44	48.00
GM_16	YE	GM_16_2_ILMN_4_18	0.04	47.27	0.04	11.26	0.28	0.00	38.16	1.86	0.88	0.01	99.88	48.28
GM_16	YE	GM_16_2_ILMN_4_19	0.05	47.17	0.04	10.97	0.25	0.00	38.01	1.90	0.94	0.02	99.40	47.88
GM_16	YE	GM_16_2_ILMN_4_20	0.10	46.75	0.49	12.99	0.23	0.00	35.75	1.87	0.98	0.01	99.25	47.44
GM_16	YE	GM_16_2_ILMN_4_21	0.07	46.87	0.05	11.57	0.22	0.00	37.80	1.94	0.88	0.04	99.51	48.21
GM_16	YE	GM_16_2_ILMN_4_22	0.06	47.13	0.06	11.49	0.24	0.00	37.93	1.92	0.90	0.04	99.87	48.26
GM_16	YE	GM_16_2_ILMN_4_23	0.09	47.02	0.06	11.65	0.23	0.00	38.00	1.82	0.89	0.04	99.87	48.49
GM_16	YE	GM_16_2_ILMN_4_25	0.09	46.53	0.06	12.30	0.21	0.00	37.65	1.80	0.89	0.05	99.67	48.71
GM_16	YE	GM_16_2_ILMN_4_27	0.09	46.46	0.05	11.62	0.23	0.00	37.55	1.85	0.87	0.01	98.86	48.01
GM_16	YE	GM_16_2_ILMN_4_29	0.16	46.84	0.70	13.73	0.21	0.00	35.52	1.82	0.76	0.02	99.79	47.88
GM_16	YE	GM_16_2_ILMN_4_32	0.07	46.43	0.06	12.57	0.24	0.00	37.46	1.83	0.87	0.02	99.63	48.77
GM_16	YE	GM_16_2_ILMN_4_33	0.07	47.02	0.08	11.79	0.20	0.00	37.93	1.89	0.89	0.01	99.97	48.55
GM_16	YE	GM_16_2_ILMN_4_34	0.04	47.36	0.05	11.20	0.24	0.00	38.20	1.87	0.90	0.03	99.93	48.28
GM_16	YE	GM_16_2_ILMN_4_35	0.10	46.99	0.06	11.48	0.25	0.00	37.82	1.89	0.90	0.06	99.64	48.14
GM_16	YE	GM_16_2_ILMN_4_36	0.06	46.87	0.08	11.84	0.22	0.00	37.63	1.88	0.91	0.05	99.66	48.28
GM_16	YE	GM_16_2_ILMN_4_37	0.08	46.98	0.09	11.46	0.24	0.00	37.78	1.85	0.88	0.05	99.46	48.09
GM_16	YE	GM_16_2_ILMN_4_38	0.05	46.66	0.07	11.56	0.24	0.00	37.42	1.89	0.94	0.01	98.88	47.82
GM_16	YE	GM_16_2_ILMN_4_39	0.15	46.82	0.13	11.66	0.24	0.00	37.52	1.86	0.91	0.01	99.39	48.02
GM_16	YE	GM_16_2_ILMN_4_40	0.06	47.05	0.18	11.97	0.20	0.00	37.49	1.90	0.90	0.02	99.89	48.26
GM_16	YE	GM_16_2_ILMN_4_41	0.05	46.58	0.04	11.99	0.23	0.00	37.57	1.85	0.89	0.07	99.40	48.36

Table S2 (continued)

Sample	Eruptive Unit	Analysis	SiO_2	TiO_2	Al_2O_3	Fe_2O_3	V_2O_3	Cr_2O_3	FeO	MnO	MgO	CaO	Total	FeO^T
GM_16	YE	GM_16_2_ILMN_4_42	0.06	46.97	0.09	11.70	0.23	0.00	37.77	1.90	0.87	0.01	99.73	48.30
GM_16	YE	GM_16_2_ILMN_4_43	0.05	47.15	0.05	10.84	0.21	0.00	38.13	1.86	0.91	0.01	99.34	47.89
GM_10	YO	GM_10_ILMN_1-6	0.17	46.81	0.17	11.27	0.25	0.00	37.53	1.86	0.80	0.01	98.92	47.68
GM_10	YO	GM_10_ILMN_1-7	0.19	47.17	0.23	10.78	0.24	0.00	37.59	1.93	0.80	0.01	99.00	47.30
GM_10	YO	GM_10_ILMN_1-10	0.19	46.82	0.21	11.24	0.21	0.00	37.38	1.99	0.81	0.01	98.91	47.50
GM_10	YO	GM_10_ILMN_1-15	0.12	47.47	0.13	10.29	0.24	0.00	38.21	1.95	0.79	0.01	99.25	47.47
GM_10	YO	GM_10_ILMN_1-18	0.17	47.14	0.21	11.20	0.22	0.00	37.61	2.01	0.79	0.02	99.39	47.69
GM_10	YO	GM_10_ILMN_1-19	0.13	47.17	0.08	10.44	0.23	0.00	38.00	1.98	0.82	0.09	99.04	47.40
GM_10	YO	GM_10_ILMN_1-20	0.14	47.02	0.08	10.66	0.27	0.00	37.77	1.99	0.81	0.08	98.86	47.37
GM_10	YO	GM_10_ILMN_1-21	0.11	47.27	0.09	10.20	0.23	0.00	38.12	2.02	0.79	0.03	98.93	47.29
GM_10	YO	GM_10_ILMN_1-22	0.11	47.33	0.06	10.26	0.23	0.00	38.31	1.99	0.81	0.01	99.14	47.54
GM_10	YO	GM_10_ILMN_5-5	0.14	47.12	0.38	11.45	0.23	0.00	36.80	1.95	0.84	0.01	99.00	47.11
GM_10	YO	GM_10_ILMN_5-19	0.16	46.63	0.26	11.29	0.21	0.00	36.99	1.93	0.80	0.03	98.36	47.15
GM_10	YO	GM_10_ILMN_4-2	0.11	47.37	0.30	10.74	0.23	0.00	37.10	2.11	0.84	0.05	98.90	46.76
GM_10	YO	GM_10_ILMN_4-4	0.18	46.99	0.40	11.15	0.24	0.00	36.62	2.02	0.80	0.02	98.49	46.66
GM_10	YO	GM_10_ILMN_4-8	0.09	47.30	0.44	11.82	0.25	0.00	36.48	2.07	0.80	0.06	99.35	47.11
GM_10	YO	GM_10_ILMN_4-20	0.14	47.49	0.57	11.72	0.23	0.00	36.22	2.07	0.83	0.02	99.36	46.77
GM_10	YO	GM_10_ILMN_4-22	0.13	47.19	0.37	11.34	0.26	0.00	36.74	2.06	0.79	0.04	99.02	46.94
GM_10	YO	GM_10_ILMN_4-23	0.11	47.25	0.37	11.31	0.25	0.00	36.78	2.06	0.81	0.02	99.03	46.97
GM_10	YO	GM_10_ILMN_4-24	0.12	47.62	0.36	10.57	0.23	0.00	37.22	2.11	0.81	0.00	99.09	46.73

Table 3 Titanomagnetite analyses

Sample	Eruptive Unit	Analysis	SiO_2	TiO_2	Al_2O_3	Fe_2O_3	V_2O_3	Cr_2O_3	FeO	MnO	MgO	CaO	Total	FeO^T
GM-18	OB	GM_18_2_TMTE_2_4	0.11	8.35	0.75	50.86	0.06	0.00	36.78	1.30	0.19	0.00	98.72	82.55
GM-18	OB	GM_18_2_TMTE_2_5	0.12	8.44	0.79	51.48	0.04	0.00	37.22	1.35	0.22	0.00	99.90	83.54
GM-18	OB	GM_18_2_TMTE_2_6	0.08	8.21	0.77	51.73	0.03	0.00	36.92	1.30	0.22	0.01	99.49	83.47
GM-18	OB	GM_18_2_TMTE_2_7	0.09	8.29	0.76	51.49	0.03	0.00	36.89	1.34	0.22	0.00	99.36	83.23
GM-18	OB	GM_18_2_TMTE_2_8	0.10	8.26	0.78	51.62	0.06	0.00	36.94	1.30	0.22	0.01	99.51	83.39
GM-18	OB	GM_18_2_TMTE_2_9	0.09	8.68	0.80	51.48	0.04	0.00	37.47	1.36	0.23	0.01	100.44	83.79
GM-18	OB	GM_18_2_TMTE_2_10	0.09	8.46	0.80	51.22	0.04	0.00	37.18	1.33	0.23	0.02	99.59	83.27
GM-18	OB	GM_18_2_TMTE_2_11	0.08	8.12	0.76	52.35	0.04	0.00	37.01	1.34	0.22	0.01	100.14	84.12
GM-18	OB	GM_18_2_TMTE_2_12	0.08	8.16	0.78	52.14	0.05	0.00	36.93	1.35	0.22	0.01	100.01	83.84
GM-18	OB	GM_18_2_TMTE_2_13	0.11	7.55	0.86	52.80	0.04	0.00	36.38	1.26	0.22	0.01	99.44	83.89
GM-18	OB	GM_18_2_TMTE_2_14	0.08	8.38	0.81	51.72	0.05	0.00	37.16	1.30	0.21	0.01	99.99	83.69
GM-18	OB	GM_18_2_TMTE_2_15	0.09	8.28	1.20	51.68	0.05	0.00	37.34	1.33	0.20	0.00	100.41	83.85
GM-18	OB	GM_18_2_TMTE_2_16	0.08	7.93	0.75	52.36	0.03	0.00	36.73	1.23	0.21	0.01	99.61	83.85
GM-18	OB	GM_18_2_TMTE_2_17	0.09	7.61	0.84	52.59	0.05	0.00	36.35	1.23	0.20	0.01	99.16	83.68
GM-18	OB	GM_18_2_TMTE_1_1	0.12	8.01	0.81	52.19	0.04	0.00	36.84	1.25	0.21	0.01	99.74	83.80
GM-18	OB	GM_18_2_TMTE_1_2	0.11	7.89	0.83	52.24	0.03	0.00	36.92	1.25	0.19	0.02	99.61	83.93
GM-18	OB	GM_18_2_TMTE_1_3	0.06	7.94	0.77	52.57	0.03	0.00	36.76	1.30	0.21	0.00	99.85	84.06
GM-18	OB	GM_18_2_TMTE_1_4	0.09	7.90	0.80	52.31	0.04	0.00	36.67	1.30	0.21	0.00	99.53	83.74
GM-18	OB	GM_18_2_TMTE_1_5	0.08	7.94	0.82	52.00	0.03	0.00	36.61	1.25	0.22	0.01	99.24	83.41
GM-18	OB	GM_18_2_TMTE_1_6	0.10	7.95	0.78	52.35	0.02	0.00	36.87	1.23	0.20	0.00	99.68	83.98
GM-18	OB	GM_18_2_TMTE_1_7	0.10	7.88	0.79	52.44	0.03	0.00	36.68	1.23	0.22	0.01	99.64	83.87
GM-18	OB	GM_18_2_TMTE_3_1	0.16	7.83	0.84	52.58	0.03	0.00	36.60	1.33	0.20	0.03	99.93	83.92
GM-18	OB	GM_18_2_TMTE_3_2	0.16	7.84	0.81	52.80	0.06	0.00	36.81	1.29	0.23	0.01	100.28	84.32
GM-18	OB	GM_18_2_TMTE_3_3	0.14	7.88	0.83	52.61	0.02	0.00	36.76	1.28	0.23	0.02	100.02	84.10
GM-18	OB	GM_18_2_TMTE_3_4	0.13	7.88	0.82	52.57	0.04	0.00	36.85	1.32	0.21	0.00	100.03	84.15
GM-18	OB	GM_18_2_TMTE_3_5	0.13	7.68	0.79	52.94	0.03	0.00	36.70	1.30	0.22	0.01	99.99	84.34
GM-18	OB	GM_18_2_TMTE_3_6	0.15	7.88	1.05	52.06	0.03	0.00	36.80	1.32	0.20	0.01	99.77	83.65
GM-18	OB	GM_18_2_TMTE_4_1	0.05	8.26	0.77	52.25	0.02	0.00	37.19	1.28	0.22	0.00	100.22	84.21
GM-18	OB	GM_18_2_TMTE_4_2	0.10	8.40	0.77	51.71	0.05	0.00	37.29	1.27	0.21	0.00	100.07	83.82
GM-18	OB	GM_18_2_TMTE_4_3	0.07	8.34	0.82	51.75	0.02	0.00	37.07	1.30	0.24	0.01	99.85	83.63
GM-18	OB	GM_18_2_TMTE_4_4	0.06	8.09	0.80	51.88	0.04	0.00	36.82	1.30	0.23	0.03	99.41	83.50
GM-18	OB	GM_18_2_TMTE_4_5	0.06	8.17	0.79	51.98	0.05	0.00	37.02	1.26	0.21	0.01	99.73	83.79
GM-18	OB	GM_18_2_TMTE_4_6	0.09	8.27	0.81	52.18	0.04	0.00	37.16	1.25	0.22	0.02	100.30	84.11

Table 3: (continued)

Sample	Eruptive Unit	Analysis	SiO_2	TiO_2	Al_2O_3	Fe_2O_3	V_2O_3	Cr_2O_3	FeO	MnO	MgO	CaO	Total	FeO^T
GM-18	OB	GM_18_2_TMTE_4_7	0.08	8.16	0.79	52.14	0.03	0.00	37.01	1.29	0.23	0.01	100.00	83.93
GM-18	OB	GM_18_2_TMTE_4_8	0.10	8.34	0.78	52.03	0.02	0.00	37.29	1.27	0.23	0.01	100.24	84.11
GM-18	OB	GM_18_2_TMTE_4_9	0.08	8.26	0.82	52.11	0.05	0.00	37.18	1.29	0.22	0.00	100.23	84.07
GM-18	OB	GM_18_2_TMTE_4_10	0.06	8.24	0.75	52.01	0.05	0.00	36.93	1.31	0.22	0.01	99.82	83.73
GM-18	OB	GM_18_2_TMTE_4_11	0.09	7.99	0.79	52.31	0.05	0.00	36.85	1.24	0.21	0.01	99.81	83.92
GM-18	OB	GM_18_2_TMTE_4_12	0.06	8.11	0.79	52.52	0.03	0.00	37.00	1.31	0.22	0.01	100.27	84.26
GM-18	OB	GM_18_2_TMTE_4_13	0.05	8.11	0.86	52.44	0.04	0.00	36.98	1.35	0.20	0.00	100.30	84.17
GM-18	OB	GM_18_2_TMTE_4_14	0.07	7.92	0.81	52.63	0.02	0.00	36.78	1.29	0.23	0.00	99.97	84.14
GM-18	OB	GM_18_2_TMTE_4_15	0.08	8.08	0.79	52.38	0.02	0.00	36.70	1.31	0.23	0.03	99.92	83.83
GM-18	OB	GM_18_2_TMTE_4_16	0.07	8.15	0.79	52.17	0.03	0.00	36.93	1.28	0.21	0.01	99.88	83.87
GM-18	OB	GM_18_2_TMTE_4_17	0.07	8.25	0.84	52.05	0.03	0.00	37.14	1.25	0.23	0.01	100.13	83.98
GM-18	OB	GM_18_2_TMTE_4_18	0.07	8.25	0.81	51.84	0.03	0.00	37.14	1.23	0.21	0.01	99.79	83.79
GM-18	OB	GM_18_2_TMTE_4_19	0.06	8.20	0.79	52.27	0.06	0.00	36.96	1.30	0.21	0.05	100.03	83.99
GM-18	OB	GM_18_2_TMTE_4_20	0.10	8.18	0.80	52.18	0.05	0.00	37.00	1.26	0.22	0.03	100.04	83.95
GM-18	OB	GM_18_2_TMTE_4_21	0.08	8.21	0.77	52.26	0.03	0.00	37.12	1.27	0.20	0.01	100.21	84.14
GM-18	OB	GM_18_2_TMTE_4_22	0.06	8.38	0.82	51.92	0.06	0.00	37.22	1.26	0.21	0.01	100.27	83.95
GM-18	OB	GM_18_2_TMTE_4_23	0.04	8.38	0.80	51.89	0.06	0.00	37.29	1.30	0.22	0.01	100.17	83.99
GM-18	OB	GM_18_2_TMTE_5_1	0.08	8.29	0.76	51.82	0.04	0.00	36.98	1.27	0.24	0.01	99.77	83.61
GM-18	OB	GM_18_2_TMTE_5_2	0.10	8.24	0.76	52.11	0.05	0.00	37.04	1.32	0.21	0.01	100.13	83.93
GM-18	OB	GM_18_2_TMTE_5_3	0.13	8.36	0.76	51.61	0.02	0.00	37.30	1.29	0.22	0.02	99.89	83.74
GM-18	OB	GM_18_2_TMTE_5_4	0.07	8.35	0.82	51.64	0.04	0.00	37.03	1.32	0.22	0.01	99.72	83.50
GM-18	OB	GM_18_2_TMTE_5_5	0.08	8.22	0.78	51.84	0.03	0.00	36.87	1.30	0.22	0.01	99.61	83.52
GM-18	OB	GM_18_2_TMTE_5_6	0.08	8.31	0.76	51.67	0.05	0.00	37.04	1.33	0.23	0.01	99.70	83.53
GM-18	OB	GM_18_2_TMTE_5_7	0.07	8.27	1.33	51.14	0.03	0.00	37.14	1.26	0.21	0.00	99.73	83.16
GM-18	OB	GM_18_2_TMTE_5_8	0.09	8.23	0.78	52.02	0.04	0.00	37.00	1.33	0.21	0.01	99.93	83.81
GM-18	OB	GM_18_2_TMTE_5_9	0.07	8.23	0.76	51.81	0.03	0.00	36.91	1.33	0.23	0.01	99.57	83.52
GM-18	OB	GM_18_2_TMTE_5_10	0.09	8.35	0.80	51.70	0.06	0.00	37.32	1.29	0.24	0.04	100.05	83.84
GM-18	OB	GM_18_2_TMTE_5_11	0.11	8.30	0.85	51.47	0.04	0.00	37.09	1.28	0.21	0.00	99.57	83.41
GM-18	OB	GM_18_2_TMTE_5_12	0.10	8.32	0.76	51.72	0.05	0.00	37.12	1.34	0.22	0.01	99.87	83.65
GM-18	OB	GM_18_2_TMTE_5_13	0.10	8.16	0.82	51.66	0.03	0.00	36.92	1.27	0.23	0.02	99.44	83.41
GM-18	OB	GM_18_2_TMTE_5_14	0.07	8.46	0.79	51.75	0.05	0.00	37.32	1.28	0.23	0.01	100.16	83.89
GM-18	OB	GM_18_2_TMTE_5_15	0.12	8.33	0.80	51.79	0.03	0.00	37.28	1.29	0.22	0.01	100.08	83.88
GM-18	OB	GM_18_2_TMTE_5_16	0.10	8.33	0.77	52.28	0.05	0.00	37.23	1.32	0.23	0.02	100.60	84.27

Table 3: (continued)

Sample	Eruptive Unit	Analysis	SiO_2	TiO_2	Al_2O_3	Fe_2O_3	V_2O_3	Cr_2O_3	FeO	MnO	MgO	CaO	Total	FeO^T
GM-18	OB	GM_18_2_TMTE_5_17	0.08	8.40	0.78	51.89	0.02	0.00	37.20	1.29	0.22	0.01	100.17	83.88
GM-18	OB	GM_18_2_TMTE_5_18	0.07	8.25	0.78	52.04	0.04	0.00	37.10	1.27	0.22	0.01	100.03	83.92
GM-18	OB	GM_18_2_TMTE_5_19	0.10	8.24	0.76	51.78	0.03	0.00	37.10	1.32	0.21	0.01	99.70	83.70
GM-18	OB	GM_18_2_TMTE_6_1	0.07	7.64	0.82	53.19	0.05	0.00	35.98	1.80	0.21	0.01	100.11	83.84
GM-18	OB	GM_18_2_TMTE_6_2	0.07	7.75	0.79	52.76	0.04	0.00	35.98	1.80	0.19	0.00	99.72	83.46
GM-18	OB	GM_18_2_TMTE_6_3	0.11	7.80	0.77	52.78	0.02	0.00	35.97	1.80	0.21	0.02	99.88	83.46
GM-18	OB	GM_18_2_TMTE_6_4	0.12	7.46	0.78	53.28	0.04	0.00	35.77	1.81	0.20	0.00	99.82	83.71
GM-18	OB	GM_18_2_TMTE_6_5	0.12	7.72	0.80	52.59	0.03	0.00	36.07	1.76	0.19	0.01	99.60	83.39
GM-18	OB	GM_18_2_TMTE_6_7	0.11	7.49	0.78	53.13	0.02	0.00	35.85	1.71	0.18	0.01	99.59	83.66
GM-18	OB	GM_18_2_TMTE_6_8	0.10	7.71	0.80	53.08	0.05	0.00	36.01	1.78	0.20	0.01	100.11	83.78
GM-18	OB	GM_18_2_TMTE_6_9	0.12	7.46	0.79	53.07	0.02	0.00	35.71	1.75	0.21	0.01	99.47	83.47
GM-18	OB	GM_18_2_TMTE_6_10	0.11	7.61	0.81	52.96	0.04	0.00	35.98	1.74	0.20	0.01	99.76	83.63
GM-18	OB	GM_18_2_TMTE_6_11	0.12	7.50	0.79	53.05	0.05	0.00	35.78	1.75	0.19	0.00	99.57	83.51
GM-18	OB	GM_18_2_TMTE_6_12	0.09	7.63	0.78	52.89	0.04	0.00	35.91	1.78	0.20	0.01	99.62	83.50
GM-18	OB	GM_18_2_TMTE_6_14	0.08	6.99	0.98	53.53	0.05	0.00	35.22	1.72	0.19	0.02	99.14	83.38
GM-18	OB	GM_18_2_TMTE_7_1	0.14	8.01	0.81	52.51	0.05	0.00	36.90	1.32	0.24	0.02	100.24	84.15
GM-18	OB	GM_18_2_TMTE_7_2	0.18	8.19	0.78	51.91	0.05	0.00	37.18	1.33	0.23	0.01	100.08	83.90
GM-18	OB	GM_18_2_TMTE_7_3	0.18	8.10	0.77	52.27	0.03	0.00	37.02	1.35	0.23	0.02	100.18	84.06
GM-18	OB	GM_18_2_TMTE_7_4	0.16	8.08	0.78	51.93	0.05	0.00	37.03	1.32	0.21	0.01	99.76	83.76
GM-18	OB	GM_18_2_TMTE_7_5	0.16	8.20	0.79	51.78	0.04	0.00	36.97	1.37	0.24	0.00	99.82	83.57
GM-18	OB	GM_18_2_TMTE_7_6	0.15	8.17	0.77	51.92	0.06	0.00	36.86	1.35	0.23	0.02	99.81	83.57
GM-18	OB	GM_18_2_TMTE_7_7	0.19	8.18	0.76	51.75	0.03	0.00	37.14	1.29	0.25	0.02	99.83	83.71
GM-18	OB	GM_18_2_TMTE_7_8	0.13	8.05	0.76	52.23	0.06	0.00	36.77	1.28	0.22	0.03	99.80	83.77
GM-18	OB	GM_18_2_TMTE_8_1	0.11	8.15	0.75	52.02	0.05	0.00	36.91	1.29	0.21	0.01	99.79	83.72
GM-18	OB	GM_18_2_TMTE_8_2	0.13	8.15	0.75	52.05	0.03	0.00	36.94	1.31	0.22	0.01	99.82	83.78
GM-18	OB	GM_18_2_TMTE_8_3	0.08	8.07	0.82	52.33	0.01	0.00	36.89	1.33	0.22	0.00	99.99	83.98
GM-18	OB	GM_18_2_TMTE_8_4	0.13	8.08	0.83	52.16	0.03	0.00	36.98	1.32	0.20	0.00	100.01	83.92
GM-18	OB	GM_18_2_TMTE_8_5	0.14	8.04	0.76	52.25	0.04	0.00	36.86	1.33	0.20	0.01	99.88	83.88
GM-18	OB	GM_18_2_TMTE_8_6	0.12	8.03	0.80	52.13	0.03	0.00	36.81	1.33	0.22	0.01	99.75	83.72
GM-18	OB	GM_18_2_TMTE_8_7	0.12	8.04	0.77	52.11	0.05	0.00	36.98	1.26	0.21	0.01	99.74	83.87
GM-18	OB	GM_18_2_TMTE_8_8	0.12	8.15	0.78	51.90	0.04	0.00	36.94	1.25	0.24	0.00	99.65	83.64
GM-18	OB	GM_18_2_TMTE_8_9	0.14	8.15	0.76	51.97	0.03	0.00	37.00	1.32	0.21	0.00	99.82	83.76
GM-18	OB	GM_18_2_TMTE_8_10	0.12	7.97	0.78	52.24	0.04	0.00	36.64	1.34	0.22	0.01	99.66	83.65

Table 3: (continued)

Sample	Eruptive Unit	Analysis	SiO_2	TiO_2	Al_2O_3	Fe_2O_3	V_2O_3	Cr_2O_3	FeO	MnO	MgO	CaO	Total	FeO^T
GM-18	OB	GM_18_2_TMTE_8_11	0.13	7.95	0.83	52.00	0.05	0.00	36.81	1.31	0.22	0.02	99.50	83.60
GM-18	OB	GM_18_2_TMTE_8_12	0.17	7.60	0.86	52.60	0.03	0.00	36.46	1.28	0.23	0.01	99.47	83.79
GM-18	OB	GM_18_2_TMTE_8_13	0.14	7.78	0.80	52.59	0.05	0.00	36.80	1.32	0.20	0.02	99.86	84.12
GM-18	OB	GM_18_2_TMTE_8_14	0.13	8.08	0.79	51.88	0.03	0.00	36.85	1.31	0.20	0.00	99.53	83.53
GM-18	OB	GM_18_2_TMTE_8_15	0.12	8.08	0.79	52.09	0.05	0.00	36.90	1.35	0.23	0.01	99.86	83.77
GM-18	OB	GM_18_2_TMTE_8_16	0.13	8.11	0.79	51.57	0.03	0.00	36.76	1.29	0.22	0.01	99.17	83.17
GM-18	OB	GM_18_2_TMTE_8_17	0.14	7.93	0.77	52.20	0.04	0.00	36.88	1.26	0.21	0.01	99.58	83.85
GM-18	OB	GM_18_2_TMTE_8_18	0.13	8.10	0.77	51.85	0.04	0.00	36.77	1.29	0.22	0.02	99.45	83.42
GM-18	OB	GM_18_2_TMTE_8_19	0.09	8.06	0.72	52.08	0.01	0.00	36.86	1.26	0.20	0.01	99.50	83.72
GM-18	OB	GM_18_2_TMTE_9_1	0.16	8.06	0.80	51.89	0.05	0.00	37.01	1.27	0.21	0.02	99.67	83.70
GM-18	OB	GM_18_2_TMTE_9_2	0.12	7.92	0.79	52.30	0.04	0.00	36.57	1.33	0.24	0.02	99.55	83.63
GM-18	OB	GM_18_2_TMTE_9_3	0.13	7.98	0.81	52.20	0.06	0.00	36.82	1.36	0.22	0.01	99.78	83.79
GM-18	OB	GM_18_2_TMTE_9_4	0.14	7.91	0.78	52.15	0.02	0.00	36.59	1.35	0.22	0.00	99.39	83.52
GM-18	OB	GM_18_2_TMTE_9_5	0.13	7.99	0.87	52.16	0.05	0.00	36.88	1.29	0.23	0.00	99.82	83.82
GM-18	OB	GM_18_2_TMTE_9_6	0.13	7.95	0.86	52.19	0.04	0.00	36.68	1.32	0.23	0.00	99.69	83.64
GM-18	OB	GM_18_2_TMTE_9_7	0.14	7.91	0.80	52.41	0.03	0.00	36.73	1.30	0.24	0.00	99.86	83.89
GM-18	OB	GM_18_2_TMTE_9_8	0.10	7.81	0.78	52.44	0.02	0.00	36.72	1.27	0.21	0.02	99.53	83.90
GM-18	OB	GM_18_2_TMTE_9_9	0.14	7.76	0.83	52.32	0.04	0.00	36.59	1.27	0.21	0.01	99.40	83.67
GM-18	OB	GM_18_2_TMTE_9_10	0.11	8.11	0.81	51.97	0.05	0.00	36.81	1.29	0.24	0.01	99.66	83.58
GM-18	OB	GM_18_2_TMTE_9_11	0.11	7.62	0.85	52.66	0.05	0.00	36.40	1.23	0.22	0.02	99.31	83.79
GM-18	OB	GM_18_2_TMTE_9_12	0.12	7.65	0.83	52.62	0.04	0.00	36.40	1.23	0.23	0.01	99.34	83.75
GM-18	OB	GM_18_2_TMTE_9_13	0.12	7.70	0.80	52.65	0.03	0.00	36.51	1.28	0.22	0.00	99.53	83.89
GM-18	OB	GM_18_2_TMTE_9_14	0.14	7.81	0.85	52.33	0.03	0.00	36.60	1.32	0.23	0.00	99.52	83.69
GM-18	OB	GM_18_2_TMTE_9_15	0.14	7.57	0.75	52.70	0.03	0.00	36.34	1.27	0.20	0.01	99.24	83.77
GM-18	OB	GM_18_2_TMTE_9_16	0.14	7.61	0.82	52.80	0.07	0.00	36.41	1.29	0.22	0.02	99.62	83.92
GM-18	OB	GM_18_2_TMTE_9_17	0.13	7.80	0.82	52.54	0.07	0.00	36.68	1.29	0.22	0.00	99.77	83.96
GM-18	OB	GM_18_2_TMTE_9_18	0.11	7.73	0.77	52.50	0.04	0.00	36.41	1.33	0.23	0.01	99.37	83.65
GM-18	OB	GM_18_2_TMTE_9_19	0.12	7.77	0.80	52.60	0.04	0.00	36.66	1.25	0.21	0.00	99.70	83.99
GM-18	OB	GM_18_2_TMTE_9_20	0.12	7.65	0.82	52.97	0.05	0.00	36.56	1.29	0.24	0.00	99.92	84.23
GM-18	OB	GM_18_2_TMTE_9_21	0.13	7.76	0.79	52.40	0.04	0.00	36.65	1.26	0.21	0.01	99.43	83.80
GM-18	OB	GM_18_2_TMTE_9_22	0.14	7.59	0.78	53.02	0.03	0.00	36.57	1.24	0.23	0.01	99.88	84.28
GM-18	OB	GM_18_2_TMTE_10_1	0.11	8.65	0.82	51.00	0.04	0.00	37.40	1.31	0.24	0.00	99.79	83.29
GM-18	OB	GM_18_2_TMTE_10_2	0.12	8.56	0.83	51.21	0.04	0.00	37.42	1.27	0.23	0.00	99.93	83.50

Table 3: (continued)

Sample	Eruptive Unit	Analysis	SiO_2	TiO_2	Al_2O_3	Fe_2O_3	V_2O_3	Cr_2O_3	FeO	MnO	MgO	CaO	Total	FeO^T
GM-18	OB	GM_18_2_TMTE_10_3	0.11	8.58	0.77	51.26	0.06	0.00	37.49	1.30	0.23	0.01	99.99	83.61
GM-18	OB	GM_18_2_TMTE_10_4	0.16	8.71	0.79	51.02	0.06	0.00	37.66	1.27	0.25	0.00	100.17	83.57
GM-18	OB	GM_18_2_TMTE_10_5	0.11	8.67	0.76	50.94	0.07	0.00	37.48	1.28	0.23	0.00	99.74	83.32
GM-18	OB	GM_18_2_TMTE_10_6	0.11	8.63	0.82	51.01	0.06	0.00	37.34	1.31	0.24	0.01	99.78	83.24
GM-18	OB	GM_18_2_TMTE_10_7	0.16	8.74	0.91	50.73	0.06	0.00	37.63	1.25	0.22	0.02	99.97	83.27
GM-18	OB	GM_18_2_TMTE_10_8	0.19	8.58	0.81	51.26	0.03	0.00	37.66	1.26	0.24	0.01	100.27	83.78
GM-18	OB	GM_18_2_TMTE_10_9	0.14	8.74	0.77	51.25	0.05	0.00	37.86	1.29	0.22	0.01	100.49	83.98
GM-18	OB	GM_18_2_TMTE_10_10	0.14	8.65	0.79	51.32	0.04	0.00	37.63	1.27	0.22	0.01	100.33	83.81
GM-18	OB	GM_18_2_TMTE_10_11	0.11	8.34	0.78	51.19	0.04	0.00	36.88	1.31	0.23	0.02	99.09	82.94
GM-18	OB	GM_18_2_TMTE_10_12	0.12	8.62	0.76	51.17	0.05	0.00	37.38	1.28	0.24	0.01	99.86	83.43
GM-18	OB	GM_18_2_TMTE_10_13	0.13	8.68	0.79	51.11	0.04	0.00	37.49	1.27	0.23	0.01	100.07	83.49
GM-18	OB	GM_18_2_TMTE_10_14	0.13	8.65	0.80	51.31	0.04	0.00	37.71	1.23	0.22	0.00	100.32	83.88
GM-18	OB	GM_18_2_TMTE_10_15	0.12	8.57	0.84	51.28	0.05	0.00	37.47	1.29	0.23	0.00	100.10	83.62
GM-18	OB	GM_18_2_TMTE_11_1	0.13	7.72	0.82	52.85	0.03	0.00	36.71	1.27	0.22	0.00	99.98	84.27
GM-18	OB	GM_18_2_TMTE_11_2	0.13	7.41	0.80	52.98	0.04	0.00	36.14	1.25	0.22	0.01	99.21	83.82
GM-18	OB	GM_18_2_TMTE_11_3	0.17	7.48	0.84	53.12	0.04	0.00	36.50	1.31	0.21	0.02	99.95	84.30
GM-18	OB	GM_18_2_TMTE_11_4	0.14	7.73	0.77	52.74	0.04	0.00	36.67	1.30	0.22	0.01	99.83	84.13
GM-18	OB	GM_18_2_TMTE_11_5	0.14	7.81	0.74	53.03	0.02	0.00	36.81	1.33	0.22	0.01	100.39	84.53
GM-18	OB	GM_18_2_TMTE_11_6	0.15	7.57	0.77	53.10	0.05	0.00	36.53	1.29	0.20	0.00	99.91	84.31
GM-18	OB	GM_18_2_TMTE_11_7	0.14	7.54	0.79	53.22	0.03	0.00	36.61	1.23	0.21	0.01	100.01	84.51
GM-18	OB	GM_18_2_TMTE_11_8	0.16	7.47	0.76	52.91	0.04	0.00	36.36	1.29	0.21	0.01	99.41	83.97
GM-18	OB	GM_18_2_TMTE_11_9	0.10	7.76	0.81	52.99	0.02	0.00	36.68	1.29	0.23	0.00	100.13	84.37
GM-18	OB	GM_18_2_TMTE_11_10	0.15	7.98	0.73	52.66	0.07	0.00	37.02	1.33	0.24	0.01	100.37	84.41
GM-18	OB	GM_18_2_TMTE _12_1	0.19	8.11	0.80	51.83	0.02	0.00	37.09	1.22	0.21	0.00	99.73	83.73
GM-18	OB	GM_18_2_TMTE _12_2	0.18	7.93	0.78	52.26	0.04	0.00	36.97	1.24	0.21	0.00	99.83	84.00
GM-18	OB	GM_18_2_TMTE _12_3	0.19	8.22	0.77	51.49	0.03	0.00	37.18	1.29	0.20	0.02	99.61	83.52
GM-18	OB	GM_18_2_TMTE _12_4	0.20	7.60	0.81	52.76	0.04	0.00	36.58	1.21	0.22	0.00	99.68	84.05
GM-18	OB	GM_18_2_TMTE _12_5	0.17	7.89	0.80	52.24	0.04	0.00	36.87	1.22	0.21	0.01	99.66	83.88
GM-18	OB	GM_18_2_TMTE _12_6	0.15	7.98	0.79	51.96	0.05	0.00	36.83	1.23	0.22	0.00	99.45	83.58
GM-18	OB	GM_18_2_TMTE _12_7	0.18	8.17	0.78	51.80	0.05	0.00	37.23	1.27	0.21	0.02	99.91	83.84
GM-18	OB	GM_18_2_TMTE _12_8	0.18	7.97	0.83	52.22	0.02	0.00	36.94	1.30	0.23	0.00	99.88	83.93
GM-18	OB	GM_18_2_TMTE_13_1	0.10	8.28	0.76	51.82	0.05	0.00	36.68	1.66	0.20	0.01	99.84	83.32
GM-18	OB	GM_18_2_TMTE_13_2	0.09	8.26	0.75	51.67	0.03	0.00	36.63	1.62	0.23	0.02	99.53	83.13

Table 3: (continued)

Sample	Eruptive Unit	Analysis	SiO_2	TiO_2	Al_2O_3	Fe_2O_3	V_2O_3	Cr_2O_3	FeO	MnO	MgO	CaO	Total	FeO^T
GM-18	OB	GM_18_2_TMTE_13_3	0.10	8.05	0.79	52.23	0.01	0.00	36.53	1.64	0.21	0.01	99.87	83.53
GM-18	OB	GM_18_2_TMTE_13_4	0.10	8.25	0.77	51.75	0.05	0.00	36.56	1.64	0.20	0.01	99.66	83.13
GM-18	OB	GM_18_2_TMTE_13_5	0.09	8.27	0.76	51.91	0.06	0.00	36.68	1.69	0.22	0.00	99.96	83.39
GM-18	OB	GM_18_2_TMTE_13_6	0.10	8.20	0.80	51.74	0.05	0.00	36.61	1.64	0.21	0.01	99.63	83.17
GM-18	OB	GM_18_2_TMTE_13_7	0.11	8.22	0.74	52.09	0.04	0.00	36.55	1.75	0.21	0.00	100.06	83.42
GM-18	OB	GM_18_2_TMTE_13_8	0.07	8.23	0.79	51.61	0.04	0.00	36.43	1.66	0.21	0.01	99.40	82.87
GM-18	OB	GM_18_2_TMTE_13_9	0.10	8.21	0.75	51.87	0.04	0.00	36.64	1.63	0.20	0.00	99.72	83.31
GM-18	OB	GM_18_2_TMTE_13_10	0.09	8.23	0.77	51.83	0.02	0.00	36.62	1.64	0.23	0.01	99.69	83.26
GM-18	OB	GM_18_2_TMTE_13_11	0.08	8.14	0.77	52.27	0.05	0.00	36.47	1.64	0.21	0.02	99.96	83.50
GM-18	OB	GM_18_2_TMTE_13_12	0.09	8.04	0.82	52.34	0.05	0.00	36.62	1.64	0.21	0.02	100.10	83.72
GM-18	OB	GM_18_2_TMTE_13_13	0.08	8.20	0.75	52.23	0.02	0.00	36.71	1.59	0.19	0.01	100.05	83.71
GM-18	OB	GM_18_2_TMTE_13_14	0.10	7.23	0.73	53.39	0.05	0.00	35.71	1.54	0.17	0.00	99.20	83.75
GM-18	OB	GM_18_2_TMTE_13_16	0.10	7.43	0.72	53.08	0.03	0.00	35.84	1.57	0.19	0.00	99.22	83.60
GM-18	OB	GM_18_2_TMTE_13_17	0.07	7.33	0.77	53.21	0.03	0.00	35.67	1.51	0.21	0.01	99.09	83.55
GM-18	OB	GM_18_2_TMTE_13_18	0.09	7.34	0.79	52.99	0.03	0.00	35.61	1.59	0.20	0.01	98.96	83.29
GM-18	OB	GM_18_2_TMTE_13_19	0.08	7.86	0.79	52.10	0.05	0.00	36.04	1.61	0.22	0.01	99.02	82.92
GM-18	OB	GM_18_2_TMTE_13_20	0.10	7.95	0.80	51.83	0.04	0.00	36.23	1.57	0.22	0.00	99.03	82.87
GM-18	OB	GM_18_2_TMTE_13_21	0.13	7.69	0.79	52.53	0.03	0.00	36.10	1.56	0.22	0.00	99.35	83.37
GM-18	OB	GM_18_2_TMTE_14_1	0.08	8.01	0.79	51.95	0.04	0.00	36.40	1.47	0.20	0.01	99.24	83.14
GM-18	OB	GM_18_2_TMTE_14_2	0.08	8.24	0.78	51.95	0.05	0.00	36.90	1.38	0.20	0.01	99.86	83.64
GM-18	OB	GM_18_2_TMTE_14_3	0.08	8.11	0.83	52.16	0.02	0.00	36.92	1.37	0.20	0.00	99.91	83.86
GM-18	OB	GM_18_2_TMTE_14_4	0.08	8.00	0.80	52.35	0.03	0.00	36.84	1.32	0.22	0.02	99.90	83.95
GM-18	OB	GM_18_2_TMTE_14_5	0.02	8.03	0.81	52.05	0.05	0.00	36.54	1.42	0.20	0.00	99.32	83.38
GM-18	OB	GM_18_2_TMTE_14_6	0.05	8.11	0.76	52.20	0.01	0.00	36.73	1.39	0.23	0.00	99.74	83.71
GM-18	OB	GM_18_2_TMTE_14_7	0.08	8.10	0.82	52.05	0.05	0.00	36.56	1.55	0.22	0.00	99.72	83.40
GM-18	OB	GM_18_2_TMTE_14_8	0.10	7.89	0.80	52.52	0.04	0.00	36.28	1.64	0.22	0.00	99.83	83.54
GM-18	OB	GM_18_2_TMTE_14_9	0.10	7.81	0.76	52.44	0.02	0.00	36.30	1.58	0.21	0.01	99.44	83.48
GM-18	OB	GM_18_2_TMTE_14_10	0.09	7.68	0.76	52.74	0.04	0.00	36.01	1.65	0.20	0.00	99.47	83.47
GM-18	OB	GM_18_2_TMTE_14_11	0.08	7.87	0.78	52.64	0.03	0.00	36.30	1.59	0.20	0.01	99.82	83.67
GM-18	OB	GM_18_2_TMTE_14_12	0.06	7.91	0.83	52.60	0.04	0.00	36.51	1.55	0.17	0.01	99.94	83.84
GM-18	OB	GM_18_2_TMTE_14_13	0.07	7.86	0.81	52.01	0.04	0.00	36.30	1.51	0.20	0.01	99.03	83.10
GM-18	OB	GM_18_2_TMTE_14_14	0.08	7.91	0.81	52.27	0.03	0.00	36.45	1.52	0.20	0.01	99.50	83.49
GM-18	OB	GM_18_2_TMTE_14_15	0.07	8.06	0.85	52.13	0.04	0.00	36.60	1.46	0.20	0.01	99.71	83.51

Table 3: (continued)

Sample	Eruptive Unit	Analysis	SiO_2	TiO_2	Al_2O_3	Fe_2O_3	V_2O_3	Cr_2O_3	FeO	MnO	MgO	CaO	Total	FeO^T
GM-18	OB	GM_18_2_TMTE_14_16	0.09	8.06	0.86	52.47	0.03	0.00	36.85	1.46	0.22	0.00	100.30	84.06
GM-18	OB	GM_18_2_TMTE_14_17	0.05	8.05	0.79	52.09	0.05	0.00	36.50	1.49	0.22	0.01	99.48	83.37
GM-18	OB	GM_18_2_TMTE_15_1	0.10	7.95	0.79	52.46	0.04	0.00	36.75	1.36	0.26	0.02	99.94	83.96
GM-18	OB	GM_18_2_TMTE_15_2	0.10	7.90	0.76	52.26	0.05	0.00	36.54	1.38	0.23	0.01	99.48	83.57
GM-18	OB	GM_18_2_TMTE_15_3	0.13	7.84	0.85	52.25	0.05	0.00	36.58	1.35	0.21	0.01	99.46	83.60
GM-18	OB	GM_18_2_TMTE_15_4	0.11	7.83	0.78	52.22	0.03	0.00	36.49	1.32	0.23	0.01	99.23	83.49
GM-18	OB	GM_18_2_TMTE_15_5	0.13	7.57	0.79	52.63	0.05	0.00	36.31	1.32	0.22	0.01	99.21	83.67
GM-18	OB	GM_18_2_TMTE_15_6	0.13	7.56	0.81	52.63	0.05	0.00	36.23	1.30	0.22	0.02	99.12	83.59
GM-18	OB	GM_18_2_TMTE_15_7	0.13	7.64	0.81	52.54	0.02	0.00	36.30	1.31	0.23	0.00	99.22	83.58
GM-18	OB	GM_18_2_TMTE_15_8	0.11	7.64	0.78	52.77	0.03	0.00	36.32	1.32	0.23	0.01	99.44	83.81
GM-18	OB	GM_18_2_TMTE_15_9	0.13	7.72	0.80	52.71	0.04	0.00	36.56	1.31	0.24	0.01	99.73	83.99
GM-18	OB	GM_18_2_TMTE_15_10	0.14	7.53	0.79	52.74	0.02	0.00	36.22	1.27	0.21	0.02	99.19	83.68
GM-18	OB	GM_18_2_TMTE_15_11	0.13	7.47	0.79	53.22	0.02	0.00	36.30	1.28	0.22	0.01	99.70	84.19
GM-18	OB	GM_18_2_TMTE_15_12	0.13	7.41	0.79	52.73	0.05	0.00	36.04	1.30	0.22	0.00	98.91	83.48
GM-18	OB	GM_18_2_TMTE_15_13	0.15	7.28	0.83	53.18	0.07	0.00	36.00	1.29	0.21	0.02	99.29	83.85
GM-18	OB	GM_18_2_TMTE_15_14	0.13	7.24	0.83	53.05	0.02	0.00	35.91	1.32	0.22	0.01	98.95	83.65
GM-18	OB	GM_18_2_TMTE_15_15	0.11	7.42	0.79	52.74	0.03	0.00	36.17	1.30	0.20	0.03	98.94	83.63
GM-18	OB	GM_18_2_TMTE_15_16	0.12	7.29	0.84	52.87	0.03	0.00	35.95	1.27	0.24	0.01	98.79	83.53
GM-18	OB	GM_18_2_TMTE_15_17	0.14	7.18	0.79	53.23	0.07	0.00	35.92	1.25	0.23	0.01	99.00	83.81
GM-18	OB	GM_18_2_TMTE_16_1	0.09	8.11	0.76	51.95	0.04	0.00	36.86	1.29	0.21	0.01	99.56	83.61
GM-18	OB	GM_18_2_TMTE_16_2	0.07	8.13	0.77	52.25	0.05	0.00	37.04	1.28	0.22	0.01	100.01	84.06
GM-18	OB	GM_18_2_TMTE_16_3	0.09	8.10	0.81	51.78	0.03	0.00	36.75	1.33	0.21	0.00	99.28	83.34
GM-18	OB	GM_18_2_TMTE_16_4	0.07	8.03	0.75	52.07	0.04	0.00	36.58	1.37	0.23	0.01	99.35	83.43
GM-18	OB	GM_18_2_TMTE_16_6	0.11	7.57	0.81	52.44	0.05	0.00	36.22	1.22	0.23	0.00	98.88	83.40
GM-18	OB	GM_18_2_TMTE_16_7	0.10	7.74	0.80	52.60	0.02	0.00	36.57	1.24	0.23	0.00	99.54	83.91
GM-18	OB	GM_18_2_TMTE_16_8	0.10	7.88	1.31	52.04	0.03	0.00	36.91	1.28	0.21	0.00	99.97	83.74
GM-18	OB	GM_18_2_TMTE_16_9	0.09	7.74	0.82	52.13	0.04	0.00	36.16	1.35	0.23	0.00	98.87	83.07
GM-18	OB	GM_18_2_TMTE_16_10	0.10	8.03	0.78	52.01	0.06	0.00	36.71	1.31	0.22	0.01	99.50	83.51
GM-18	OB	GM_18_2_TMTE_16_11	0.09	8.04	0.80	51.85	0.04	0.00	36.67	1.28	0.22	0.00	99.25	83.33
GM-18	OB	GM_18_2_TMTE_16_12	0.09	8.10	0.78	52.09	0.06	0.00	36.84	1.30	0.22	0.00	99.75	83.71
GM-18	OB	GM_18_2_TMTE_16_13	0.10	7.88	0.73	52.37	0.05	0.00	36.68	1.29	0.22	0.01	99.54	83.80
GM-18	OB	GM_18_2_TMTE_16_14	0.11	8.14	0.79	51.94	0.03	0.00	36.88	1.36	0.22	0.00	99.70	83.62
GM-18	OB	GM_18_2_TMTE_16_15	0.08	7.70	0.80	52.30	0.03	0.00	36.19	1.25	0.22	0.01	98.85	83.25

Table 3: (continued)

Sample	Eruptive Unit	Analysis	SiO_2	TiO_2	Al_2O_3	Fe_2O_3	V_2O_3	Cr_2O_3	FeO	MnO	MgO	CaO	Total	FeO^T
GM-18	OB	GM_18_2_TMTE_16_16	0.09	8.05	0.79	51.92	0.04	0.00	36.67	1.27	0.23	0.01	99.29	83.39
GM-18	OB	GM_18_2_TMTE_18_1	0.13	8.31	0.77	51.43	0.01	0.00	36.82	1.43	0.22	0.02	99.36	83.10
GM-18	OB	GM_18_2_TMTE_18_2	0.12	8.37	0.78	51.49	0.05	0.00	37.23	1.32	0.21	0.00	99.75	83.56
GM-18	OB	GM_18_2_TMTE_18_3	0.14	8.50	0.78	50.98	0.04	0.00	37.24	1.37	0.21	0.01	99.46	83.11
GM-18	OB	GM_18_2_TMTE_18_4	0.09	8.49	0.74	51.44	0.06	0.00	37.06	1.44	0.22	0.00	99.84	83.35
GM-18	OB	GM_18_2_TMTE_18_5	0.12	8.52	0.81	50.91	0.04	0.00	37.14	1.36	0.23	0.01	99.40	82.95
GM-18	OB	GM_18_2_TMTE_18_6	0.11	8.35	0.77	51.25	0.08	0.00	36.98	1.36	0.22	0.01	99.41	83.10
GM-18	OB	GM_18_2_TMTE_18_7	0.10	8.41	0.79	51.21	0.06	0.00	37.06	1.37	0.23	0.01	99.45	83.14
GM-18	OB	GM_18_2_TMTE_18_8	0.08	8.46	0.74	51.45	0.04	0.00	37.16	1.29	0.21	0.00	99.71	83.45
GM-18	OB	GM_18_2_TMTE_18_9	0.10	8.50	0.73	51.42	0.02	0.00	37.22	1.39	0.22	0.01	99.83	83.49
GM-18	OB	GM_18_2_TMTE_18_10	0.13	8.50	0.76	51.43	0.02	0.00	37.37	1.40	0.21	0.02	100.09	83.65
GM-18	OB	GM_18_2_TMTE_18_11	0.12	8.51	0.80	51.18	0.04	0.00	37.24	1.42	0.21	0.01	99.76	83.29
GM-18	OB	GM_18_2_TMTE_18_12	0.14	8.41	0.78	51.49	0.03	0.00	37.22	1.38	0.21	0.01	99.93	83.55
GM-18	OB	GM_18_2_TMTE_18_13	0.11	8.45	0.82	51.33	0.05	0.00	37.09	1.36	0.21	0.01	99.69	83.28
GM-18	OB	GM_18_2_TMTE_18_14	0.12	8.43	0.76	51.38	0.05	0.00	37.12	1.40	0.23	0.01	99.76	83.36
GM-18	OB	GM_18_2_TMTE_18_15	0.10	8.44	0.78	51.28	0.05	0.00	37.07	1.43	0.21	0.02	99.63	83.21
GM-18	OB	GM_18_2_TMTE_18_16	0.09	8.25	0.83	51.38	0.06	0.00	36.71	1.44	0.24	0.01	99.28	82.94
GM-18	OB	GM_18_2_TMTE_18_17	0.12	8.27	0.78	51.27	0.06	0.00	36.71	1.45	0.22	0.00	99.16	82.85
GM-18	OB	GM_18_2_TMTE_18_18	0.13	8.32	0.79	51.48	0.05	0.00	36.85	1.47	0.24	0.00	99.61	83.17
GM-18	OB	GM_18_2_TMTE_18_19	0.08	8.15	0.76	51.83	0.05	0.00	36.63	1.42	0.22	0.00	99.43	83.27
GM-18	OB	GM_18_2_TMTE_18_20	0.09	7.99	0.76	52.02	0.02	0.00	36.43	1.43	0.20	0.01	99.26	83.25
GM-18	OB	GM_18_2_TMTE_19_1	0.14	8.46	0.79	51.23	0.02	0.00	37.06	1.36	0.23	0.02	99.52	83.16
GM-18	OB	GM_18_2_TMTE_19_2	0.14	8.49	0.79	51.14	0.03	0.00	37.27	1.35	0.21	0.02	99.68	83.28
GM-18	OB	GM_18_2_TMTE_19_3	0.11	8.28	0.79	51.65	0.05	0.00	37.12	1.31	0.22	0.01	99.72	83.59
GM-18	OB	GM_18_2_TMTE_19_4	0.12	8.49	0.77	51.35	0.04	0.00	37.21	1.32	0.23	0.01	99.81	83.42
GM-18	OB	GM_18_2_TMTE_19_5	0.17	8.46	0.82	51.04	0.05	0.00	37.26	1.31	0.22	0.00	99.54	83.19
GM-18	OB	GM_18_2_TMTE_19_6	0.12	8.44	0.78	51.09	0.05	0.00	37.18	1.27	0.22	0.01	99.40	83.15
GM-18	OB	GM_18_2_TMTE_19_7	0.12	8.26	0.79	51.39	0.03	0.00	36.88	1.36	0.21	0.01	99.31	83.12
GM-18	OB	GM_18_2_TMTE_19_8	0.13	8.40	0.84	51.17	0.04	0.00	37.19	1.31	0.20	0.00	99.48	83.24
GM-18	OB	GM_18_2_TMTE_19_9	0.12	8.43	0.76	51.09	0.05	0.00	37.02	1.27	0.23	0.01	99.22	82.99
GM-18	OB	GM_18_2_TMTE_19_10	0.12	8.32	0.83	51.37	0.04	0.00	36.97	1.32	0.24	0.01	99.50	83.19
GM-18	OB	GM_18_2_TMTE_19_11	0.11	8.53	0.78	50.68	0.04	0.00	37.13	1.32	0.23	0.02	99.01	82.73
GM-18	OB	GM_18_2_TMTE_19_12	0.14	8.43	0.80	51.30	0.05	0.00	37.27	1.33	0.21	0.01	99.77	83.43

Table 3: (continued)

Sample	Eruptive Unit	Analysis	SiO_2	TiO_2	Al_2O_3	Fe_2O_3	V_2O_3	Cr_2O_3	FeO	MnO	MgO	CaO	Total	FeO^T
GM-18	OB	GM_18_2_TMTE_19_13	0.13	8.43	0.86	50.96	0.03	0.00	37.08	1.34	0.23	0.01	99.32	82.93
GM-18	OB	GM_18_2_TMTE_19_14	0.15	8.36	0.81	51.28	0.04	0.00	37.07	1.31	0.23	0.01	99.48	83.22
GM-18	OB	GM_18_2_TMTE_20_1	0.12	8.13	0.79	51.95	0.04	0.00	37.07	1.25	0.21	0.00	99.73	83.82
GM-18	OB	GM_18_2_TMTE_20_2	0.10	8.24	0.77	51.83	0.04	0.00	37.14	1.23	0.22	0.01	99.82	83.78
GM-18	OB	GM_18_2_TMTE_20_3	0.12	8.33	0.78	51.55	0.02	0.00	37.08	1.30	0.22	0.00	99.67	83.46
GM-18	OB	GM_18_2_TMTE_20_4	0.10	8.17	0.81	51.76	0.02	0.00	36.88	1.27	0.23	0.01	99.46	83.45
GM-18	OB	GM_18_2_TMTE_20_5	0.09	8.23	0.79	51.57	0.05	0.00	36.87	1.26	0.23	0.00	99.35	83.28
GM-18	OB	GM_18_2_TMTE_20_6	0.12	8.16	0.82	51.85	0.05	0.00	37.00	1.25	0.23	0.01	99.70	83.65
GM-18	OB	GM_18_2_TMTE_20_7	0.08	8.23	0.73	51.76	0.05	0.00	37.05	1.24	0.23	0.02	99.59	83.62
GM-18	OB	GM_18_2_TMTE_20_8	0.09	8.25	0.79	51.43	0.02	0.00	36.97	1.29	0.23	0.02	99.27	83.25
GM-18	OB	GM_18_2_TMTE_20_9	0.10	8.36	0.78	51.40	0.04	0.00	37.03	1.31	0.22	0.00	99.51	83.28
GM-18	OB	GM_18_2_TMTE_20_10	0.08	8.25	0.79	51.58	0.03	0.00	37.08	1.27	0.22	0.02	99.46	83.50
GM-18	OB	GM_18_2_TMTE_20_11	0.08	8.33	0.82	51.61	0.04	0.00	37.15	1.25	0.22	0.01	99.77	83.59
GM-18	OB	GM_18_2_TMTE_20_12	0.08	8.25	0.79	51.93	0.03	0.00	37.09	1.28	0.21	0.00	99.90	83.82
GM-18	OB	GM_18_2_TMTE_20_13	0.10	8.34	0.77	51.51	0.03	0.00	36.98	1.26	0.23	0.02	99.49	83.33
GM-18	OB	GM_18_2_TMTE_20_14	0.11	8.26	0.79	51.96	0.05	0.00	37.08	1.25	0.22	0.03	99.95	83.84
GM-18	OB	GM_18_2_TMTE_20_15	0.10	8.30	0.78	51.71	0.03	0.00	37.10	1.30	0.21	0.00	99.78	83.63
GM-18	OB	GM_18_2_TMTE_20_16	0.12	8.42	0.77	51.66	0.04	0.00	37.46	1.26	0.21	0.01	100.15	83.95
GM-18	OB	GM_18_2_TMTE_20_17	0.11	8.31	0.78	51.75	0.04	0.00	37.13	1.31	0.22	0.01	99.92	83.70
GM-18	OB	GM_18_2_TMTE_21_3	0.20	8.16	0.77	51.99	0.04	0.00	36.86	1.57	0.22	0.00	100.07	83.65
GM-18	OB	GM_18_2_TMTE_21_5	0.19	7.49	0.80	53.05	0.06	0.00	36.28	1.44	0.23	0.01	99.78	84.02
GM-18	OB	GM_18_2_TMTE_21_7	0.19	7.40	0.77	52.81	0.04	0.00	35.95	1.47	0.21	0.01	99.09	83.47
GM-18	OB	GM_18_2_TMTE_21_9	0.18	8.12	0.78	52.07	0.04	0.00	36.69	1.63	0.24	0.00	100.08	83.54
GM-18	OB	GM_18_2_TMTE_21_11	0.19	8.20	0.76	52.04	0.03	0.00	36.86	1.66	0.24	0.01	100.25	83.68
GM-18	OB	GM_18_2_TMTE_21_12	0.19	7.89	0.83	52.43	0.04	0.00	36.61	1.49	0.23	0.02	99.99	83.79
GM-18	OB	GM_18_2_TMTE_21_13	0.18	7.97	0.81	52.01	0.04	0.00	36.70	1.53	0.21	0.00	99.62	83.50
GM-18	OB	GM_18_3_TMTE_22_1	0.05	8.09	0.74	52.18	0.03	0.00	36.76	1.34	0.21	0.00	99.63	83.71
GM-18	OB	GM_18_3_TMTE_22_2	0.08	8.17	0.78	52.32	0.03	0.00	37.05	1.35	0.23	0.01	100.26	84.13
GM-18	OB	GM_18_3_TMTE_22_3	0.10	7.86	0.80	52.71	0.03	0.00	36.63	1.38	0.23	0.00	100.01	84.05
GM-18	OB	GM_18_3_TMTE_22_4	0.05	7.96	0.81	52.95	0.06	0.00	36.86	1.33	0.24	0.00	100.53	84.50
GM-18	OB	GM_18_3_TMTE_22_5	0.08	8.04	0.82	52.28	0.04	0.00	36.85	1.38	0.22	0.01	99.89	83.90
GM-18	OB	GM_18_3_TMTE_22_6	0.15	7.37	0.84	53.25	0.04	0.00	36.28	1.29	0.21	0.01	99.68	84.20
GM-18	OB	GM_18_3_TMTE_22_7	0.07	7.82	0.84	53.20	0.05	0.00	36.73	1.34	0.22	0.01	100.58	84.60

Table 3: (continued)

Sample	Eruptive Unit	Analysis	SiO_2	TiO_2	Al_2O_3	Fe_2O_3	V_2O_3	Cr_2O_3	FeO	MnO	MgO	CaO	Total	FeO^T
GM-18	OB	GM_18_3_TMTE_23_1	0.06	8.17	0.76	52.00	0.03	0.00	36.68	1.44	0.21	0.02	99.57	83.47
GM-18	OB	GM_18_3_TMTE_23_2	0.07	8.08	0.78	51.84	0.06	0.00	36.58	1.38	0.21	0.00	99.28	83.23
GM-18	OB	GM_18_3_TMTE_23_3	0.09	8.19	0.81	51.86	0.01	0.00	36.84	1.46	0.22	0.00	99.66	83.51
GM-18	OB	GM_18_3_TMTE_23_4	0.08	8.20	0.80	52.05	0.05	0.00	36.78	1.48	0.22	0.01	99.95	83.61
GM-18	OB	GM_18_3_TMTE_23_5	0.09	8.38	0.77	51.65	0.07	0.00	36.89	1.44	0.22	0.02	99.78	83.37
GM-18	OB	GM_18_3_TMTE_23_6	0.09	8.13	0.70	52.06	0.04	0.00	36.78	1.44	0.21	0.01	99.69	83.63
GM-18	OB	GM_18_3_TMTE_23_7	0.08	8.28	0.79	51.76	0.04	0.00	36.75	1.51	0.22	0.00	99.72	83.32
GM-18	OB	GM_18_3_TMTE_23_8	0.07	8.05	0.79	52.14	0.03	0.00	36.80	1.39	0.21	0.01	99.63	83.71
GM-18	OB	GM_18_3_TMTE_23_9	0.08	8.11	0.72	52.35	0.04	0.00	36.78	1.42	0.23	0.01	100.01	83.89
GM-18	OB	GM_18_3_TMTE_23_10	0.08	8.09	0.78	52.15	0.04	0.00	36.84	1.44	0.21	0.02	99.85	83.76
GM-18	OB	GM_18_3_TMTE_23_11	0.09	8.07	0.81	52.30	0.02	0.00	36.70	1.46	0.23	0.00	99.97	83.76
GM-18	OB	GM_18_3_TMTE_23_12	0.07	8.22	0.81	51.95	0.01	0.00	36.77	1.45	0.21	0.01	99.77	83.51
GM-18	OB	GM_18_3_TMTE_23_13	0.05	8.24	0.79	51.91	0.03	0.00	36.95	1.40	0.21	0.01	99.80	83.67
GM-18	OB	GM_18_3_TMTE_23_14	0.07	8.15	0.78	51.93	0.06	0.00	36.66	1.52	0.23	0.01	99.63	83.39
GM-18	OB	GM_18_3_TMTE_23_15	0.06	8.16	0.87	52.07	0.04	0.00	36.71	1.48	0.23	0.01	99.88	83.56
GM-18	OB	GM_18_3_TMTE_23_16	0.09	8.11	0.77	52.01	0.06	0.00	36.82	1.41	0.23	0.02	99.71	83.62
GM-18	OB	GM_18_3_TMTE_23_17	0.08	8.17	0.78	52.11	0.04	0.00	36.84	1.37	0.21	0.02	99.86	83.73
GM-18	OB	GM_18_3_TMTE_24_1	0.12	8.25	0.76	52.25	0.02	0.00	37.19	1.30	0.24	0.00	100.42	84.20
GM-18	OB	GM_18_3_TMTE_24_2	0.12	8.30	0.81	51.76	0.04	0.00	37.24	1.31	0.22	0.01	100.00	83.81
GM-18	OB	GM_18_3_TMTE_24_3	0.13	8.30	0.79	51.58	0.04	0.00	37.05	1.31	0.21	0.01	99.68	83.46
GM-18	OB	GM_18_3_TMTE_24_4	0.11	8.24	0.78	51.84	0.04	0.00	37.07	1.34	0.22	0.01	99.86	83.71
GM-18	OB	GM_18_3_TMTE_24_5	0.10	7.97	0.79	52.39	0.03	0.00	36.96	1.29	0.21	0.02	99.93	84.11
GM-18	OB	GM_18_3_TMTE_24_6	0.14	7.61	0.80	53.28	0.02	0.00	36.67	1.30	0.20	0.00	100.28	84.61
GM-18	OB	GM_18_3_TMTE_24_7	0.12	7.66	0.79	53.21	0.03	0.00	36.64	1.30	0.22	0.00	100.21	84.52
GM-18	OB	GM_18_3_TMTE_24_8	0.14	7.71	0.76	52.74	0.05	0.00	36.55	1.28	0.24	0.00	99.71	84.00
GM-18	OB	GM_18_3_TMTE_24_9	0.10	7.98	0.76	52.45	0.05	0.00	36.80	1.29	0.23	0.01	99.88	84.00
GM-18	OB	GM_18_3_TMTE_24_10	0.14	7.98	0.79	52.53	0.04	0.00	37.12	1.29	0.20	0.02	100.31	84.39
GM-18	OB	GM_18_3_TMTE_24_11	0.08	7.54	0.77	53.42	0.03	0.00	36.47	1.23	0.23	0.00	100.03	84.55
GM-18	OB	GM_18_3_TMTE_24_12	0.12	7.54	0.80	53.38	0.03	0.00	36.64	1.23	0.21	0.00	100.18	84.67
GM-18	OB	GM_18_3_TMTE_24_13	0.11	7.51	0.80	53.13	0.06	0.00	36.29	1.26	0.23	0.02	99.65	84.10
GM-18	OB	GM_18_3_TMTE_24_14	0.09	7.80	0.76	52.55	0.05	0.00	36.50	1.30	0.23	0.01	99.52	83.79
GM-18	OB	GM_18_3_TMTE_24_15	0.07	8.11	0.77	52.33	0.03	0.00	36.96	1.29	0.22	0.00	100.00	84.05
GM-18	OB	GM_18_3_TMTE_24_16	0.10	8.07	0.76	52.28	0.05	0.00	36.96	1.28	0.23	0.00	99.93	84.01

Table 3: (continued)

Sample	Eruptive Unit	Analysis	SiO_2	TiO_2	Al_2O_3	Fe_2O_3	V_2O_3	Cr_2O_3	FeO	MnO	MgO	CaO	Total	FeO^T
GM-18	OB	GM_18_3_TMTE_24_17	0.07	8.22	0.77	52.09	0.04	0.00	36.95	1.35	0.23	0.01	99.93	83.82
GM-18	OB	GM_18_3_TMTE_24_18	0.12	8.07	0.75	52.38	0.05	0.00	37.09	1.26	0.21	0.00	100.14	84.23
GM-18	OB	GM_18_3_TMTE_24_19	0.11	7.78	0.78	52.68	0.00	0.00	36.66	1.25	0.21	0.00	99.74	84.07
GM-18	OB	GM_18_3_TMTE_24_20	0.14	8.00	0.81	52.33	0.04	0.00	36.93	1.28	0.22	0.00	100.04	84.02
GM-18	OB	GM_18_3_TMTE_24_21	0.12	8.34	0.77	52.00	0.05	0.00	37.35	1.34	0.22	0.01	100.44	84.14
GM-18	OB	GM_18_3_TMTE_24_22	0.12	7.73	0.81	53.01	0.04	0.00	36.73	1.29	0.21	0.00	100.18	84.43
GM-18	OB	GM_18_3_TMTE_25_1	0.09	8.24	0.79	52.00	0.02	0.00	37.16	1.35	0.21	0.02	100.06	83.95
GM-18	OB	GM_18_3_TMTE_25_2	0.09	8.37	0.75	51.86	0.03	0.00	37.27	1.32	0.22	0.02	100.13	83.93
GM-18	OB	GM_18_3_TMTE_25_3	0.07	8.30	0.76	52.08	0.07	0.00	37.17	1.32	0.24	0.01	100.26	84.04
GM-18	OB	GM_18_3_TMTE_25_4	0.08	8.40	0.73	52.26	0.05	0.00	37.33	1.35	0.22	0.01	100.68	84.35
GM-18	OB	GM_18_3_TMTE_25_5	0.11	8.37	0.78	52.18	0.04	0.00	37.42	1.36	0.21	0.00	100.67	84.37
GM-18	OB	GM_18_3_TMTE_25_6	0.08	8.40	0.77	51.83	0.03	0.00	37.28	1.33	0.19	0.01	100.10	83.92
GM-18	OB	GM_18_3_TMTE_25_7	0.05	8.29	0.77	52.16	0.04	0.00	37.09	1.37	0.22	0.01	100.18	84.03
GM-18	OB	GM_18_3_TMTE_25_8	0.08	8.18	0.79	52.33	0.02	0.00	37.02	1.34	0.22	0.00	100.24	84.11
GM-18	OB	GM_18_3_TMTE_25_9	0.08	8.30	0.79	51.87	0.03	0.00	37.01	1.34	0.22	0.02	99.85	83.68
GM-18	OB	GM_18_3_TMTE_25_10	0.09	8.30	0.77	51.98	0.01	0.00	37.29	1.33	0.22	0.02	100.16	84.06
GM-18	OB	GM_18_3_TMTE_25_11	0.10	8.37	0.78	51.85	0.05	0.00	37.33	1.31	0.22	0.00	100.23	83.99
GM-18	OB	GM_18_3_TMTE_25_12	0.08	7.84	0.79	52.91	0.05	0.00	36.64	1.29	0.22	0.03	100.05	84.25
GM-18	OB	GM_18_3_TMTE_25_13	0.10	7.83	0.77	53.03	0.01	0.00	36.68	1.36	0.21	0.01	100.27	84.39
GM-18	OB	GM_18_3_TMTE_25_14	0.07	8.00	0.78	52.67	0.04	0.00	36.94	1.31	0.20	0.01	100.26	84.34
GM-18	OB	GM_18_3_TMTE_25_15	0.09	7.87	0.75	52.97	0.04	0.00	36.79	1.34	0.22	0.01	100.31	84.46
GM-18	OB	GM_18_3_TMTE_25_16	0.08	7.97	0.78	52.83	0.03	0.00	36.83	1.36	0.22	0.00	100.38	84.37
GM-18	OB	GM_18_3_TMTE_25_17	0.08	7.61	0.78	53.25	0.03	0.00	36.54	1.27	0.21	0.01	99.96	84.46
GM-18	OB	GM_18_3_TMTE_26_1	0.07	8.19	0.79	51.97	0.04	0.00	37.01	1.31	0.21	0.01	99.83	83.78
GM-18	OB	GM_18_3_TMTE_26_2	0.08	7.99	0.79	52.35	0.05	0.00	36.78	1.28	0.22	0.00	99.77	83.89
GM-18	OB	GM_18_3_TMTE_26_3	0.11	8.16	0.80	52.17	0.02	0.00	36.99	1.28	0.22	0.01	100.02	83.93
GM-18	OB	GM_18_3_TMTE_26_4	0.09	8.01	0.78	52.33	0.04	0.00	36.83	1.30	0.23	0.00	99.85	83.92
GM-18	OB	GM_18_3_TMTE_26_5	0.10	8.05	0.76	52.44	0.03	0.00	36.96	1.27	0.20	0.01	100.08	84.14
GM-18	OB	GM_18_3_TMTE_26_6	0.06	8.14	0.77	52.22	0.05	0.00	36.93	1.31	0.22	0.01	99.95	83.92
GM-18	OB	GM_18_3_TMTE_26_7	0.10	8.04	0.79	52.03	0.04	0.00	36.76	1.32	0.21	0.00	99.56	83.58
GM-18	OB	GM_18_3_TMTE_26_8	0.09	8.18	1.01	51.99	0.03	0.00	37.21	1.28	0.21	0.00	100.24	84.00
GM-18	OB	GM_18_3_TMTE_26_9	0.06	7.96	0.78	52.71	0.06	0.00	36.88	1.25	0.21	0.01	100.22	84.31
GM-18	OB	GM_18_3_TMTE_26_10	0.08	7.59	0.86	52.91	0.04	0.00	36.42	1.21	0.20	0.01	99.58	84.03

Table 3: (continued)

Sample	Eruptive Unit	Analysis	SiO_2	TiO_2	Al_2O_3	Fe_2O_3	V_2O_3	Cr_2O_3	FeO	MnO	MgO	CaO	Total	FeO^T
GM-18	OB	GM_18_3_TMTE_26_11	0.08	7.85	0.88	52.57	0.02	0.00	36.75	1.27	0.23	0.01	99.89	84.05
GM-18	OB	GM_18_3_TMTE_26_12	0.07	8.02	0.89	52.44	0.03	0.00	36.90	1.31	0.20	0.01	100.10	84.09
GM-18	OB	GM_18_3_TMTE_26_13	0.09	7.85	0.81	52.69	0.04	0.00	36.73	1.25	0.21	0.01	99.93	84.14
GM-18	OB	GM_18_3_TMTE_26_14	0.08	7.92	0.77	52.35	0.02	0.00	36.66	1.27	0.22	0.01	99.57	83.77
GM-18	OB	GM_18_3_TMTE_26_15	0.10	8.09	0.81	52.07	0.05	0.00	37.03	1.28	0.21	0.02	99.87	83.89
GM-18	OB	GM_18_3_TMTE_26_16	0.12	8.05	0.76	52.21	0.06	0.00	36.93	1.29	0.22	0.00	99.85	83.91
GM-18	OB	GM_18_3_TMTE_26_17	0.08	7.79	0.81	52.96	0.03	0.00	36.79	1.23	0.21	0.01	100.16	84.44
GM-18	OB	GM_18_3_TMTE_26_18	0.09	7.60	0.78	53.37	0.03	0.00	36.43	1.31	0.23	0.00	100.16	84.45
GM-18	OB	GM_18_3_TMTE_26_19	0.07	7.96	0.79	52.57	0.04	0.00	36.78	1.33	0.21	0.01	100.00	84.08
GM-18	OB	GM_18_3_TMTE_27_16	0.11	7.82	0.78	52.33	0.04	0.00	36.48	1.31	0.22	0.00	99.41	83.57
GM-18	OB	GM_18_3_TMTE_27_17	0.08	8.06	0.77	51.96	0.06	0.00	36.71	1.35	0.23	0.01	99.42	83.46
GM-18	OB	GM_18_3_TMTE_27_18	0.09	8.28	0.74	51.76	0.01	0.00	36.99	1.35	0.23	0.01	99.71	83.57
GM-18	OB	GM_18_3_TMTE_27_20	0.08	8.13	0.77	52.43	0.04	0.00	36.89	1.38	0.22	0.00	100.25	84.07
GM-18	OB	GM_18_3_TMTE_28_1	0.15	8.36	0.80	51.36	0.04	0.00	37.14	1.30	0.23	0.00	99.62	83.36
GM-18	OB	GM_18_3_TMTE_28_2	0.16	8.16	0.78	51.70	0.07	0.00	36.91	1.35	0.22	0.00	99.59	83.43
GM-18	OB	GM_18_3_TMTE_28_3	0.16	8.22	0.78	51.77	0.02	0.00	36.94	1.34	0.24	0.01	99.73	83.52
GM-18	OB	GM_18_3_TMTE_28_4	0.16	8.29	0.75	51.59	0.03	0.00	37.11	1.28	0.23	0.00	99.72	83.53
GM-18	OB	GM_18_3_TMTE_28_5	0.17	8.36	0.78	51.42	0.05	0.00	37.37	1.32	0.20	0.02	99.89	83.64
GM-18	OB	GM_18_3_TMTE_28_6	0.14	8.25	0.76	51.66	0.05	0.00	37.03	1.26	0.24	0.01	99.64	83.52
GM-18	OB	GM_18_3_TMTE_28_7	0.17	8.33	0.78	51.84	0.05	0.00	37.39	1.34	0.21	0.01	100.37	84.04
GM-18	OB	GM_18_3_TMTE_28_8	0.13	8.42	0.76	51.58	0.03	0.00	37.27	1.33	0.21	0.00	100.01	83.69
GM-18	OB	GM_18_3_TMTE_28_9	0.16	7.85	0.78	52.45	0.01	0.00	36.69	1.38	0.22	0.01	99.80	83.89
GM-18	OB	GM_18_3_TMTE_28_10	0.16	8.21	0.79	51.80	0.01	0.00	36.94	1.38	0.24	0.01	99.75	83.56
GM-18	OB	GM_18_3_TMTE_28_11	0.18	8.20	0.82	51.53	0.04	0.00	37.11	1.37	0.21	0.02	99.64	83.48
GM-18	OB	GM_18_3_TMTE_29_1	0.05	8.56	0.76	51.55	0.07	0.00	37.27	1.40	0.21	0.01	100.16	83.66
GM-18	OB	GM_18_3_TMTE_29_2	0.09	8.45	0.79	51.30	0.04	0.00	37.04	1.42	0.21	0.01	99.57	83.21
GM-18	OB	GM_18_3_TMTE_29_4	0.12	8.58	0.80	51.19	0.04	0.00	37.13	1.46	0.20	0.03	99.76	83.19
GM-18	OB	GM_18_3_TMTE_29_5	0.09	8.54	0.77	51.20	0.03	0.00	37.15	1.43	0.22	0.00	99.63	83.22
GM-18	OB	GM_18_3_TMTE_29_6	0.08	8.47	0.77	51.42	0.04	0.00	36.98	1.42	0.20	0.03	99.63	83.25
GM-18	OB	GM_18_3_TMTE_29_7	0.06	8.51	0.78	51.72	0.04	0.00	37.20	1.51	0.22	0.00	100.25	83.74
GM-18	OB	GM_18_3_TMTE_29_8	0.08	8.42	0.79	51.59	0.03	0.00	37.02	1.44	0.21	0.00	99.87	83.44
GM-18	OB	GM_18_3_TMTE_29_9	0.08	8.54	0.78	51.50	0.06	0.00	37.35	1.44	0.20	0.02	100.22	83.70
GM-18	OB	GM_18_3_TMTE_29_10	0.09	8.55	0.78	51.33	0.03	0.00	37.32	1.42	0.21	0.02	99.95	83.51

Table 3: (continued)

Sample	Eruptive Unit	Analysis	SiO_2	TiO_2	Al_2O_3	Fe_2O_3	V_2O_3	Cr_2O_3	FeO	MnO	MgO	CaO	Total	FeO^T
GM-18	OB	GM_18_3_TMTE_29_11	0.06	8.42	0.80	51.65	0.05	0.00	37.09	1.43	0.20	0.00	99.96	83.57
GM-18	OB	GM_18_3_TMTE_29_12	0.10	8.37	0.77	51.73	0.05	0.00	37.06	1.47	0.21	0.00	100.00	83.61
GM-18	OB	GM_18_3_TMTE_29_13	0.07	8.58	0.75	51.41	0.03	0.00	37.21	1.45	0.22	0.00	99.95	83.47
GM-18	OB	GM_18_3_TMTE_29_14	0.08	8.57	0.77	51.17	0.04	0.00	37.28	1.42	0.21	0.02	99.76	83.33
GM-18	OB	GM_18_3_TMTE_29_15	0.09	8.68	0.79	51.15	0.02	0.00	37.44	1.40	0.21	0.01	100.02	83.47
GM-18	OB	GM_18_3_TMTE_29_16	0.08	8.49	0.79	51.43	0.02	0.00	37.07	1.45	0.21	0.01	99.82	83.35
GM-18	OB	GM_18_3_TMTE_29_17	0.10	8.42	0.77	51.96	0.03	0.00	37.09	1.49	0.22	0.02	100.33	83.85
GM-18	OB	GM_18_3_TMTE_29_18	0.09	8.59	0.75	51.36	0.06	0.00	37.20	1.44	0.22	0.02	99.94	83.42
GM-18	OB	GM_18_3_TMTE_29_19	0.09	8.60	0.75	51.17	0.05	0.00	37.18	1.52	0.19	0.01	99.81	83.23
GM-18	OB	GM_18_3_TMTE_29_20	0.09	8.16	0.78	52.08	0.04	0.00	36.80	1.60	0.19	0.00	99.93	83.67
GM-18	OB	GM_18_3_TMTE_29_21	0.08	8.12	0.75	51.91	0.02	0.00	36.56	1.64	0.17	0.01	99.50	83.27
GM-18	OB	GM_18_3_TMTE_29_22	0.09	7.38	0.74	53.42	0.04	0.00	35.96	1.58	0.18	0.00	99.64	84.03
GM-18	OB	GM_18_3_TMTE_29_23	0.10	8.33	0.80	51.80	0.04	0.00	36.99	1.57	0.21	0.01	100.05	83.60
GM-18	OB	GM_18_3_TMTE_29_24	0.10	7.58	0.81	53.03	0.05	0.00	36.27	1.53	0.19	0.01	99.80	83.99
GM-18	OB	GM_18_3_TMTE_30_1	0.13	8.06	0.79	52.35	0.02	0.00	36.87	1.53	0.20	0.00	100.13	83.98
GM-18	OB	GM_18_3_TMTE_30_2	0.11	8.18	0.80	52.44	0.05	0.00	36.92	1.58	0.21	0.01	100.61	84.11
GM-18	OB	GM_18_3_TMTE_30_3	0.16	8.21	0.78	52.26	0.03	0.00	37.06	1.55	0.17	0.01	100.51	84.09
GM-18	OB	GM_18_3_TMTE_30_4	0.13	8.11	0.83	52.27	0.02	0.00	36.83	1.63	0.19	0.01	100.25	83.86
GM-18	OB	GM_18_3_TMTE_30_5	0.13	7.29	0.69	54.05	0.05	0.00	35.98	1.72	0.16	0.00	100.35	84.61
GM-18	OB	GM_18_3_TMTE_30_6	0.11	8.01	0.75	52.22	0.04	0.00	36.58	1.67	0.17	0.02	99.75	83.57
GM-18	OB	GM_18_3_TMTE_30_7	0.09	8.04	0.75	52.58	0.03	0.00	36.70	1.55	0.21	0.00	100.24	84.01
GM-18	OB	GM_18_3_TMTE_30_8	0.13	7.73	0.82	52.92	0.04	0.00	36.56	1.46	0.20	0.00	100.09	84.18
GM-18	OB	GM_18_3_TMTE_30_9	0.12	8.01	0.80	52.77	0.02	0.00	36.98	1.45	0.18	0.01	100.57	84.46
GM-18	OB	GM_18_3_TMTE_30_10	0.14	7.35	0.77	53.19	0.03	0.00	36.15	1.33	0.19	0.01	99.41	84.01
GM-18	OB	GM_18_3_TMTE_30_11	0.14	7.99	0.80	52.71	0.02	0.00	36.96	1.44	0.21	0.00	100.51	84.39
GM-18	OB	GM_18_3_TMTE_30_12	0.13	8.10	0.81	52.19	0.04	0.00	37.00	1.43	0.20	0.01	100.09	83.96
GM-18	OB	GM_18_3_TMTE_30_13	0.12	8.00	0.80	52.42	0.03	0.00	36.83	1.41	0.22	0.01	100.08	84.00
GM-18	OB	GM_18_3_TMTE_30_14	0.14	7.88	0.80	52.48	0.03	0.00	36.82	1.38	0.19	0.01	99.93	84.04
GM-18	OB	GM_18_3_TMTE_30_15	0.14	8.17	0.76	52.18	0.04	0.00	37.11	1.43	0.21	0.01	100.24	84.06
GM-18	OB	GM_18_3_TMTE_30_16	0.13	8.19	0.81	52.31	0.03	0.00	37.11	1.46	0.19	0.00	100.48	84.19
GM-18	OB	GM_18_3_TMTE_30_17	0.14	8.20	0.77	52.13	0.06	0.00	37.02	1.51	0.20	0.00	100.28	83.93
GM-18	OB	GM_18_3_TMTE_30_18	0.10	8.09	0.78	52.19	0.01	0.00	36.75	1.51	0.19	0.00	99.86	83.71
GM-18	OB	GM_18_3_TMTE_31_1	0.11	8.19	0.96	51.82	0.03	0.00	37.01	1.41	0.20	0.00	99.95	83.64

Table 3: (continued)

Sample	Eruptive Unit	Analysis	SiO_2	TiO_2	Al_2O_3	Fe_2O_3	V_2O_3	Cr_2O_3	FeO	MnO	MgO	CaO	Total	FeO^T
GM-18	OB	GM_18_3_TMTE_31_2	0.09	8.33	0.75	51.83	0.04	0.00	37.13	1.35	0.22	0.01	99.98	83.76
GM-18	OB	GM_18_3_TMTE_31_3	0.11	8.36	0.73	52.26	0.03	0.00	37.21	1.43	0.23	0.00	100.62	84.24
GM-18	OB	GM_18_3_TMTE_31_4	0.10	8.28	0.74	51.84	0.03	0.00	36.96	1.40	0.20	0.00	99.88	83.61
GM-18	OB	GM_18_3_TMTE_31_5	0.09	8.12	0.77	52.41	0.05	0.00	37.07	1.40	0.19	0.02	100.34	84.23
GM-18	OB	GM_18_3_TMTE_31_6	0.08	8.22	0.77	52.27	0.04	0.00	36.94	1.37	0.22	0.02	100.21	83.97
GM-18	OB	GM_18_3_TMTE_31_7	0.09	8.19	0.78	52.48	0.05	0.00	36.97	1.43	0.23	0.01	100.54	84.19
GM-18	OB	GM_18_3_TMTE_31_8	0.11	8.32	0.76	52.19	0.03	0.00	37.24	1.38	0.21	0.00	100.52	84.20
GM-18	OB	GM_18_3_TMTE_31_9	0.12	8.00	0.79	52.73	0.05	0.00	36.94	1.36	0.22	0.00	100.47	84.40
GM-18	OB	GM_18_3_TMTE_31_10	0.11	7.94	0.73	52.77	0.05	0.00	36.82	1.39	0.21	0.00	100.27	84.31
GM-18	OB	GM_18_3_TMTE_31_11	0.08	8.24	0.77	52.49	0.04	0.00	37.21	1.43	0.21	0.00	100.66	84.44
GM-18	OB	GM_18_3_TMTE_31_12	0.11	8.27	0.75	52.20	0.03	0.00	37.05	1.45	0.21	0.01	100.35	84.02
GM-18	OB	GM_18_3_TMTE_31_13	0.12	8.23	0.83	52.18	0.02	0.00	37.09	1.50	0.20	0.01	100.44	84.05
GM-18	OB	GM_18_3_TMTE_32_1	0.10	8.14	0.79	52.19	0.03	0.00	36.90	1.36	0.23	0.00	100.00	83.86
GM-18	OB	GM_18_3_TMTE_32_2	0.07	7.83	0.77	52.77	0.06	0.00	36.54	1.37	0.23	0.00	99.91	84.03
GM-18	OB	GM_18_3_TMTE_32_3	0.03	8.04	0.78	52.29	0.04	0.00	36.69	1.38	0.22	0.01	99.70	83.74
GM-18	OB	GM_18_3_TMTE_32_4	0.06	8.06	0.78	52.06	0.06	0.00	36.54	1.42	0.22	0.00	99.49	83.39
GM-18	OB	GM_18_3_TMTE_32_5	0.07	7.95	0.79	52.17	0.04	0.00	36.57	1.36	0.20	0.00	99.41	83.51
GM-18	OB	GM_18_3_TMTE_32_6	0.09	8.10	0.78	52.30	0.02	0.00	36.92	1.36	0.22	0.00	99.99	83.98
GM-18	OB	GM_18_3_TMTE_32_7	0.08	8.18	0.79	52.03	0.05	0.00	37.02	1.34	0.22	0.02	99.94	83.84
GM-18	OB	GM_18_3_TMTE_32_8	0.10	8.08	0.77	52.02	0.04	0.00	36.87	1.31	0.24	0.02	99.67	83.68
GM-18	OB	GM_18_3_TMTE_32_9	0.04	7.97	0.80	52.75	0.05	0.00	36.69	1.36	0.24	0.00	100.20	84.15
GM-18	OB	GM_18_3_TMTE _33_5	0.19	8.11	0.82	52.04	0.06	0.00	37.19	1.26	0.23	0.01	100.16	84.03
GM-01	OC	GM-01 Tmte 102	0.19	6.88	0.70	54.41	0.02	0.00	34.40	2.61	0.26	0.00	99.79	83.36
GM-01	OC	GM-01 Tmte 103	0.07	7.21	0.70	54.16	0.02	0.00	34.50	2.67	0.24	0.00	99.98	83.23
GM-01	OC	GM-01 Tmte 104	0.06	7.08	0.70	54.07	0.06	0.00	34.34	2.65	0.27	0.00	99.53	83.00
GM-01	OC	GM-01 Tmte 105	0.05	7.28	0.69	54.12	0.03	0.00	34.59	2.63	0.26	0.00	100.05	83.29
GM-01	OC	GM-01 Tmte 106	0.06	6.94	0.72	54.46	0.03	0.00	34.13	2.77	0.23	0.00	99.67	83.14
GM-01	OC	GM-01 Tmte 107	0.08	6.74	0.68	54.93	0.04	0.00	34.03	2.71	0.25	0.00	99.75	83.46
GM-01	OC	GM-01 Tmte 108	0.07	7.14	0.68	54.31	0.04	0.00	34.46	2.73	0.25	0.00	100.04	83.33
GM-01	OC	GM-01 Tmte 110	0.10	7.03	0.73	54.23	0.04	0.00	34.35	2.62	0.27	0.00	99.72	83.14
GM-01	OC	GM-01 Tmte 111	0.08	7.15	0.69	54.24	0.05	0.00	34.57	2.55	0.24	0.00	100.01	83.38
GM-01	OC	GM-01 Tmte 113	0.11	7.20	0.70	54.05	0.04	0.00	34.57	2.65	0.27	0.00	99.92	83.20
GM-01	OC	GM-01 Tmte 114	0.06	7.12	0.72	54.62	0.02	0.00	34.60	2.61	0.24	0.00	100.45	83.75

Table 3: (continued)

Sample	Eruptive Unit	Analysis	SiO_2	TiO_2	Al_2O_3	Fe_2O_3	V_2O_3	Cr_2O_3	FeO	MnO	MgO	CaO	Total	FeO^T
GM-01	OC	GM-01 Tmte 115	0.04	7.06	0.69	54.52	0.02	0.00	34.29	2.74	0.22	0.00	100.03	83.35
GM-01	OC	GM-01 Tmte 116	0.05	7.26	0.71	54.29	0.06	0.00	34.72	2.65	0.24	0.00	100.33	83.57
GM-01	OC	GM-01 Tmte 117	0.13	7.19	0.70	54.00	0.04	0.00	34.58	2.67	0.25	0.00	99.95	83.18
GM-01	OC	GM-01 Tmte 118	0.14	6.85	0.73	54.37	0.03	0.00	34.10	2.70	0.25	0.00	99.58	83.02
GM-01	OC	GM-01 Tmte 119	0.16	6.97	0.72	54.28	0.03	0.00	34.43	2.61	0.26	0.00	99.77	83.27
GM-01	OC	GM-01 Tmte 120	0.14	7.06	0.70	54.36	0.04	0.00	34.64	2.62	0.25	0.00	100.12	83.55
GM-01	OC	GM-01 Tmte 121	0.11	7.24	0.68	53.83	0.04	0.00	34.48	2.72	0.24	0.00	99.69	82.92
GM-01	OC	GM-01 Tmte 122	0.13	6.86	0.70	54.50	0.04	0.00	34.30	2.62	0.23	0.00	99.69	83.34
GM-01	OC	GM-01 Tmte 123	0.16	7.28	0.70	53.59	0.05	0.00	34.65	2.67	0.24	0.00	99.68	82.87
GM-01	OC	GM-01 Tmte 125	0.12	6.69	0.68	55.16	0.03	0.00	34.11	2.75	0.22	0.00	100.14	83.74
GM-01	OC	GM-01 Tmte 126	0.16	7.12	0.68	54.21	0.02	0.00	34.51	2.76	0.26	0.00	100.15	83.29
GM-01	OC	GM-01 Tmte 127	0.10	6.94	0.72	54.44	0.03	0.00	34.20	2.74	0.26	0.00	99.79	83.19
GM-01	OC	GM-01 Tmte 128	0.12	6.68	0.67	55.06	0.03	0.00	34.11	2.65	0.25	0.00	99.91	83.65
GM-01	OC	GM-01 Tmte 129	0.08	7.23	0.67	54.20	0.05	0.00	34.44	2.81	0.26	0.00	100.12	83.21
GM-01	OC	GM-01 Tmte 130	0.10	7.00	0.72	54.45	0.04	0.00	34.28	2.76	0.24	0.00	100.02	83.28
GM-01	OC	GM-01 Tmte 131	0.08	7.29	0.71	54.05	0.03	0.00	34.70	2.62	0.24	0.00	100.15	83.34
GM-01	OC	GM-01 Tmte 132	0.09	7.18	0.70	53.94	0.06	0.00	34.36	2.77	0.22	0.00	99.71	82.90
GM-01	OC	GM-01 Tmte 133	0.16	7.12	0.71	54.03	0.03	0.00	34.55	2.68	0.24	0.00	99.88	83.17
GM-01	OC	GM-01 Tmte 134	0.16	7.24	0.70	53.90	0.04	0.00	34.68	2.66	0.24	0.00	100.08	83.19
GM-01	OC	GM-01 Tmte 135	0.17	7.07	0.69	54.38	0.02	0.00	34.60	2.69	0.24	0.00	100.25	83.53
GM-01	OC	GM-01 Tmte 136	0.12	7.22	0.70	54.00	0.02	0.00	34.49	2.79	0.27	0.00	99.94	83.09
GM-01	OC	GM-01 Tmte 137	0.09	7.28	0.74	53.67	0.03	0.00	34.41	2.69	0.28	0.00	99.64	82.71
GM-01	OC	GM-01 Tmte 138	0.08	7.23	0.70	53.88	0.05	0.00	34.59	2.56	0.26	0.00	99.71	83.07
GM-01	OC	GM-01 Tmte 139	0.12	7.12	0.72	54.08	0.05	0.00	34.41	2.68	0.26	0.00	99.87	83.08
GM-01	OC	GM-01 Tmte 140	0.10	7.15	0.70	54.14	0.03	0.00	34.36	2.82	0.25	0.00	99.95	83.08
GM-01	OC	GM-01 Tmte 141	0.10	7.10	0.67	54.38	0.04	0.00	34.39	2.74	0.27	0.00	100.05	83.33
GM-01	OC	GM-01 Tmte 142	0.17	7.13	0.70	53.89	0.02	0.00	34.50	2.69	0.25	0.00	99.73	82.99
GM-01	OC	GM-01 Tmte 143	0.19	7.28	0.70	53.57	0.02	0.00	34.70	2.71	0.24	0.00	99.73	82.90
GM-01	OC	GM-01 Tmte 144	0.17	7.24	0.73	53.80	0.02	0.00	34.63	2.69	0.26	0.00	99.95	83.05
GM-01	OC	GM-01 Tmte 145	0.11	7.14	0.72	54.22	0.03	0.00	34.42	2.77	0.27	0.00	100.04	83.21
GM-01	OC	GM-01 Tmte 146	0.09	7.19	0.68	54.18	0.03	0.00	34.51	2.71	0.25	0.00	100.05	83.26
GM-01	OC	GM-01 Tmte 147	0.10	7.18	0.69	54.00	0.04	0.00	34.35	2.76	0.24	0.00	99.82	82.94
GM-01	OC	GM-01 Tmte 148	0.10	7.20	0.72	54.02	0.01	0.00	34.52	2.69	0.26	0.00	99.88	83.13

Table 3: (continued)

Sample	Eruptive Unit	Analysis	SiO_2	TiO_2	Al_2O_3	Fe_2O_3	V_2O_3	Cr_2O_3	FeO	MnO	MgO	CaO	Total	FeO^T
GM-01	OC	GM-01 Tmte 149	0.11	7.15	0.70	53.84	0.03	0.00	34.50	2.61	0.23	0.00	99.54	82.95
GM-01	OC	GM-01 Tmte 150	0.11	7.09	0.71	53.98	0.02	0.00	34.38	2.73	0.20	0.00	99.65	82.95
GM-01	OC	GM-01 Tmte 151	0.15	6.88	0.74	54.41	0.03	0.00	34.36	2.59	0.24	0.00	99.75	83.32
GM-01	OC	GM-01 Tmte 152	0.09	7.18	0.70	54.54	0.03	0.00	34.67	2.69	0.25	0.00	100.53	83.74
GM-01	OC	GM-01 Tmte 153	0.10	6.94	0.72	55.06	0.02	0.00	34.48	2.70	0.27	0.00	100.65	84.03
GM-01	OC	GM-01 Tmte 154	0.11	7.23	0.72	54.22	0.04	0.00	34.69	2.72	0.26	0.00	100.31	83.48
GM-01	OC	GM-01 Tmte 155	0.08	7.21	0.70	54.11	0.04	0.00	34.51	2.70	0.26	0.00	99.92	83.20
GM-01	OC	GM-01 Tmte 161	0.14	6.98	0.71	54.28	0.02	0.00	34.39	2.66	0.25	0.00	99.80	83.24
GM-01	OC	GM-01 Tmte 173	0.15	7.19	0.71	53.81	0.05	0.00	34.53	2.67	0.27	0.00	99.76	82.96
GM-01	OC	GM-01 Tmte 174	0.05	6.75	0.69	54.94	0.01	0.00	34.05	2.65	0.24	0.00	99.75	83.49
GM-01	OC	GM-01 Tmte 175	0.16	7.17	0.69	54.04	0.04	0.00	34.63	2.71	0.26	0.00	100.01	83.25
GM-01	OC	GM-01 Tmte 179	0.11	7.22	0.67	54.10	0.04	0.00	34.70	2.62	0.26	0.00	100.00	83.38
GM-01	OC	GM-01 Tmte 181	0.18	6.62	0.68	54.90	0.01	0.00	34.19	2.53	0.24	0.00	99.73	83.59
GM-01	OC	GM-01 Tmte 182	0.14	7.07	0.70	53.93	0.02	0.00	34.45	2.60	0.25	0.00	99.56	82.98
GM-01	OC	GM-01 Tmte 184	0.20	7.14	0.70	53.98	0.02	0.00	34.65	2.67	0.24	0.00	99.99	83.22
GM-01	OC	GM-01 Tmte 185	0.15	6.87	0.73	54.43	0.05	0.00	34.33	2.65	0.23	0.00	99.76	83.31
GM-01	OC	GM-01 Tmte 186	0.17	7.12	0.64	53.88	0.06	0.00	34.53	2.62	0.25	0.00	99.62	83.01
GM-01	OC	GM-01 Tmte 187	0.18	7.33	0.69	53.50	0.02	0.00	34.72	2.65	0.27	0.00	99.78	82.86
GM-01	OC	GM-01 Tmte 188	0.06	7.17	0.69	54.38	0.02	0.00	34.21	2.92	0.24	0.00	100.21	83.15
GM-01	OC	GM-01 Tmte 189	0.09	7.27	0.70	53.93	0.03	0.00	34.43	2.81	0.23	0.00	99.90	82.96
GM-01	OC	GM-01 Tmte 190	0.06	7.23	0.71	53.89	0.01	0.00	34.52	2.58	0.27	0.00	99.65	83.01
GM-01	OC	GM-01 Tmte 191	0.08	7.17	0.69	54.24	0.05	0.00	34.41	2.74	0.26	0.00	100.08	83.22
GM-01	OC	GM-01 Tmte 192	0.07	7.34	0.72	53.75	0.04	0.00	34.60	2.65	0.25	0.00	99.79	82.97
GM-01	OC	GM-01 Tmte 193	0.10	7.19	0.65	54.16	0.04	0.00	34.57	2.68	0.24	0.00	99.94	83.31
GM-01	OC	GM-01 Tmte 194	0.07	7.20	0.71	54.03	0.04	0.00	34.45	2.66	0.27	0.00	99.83	83.07
GM-01	OC	GM-01 Tmte 195	0.07	7.22	0.66	54.13	0.04	0.00	34.48	2.71	0.26	0.00	99.88	83.19
GM-01	OC	GM-01 Tmte 196	0.07	6.88	0.71	54.58	0.04	0.00	34.15	2.65	0.26	0.00	99.61	83.26
GM-01	OC	GM-01 Tmte 197	0.08	7.36	0.70	53.94	0.02	0.00	34.77	2.61	0.25	0.00	100.07	83.31
GM-01	OC	GM-01 Tmte 198	0.08	7.17	0.68	54.26	0.02	0.00	34.46	2.70	0.26	0.00	100.08	83.29
GM-01	OC	GM-01 Tmte 199	0.06	7.21	0.72	54.00	0.05	0.00	34.32	2.77	0.27	0.00	99.77	82.92
GM-01	OC	GM-01 Tmte 200	0.10	7.20	0.71	53.92	0.05	0.00	34.40	2.79	0.25	0.00	99.75	82.92
GM-07a	OL	GM_07a_1_TMTE_1_1	0.09	8.74	0.73	50.66	0.05	0.00	36.92	1.72	0.21	0.00	99.36	82.50
GM-07a	OL	GM_07a_1_TMTE_1_2	0.14	8.69	0.77	50.44	0.05	0.00	36.76	1.68	0.22	0.01	99.10	82.15

Table 3: (continued)

Sample	Eruptive Unit	Analysis	SiO_2	TiO_2	Al_2O_3	Fe_2O_3	V_2O_3	Cr_2O_3	FeO	MnO	MgO	CaO	Total	FeO^T
GM-07a	OL	GM_07a_1_TMTE_1_3	0.10	9.02	0.73	50.57	0.03	0.00	37.32	1.75	0.24	0.01	99.98	82.82
GM-07a	OL	GM_07a_1_TMTE_1_4	0.11	8.75	0.77	50.94	0.03	0.00	37.00	1.66	0.24	0.02	99.84	82.84
GM-07a	OL	GM_07a_1_TMTE_1_5	0.12	8.83	0.80	50.71	0.02	0.00	37.15	1.72	0.24	0.00	99.87	82.79
GM-07a	OL	GM_07a_1_TMTE_1_6	0.10	8.95	0.77	50.85	0.03	0.00	37.44	1.77	0.21	0.02	100.42	83.20
GM-07a	OL	GM_07a_1_TMTE_1_7	0.11	8.68	0.77	51.00	0.06	0.00	37.04	1.71	0.23	0.01	99.87	82.94
GM-07a	OL	GM_07a_1_TMTE_1_9	0.09	8.63	0.78	51.05	0.04	0.00	36.87	1.69	0.24	0.00	99.68	82.81
GM-07a	OL	GM_07a_1_TMTE_1_13	0.13	8.82	0.78	50.52	0.04	0.00	36.99	1.69	0.23	0.01	99.54	82.45
GM-07a	OL	GM_07a_1_TMTE_1_15	0.16	8.68	0.78	51.06	0.06	0.00	37.18	1.67	0.23	0.00	100.14	83.13
GM-07a	OL	GM_07a_1_TMTE_1_16	0.15	8.77	0.77	50.67	0.02	0.00	37.12	1.70	0.23	0.00	99.68	82.72
GM-07a	OL	GM_07a_1_TMTE_1_17	0.19	8.80	0.78	50.69	0.01	0.00	37.17	1.74	0.23	0.01	99.93	82.78
GM-07a	OL	GM_07a_1_TMTE_1_18	0.15	8.72	0.79	51.00	0.05	0.00	37.18	1.72	0.22	0.01	100.09	83.08
GM-07a	OL	GM_07a_1_TMTE_1_19	0.12	8.69	0.71	51.05	0.03	0.00	37.07	1.69	0.22	0.00	99.84	83.00
GM-07a	OL	GM_07a_1_TMTE_1_21	0.12	8.70	0.76	50.88	0.01	0.00	37.00	1.73	0.23	0.01	99.71	82.78
GM-07a	OL	GM_07a_1_TMTE_1_23	0.11	8.94	0.84	50.65	0.03	0.00	37.14	1.79	0.25	0.01	100.08	82.72
GM-07a	OL	GM_07a_1_TMTE_1_24	0.09	8.79	0.77	50.97	0.06	0.00	37.19	1.70	0.24	0.01	100.09	83.06
GM-07a	OL	GM_07a_1_TMTE_1_25	0.11	8.73	0.77	50.64	0.04	0.00	36.90	1.72	0.22	0.01	99.39	82.47
GM-07a	OL	GM_07a_1_TMTE_2_1	0.10	8.88	0.81	50.48	0.05	0.00	37.18	1.71	0.21	0.01	99.67	82.60
GM-07a	OL	GM_07a_1_TMTE_2_2	0.14	8.85	0.75	50.84	0.03	0.00	37.21	1.72	0.25	0.01	100.09	82.95
GM-07a	OL	GM_07a_1_TMTE_2_3	0.10	8.70	0.78	50.86	0.03	0.00	37.04	1.72	0.24	0.02	99.71	82.81
GM-07a	OL	GM_07a_1_TMTE_2_4	0.13	8.74	0.79	50.86	0.05	0.00	37.08	1.70	0.23	0.00	99.88	82.85
GM-07a	OL	GM_07a_1_TMTE_2_5	0.10	8.83	0.79	50.67	0.07	0.00	37.19	1.73	0.23	0.00	99.81	82.79
GM-07a	OL	GM_07a_1_TMTE_2_6	0.06	8.78	0.80	50.94	0.02	0.00	37.11	1.73	0.24	0.01	99.90	82.95
GM-07a	OL	GM_07a_1_TMTE_2_7	0.08	8.98	0.82	50.45	0.03	0.00	37.21	1.76	0.23	0.01	99.87	82.60
GM-07a	OL	GM_07a_1_TMTE_2_8	0.05	8.98	0.83	51.03	0.04	0.00	37.45	1.70	0.22	0.00	100.58	83.36
GM-07a	OL	GM_07a_1_TMTE_2_9	0.06	8.92	0.80	50.33	0.05	0.00	37.09	1.69	0.23	0.01	99.44	82.38
GM-07a	OL	GM_07a_1_TMTE_2_10	0.08	8.76	0.73	50.73	0.07	0.00	37.05	1.72	0.24	0.01	99.56	82.70
GM-07a	OL	GM_07a_1_TMTE_2_11	0.13	8.80	1.26	50.36	0.04	0.00	37.17	1.78	0.23	0.01	100.09	82.49
GM-07a	OL	GM_07a_1_TMTE_3_1	0.09	9.01	0.74	50.22	0.03	0.00	36.96	2.01	0.22	0.02	99.58	82.15
GM-07a	OL	GM_07a_1_TMTE_3_2	0.10	8.92	0.73	50.57	0.04	0.00	36.93	1.90	0.24	0.00	99.75	82.44
GM-07a	OL	GM_07a_1_TMTE_3_3	0.08	8.95	0.79	50.53	0.04	0.00	36.94	1.90	0.23	0.01	99.78	82.41
GM-07a	OL	GM_07a_1_TMTE_3_4	0.12	8.95	0.86	50.43	0.03	0.00	37.07	1.96	0.23	0.01	99.92	82.45
GM-07a	OL	GM_07a_1_TMTE_3_5	0.11	9.00	0.74	50.70	0.04	0.00	37.21	1.97	0.20	0.01	100.26	82.83
GM-07a	OL	GM_07a_1_TMTE_3_6	0.10	9.11	0.78	50.51	0.03	0.00	37.33	1.94	0.23	0.01	100.33	82.78

Table 3: (continued)

Sample	Eruptive Unit	Analysis	SiO_2	TiO_2	Al_2O_3	Fe_2O_3	V_2O_3	Cr_2O_3	FeO	MnO	MgO	CaO	Total	FeO^T
GM-07a	OL	GM_07a_1_TMTE_3_8	0.09	9.01	0.74	50.61	0.02	0.00	37.14	1.84	0.23	0.00	100.04	82.69
GM-07a	OL	GM_07a_1_TMTE_3_9	0.10	8.90	0.75	50.75	0.05	0.00	36.99	1.93	0.23	0.01	99.98	82.66
GM-07a	OL	GM_07a_1_TMTE_3_10	0.11	9.04	0.74	50.42	0.03	0.00	36.91	2.04	0.22	0.01	99.87	82.28
GM-07a	OL	GM_07a_1_TMTE_3_11	0.10	9.05	0.81	50.34	0.05	0.00	36.94	2.05	0.25	0.00	99.94	82.24
GM-07a	OL	GM_07a_1_TMTE_3_12	0.11	8.62	0.74	51.00	0.02	0.00	36.62	1.95	0.22	0.00	99.58	82.51
GM-07a	OL	GM_07a_1_TMTE_3_13	0.10	8.62	0.78	51.42	0.03	0.00	36.89	1.83	0.25	0.00	100.25	83.17
GM-07a	OL	GM_07a_1_TMTE_4_3	0.13	8.73	0.75	50.84	0.04	0.00	36.92	1.72	0.24	0.01	99.73	82.66
GM-07a	OL	GM_07a_1_TMTE_4_5	0.13	8.88	0.78	50.46	0.06	0.00	37.21	1.71	0.23	0.00	99.70	82.62
GM-07a	OL	GM_07a_1_TMTE_4_6	0.09	8.96	0.77	50.96	0.03	0.00	37.44	1.69	0.22	0.01	100.45	83.29
GM-07a	OL	GM_07a_1_TMTE_4_7	0.11	8.88	0.75	50.70	0.02	0.00	37.18	1.74	0.22	0.00	99.89	82.80
GM-07a	OL	GM_07a_1_TMTE_4_8	0.17	8.52	0.79	50.31	0.05	0.00	36.39	1.64	0.22	0.05	98.40	81.66
GM-07a	OL	GM_07a_1_TMTE_4_9	0.11	8.91	0.88	50.85	0.04	0.00	37.33	1.77	0.24	0.01	100.39	83.08
GM-07a	OL	GM_07a_1_TMTE_4_10	0.10	8.57	0.79	51.34	0.04	0.00	36.93	1.66	0.21	0.01	99.97	83.12
GM-07a	OL	GM_07a_1_TMTE_4_11	0.13	8.60	0.77	51.48	0.04	0.00	37.07	1.73	0.23	0.01	100.34	83.39
GM-07a	OL	GM_07a_1_TMTE_4_12	0.14	8.74	0.78	51.23	0.04	0.00	37.19	1.77	0.22	0.01	100.43	83.30
GM-07a	OL	GM_07a_1_TMTE_4_13	0.14	8.77	0.73	51.16	0.05	0.00	37.26	1.71	0.23	0.01	100.33	83.30
GM-07a	OL	GM_07a_1_TMTE_4_14	0.13	8.87	0.78	51.13	0.04	0.00	37.34	1.77	0.22	0.01	100.59	83.35
GM-07a	OL	GM_07a_1_TMTE_4_15	0.11	8.87	0.87	50.47	0.03	0.00	36.94	1.91	0.23	0.01	99.80	82.36
GM-07a	OL	GM_07a_1_TMTE_4_16	0.10	8.79	0.75	51.21	0.04	0.00	37.20	1.76	0.25	0.01	100.41	83.28
GM-07a	OL	GM_07a_1_TMTE_4_17	0.11	8.79	0.81	49.95	0.03	0.00	36.66	1.86	0.23	0.02	98.74	81.61
GM-07a	OL	GM_07a_1_TMTE_4_18	0.08	8.81	0.76	50.89	0.02	0.00	37.11	1.80	0.24	0.02	99.94	82.90
GM-07a	OL	GM_07a_1_TMTE_4_19	0.15	8.90	0.78	50.49	0.04	0.00	37.35	1.71	0.22	0.01	99.93	82.79
GM-07a	OL	GM_07a_1_TMTE_5_2	0.12	8.78	0.76	51.13	0.05	0.00	36.50	2.34	0.22	0.01	100.24	82.51
GM-07a	OL	GM_07a_1_TMTE_5_3	0.09	8.76	0.76	51.36	0.04	0.00	36.51	2.36	0.21	0.01	100.49	82.73
GM-07a	OL	GM_07a_1_TMTE_5_4	0.07	8.90	0.78	51.04	0.02	0.00	36.52	2.44	0.22	0.00	100.37	82.45
GM-07a	OL	GM_07a_1_TMTE_5_5	0.11	8.95	0.80	51.06	0.04	0.00	36.74	2.38	0.23	0.00	100.72	82.69
GM-07a	OL	GM_07a_1_TMTE_5_6	0.10	8.79	0.87	51.45	0.03	0.00	36.69	2.37	0.22	0.00	100.91	82.99
GM-07a	OL	GM_07a_1_TMTE_5_7	0.11	8.75	0.77	51.11	0.06	0.00	36.50	2.36	0.22	0.00	100.21	82.49
GM-07a	OL	GM_07a_1_TMTE_5_8	0.09	8.88	0.82	51.11	0.04	0.00	36.76	2.32	0.21	0.01	100.59	82.75
GM-07a	OL	GM_07a_1_TMTE_5_9	0.09	8.80	0.74	51.45	0.05	0.00	36.64	2.33	0.23	0.01	100.68	82.94
GM-07a	OL	GM_07a_1_TMTE_5_10	0.08	8.68	0.73	51.44	0.04	0.00	36.28	2.42	0.21	0.01	100.25	82.57
GM-07a	OL	GM_07a_1_TMTE_5_11	0.10	8.87	0.76	51.22	0.03	0.00	36.72	2.35	0.20	0.01	100.60	82.81
GM-07a	OL	GM_07a_1_TMTE_5_12	0.10	8.82	0.75	51.16	0.05	0.00	36.34	2.45	0.22	0.02	100.34	82.38

Table 3: (continued)

Sample	Eruptive Unit	Analysis	SiO_2	TiO_2	Al_2O_3	Fe_2O_3	V_2O_3	Cr_2O_3	FeO	MnO	MgO	CaO	Total	FeO^T
GM-07a	OL	GM_07a_1_TMTE_5_13	0.08	8.73	0.78	51.57	0.06	0.00	36.30	2.46	0.22	0.03	100.66	82.70
GM-07a	OL	GM_07a_1_TMTE_5_14	0.09	8.84	0.79	51.32	0.03	0.00	36.51	2.43	0.23	0.00	100.67	82.69
GM-07a	OL	GM_07a_1_TMTE_5_15	0.11	8.72	0.79	51.18	0.06	0.00	36.34	2.44	0.21	0.01	100.24	82.39
GM-07a	OL	GM_07a_1_TMTE_5_16	0.09	8.89	0.77	51.00	0.05	0.00	36.48	2.45	0.24	0.01	100.31	82.37
GM-07a	OL	GM_07a_1_TMTE_5_17	0.08	8.88	0.78	51.50	0.04	0.00	36.74	2.36	0.20	0.02	100.93	83.09
GM-07a	OL	GM_07a_1_TMTE_6_2	0.14	8.43	0.77	52.03	0.05	0.00	36.70	2.03	0.22	0.02	100.67	83.53
GM-07a	OL	GM_07a_1_TMTE_6_3	0.13	8.54	0.74	51.44	0.04	0.00	36.66	2.03	0.22	0.02	100.17	82.95
GM-07a	OL	GM_07a_1_TMTE_6_4	0.13	8.44	0.78	51.77	0.03	0.00	36.59	2.05	0.23	0.00	100.34	83.18
GM-07a	OL	GM_07a_1_TMTE_6_5	0.18	8.55	0.75	50.75	0.05	0.00	36.49	2.04	0.22	0.00	99.30	82.16
GM-07a	OL	GM_07a_1_TMTE_6_6	0.16	8.53	0.80	51.70	0.03	0.00	36.72	2.01	0.23	0.01	100.55	83.24
GM-07a	OL	GM_07a_1_TMTE_6_7	0.12	7.93	0.76	52.78	0.06	0.00	36.08	2.04	0.20	0.01	100.34	83.57
GM-07a	OL	GM_07a_1_TMTE_6_8	0.14	7.80	0.75	53.04	0.05	0.00	36.07	1.98	0.21	0.01	100.38	83.80
GM-07a	OL	GM_07a_1_TMTE_6_9	0.12	7.70	0.78	53.53	0.03	0.00	36.11	1.95	0.20	0.00	100.79	84.28
GM-07a	OL	GM_07a_1_TMTE_6_10	0.12	7.35	0.81	53.74	0.02	0.00	35.81	1.88	0.19	0.02	100.26	84.17
GM-07a	OL	GM_07a_1_TMTE_6_12	0.10	7.63	0.84	53.48	0.03	0.00	36.28	1.65	0.22	0.00	100.55	84.41
GM-07a	OL	GM_07a_1_TMTE_6_13	0.10	7.67	0.82	53.36	0.03	0.00	36.33	1.66	0.24	0.01	100.41	84.34
GM-07a	OL	GM_07a_1_TMTE_6_14	0.09	7.80	0.76	53.22	0.03	0.00	36.37	1.66	0.23	0.01	100.45	84.26
GM-07a	OL	GM_07a_1_TMTE_6_15	0.10	7.97	0.78	52.49	0.03	0.00	36.37	1.74	0.22	0.01	99.99	83.60
GM-07a	OL	GM_07a_1_TMTE_7_1	0.09	8.91	0.75	51.04	0.04	0.00	37.06	1.99	0.23	0.01	100.45	82.99
GM-07a	OL	GM_07a_1_TMTE_7_2	0.07	8.95	0.79	51.02	0.04	0.00	37.00	2.02	0.24	0.01	100.43	82.91
GM-07a	OL	GM_07a_1_TMTE_7_3	0.06	8.35	0.81	52.00	0.02	0.00	36.66	1.79	0.23	0.01	100.18	83.46
GM-07a	OL	GM_07a_1_TMTE_7_4	0.08	8.47	0.83	51.63	0.05	0.00	36.70	1.90	0.23	0.01	100.17	83.16
GM-07a	OL	GM_07a_1_TMTE_7_5	0.07	8.77	0.82	51.25	0.05	0.00	37.06	1.91	0.23	0.01	100.43	83.18
GM-07a	OL	GM_07a_1_TMTE_7_6	0.06	8.73	0.78	50.94	0.02	0.00	36.81	1.86	0.25	0.02	99.75	82.65
GM-07a	OL	GM_07a_1_TMTE_7_7	0.09	8.94	0.78	50.68	0.04	0.00	37.12	1.92	0.22	0.01	100.06	82.73
GM-07a	OL	GM_07a_1_TMTE_7_8	0.07	8.95	0.72	51.04	0.04	0.00	36.90	2.05	0.22	0.02	100.36	82.83
GM-07a	OL	GM_07a_1_TMTE_7_10	0.06	8.87	0.77	51.49	0.05	0.00	37.05	2.07	0.22	0.01	100.97	83.38
GM-07a	OL	GM_07a_1_TMTE_7_11	0.09	8.80	0.75	51.25	0.03	0.00	36.87	2.07	0.22	0.01	100.45	82.99
GM-07a	OL	GM_07a_1_TMTE_7_12	0.06	8.84	0.84	50.66	0.05	0.00	36.91	1.85	0.26	0.01	99.75	82.50
GM-07a	OL	GM_07a_1_TMTE_7_13	0.12	8.68	0.79	51.22	0.05	0.00	36.90	1.90	0.25	0.01	100.17	82.99
GM-07a	OL	GM_07a_1_TMTE_7_14	0.06	8.52	0.78	51.80	0.04	0.00	36.81	1.86	0.22	0.00	100.38	83.42
GM-07a	OL	GM_07a_1_TMTE_7_15	0.10	7.63	0.80	53.15	0.04	0.00	36.09	1.71	0.21	0.01	100.01	83.92
GM-07a	OL	GM_07a_1_TMTE_8_1	0.09	8.77	0.84	51.08	0.04	0.00	37.10	1.71	0.24	0.01	100.22	83.07

Table 3: (continued)

Sample	Eruptive Unit	Analysis	SiO_2	TiO_2	Al_2O_3	Fe_2O_3	V_2O_3	Cr_2O_3	FeO	MnO	MgO	CaO	Total	FeO^T
GM-07a	OL	GM_07a_1_TMTE_8_2	0.08	8.92	0.76	50.91	0.06	0.00	37.24	1.78	0.24	0.01	100.27	83.05
GM-07a	OL	GM_07a_1_TMTE_8_3	0.07	8.86	0.83	50.95	0.06	0.00	37.22	1.72	0.23	0.00	100.22	83.07
GM-07a	OL	GM_07a_1_TMTE_8_4	0.08	8.79	0.75	50.84	0.04	0.00	37.09	1.75	0.23	0.02	99.85	82.84
GM-07a	OL	GM_07a_1_TMTE_8_5	0.09	8.96	0.76	50.70	0.03	0.00	37.31	1.73	0.23	0.00	100.09	82.94
GM-07a	OL	GM_07a_1_TMTE_8_6	0.11	9.06	0.77	50.71	0.06	0.00	37.53	1.72	0.25	0.00	100.47	83.16
GM-07a	OL	GM_07a_1_TMTE_8_7	0.10	8.68	0.76	51.40	0.02	0.00	37.09	1.75	0.23	0.01	100.33	83.34
GM-07a	OL	GM_07a_1_TMTE_8_8	0.07	8.90	0.76	50.84	0.04	0.00	37.27	1.73	0.23	0.01	100.13	83.01
GM-07a	OL	GM_07a_1_TMTE_8_9	0.08	8.87	0.83	51.05	0.02	0.00	37.15	1.74	0.22	0.02	100.31	83.08
GM-07a	OL	GM_07a_1_TMTE_8_10	0.08	8.86	0.81	51.09	0.05	0.00	37.28	1.73	0.23	0.00	100.42	83.26
GM-07a	OL	GM_07a_1_TMTE_8_11	0.08	8.83	0.73	51.24	0.04	0.00	37.18	1.70	0.23	0.02	100.33	83.28
GM-07a	OL	GM_07a_1_TMTE_8_12	0.08	8.79	0.78	50.41	0.05	0.00	36.89	1.69	0.23	0.00	99.20	82.26
GM-07a	OL	GM_07a_1_TMTE_8_13	0.08	8.87	0.91	50.25	0.07	0.00	36.98	1.72	0.23	0.01	99.40	82.20
GM-07a	OL	GM_07a_1_TMTE_8_14	0.10	8.90	0.80	51.01	0.03	0.00	37.28	1.73	0.24	0.01	100.41	83.18
GM-07a	OL	GM_07a_1_TMTE_8_15	0.13	8.79	0.79	50.91	0.06	0.00	37.19	1.73	0.23	0.01	100.16	83.00
GM-07a	OL	GM_07a_1_TMTE_8_16	0.09	8.80	0.76	50.91	0.05	0.00	37.10	1.74	0.22	0.01	99.97	82.91
GM-07a	OL	GM_07a_1_TMTE_9_2	0.11	8.71	0.82	51.01	0.03	0.00	36.91	1.78	0.23	0.02	99.90	82.82
GM-07a	OL	GM_07a_1_TMTE_9_4	0.09	8.75	0.79	51.33	0.05	0.00	37.13	1.80	0.24	0.01	100.49	83.31
GM-07a	OL	GM_07a_1_TMTE_9_5	0.12	8.78	0.80	51.02	0.04	0.00	37.23	1.75	0.25	0.01	100.20	83.14
GM-07a	OL	GM_07a_1_TMTE_9_6	0.10	8.80	0.79	50.89	0.04	0.00	37.16	1.78	0.24	0.01	100.08	82.95
GM-07a	OL	GM_07a_1_TMTE_9_7	0.14	8.86	0.82	50.99	0.03	0.00	37.55	1.74	0.23	0.02	100.56	83.44
GM-07a	OL	GM_07a_1_TMTE_9_8	0.10	8.76	0.74	51.21	0.06	0.00	37.01	1.81	0.22	0.01	100.29	83.10
GM-07a	OL	GM_07a_1_TMTE_9_9	0.09	8.79	0.80	51.41	0.04	0.00	37.23	1.77	0.24	0.00	100.69	83.49
GM-07a	OL	GM_07a_1_TMTE_9_10	0.12	8.71	0.79	51.29	0.06	0.00	37.16	1.77	0.23	0.00	100.43	83.31
GM-07a	OL	GM_07a_1_TMTE_9_11	0.11	8.81	0.83	51.17	0.04	0.00	37.09	1.80	0.23	0.03	100.40	83.13
GM-07a	OL	GM_07a_1_TMTE_9_12	0.14	8.79	0.77	50.82	0.07	0.00	37.05	1.83	0.23	0.00	100.02	82.78
GM-07a	OL	GM_07a_1_TMTE_9_14	0.09	8.81	0.94	50.87	0.03	0.00	37.12	1.84	0.23	0.00	100.19	82.90
GM-07a	OL	GM_07a_1_TMTE_9_15	0.10	8.72	0.80	51.13	0.05	0.00	37.13	1.76	0.23	0.00	100.15	83.14
GM-07a	OL	GM_07a_1_TMTE_9_16	0.11	8.87	0.81	50.62	0.03	0.00	37.26	1.73	0.22	0.02	99.94	82.80
GM-07a	OL	GM_07a_1_TMTE_10_3	0.11	8.61	1.50	50.57	0.04	0.00	37.03	1.73	0.25	0.01	100.19	82.53
GM-07a	OL	GM_07a_1_TMTE_10_4	0.12	8.76	0.77	51.29	0.03	0.00	37.27	1.74	0.25	0.01	100.50	83.42
GM-07a	OL	GM_07a_1_TMTE_10_5	0.08	8.76	0.78	51.00	0.02	0.00	37.06	1.76	0.23	0.00	99.94	82.95
GM-07a	OL	GM_07a_1_TMTE_10_6	0.08	8.94	0.81	51.02	0.05	0.00	37.33	1.77	0.24	0.00	100.57	83.25
GM-07a	OL	GM_07a_1_TMTE_10_7	0.10	8.89	0.81	50.82	0.03	0.00	37.23	1.74	0.23	0.01	100.15	82.95

Table 3: (continued)

Sample	Eruptive Unit	Analysis	SiO_2	TiO_2	Al_2O_3	Fe_2O_3	V_2O_3	Cr_2O_3	FeO	MnO	MgO	CaO	Total	FeO^T
GM-07a	OL	GM_07a_1_TMTE_10_8	0.10	8.93	0.89	50.69	0.05	0.00	37.24	1.78	0.23	0.00	100.25	82.86
GM-07a	OL	GM_07a_1_TMTE_10_9	0.11	8.72	1.41	50.06	0.05	0.00	37.01	1.76	0.24	0.00	99.64	82.06
GM-07a	OL	GM_07a_1_TMTE_10_10	0.11	8.84	0.79	51.33	0.04	0.00	37.41	1.70	0.25	0.01	100.80	83.60
GM-07a	OL	GM_07a_1_TMTE_10_11	0.08	8.86	1.26	50.42	0.05	0.00	37.29	1.76	0.25	0.01	100.26	82.66
GM-07a	OL	GM_07a_1_TMTE_10_14	0.10	8.94	0.81	50.77	0.06	0.00	37.31	1.75	0.23	0.00	100.30	83.00
GM-07a	OL	GM_07a_1_TMTE_10_16	0.11	8.43	0.77	51.43	0.04	0.00	36.63	1.76	0.21	0.02	99.66	82.91
GM-07a	OL	GM_07a_1_TMTE_10_17	0.10	8.65	0.97	51.04	0.04	0.00	36.91	1.75	0.23	0.02	100.03	82.84
GM-07a	OL	GM_07a_1_TMTE_11_1	0.14	9.00	0.79	50.35	0.03	0.00	37.26	1.75	0.25	0.00	99.87	82.56
GM-07a	OL	GM_07a_1_TMTE_11_2	0.10	9.01	0.79	50.52	0.05	0.00	37.25	1.72	0.26	0.01	100.03	82.71
GM-07a	OL	GM_07a_1_TMTE_11_3	0.12	9.04	0.81	50.30	0.03	0.00	37.30	1.79	0.25	0.00	99.92	82.56
GM-07a	OL	GM_07a_1_TMTE_11_4	0.12	9.03	0.79	50.69	0.02	0.00	37.42	1.80	0.24	0.01	100.39	83.04
GM-07a	OL	GM_07a_1_TMTE_11_5	0.15	8.90	0.77	50.41	0.05	0.00	37.26	1.74	0.21	0.01	99.80	82.62
GM-07a	OL	GM_07a_1_TMTE_11_6	0.13	8.87	0.80	51.06	0.03	0.00	37.25	1.77	0.24	0.02	100.44	83.20
GM-07a	OL	GM_07a_1_TMTE_11_8	0.12	9.04	0.80	50.53	0.06	0.00	37.53	1.74	0.23	0.02	100.35	82.99
GM-07a	OL	GM_07a_1_TMTE_11_9	0.16	8.97	0.85	50.43	0.05	0.00	37.32	1.80	0.24	0.00	100.13	82.70
GM-07a	OL	GM_07a_1_TMTE_11_10	0.10	8.93	0.79	50.73	0.06	0.00	37.25	1.77	0.24	0.01	100.22	82.90
GM-07a	OL	GM_07a_1_TMTE_11_11	0.12	9.08	0.73	50.34	0.03	0.00	37.34	1.80	0.23	0.00	99.92	82.63
GM-07a	OL	GM_07a_1_TMTE_11_12	0.14	8.53	0.79	51.21	0.03	0.00	36.94	1.72	0.24	0.01	99.85	83.02
GM-07a	OL	GM_07a_1_TMTE_11_13	0.14	8.73	0.79	50.83	0.05	0.00	37.05	1.76	0.24	0.01	99.88	82.79
GM-07a	OL	GM_07a_1_TMTE_11_14	0.11	8.98	0.75	50.57	0.05	0.00	37.23	1.78	0.25	0.00	99.99	82.74
GM-07a	OL	GM_07a_1_TMTE_11_16	0.12	8.83	0.76	50.95	0.04	0.00	37.19	1.80	0.23	0.01	100.24	83.04
GM-07a	OL	GM_07a_1_TMTE_11_17	0.14	8.80	0.74	51.00	0.04	0.00	37.08	1.83	0.24	0.00	100.17	82.97
GM-07a	OL	GM_07a_1_TMTE_11_18	0.13	8.79	0.81	51.20	0.05	0.00	37.09	1.80	0.24	0.02	100.47	83.16
GM-07a	OL	GM_07a_1_TMTE_12_1	0.17	8.76	0.77	50.76	0.05	0.00	37.39	1.38	0.24	0.01	99.87	83.07
GM-07a	OL	GM_07a_1_TMTE_12_2	0.19	8.80	0.75	50.72	0.03	0.00	37.47	1.47	0.25	0.00	99.99	83.10
GM-07a	OL	GM_07a_1_TMTE_12_4	0.18	8.80	0.79	50.70	0.07	0.00	37.54	1.43	0.23	0.00	100.04	83.16
GM-07a	OL	GM_07a_1_TMTE_12_5	0.19	8.86	0.77	50.73	0.05	0.00	37.67	1.42	0.24	0.00	100.23	83.32
GM-07a	OL	GM_07a_1_TMTE_12_6	0.18	8.91	0.76	50.70	0.04	0.00	37.69	1.47	0.25	0.01	100.29	83.31
GM-07a	OL	GM_07a_1_TMTE_12_8	0.16	8.87	0.73	50.76	0.05	0.00	37.57	1.45	0.25	0.00	100.11	83.25
GM-07a	OL	GM_07a_1_TMTE_12_9	0.18	8.87	0.79	50.69	0.05	0.00	37.61	1.48	0.26	0.00	100.16	83.23
GM-07a	OL	GM_07a_1_TMTE_12_12	0.19	8.84	0.76	50.90	0.06	0.00	37.74	1.37	0.25	0.00	100.39	83.54
GM-07a	OL	GM_07a_1_TMTE_12_13	0.19	8.06	0.80	52.13	0.04	0.00	36.79	1.47	0.26	0.01	99.96	83.70
GM-07a	OL	GM_07a_1_TMTE_12_14	0.17	8.87	0.83	50.66	0.06	0.00	37.59	1.47	0.25	0.01	100.16	83.18

Table 3: (continued)

Sample	Eruptive Unit	Analysis	SiO_2	TiO_2	Al_2O_3	Fe_2O_3	V_2O_3	Cr_2O_3	FeO	MnO	MgO	CaO	Total	FeO^T
GM-07a	OL	GM_07a_1_TMTE_12_15	0.17	8.52	0.73	51.32	0.03	0.00	37.21	1.50	0.24	0.00	99.94	83.39
GM-07a	OL	GM_07a_1_TMTE_12_16	0.17	8.89	0.74	50.26	0.06	0.00	37.37	1.50	0.24	0.01	99.56	82.59
GM-07a	OL	GM_07a_2_TMTE_13_1	0.14	8.81	0.83	50.78	0.04	0.00	37.21	1.73	0.23	0.01	100.11	82.90
GM-07a	OL	GM_07a_2_TMTE_13_2	0.12	8.84	0.76	50.82	0.03	0.00	37.26	1.68	0.22	0.01	99.99	82.99
GM-07a	OL	GM_07a_2_TMTE_13_3	0.11	8.73	0.80	50.84	0.02	0.00	36.87	1.72	0.22	0.03	99.63	82.62
GM-07a	OL	GM_07a_2_TMTE_13_4	0.14	8.78	0.89	50.72	0.02	0.00	36.98	1.69	0.22	0.05	99.80	82.63
GM-07a	OL	GM_07a_2_TMTE_13_5	0.14	8.64	0.79	50.67	0.03	0.00	36.84	1.73	0.23	0.01	99.31	82.44
GM-07a	OL	GM_07a_2_TMTE_13_6	0.12	8.71	0.83	50.80	0.04	0.00	37.06	1.68	0.22	0.00	99.75	82.77
GM-07a	OL	GM_07a_2_TMTE_13_7	0.14	8.62	0.79	50.78	0.03	0.00	36.97	1.72	0.21	0.01	99.53	82.66
GM-07a	OL	GM_07a_2_TMTE_13_8	0.15	8.81	0.80	50.64	0.04	0.00	37.16	1.66	0.23	0.03	99.74	82.73
GM-07a	OL	GM_07a_2_TMTE_13_9	0.11	8.73	0.76	50.23	0.08	0.00	36.66	1.77	0.25	0.00	98.88	81.86
GM-07a	OL	GM_07a_2_TMTE_13_10	0.10	8.80	0.77	50.70	0.03	0.00	37.03	1.74	0.24	0.00	99.67	82.66
GM-07a	OL	GM_07a_2_TMTE_13_11	0.11	8.66	0.78	50.54	0.04	0.00	36.83	1.74	0.22	0.00	99.14	82.30
GM-07a	OL	GM_07a_2_TMTE_13_12	0.12	8.82	0.76	50.21	0.05	0.00	37.00	1.74	0.22	0.01	99.15	82.18
GM-07a	OL	GM_07a_2_TMTE_13_13	0.10	8.83	0.77	50.39	0.03	0.00	36.84	1.74	0.21	0.02	99.21	82.18
GM-07a	OL	GM_07a_2_TMTE_13_14	0.13	8.69	0.78	50.83	0.07	0.00	36.95	1.74	0.23	0.00	99.75	82.69
GM-07a	OL	GM_07a_2_TMTE_13_15	0.13	8.92	0.77	50.51	0.03	0.00	37.04	1.72	0.23	0.03	99.70	82.49
GM-07a	OL	GM_07a_2_TMTE_13_16	0.13	8.82	0.77	50.88	0.05	0.00	36.77	1.71	0.21	0.09	99.72	82.55
GM-07a	OL	GM_07a_2_TMTE_2_1	0.12	8.86	0.77	50.80	0.05	0.00	37.34	1.70	0.23	0.00	100.09	83.05
GM-07a	OL	GM_07a_2_TMTE_2_2	0.14	8.90	0.78	50.52	0.05	0.00	37.25	1.67	0.23	0.02	99.80	82.72
GM-07a	OL	GM_07a_2_TMTE_2_3	0.16	8.89	0.76	50.62	0.05	0.00	37.25	1.72	0.24	0.02	99.96	82.80
GM-07a	OL	GM_07a_2_TMTE_2_4	0.14	8.85	0.77	50.69	0.04	0.00	37.31	1.75	0.22	0.01	100.02	82.92
GM-07a	OL	GM_07a_2_TMTE_2_5	0.15	8.78	0.77	50.76	0.03	0.00	37.36	1.67	0.21	0.01	99.94	83.04
GM-07a	OL	GM_07a_2_TMTE_2_7	0.15	8.91	0.79	50.78	0.03	0.00	37.37	1.70	0.22	0.01	100.26	83.07
GM-07a	OL	GM_07a_2_TMTE_2_9	0.17	8.82	1.00	50.51	0.04	0.00	37.50	1.69	0.21	0.02	100.17	82.95
GM-07a	OL	GM_07a_2_TMTE_2_10	0.11	8.87	0.80	50.71	0.05	0.00	37.22	1.68	0.23	0.01	99.96	82.85
GM-07a	OL	GM_07a_2_TMTE_2_11	0.11	8.74	0.76	50.95	0.04	0.00	36.97	1.66	0.22	0.03	99.80	82.82
GM-07a	OL	GM_07a_2_TMTE_2_12	0.16	8.79	0.78	50.51	0.06	0.00	37.14	1.68	0.24	0.01	99.66	82.60
GM-07a	OL	GM_07a_2_TMTE_2_13	0.14	8.88	0.78	50.81	0.04	0.00	37.37	1.69	0.23	0.01	100.20	83.09
GM-07a	OL	GM_07a_2_TMTE_2_14	0.15	8.78	0.74	50.61	0.03	0.00	37.20	1.73	0.21	0.01	99.63	82.74
GM-07a	OL	GM_07a_2_TMTE_2_15	0.13	8.91	0.74	50.83	0.06	0.00	37.32	1.75	0.21	0.00	100.26	83.06
GM-07a	OL	GM_07a_2_TMTE_2_16	0.13	8.86	0.74	50.87	0.07	0.00	37.29	1.72	0.24	0.00	100.17	83.06
GM-07a	OL	GM_07a_2_TMTE_3_1	0.20	8.94	0.78	50.22	0.08	0.00	37.28	1.87	0.20	0.00	99.81	82.47

Table 3: (continued)

Sample	Eruptive Unit	Analysis	SiO_2	TiO_2	Al_2O_3	Fe_2O_3	V_2O_3	Cr_2O_3	FeO	MnO	MgO	CaO	Total	FeO^T
GM-07a	OL	GM_07a_2_TMTE_3_5	0.14	8.85	0.78	50.53	0.03	0.00	37.04	1.74	0.24	0.00	99.72	82.51
GM-07a	OL	GM_07a_2_TMTE_3_7	0.19	8.89	0.77	50.38	0.02	0.00	37.26	1.78	0.23	0.01	99.80	82.59
GM-07a	OL	GM_07a_2_TMTE_3_8	0.18	8.87	0.76	50.30	0.04	0.00	37.02	1.81	0.22	0.01	99.54	82.29
GM-07a	OL	GM_07a_2_TMTE_3_9	0.19	8.91	0.77	50.49	0.03	0.00	37.21	1.82	0.26	0.01	99.99	82.64
GM-07a	OL	GM_07a_2_TMTE_3_10	0.18	8.59	0.81	50.43	0.04	0.00	36.81	1.75	0.22	0.01	99.10	82.19
GM-07a	OL	GM_07a_2_TMTE_3_11	0.19	8.69	0.81	50.89	0.06	0.00	37.22	1.79	0.22	0.02	100.11	83.01
GM-07a	OL	GM_07a_2_TMTE_3_12	0.19	8.66	0.80	50.74	0.03	0.00	36.97	1.78	0.22	0.00	99.71	82.63
GM-07a	OL	GM_07a_2_TMTE_3_13	0.17	8.75	0.74	50.85	0.06	0.00	37.09	1.81	0.23	0.00	99.99	82.85
GM-07a	OL	GM_07a_2_TMTE_3_17	0.19	8.81	0.81	50.43	0.02	0.00	37.13	1.83	0.22	0.01	99.72	82.51
GM-07a	OL	GM_07a_2_TMTE_3_18	0.17	8.80	0.78	50.60	0.04	0.00	37.11	1.80	0.23	0.01	99.79	82.64
GM-07a	OL	GM_07a_2_TMTE_4_1	0.10	8.96	0.78	50.58	0.03	0.00	37.18	1.76	0.25	0.01	99.94	82.69
GM-07a	OL	GM_07a_2_TMTE_4_2	0.13	9.02	0.75	50.23	0.04	0.00	37.25	1.77	0.24	0.00	99.68	82.44
GM-07a	OL	GM_07a_2_TMTE_4_3	0.11	8.94	0.74	50.61	0.02	0.00	37.21	1.73	0.22	0.00	99.90	82.74
GM-07a	OL	GM_07a_2_TMTE_4_4	0.13	8.94	0.76	50.38	0.04	0.00	37.23	1.77	0.23	0.01	99.77	82.56
GM-07a	OL	GM_07a_2_TMTE_4_5	0.10	8.78	0.82	51.05	0.04	0.00	37.19	1.70	0.24	0.00	100.21	83.13
GM-07a	OL	GM_07a_2_TMTE_4_6	0.12	8.85	0.81	50.86	0.02	0.00	37.33	1.71	0.22	0.00	100.20	83.10
GM-07a	OL	GM_07a_2_TMTE_4_7	0.12	8.85	0.79	50.63	0.06	0.00	37.12	1.72	0.22	0.00	99.86	82.68
GM-07a	OL	GM_07a_2_TMTE_4_9	0.12	9.08	0.77	50.64	0.04	0.00	37.55	1.72	0.24	0.00	100.44	83.11
GM-07a	OL	GM_07a_2_TMTE_4_10	0.10	9.03	0.75	50.43	0.05	0.00	37.32	1.74	0.23	0.00	99.90	82.70
GM-07a	OL	GM_07a_2_TMTE_4_11	0.10	8.98	0.77	51.03	0.03	0.00	37.35	1.77	0.23	0.02	100.58	83.27
GM-07a	OL	GM_07a_2_TMTE_4_12	0.11	8.96	0.77	50.27	0.04	0.00	37.14	1.73	0.23	0.00	99.53	82.38
GM-07a	OL	GM_07a_2_TMTE_4_13	0.10	8.88	0.75	50.57	0.07	0.00	37.25	1.67	0.22	0.02	99.82	82.75
GM-07a	OL	GM_07a_2_TMTE_4_14	0.11	8.85	0.81	50.66	0.04	0.00	37.05	1.78	0.23	0.00	99.88	82.63
GM-07a	OL	GM_07a_2_TMTE_4_15	0.09	9.07	0.78	50.76	0.02	0.00	37.51	1.75	0.24	0.01	100.54	83.19
GM-07a	OL	GM_07a_2_TMTE_4_17	0.12	8.96	0.78	49.98	0.04	0.00	37.10	1.68	0.27	0.02	99.24	82.08
GM-07a	OL	GM_07a_2_TMTE_5_1	0.16	9.07	0.82	49.79	0.03	0.00	36.50	2.42	0.22	0.01	99.37	81.31
GM-07a	OL	GM_07a_2_TMTE_5_2	0.12	8.94	0.78	50.42	0.04	0.00	36.47	2.45	0.23	0.02	99.82	81.84
GM-07a	OL	GM_07a_2_TMTE_5_3	0.15	8.40	0.78	51.85	0.05	0.00	36.05	2.40	0.22	0.03	100.33	82.71
GM-07a	OL	GM_07a_2_TMTE_5_4	0.10	8.54	0.71	51.38	0.05	0.00	36.04	2.47	0.21	0.01	99.88	82.28
GM-07a	OL	GM_07a_2_TMTE_5_5	0.13	8.79	0.70	50.96	0.05	0.00	36.42	2.46	0.21	0.01	100.07	82.28
GM-07a	OL	GM_07a_2_TMTE_5_6	0.13	8.84	0.76	50.93	0.05	0.00	36.45	2.44	0.22	0.01	100.21	82.28
GM-07a	OL	GM_07a_2_TMTE_5_7	0.15	8.89	0.76	50.54	0.02	0.00	36.46	2.41	0.21	0.00	99.84	81.94
GM-07a	OL	GM_07a_2_TMTE_5_10	0.17	8.85	0.83	50.27	0.04	0.00	36.36	2.42	0.21	0.00	99.52	81.59

Table 3: (continued)

Sample	Eruptive Unit	Analysis	SiO_2	TiO_2	Al_2O_3	Fe_2O_3	V_2O_3	Cr_2O_3	FeO	MnO	MgO	CaO	Total	FeO^T
GM-07a	OL	GM_07a_2_TMTE_5_11	0.14	8.93	0.79	50.55	0.05	0.00	36.71	2.35	0.21	0.01	100.05	82.20
GM-07a	OL	GM_07a_2_TMTE_5_12	0.12	9.03	0.72	50.26	0.04	0.00	36.56	2.34	0.22	0.00	99.66	81.79
GM-07a	OL	GM_07a_2_TMTE_5_15	0.11	8.72	0.80	50.98	0.04	0.00	36.21	2.48	0.23	0.01	99.97	82.09
GM-07a	OL	GM_07a_2_TMTE_5_16	0.12	8.71	0.80	50.84	0.04	0.00	36.25	2.37	0.23	0.00	99.72	81.99
GM-07a	OL	GM_07a_2_TMTE_6_1	0.12	8.87	0.79	50.63	0.06	0.00	37.21	1.71	0.22	0.00	99.91	82.78
GM-07a	OL	GM_07a_2_TMTE_6_2	0.10	8.95	0.77	50.87	0.03	0.00	37.34	1.78	0.23	0.01	100.29	83.11
GM-07a	OL	GM_07a_2_TMTE_6_3	0.13	8.81	0.76	50.48	0.04	0.00	37.01	1.75	0.23	0.01	99.46	82.44
GM-07a	OL	GM_07a_2_TMTE_6_4	0.12	8.90	0.78	50.61	0.04	0.00	37.31	1.76	0.22	0.01	99.95	82.84
GM-07a	OL	GM_07a_2_TMTE_6_5	0.12	8.83	0.79	50.85	0.04	0.00	37.07	1.79	0.23	0.01	100.04	82.83
GM-07a	OL	GM_07a_2_TMTE_6_6	0.15	8.84	0.75	50.76	0.03	0.00	37.05	1.75	0.25	0.02	99.90	82.73
GM-07a	OL	GM_07a_2_TMTE_6_7	0.13	8.71	0.76	50.85	0.02	0.00	37.04	1.71	0.21	0.01	99.78	82.79
GM-07a	OL	GM_07a_2_TMTE_6_8	0.11	8.89	0.78	51.09	0.05	0.00	37.36	1.73	0.23	0.01	100.53	83.34
GM-07a	OL	GM_07a_2_TMTE_6_9	0.10	8.68	0.77	51.09	0.05	0.00	36.89	1.81	0.23	0.00	99.88	82.86
GM-07a	OL	GM_07a_2_TMTE_6_10	0.12	8.78	0.74	51.33	0.06	0.00	37.33	1.75	0.21	0.01	100.57	83.51
GM-07a	OL	GM_07a_2_TMTE_6_11	0.09	8.95	0.78	50.42	0.03	0.00	37.15	1.75	0.23	0.00	99.66	82.52
GM-07a	OL	GM_07a_2_TMTE_6_12	0.09	8.86	0.75	50.90	0.04	0.00	37.15	1.76	0.24	0.00	100.05	82.96
GM-07a	OL	GM_07a_2_TMTE_6_13	0.11	8.78	0.84	50.66	0.03	0.00	36.84	1.77	0.23	0.01	99.67	82.43
GM-07a	OL	GM_07a_2_TMTE_6_14	0.10	8.80	0.77	50.72	0.06	0.00	36.97	1.78	0.24	0.01	99.73	82.61
GM-07a	OL	GM_07a_2_TMTE_6_15	0.07	8.80	0.76	50.82	0.06	0.00	36.87	1.83	0.23	0.00	99.77	82.60
GM-07a	OL	GM_07a_2_TMTE_6_16	0.07	8.86	0.80	50.77	0.05	0.00	36.87	1.86	0.24	0.01	99.87	82.56
GM-07a	OL	GM_07a_2_TMTE_7_2	0.15	8.94	0.78	50.28	0.02	0.00	37.11	1.84	0.23	0.01	99.61	82.35
GM-07a	OL	GM_07a_2_TMTE_7_4	0.13	8.82	0.79	50.92	0.07	0.00	37.13	1.80	0.23	0.00	100.24	82.95
GM-07a	OL	GM_07a_2_TMTE_7_5	0.15	8.93	0.76	50.69	0.04	0.00	37.20	1.93	0.23	0.00	100.18	82.81
GM-07a	OL	GM_07a_2_TMTE_7_6	0.13	8.84	0.81	50.77	0.03	0.00	37.02	1.90	0.23	0.01	100.02	82.70
GM-07a	OL	GM_07a_2_TMTE_7_7	0.14	8.77	0.74	50.55	0.04	0.00	36.68	2.05	0.23	0.01	99.50	82.17
GM-07a	OL	GM_07a_2_TMTE_7_8	0.16	8.83	0.80	50.64	0.03	0.00	36.82	2.05	0.24	0.01	99.95	82.39
GM-07a	OL	GM_07a_2_TMTE_7_9	0.20	8.72	0.80	50.58	0.03	0.00	36.65	2.00	0.24	0.01	99.58	82.17
GM-07a	OL	GM_07a_2_TMTE_7_10	0.13	8.99	0.77	50.86	0.04	0.00	37.04	2.04	0.25	0.02	100.46	82.81
GM-07a	OL	GM_07a_2_TMTE_7_12	0.14	8.83	0.78	50.58	0.01	0.00	36.79	2.07	0.22	0.00	99.71	82.30
GM-07a	OL	GM_07a_2_TMTE_7_13	0.12	9.01	0.77	50.52	0.03	0.00	36.91	2.06	0.23	0.01	100.06	82.36
GM-07a	OL	GM_07a_2_TMTE_7_14	0.14	8.87	0.84	50.70	0.05	0.00	37.01	1.97	0.25	0.00	100.14	82.63
GM-07a	OL	GM_07a_2_TMTE_7_15	0.15	8.77	0.79	50.98	0.04	0.00	36.79	2.02	0.23	0.01	100.16	82.66
GM-07a	OL	GM_07a_2_TMTE_7_16	0.12	8.64	0.79	50.88	0.04	0.00	36.54	2.03	0.23	0.01	99.61	82.32

Table 3: (continued)

Sample	Eruptive Unit	Analysis	SiO_2	TiO_2	Al_2O_3	Fe_2O_3	V_2O_3	Cr_2O_3	FeO	MnO	MgO	CaO	Total	FeO^T
GM-07a	OL	GM_07a_2_TMTE_7_17	0.19	8.76	1.02	50.10	0.03	0.00	36.90	1.96	0.24	0.01	99.45	81.98
GM-07a	OL	GM_07a_2_TMTE_7_18	0.14	8.09	0.79	52.18	0.05	0.00	36.35	1.77	0.22	0.01	99.99	83.30
GM-07a	OL	GM_07a_2_TMTE_7_20	0.15	7.94	0.76	52.24	0.04	0.00	36.27	1.76	0.21	0.01	99.63	83.28
GM-07a	OL	GM_07a_2_TMTE_7_21	0.18	8.53	0.76	51.37	0.04	0.00	36.96	1.86	0.22	0.01	100.18	83.18
GM-07a	OL	GM_07a_2_TMTE_8_1	0.19	9.05	0.73	50.08	0.05	0.00	37.09	1.94	0.23	0.01	99.68	82.16
GM-07a	OL	GM_07a_2_TMTE_8_2	0.19	8.74	0.75	50.56	0.02	0.00	36.96	1.84	0.23	0.00	99.56	82.46
GM-07a	OL	GM_07a_2_TMTE_8_3	0.20	8.80	0.79	50.73	0.03	0.00	37.08	1.80	0.24	0.01	100.07	82.73
GM-07a	OL	GM_07a_2_TMTE_8_5	0.19	8.88	0.77	50.75	0.03	0.00	37.42	1.80	0.22	0.01	100.30	83.09
GM-07a	OL	GM_07a_2_TMTE_8_6	0.18	8.55	0.79	50.89	0.03	0.00	36.60	1.93	0.23	0.01	99.48	82.39
GM-07a	OL	GM_07a_2_TMTE_8_8	0.18	9.07	0.78	49.97	0.05	0.00	37.37	1.86	0.22	0.01	99.73	82.33
GM-07a	OL	GM_07a_2_TMTE_8_9	0.17	8.91	0.77	50.13	0.03	0.00	36.75	1.99	0.23	0.02	99.34	81.85
GM-07a	OL	GM_07a_2_TMTE_8_10	0.19	8.91	0.71	50.42	0.04	0.00	37.04	1.96	0.22	0.00	99.79	82.42
GM-07a	OL	GM_07a_2_TMTE_8_13	0.19	8.92	0.77	50.54	0.04	0.00	37.31	1.76	0.25	0.01	100.02	82.79
GM-07a	OL	GM_07a_2_TMTE_8_14	0.19	8.83	0.79	50.20	0.05	0.00	37.00	1.77	0.22	0.00	99.41	82.17
GM-07a	OL	GM_07a_2_TMTE_8_15	0.20	8.90	0.74	50.50	0.03	0.00	37.13	1.83	0.24	0.01	99.91	82.57
GM-07a	OL	GM_07a_2_TMTE_8_16	0.20	8.79	0.75	50.83	0.06	0.00	37.29	1.79	0.22	0.01	100.16	83.03
GM-07a	OL	GM_07a_2_TMTE_9_2	0.13	8.70	0.77	50.61	0.04	0.00	36.80	1.82	0.22	0.01	99.40	82.34
GM-07a	OL	GM_07a_2_TMTE_9_3	0.16	8.83	0.74	50.49	0.03	0.00	36.90	1.90	0.22	0.00	99.61	82.33
GM-07a	OL	GM_07a_2_TMTE_9_4	0.13	8.80	0.77	50.53	0.05	0.00	36.72	1.83	0.24	0.02	99.45	82.19
GM-07a	OL	GM_07a_2_TMTE_9_5	0.13	8.78	0.82	50.45	0.03	0.00	36.79	1.91	0.23	0.02	99.50	82.19
GM-07a	OL	GM_07a_2_TMTE_9_6	0.10	8.76	0.84	50.50	0.05	0.00	36.73	1.83	0.22	0.00	99.43	82.17
GM-07a	OL	GM_07a_2_TMTE_9_7	0.11	8.59	0.78	50.93	0.05	0.00	36.72	1.75	0.21	0.00	99.53	82.55
GM-07a	OL	GM_07a_2_TMTE_9_8	0.14	8.70	0.99	50.11	0.05	0.00	36.67	1.78	0.24	0.01	99.05	81.77
GM-07a	OL	GM_07a_2_TMTE_9_10	0.14	8.71	1.03	50.15	0.06	0.00	36.74	1.87	0.21	0.01	99.25	81.87
GM-07a	OL	GM_07a_2_TMTE_9_12	0.12	8.75	0.76	50.37	0.03	0.00	36.64	1.87	0.23	0.00	99.10	81.96
GM-07a	OL	GM_07a_2_TMTE_9_13	0.12	8.68	0.79	50.78	0.05	0.00	36.67	1.89	0.23	0.01	99.53	82.36
GM-07a	OL	GM_07a_2_TMTE_9_14	0.12	8.77	0.83	50.58	0.05	0.00	36.68	1.87	0.25	0.01	99.56	82.20
GM-07a	OL	GM_07a_2_TMTE_9_15	0.14	8.64	0.76	50.50	0.04	0.00	36.53	1.84	0.23	0.00	99.10	81.98
GM-07a	OL	GM_07a_2_TMTE_9_16	0.14	8.72	0.76	50.85	0.04	0.00	36.90	1.83	0.23	0.01	99.86	82.66
GM-07a	OL	GM_07a_2_TMTE_9_17	0.10	8.36	0.74	51.06	0.06	0.00	36.21	1.87	0.23	0.01	99.00	82.16
GM-07a	OL	GM_07a_2_TMTE_9_18	0.16	8.25	1.06	50.31	0.04	0.00	36.16	1.74	0.23	0.01	98.22	81.43
GM-07a	OL	GM_07a_2_TMTE_10_1	0.16	8.83	0.75	49.94	0.04	0.00	36.92	1.81	0.22	0.01	98.89	81.86
GM-07a	OL	GM_07a_2_TMTE_10_2	0.12	8.91	0.78	50.40	0.04	0.00	37.14	1.70	0.24	0.00	99.65	82.49

Table 3: (continued)

Sample	Eruptive Unit	Analysis	SiO_2	TiO_2	Al_2O_3	Fe_2O_3	V_2O_3	Cr_2O_3	FeO	MnO	MgO	CaO	Total	FeO^T
GM-07a	OL	GM_07a_2_TMTE_10_3	0.16	8.60	0.78	50.57	0.03	0.00	36.86	1.69	0.22	0.01	99.21	82.37
GM-07a	OL	GM_07a_2_TMTE_10_4	0.14	8.69	0.80	50.39	0.04	0.00	36.77	1.74	0.26	0.00	99.14	82.11
GM-07a	OL	GM_07a_2_TMTE_10_5	0.14	8.80	0.73	50.26	0.05	0.00	36.88	1.77	0.24	0.01	99.16	82.10
GM-07a	OL	GM_07a_2_TMTE_10_6	0.17	8.76	0.82	50.42	0.07	0.00	37.06	1.74	0.22	0.00	99.54	82.43
GM-07a	OL	GM_07a_2_TMTE_10_7	0.13	8.83	0.78	50.19	0.05	0.00	37.02	1.73	0.23	0.02	99.27	82.18
GM-07a	OL	GM_07a_2_TMTE_10_8	0.16	8.84	0.82	50.17	0.04	0.00	37.09	1.73	0.23	0.01	99.38	82.24
GM-07a	OL	GM_07a_2_TMTE_10_9	0.11	8.77	0.79	50.74	0.04	0.00	36.95	1.77	0.25	0.00	99.72	82.61
GM-07a	OL	GM_07a_2_TMTE_10_10	0.14	8.48	0.83	51.19	0.02	0.00	36.84	1.74	0.24	0.01	99.73	82.91
GM-07a	OL	GM_07a_2_TMTE_10_11	0.15	8.41	0.83	51.11	0.02	0.00	36.68	1.66	0.24	0.01	99.36	82.68
GM-07a	OL	GM_07a_2_TMTE_10_12	0.16	8.45	0.73	51.33	0.03	0.00	36.93	1.69	0.24	0.02	99.83	83.12
GM-07a	OL	GM_07a_2_TMTE_10_13	0.17	8.67	0.77	50.75	0.02	0.00	36.92	1.77	0.24	0.00	99.57	82.58
GM-07a	OL	GM_07a_2_TMTE_10_14	0.17	8.86	0.82	50.01	0.03	0.00	36.98	1.74	0.22	0.01	99.14	81.98
GM-07a	OL	GM_07a_2_TMTE_10_15	0.16	8.58	0.75	50.78	0.04	0.00	36.84	1.71	0.23	0.00	99.38	82.53
GM-07a	OL	GM_07a_2_TMTE_10_16	0.16	8.63	0.77	51.11	0.04	0.00	37.07	1.77	0.22	0.01	100.10	83.07
GM-07a	OL	GM_07a_2_TMTE_10_17	0.13	8.81	0.81	50.23	0.04	0.00	36.85	1.76	0.26	0.00	99.22	82.05
GM-07a	OL	GM_07a_2_TMTE_11_1	0.08	8.80	0.78	50.78	0.02	0.00	36.61	2.16	0.22	0.01	99.78	82.30
GM-07a	OL	GM_07a_2_TMTE_11_2	0.09	8.96	0.88	50.58	0.05	0.00	36.80	2.21	0.24	0.00	100.09	82.32
GM-07a	OL	GM_07a_2_TMTE_11_3	0.11	8.77	0.99	50.37	0.03	0.00	36.41	2.18	0.23	0.02	99.45	81.74
GM-07a	OL	GM_07a_2_TMTE_11_4	0.11	8.62	0.80	50.98	0.02	0.00	36.41	2.23	0.22	0.01	99.72	82.28
GM-07a	OL	GM_07a_2_TMTE_11_5	0.10	8.48	0.73	51.65	0.03	0.00	36.24	2.19	0.22	0.01	100.06	82.71
GM-07a	OL	GM_07a_2_TMTE_11_6	0.10	8.64	0.72	51.33	0.06	0.00	36.52	2.18	0.21	0.01	100.07	82.71
GM-07a	OL	GM_07a_2_TMTE_11_7	0.07	8.56	0.74	51.27	0.03	0.00	36.27	2.21	0.20	0.01	99.74	82.41
GM-07a	OL	GM_07a_2_TMTE_11_8	0.10	8.28	0.74	51.82	0.04	0.00	36.11	2.12	0.24	0.00	99.83	82.74
GM-07a	OL	GM_07a_2_TMTE_11_9	0.11	8.90	0.71	50.38	0.01	0.00	36.52	2.17	0.22	0.01	99.37	81.85
GM-07a	OL	GM_07a_2_TMTE_11_10	0.13	8.81	0.83	50.91	0.04	0.00	36.77	2.20	0.21	0.00	100.24	82.58
GM-07a	OL	GM_07a_2_TMTE_11_11	0.12	8.65	2.02	49.10	0.04	0.00	36.49	2.13	0.23	0.01	99.13	80.66
GM-07a	OL	GM_07a_2_TMTE_11_12	0.09	8.76	0.80	51.07	0.03	0.00	36.62	2.17	0.20	0.00	100.16	82.57
GM-07a	OL	GM_07a_2_TMTE_11_14	0.08	8.78	0.80	50.78	0.05	0.00	36.40	2.25	0.22	0.01	99.71	82.10
GM-07a	OL	GM_07a_2_TMTE_11_15	0.11	8.78	0.78	50.23	0.05	0.00	36.35	2.19	0.21	0.01	99.04	81.55
GM-07a	OL	GM_07a_2_TMTE_11_17	0.08	8.57	0.77	51.10	0.05	0.00	36.22	2.22	0.22	0.00	99.56	82.20
GM-07a	OL	GM_07a_2_TMTE_11_18	0.12	8.19	0.75	51.78	0.04	0.00	35.99	2.20	0.20	0.00	99.61	82.58
GM-07a	OL	GM_07a_2_TMTE_12_1	0.13	8.78	0.79	50.07	0.05	0.00	36.53	1.91	0.23	0.01	98.79	81.59
GM-07a	OL	GM_07a_2_TMTE_12_2	0.11	8.84	0.77	50.81	0.05	0.00	36.91	1.93	0.23	0.01	99.97	82.63

Table 3: (continued)

Sample	Eruptive Unit	Analysis	SiO_2	TiO_2	Al_2O_3	Fe_2O_3	V_2O_3	Cr_2O_3	FeO	MnO	MgO	CaO	Total	FeO^T
GM-07a	OL	GM_07a_2_TMTE_12_3	0.10	8.83	0.73	50.48	0.03	0.00	36.62	1.98	0.23	0.00	99.34	82.05
GM-07a	OL	GM_07a_2_TMTE_12_4	0.12	8.53	0.76	51.15	0.05	0.00	36.60	1.91	0.23	0.01	99.69	82.63
GM-07a	OL	GM_07a_2_TMTE_12_5	0.10	8.15	0.79	51.46	0.04	0.00	36.05	1.91	0.23	0.01	99.02	82.35
GM-07a	OL	GM_07a_2_TMTE_12_6	0.11	8.47	0.80	51.22	0.05	0.00	36.54	1.88	0.22	0.00	99.60	82.63
GM-07a	OL	GM_07a_2_TMTE_12_7	0.11	8.48	0.80	51.15	0.04	0.00	36.40	1.87	0.22	0.03	99.42	82.43
GM-07a	OL	GM_07a_2_TMTE_12_8	0.13	8.69	0.71	50.85	0.04	0.00	36.81	1.88	0.23	0.01	99.62	82.57
GM-07a	OL	GM_07a_2_TMTE_12_9	0.12	8.78	0.77	50.36	0.06	0.00	36.75	1.86	0.23	0.00	99.23	82.06
GM-07a	OL	GM_07a_2_TMTE_12_10	0.11	8.89	0.74	50.82	0.03	0.00	37.17	1.84	0.23	0.01	100.11	82.90
GM-07a	OL	GM_07a_2_TMTE_12_11	0.10	8.65	0.78	51.18	0.03	0.00	36.83	1.88	0.24	0.00	99.94	82.89
GM-07a	OL	GM_07a_2_TMTE_12_12	0.14	8.74	0.73	50.66	0.05	0.00	36.72	1.90	0.23	0.02	99.47	82.31
GM-07a	OL	GM_07a_2_TMTE_12_13	0.10	8.78	0.78	50.35	0.05	0.00	36.46	2.05	0.22	0.00	99.14	81.76
GM-07a	OL	GM_07a_2_TMTE_12_14	0.10	8.76	0.76	50.85	0.04	0.00	36.68	2.06	0.21	0.01	99.84	82.44
GM-07a	OL	GM_07a_2_TMTE_12_15	0.12	8.86	0.78	50.79	0.05	0.00	36.99	1.91	0.23	0.01	100.00	82.70
GM-07a	OL	GM_07a_2_TMTE_13_1	0.12	8.83	1.31	49.37	0.02	0.00	36.60	2.04	0.22	0.01	98.83	81.03
GM-07a	OL	GM_07a_2_TMTE_13_3	0.08	8.76	0.75	50.69	0.06	0.00	36.50	2.15	0.23	0.01	99.54	82.11
GM-07a	OL	GM_07a_2_TMTE_13_4	0.12	8.87	0.82	50.36	0.06	0.00	36.65	2.15	0.21	0.00	99.59	81.97
GM-07a	OL	GM_07a_2_TMTE_13_5	0.11	8.83	0.80	50.51	0.06	0.00	36.61	2.22	0.22	0.01	99.66	82.06
GM-07a	OL	GM_07a_2_TMTE_13_6	0.13	8.74	0.82	50.37	0.06	0.00	36.51	2.16	0.22	0.01	99.30	81.83
GM-07a	OL	GM_07a_2_TMTE_13_7	0.10	8.86	0.94	51.17	0.03	0.00	36.78	2.21	0.24	0.01	100.73	82.82
GM-07a	OL	GM_07a_2_TMTE_13_8	0.13	8.32	0.89	51.85	0.03	0.00	36.34	2.11	0.19	0.02	100.25	83.00
GM-07a	OL	GM_07a_2_TMTE_13_9	0.13	8.39	0.84	51.68	0.04	0.00	36.48	2.07	0.22	0.01	100.18	82.98
GM-07a	OL	GM_07a_2_TMTE_13_10	0.14	8.30	0.73	51.82	0.05	0.00	36.32	2.14	0.20	0.01	100.04	82.95
GM-07a	OL	GM_07a_2_TMTE_13_12	0.11	8.55	0.76	51.13	0.03	0.00	36.42	2.15	0.20	0.00	99.62	82.43
GM-07a	OL	GM_07a_2_TMTE_13_13	0.11	8.74	0.79	50.99	0.07	0.00	36.68	2.04	0.23	0.01	100.00	82.56
GM-07a	OL	GM_07a_2_TMTE_13_14	0.10	8.55	0.75	51.01	0.04	0.00	36.20	2.09	0.22	0.02	99.32	82.11
GM-07a	OL	GM_07a_2_TMTE_13_15	0.07	8.64	0.78	51.05	0.07	0.00	36.50	2.07	0.22	0.01	99.67	82.44
GM-07a	OL	GM_07a_2_TMTE_14_1	0.08	8.99	0.80	50.64	0.05	0.00	37.19	1.72	0.25	0.01	100.07	82.76
GM-07a	OL	GM_07a_2_TMTE_14_2	0.09	8.84	0.76	50.82	0.07	0.00	37.12	1.72	0.24	0.00	99.96	82.85
GM-07a	OL	GM_07a_2_TMTE_14_3	0.11	8.26	0.75	51.87	0.03	0.00	36.49	1.67	0.23	0.03	99.73	83.17
GM-07a	OL	GM_07a_2_TMTE_14_4	0.07	8.77	0.73	50.93	0.05	0.00	37.05	1.70	0.21	0.00	99.81	82.88
GM-07a	OL	GM_07a_2_TMTE_14_5	0.07	8.96	0.80	50.60	0.05	0.00	37.29	1.68	0.23	0.00	99.95	82.82
GM-07a	OL	GM_07a_2_TMTE_14_6	0.06	8.89	0.76	50.96	0.03	0.00	37.25	1.69	0.22	0.01	100.12	83.10
GM-07a	OL	GM_07a_2_TMTE_14_7	0.10	8.67	0.81	51.29	0.03	0.00	36.97	1.77	0.23	0.01	100.20	83.13

Table 3: (continued)

Sample	Eruptive Unit	Analysis	SiO_2	TiO_2	Al_2O_3	Fe_2O_3	V_2O_3	Cr_2O_3	FeO	MnO	MgO	CaO	Total	FeO^T
GM-07a	OL	GM_07a_2_TMTE_14_8	0.08	8.41	0.94	51.73	0.05	0.00	36.93	1.67	0.22	0.01	100.30	83.47
GM-07a	OL	GM_07a_2_TMTE_14_9	0.08	8.69	0.76	51.18	0.02	0.00	36.97	1.76	0.24	0.00	99.96	83.02
GM-07a	OL	GM_07a_2_TMTE_14_10	0.12	8.88	0.76	50.89	0.05	0.00	37.35	1.71	0.24	0.00	100.25	83.15
GM-07a	OL	GM_07a_2_TMTE_14_11	0.08	8.70	0.77	51.16	0.04	0.00	36.98	1.73	0.24	0.00	99.99	83.01
GM-07a	OL	GM_07a_2_TMTE_14_12	0.09	8.86	0.81	50.83	0.06	0.00	37.26	1.72	0.24	0.01	100.15	83.01
GM-07a	OL	GM_07a_2_TMTE_14_13	0.09	8.81	0.77	50.84	0.03	0.00	37.12	1.73	0.23	0.00	99.89	82.87
GM-07a	OL	GM_07a_2_TMTE_14_14	0.10	8.88	0.77	50.90	0.05	0.00	37.32	1.76	0.25	0.02	100.32	83.13
GM-07a	OL	GM_07a_2_TMTE_14_15	0.10	8.87	0.74	50.75	0.06	0.00	37.16	1.72	0.22	0.00	99.96	82.83
GM-07a	OL	GM_07a_2_TMTE_14_16	0.09	8.86	0.74	50.87	0.03	0.00	37.16	1.73	0.24	0.00	100.00	82.94
GM-07a	OL	GM_07a_3_TMTE_1_3	0.15	8.32	0.75	51.62	0.03	0.00	36.73	1.68	0.23	0.00	99.79	83.18
GM-07a	OL	GM_07a_3_TMTE_1_4	0.12	8.14	0.78	52.21	0.04	0.00	36.54	1.70	0.24	0.00	100.15	83.52
GM-07a	OL	GM_07a_3_TMTE_1_5	0.12	8.10	0.79	52.24	0.03	0.00	36.65	1.69	0.23	0.01	100.10	83.65
GM-07a	OL	GM_07a_3_TMTE_1_6	0.15	8.19	0.78	52.29	0.04	0.00	36.77	1.71	0.23	0.01	100.44	83.82
GM-07a	OL	GM_07a_3_TMTE_1_7	0.14	8.05	0.81	52.37	0.03	0.00	36.62	1.69	0.23	0.01	100.14	83.74
GM-07a	OL	GM_07a_3_TMTE_1_8	0.16	7.99	0.81	52.40	0.05	0.00	36.53	1.72	0.21	0.02	100.13	83.68
GM-07a	OL	GM_07a_3_TMTE_1_9	0.13	7.78	0.81	52.80	0.03	0.00	36.31	1.62	0.20	0.01	100.00	83.83
GM-07a	OL	GM_07a_3_TMTE_1_10	0.17	7.73	0.82	52.60	0.04	0.00	36.21	1.59	0.23	0.02	99.70	83.55
GM-07a	OL	GM_07a_3_TMTE_1_15	0.10	8.23	0.80	52.43	0.04	0.00	36.78	1.68	0.23	0.01	100.60	83.96
GM-07a	OL	GM_07a_3_TMTE_1_16	0.15	7.88	0.80	52.32	0.02	0.00	36.39	1.65	0.22	0.01	99.72	83.47
GM-07a	OL	GM_07a_3_TMTE_2_1	0.18	8.47	1.87	48.90	0.07	0.00	36.82	1.69	0.17	0.01	98.40	80.82
GM-07a	OL	GM_07a_3_TMTE_2_2	0.10	8.74	0.77	51.48	0.03	0.00	37.32	1.72	0.24	0.01	100.64	83.64
GM-07a	OL	GM_07a_3_TMTE_2_3	0.06	8.75	0.78	51.69	0.05	0.00	37.21	1.76	0.24	0.01	100.84	83.73
GM-07a	OL	GM_07a_3_TMTE_2_4	0.11	8.81	0.73	51.38	0.01	0.00	37.49	1.67	0.21	0.01	100.69	83.73
GM-07a	OL	GM_07a_3_TMTE_2_5	0.10	8.87	0.78	51.12	0.04	0.00	37.22	1.78	0.23	0.02	100.47	83.22
GM-07a	OL	GM_07a_3_TMTE_2_6	0.11	8.69	0.76	51.47	0.04	0.00	37.17	1.73	0.24	0.00	100.50	83.48
GM-07a	OL	GM_07a_3_TMTE_2_7	0.09	8.69	0.75	51.82	0.06	0.00	37.15	1.75	0.22	0.02	100.89	83.78
GM-07a	OL	GM_07a_3_TMTE_2_8	0.10	8.60	0.81	51.76	0.01	0.00	37.22	1.75	0.22	0.01	100.75	83.79
GM-07a	OL	GM_07a_3_TMTE_2_9	0.13	8.47	0.79	51.64	0.03	0.00	37.00	1.70	0.22	0.01	100.28	83.47
GM-07a	OL	GM_07a_3_TMTE_2_10	0.08	8.71	0.82	51.63	0.02	0.00	37.22	1.73	0.23	0.01	100.72	83.68
GM-07a	OL	GM_07a_3_TMTE_2_11	0.07	8.55	0.77	51.99	0.02	0.00	37.00	1.74	0.22	0.02	100.63	83.78
GM-07a	OL	GM_07a_3_TMTE_2_12	0.09	8.65	0.78	51.48	0.04	0.00	37.09	1.78	0.22	0.01	100.43	83.42
GM-07a	OL	GM_07a_3_TMTE_2_13	0.09	8.75	0.75	51.33	0.02	0.00	37.13	1.73	0.22	0.01	100.35	83.32
GM-07a	OL	GM_07a_3_TMTE_2_14	0.08	8.70	0.77	51.77	0.05	0.00	37.14	1.88	0.22	0.02	100.96	83.73

Table 3: (continued)

Sample	Eruptive Unit	Analysis	SiO_2	TiO_2	Al_2O_3	Fe_2O_3	V_2O_3	Cr_2O_3	FeO	MnO	MgO	CaO	Total	FeO^T
GM-07a	OL	GM_07a_3_TMTE_2_15	0.09	8.91	0.76	51.13	0.04	0.00	37.31	1.79	0.23	0.00	100.55	83.32
GM-07a	OL	GM_07a_3_TMTE_2_16	0.09	8.70	0.76	51.74	0.06	0.00	37.22	1.74	0.24	0.00	100.87	83.78
GM-07a	OL	GM_07a_3_TMTE_2_17	0.07	8.73	0.78	51.14	0.05	0.00	36.92	1.79	0.23	0.00	100.06	82.93
GM-07a	OL	GM_07a_3_TMTE_2_18	0.12	8.69	0.71	51.55	0.03	0.00	37.11	1.77	0.23	0.00	100.54	83.50
GM-07a	OL	GM_07a_3_TMTE_3_1	0.13	8.66	0.75	51.52	0.07	0.00	37.14	1.79	0.22	0.00	100.61	83.51
GM-07a	OL	GM_07a_3_TMTE_3_2	0.13	8.79	0.81	51.30	0.06	0.00	37.31	1.81	0.21	0.01	100.70	83.47
GM-07a	OL	GM_07a_3_TMTE_3_4	0.12	8.71	0.79	51.30	0.05	0.00	37.28	1.72	0.23	0.01	100.44	83.44
GM-07a	OL	GM_07a_3_TMTE_3_5	0.11	8.72	0.78	51.35	0.06	0.00	37.23	1.72	0.23	0.01	100.45	83.44
GM-07a	OL	GM_07a_3_TMTE_3_9	0.14	8.75	0.78	51.40	0.03	0.00	37.30	1.77	0.21	0.01	100.67	83.55
GM-07a	OL	GM_07a_3_TMTE_3_12	0.10	8.06	0.79	52.85	0.05	0.00	36.74	1.66	0.22	0.00	100.77	84.30
GM-07a	OL	GM_07a_3_TMTE_3_13	0.12	8.49	0.85	51.23	0.04	0.00	36.94	1.70	0.21	0.01	99.86	83.03
GM-07a	OL	GM_07a_3_TMTE_4_3	0.09	8.81	0.77	51.14	0.03	0.00	36.55	2.38	0.23	0.01	100.35	82.56
GM-07a	OL	GM_07a_3_TMTE_4_4	0.08	8.76	0.76	51.19	0.07	0.00	36.45	2.33	0.21	0.00	100.24	82.52
GM-07a	OL	GM_07a_3_TMTE_4_6	0.09	8.81	0.82	51.25	0.05	0.00	36.60	2.41	0.23	0.00	100.56	82.71
GM-07a	OL	GM_07a_3_TMTE_4_7	0.09	8.82	0.79	51.23	0.06	0.00	36.51	2.46	0.20	0.00	100.58	82.61
GM-07a	OL	GM_07a_3_TMTE_4_14	0.07	8.61	0.79	51.56	0.04	0.00	36.36	2.27	0.22	0.01	100.31	82.76
GM-07a	OL	GM_07a_3_TMTE_5_1	0.12	8.76	0.83	51.06	0.03	0.00	36.92	1.98	0.23	0.00	100.24	82.87
GM-07a	OL	GM_07a_3_TMTE_5_2	0.09	8.77	0.83	50.99	0.04	0.00	36.85	2.05	0.22	0.01	100.14	82.74
GM-07a	OL	GM_07a_3_TMTE_5_3	0.12	8.65	0.83	51.56	0.07	0.00	36.91	2.04	0.23	0.01	100.70	83.30
GM-07a	OL	GM_07a_3_TMTE_5_6	0.11	8.61	0.87	51.47	0.03	0.00	36.96	1.96	0.23	0.01	100.47	83.27
GM-07a	OL	GM_07a_3_TMTE_5_9	0.14	8.60	0.76	51.36	0.04	0.00	36.89	1.92	0.22	0.01	100.23	83.10
GM-07a	OL	GM_07a_3_TMTE_5_10	0.10	8.61	1.02	51.25	0.04	0.00	36.93	1.87	0.23	0.00	100.37	83.06
GM-07a	OL	GM_07a_3_TMTE_5_11	0.11	8.50	0.85	51.47	0.02	0.00	36.73	1.95	0.21	0.00	100.12	83.04
GM-07a	OL	GM_07a_3_TMTE_5_12	0.07	8.51	0.77	51.80	0.02	0.00	36.64	1.94	0.23	0.00	100.36	83.25
GM-07a	OL	GM_07a_3_TMTE_5_14	0.09	8.38	0.80	52.25	0.03	0.00	36.36	2.23	0.21	0.01	100.75	83.37
GM-07a	OL	GM_07a_3_TMTE_5_15	0.11	7.99	0.76	52.71	0.07	0.00	36.04	2.25	0.21	0.02	100.49	83.47
GM-07a	OL	GM_07a_3_TMTE_5_16	0.08	8.59	0.80	51.93	0.02	0.00	36.60	2.22	0.22	0.00	100.84	83.32
GM-07a	OL	GM_07a_3_TMTE_6_1	0.07	8.81	0.76	51.33	0.05	0.00	37.22	1.77	0.22	0.00	100.51	83.40
GM-07a	OL	GM_07a_3_TMTE_6_2	0.08	8.90	0.78	51.04	0.07	0.00	37.34	1.71	0.23	0.00	100.45	83.26
GM-07a	OL	GM_07a_3_TMTE_6_3	0.06	8.79	0.80	51.34	0.03	0.00	37.30	1.70	0.23	0.01	100.52	83.50
GM-07a	OL	GM_07a_3_TMTE_6_4	0.09	8.96	0.81	50.84	0.02	0.00	37.43	1.72	0.22	0.00	100.33	83.18
GM-07a	OL	GM_07a_3_TMTE_6_5	0.08	8.80	0.81	51.04	0.02	0.00	37.21	1.68	0.21	0.01	100.14	83.14
GM-07a	OL	GM_07a_3_TMTE_6_6	0.06	8.86	0.77	51.33	0.06	0.00	37.33	1.70	0.21	0.01	100.64	83.52

Table 3: (continued)

Sample	Eruptive Unit	Analysis	SiO_2	TiO_2	Al_2O_3	Fe_2O_3	V_2O_3	Cr_2O_3	FeO	MnO	MgO	CaO	Total	FeO^T
GM-07a	OL	GM_07a_3_TMTE_6_7	0.08	8.80	0.81	51.55	0.04	0.00	37.28	1.71	0.24	0.03	100.77	83.66
GM-07a	OL	GM_07a_3_TMTE_6_9	0.08	9.10	0.79	50.79	0.05	0.00	37.51	1.72	0.22	0.01	100.62	83.22
GM-07a	OL	GM_07a_3_TMTE_6_10	0.08	8.89	0.78	51.34	0.02	0.00	37.49	1.77	0.21	0.01	100.84	83.69
GM-07a	OL	GM_07a_3_TMTE_6_11	0.08	8.97	0.76	51.08	0.03	0.00	37.52	1.74	0.24	0.01	100.65	83.48
GM-07a	OL	GM_07a_3_TMTE_6_13	0.10	8.78	0.76	51.29	0.03	0.00	37.13	1.74	0.23	0.02	100.38	83.28
GM-07a	OL	GM_07a_3_TMTE_6_14	0.08	8.29	0.76	52.39	0.04	0.00	36.86	1.70	0.22	0.00	100.60	84.00
GM-07a	OL	GM_07a_3_TMTE_6_15	0.08	8.21	0.79	52.47	0.03	0.00	36.65	1.73	0.24	0.01	100.51	83.87
GM-07a	OL	GM_07a_3_TMTE_6_16	0.08	8.65	0.79	51.67	0.05	0.00	37.12	1.76	0.23	0.00	100.64	83.61
GM-07a	OL	GM_07a_3_TMTE_7_1	0.06	8.80	0.76	51.30	0.03	0.00	37.20	1.76	0.23	0.01	100.41	83.36
GM-07a	OL	GM_07a_3_TMTE_7_2	0.08	8.89	0.74	51.22	0.06	0.00	37.38	1.80	0.22	0.00	100.63	83.47
GM-07a	OL	GM_07a_3_TMTE_7_3	0.09	8.70	0.78	51.28	0.07	0.00	37.05	1.77	0.24	0.00	100.25	83.19
GM-07a	OL	GM_07a_3_TMTE_7_4	0.13	8.83	0.76	51.22	0.04	0.00	37.35	1.75	0.24	0.01	100.60	83.44
GM-07a	OL	GM_07a_3_TMTE_7_5	0.08	8.97	0.78	51.00	0.01	0.00	37.37	1.76	0.24	0.01	100.54	83.26
GM-07a	OL	GM_07a_3_TMTE_7_6	0.07	8.95	0.77	51.07	0.06	0.00	37.37	1.83	0.22	0.01	100.64	83.33
GM-07a	OL	GM_07a_3_TMTE_7_7	0.09	8.83	0.78	51.19	0.04	0.00	37.07	1.87	0.24	0.01	100.41	83.12
GM-07a	OL	GM_07a_3_TMTE_7_8	0.07	8.96	0.81	50.97	0.06	0.00	37.44	1.78	0.21	0.01	100.58	83.30
GM-07a	OL	GM_07a_3_TMTE_7_9	0.08	8.87	1.02	50.89	0.04	0.00	37.25	1.82	0.25	0.01	100.47	83.04
GM-07a	OL	GM_07a_3_TMTE_7_11	0.10	8.80	0.79	51.28	0.05	0.00	37.05	1.97	0.21	0.01	100.56	83.19
GM-07a	OL	GM_07a_3_TMTE_7_12	0.11	8.78	0.78	51.27	0.04	0.00	37.08	1.85	0.24	0.01	100.45	83.22
GM-07a	OL	GM_07a_3_TMTE_7_13	0.07	8.90	0.80	50.90	0.04	0.00	37.24	1.77	0.22	0.01	100.25	83.04
GM-07a	OL	GM_07a_3_TMTE_7_14	0.11	8.70	0.79	51.01	0.02	0.00	37.16	1.77	0.21	0.03	100.01	83.05
GM-07a	OL	GM_07a_3_TMTE_7_15	0.05	8.66	0.77	51.41	0.04	0.00	37.00	1.78	0.22	0.01	100.21	83.26
GM-07a	OL	GM_07a_3_TMTE_8_2	0.20	8.88	0.91	50.75	0.05	0.00	37.34	1.83	0.25	0.01	100.51	83.00
GM-07a	OL	GM_07a_3_TMTE_8_6	0.15	8.90	0.79	51.25	0.06	0.00	37.21	1.90	0.23	0.03	100.87	83.32
GM-07a	OL	GM_07a_3_TMTE_8_8	0.12	8.95	0.80	50.79	0.05	0.00	37.28	1.84	0.23	0.00	100.33	82.98
GM-07a	OL	GM_07a_3_TMTE_8_10	0.16	9.11	0.85	50.21	0.05	0.00	37.50	1.82	0.22	0.00	100.22	82.68
GM-07a	OL	GM_07a_3_TMTE_8_11	0.16	8.66	0.83	51.38	0.03	0.00	37.23	1.77	0.22	0.00	100.55	83.46
GM-07a	OL	GM_07a_3_TMTE_8_12	0.17	8.62	0.79	51.32	0.03	0.00	37.07	1.79	0.24	0.00	100.31	83.26
GM-07a	OL	GM_07a_3_TMTE_8_13	0.10	9.02	0.78	51.19	0.04	0.00	37.60	1.74	0.22	0.00	100.99	83.67
GM-07a	OL	GM_07a_3_TMTE_8_14	0.10	8.94	0.81	51.23	0.03	0.00	37.47	1.78	0.23	0.00	100.90	83.57
GM-07a	OL	GM_07a_3_TMTE_8_15	0.09	8.76	0.89	51.47	0.05	0.00	37.34	1.78	0.23	0.01	100.92	83.66
GM-07a	OL	GM_07a_3_TMTE_9_1	0.09	8.03	0.77	52.61	0.05	0.00	36.31	1.98	0.21	0.02	100.34	83.65
GM-07a	OL	GM_07a_3_TMTE_9_2	0.09	8.27	0.76	52.58	0.03	0.00	36.67	1.98	0.22	0.01	100.92	83.99

Table 3: (continued)

Sample	Eruptive Unit	Analysis	SiO_2	TiO_2	Al_2O_3	Fe_2O_3	V_2O_3	Cr_2O_3	FeO	MnO	MgO	CaO	Total	FeO^T
GM-07a	OL	GM_07a_3_TMTE_9_3	0.09	8.43	0.73	52.05	0.06	0.00	36.50	2.06	0.23	0.01	100.50	83.34
GM-07a	OL	GM_07a_3_TMTE_9_4	0.07	8.31	0.80	52.39	0.03	0.00	36.56	1.93	0.23	0.01	100.66	83.70
GM-07a	OL	GM_07a_3_TMTE_9_5	0.05	8.66	0.72	51.82	0.06	0.00	36.86	1.93	0.23	0.00	100.67	83.49
GM-07a	OL	GM_07a_3_TMTE_9_6	0.08	8.41	0.75	52.24	0.06	0.00	36.68	2.02	0.23	0.01	100.78	83.69
GM-07a	OL	GM_07a_3_TMTE_9_7	0.07	8.46	0.74	51.85	0.03	0.00	36.64	2.01	0.22	0.02	100.34	83.29
GM-07a	OL	GM_07a_3_TMTE_9_10	0.10	7.34	0.74	54.13	0.03	0.00	35.82	1.85	0.22	0.00	100.52	84.53
GM-07a	OL	GM_07a_3_TMTE_9_12	0.08	7.98	0.77	52.90	0.02	0.00	36.18	1.93	0.22	0.00	100.52	83.79
GM-07a	OL	GM_07a_3_TMTE_10_1	0.04	8.71	0.77	51.62	0.06	0.00	37.04	1.79	0.23	0.01	100.55	83.49
GM-07a	OL	GM_07a_3_TMTE_10_2	0.07	8.68	0.76	51.59	0.03	0.00	37.03	1.77	0.23	0.01	100.45	83.46
GM-07a	OL	GM_07a_3_TMTE_10_3	0.08	7.97	0.81	52.71	0.03	0.00	36.41	1.71	0.21	0.01	100.21	83.84
GM-07a	OL	GM_07a_3_TMTE_10_4	0.08	8.02	0.74	52.98	0.02	0.00	36.53	1.74	0.20	0.01	100.65	84.20
GM-07a	OL	GM_07a_3_TMTE_10_5	0.07	8.77	0.74	51.33	0.04	0.00	37.13	1.80	0.25	0.01	100.41	83.32
GM-07a	OL	GM_07a_3_TMTE_10_6	0.07	8.54	0.78	52.02	0.04	0.00	37.04	1.78	0.23	0.00	100.80	83.85
GM-07a	OL	GM_07a_3_TMTE_10_8	0.07	8.40	0.78	52.12	0.04	0.00	36.90	1.70	0.23	0.00	100.48	83.80
GM-07a	OL	GM_07a_3_TMTE_10_9	0.06	8.44	0.77	52.06	0.04	0.00	37.06	1.70	0.22	0.02	100.62	83.90
GM-07a	OL	GM_07a_3_TMTE_10_10	0.09	8.27	0.74	52.59	0.03	0.00	36.81	1.74	0.21	0.01	100.80	84.14
GM-07a	OL	GM_07a_3_TMTE_10_11	0.07	8.31	0.81	52.10	0.03	0.00	36.66	1.74	0.25	0.01	100.24	83.54
GM-07a	OL	GM_07a_3_TMTE_10_12	0.06	8.74	0.86	51.45	0.04	0.00	37.03	1.75	0.25	0.01	100.54	83.32
GM-07a	OL	GM_07a_3_TMTE_10_13	0.12	8.73	0.77	51.52	0.04	0.00	37.27	1.75	0.27	0.01	100.74	83.63
GM-07a	OL	GM_07a_3_TMTE_10_14	0.06	8.43	0.80	52.27	0.03	0.00	37.03	1.73	0.23	0.00	100.85	84.07
GM-07a	OL	GM_07a_3_TMTE_11_1	0.08	8.70	0.74	51.86	0.03	0.00	36.95	2.02	0.24	0.01	100.99	83.61
GM-07a	OL	GM_07a_3_TMTE_11_3	0.10	8.79	0.74	51.60	0.02	0.00	37.00	2.02	0.23	0.00	100.89	83.44
GM-07a	OL	GM_07a_3_TMTE_11_4	0.11	8.76	0.76	51.60	0.07	0.00	37.16	1.98	0.23	0.01	100.95	83.59
GM-07a	OL	GM_07a_3_TMTE_11_5	0.09	8.88	0.77	51.24	0.03	0.00	37.11	2.10	0.23	0.03	100.78	83.22
GM-07a	OL	GM_07a_3_TMTE_11_6	0.08	8.92	0.79	51.45	0.04	0.00	37.07	2.03	0.25	0.02	100.98	83.37
GM-07a	OL	GM_07a_3_TMTE_11_7	0.08	8.78	0.77	51.38	0.05	0.00	36.78	2.10	0.21	0.01	100.58	83.01
GM-07a	OL	GM_07a_3_TMTE_11_10	0.09	8.54	0.76	52.03	0.02	0.00	36.64	1.96	0.23	0.04	100.64	83.46
GM-07a	OL	GM_07a_3_TMTE_11_12	0.11	8.55	0.72	51.89	0.03	0.00	36.73	2.06	0.21	0.01	100.64	83.42
GM-07a	OL	GM_07a_3_TMTE_11_14	0.17	8.18	0.77	52.27	0.06	0.00	36.60	1.87	0.20	0.01	100.51	83.64
GM-07a	OL	GM_07a_3_TMTE_12_1	0.16	8.82	0.79	50.99	0.03	0.00	37.20	1.81	0.24	0.00	100.38	83.08
GM-07a	OL	GM_07a_3_TMTE_12_2	0.11	8.74	0.78	51.41	0.04	0.00	37.24	1.75	0.24	0.01	100.53	83.50
GM-07a	OL	GM_07a_3_TMTE_12_3	0.11	8.93	0.76	50.90	0.03	0.00	37.30	1.79	0.25	0.01	100.38	83.10
GM-07a	OL	GM_07a_3_TMTE_12_4	0.10	8.89	0.77	50.82	0.06	0.00	37.27	1.75	0.25	0.01	100.19	83.00

Table 3: (continued)

Sample	Eruptive Unit	Analysis	SiO_2	TiO_2	Al_2O_3	Fe_2O_3	V_2O_3	Cr_2O_3	FeO	MnO	MgO	CaO	Total	FeO^T
GM-07a	OL	GM_07a_3_TMTE_12_5	0.08	8.68	0.79	51.49	0.02	0.00	36.91	1.84	0.24	0.01	100.35	83.24
GM-07a	OL	GM_07a_3_TMTE_12_6	0.10	8.76	0.77	51.35	0.03	0.00	37.20	1.84	0.26	0.03	100.59	83.41
GM-07a	OL	GM_07a_3_TMTE_12_7	0.15	8.57	0.79	51.01	0.03	0.00	36.91	1.78	0.21	0.01	99.77	82.81
GM-07a	OL	GM_07a_3_TMTE_13_4	0.11	8.57	0.82	52.11	0.04	0.00	36.63	1.85	0.22	0.12	100.74	83.52
GM-07a	OL	GM_07a_3_TMTE_13_5	0.09	8.94	0.75	50.79	0.02	0.00	37.07	1.98	0.19	0.01	100.14	82.77
GM-07a	OL	GM_07a_3_TMTE_13_6	0.11	8.91	0.79	51.31	0.05	0.00	37.57	1.73	0.23	0.00	100.98	83.75
GM-07a	OL	GM_07a_3_TMTE_13_7	0.12	8.90	0.76	51.16	0.04	0.00	37.40	1.73	0.24	0.00	100.67	83.43
GM-07a	OL	GM_07a_3_TMTE_14_3	0.13	8.07	0.77	52.69	0.04	0.00	36.55	1.94	0.20	0.02	100.74	83.96
GM-07a	OL	GM_07a_3_TMTE_14_4	0.13	8.75	0.80	51.39	0.07	0.00	37.09	1.98	0.22	0.01	100.78	83.33
GM-07a	OL	GM_07a_3_TMTE_14_5	0.15	8.80	0.93	51.30	0.02	0.00	37.18	1.99	0.23	0.00	100.96	83.34
GM-07a	OL	GM_07a_3_TMTE_14_6	0.19	8.62	0.90	51.25	0.04	0.00	37.07	1.90	0.23	0.00	100.49	83.18
GM-07a	OL	GM_07a_3_TMTE_14_7	0.14	8.83	0.84	51.26	0.03	0.00	37.23	1.96	0.23	0.00	100.81	83.35
GM-07a	OL	GM_07a_3_TMTE_14_8	0.13	8.83	0.76	51.55	0.06	0.00	37.18	1.96	0.21	0.03	100.97	83.56
GM-07a	OL	GM_07a_3_TMTE_15_1	0.10	8.85	0.77	51.31	0.05	0.00	37.14	1.95	0.24	0.01	100.71	83.32
GM-07a	OL	GM_07a_3_TMTE_15_4	0.10	8.27	0.72	52.38	0.05	0.00	36.54	1.96	0.22	0.01	100.54	83.67
GM-07a	OL	GM_07a_3_TMTE_15_5	0.08	8.28	0.79	52.19	0.02	0.00	36.54	1.91	0.24	0.00	100.35	83.50
GM-07a	OL	GM_07a_3_TMTE_15_6	0.08	8.83	0.79	51.53	0.05	0.00	37.23	1.87	0.21	0.02	100.93	83.60
GM-07a	OL	GM_07a_3_TMTE_15_7	0.05	8.67	0.76	51.72	0.05	0.00	36.89	1.82	0.25	0.01	100.60	83.43
GM-07a	OL	GM_07a_3_TMTE_16_1	0.09	8.87	0.76	51.43	0.06	0.00	37.26	1.77	0.25	0.02	100.81	83.54
GM-07a	OL	GM_07a_3_TMTE_16_6	0.08	8.89	0.77	51.05	0.04	0.00	37.29	1.80	0.25	0.02	100.43	83.23
GM-07a	OL	GM_07a_4_TMTE_1_1	0.11	8.91	0.75	51.26	0.06	0.00	37.53	1.82	0.21	0.02	100.96	83.65
GM-07a	OL	GM_07a_4_TMTE_1_2	0.13	8.89	0.80	51.00	0.04	0.00	37.40	1.77	0.23	0.00	100.53	83.29
GM-07a	OL	GM_07a_4_TMTE_1_3	0.15	8.41	0.76	52.11	0.05	0.00	37.08	1.77	0.22	0.01	100.79	83.97
GM-07a	OL	GM_07a_4_TMTE_1_6	0.16	8.78	0.74	51.20	0.06	0.00	37.31	1.80	0.25	0.02	100.61	83.38
GM-07a	OL	GM_07a_4_TMTE_2_1	0.09	9.03	0.75	51.19	0.03	0.00	37.49	1.76	0.25	0.01	100.91	83.55
GM-07a	OL	GM_07a_4_TMTE_2_2	0.10	9.02	0.81	51.03	0.04	0.00	37.36	1.81	0.25	0.02	100.76	83.28
GM-07a	OL	GM_07a_4_TMTE_2_4	0.10	9.06	0.76	50.73	0.03	0.00	37.46	1.80	0.24	0.01	100.46	83.11
GM-07a	OL	GM_07a_4_TMTE_2_6	0.12	8.37	0.77	52.00	0.07	0.00	36.82	1.77	0.21	0.01	100.42	83.62
GM-07a	OL	GM_07a_4_TMTE_3_1	0.14	8.54	0.84	51.64	0.02	0.00	37.17	1.63	0.21	0.01	100.50	83.64
GM-07a	OL	GM_07a_4_TMTE_3_4	0.13	8.83	0.76	51.20	0.04	0.00	37.41	1.76	0.21	0.01	100.63	83.48
GM-07a	OL	GM_07a_4_TMTE_4_2	0.10	8.81	0.80	51.24	0.04	0.00	37.43	1.74	0.20	0.01	100.61	83.54
GM-07a	OL	GM_07a_4_TMTE_4_4	0.10	9.02	0.79	51.08	0.05	0.00	37.54	1.81	0.23	0.00	100.92	83.50
GM-07a	OL	GM_07a_4_TMTE_4_5	0.08	8.80	0.75	51.61	0.01	0.00	37.32	1.71	0.24	0.01	100.84	83.76

Table 3: (continued)

Sample	Eruptive Unit	Analysis	SiO_2	TiO_2	Al_2O_3	Fe_2O_3	V_2O_3	Cr_2O_3	FeO	MnO	MgO	CaO	Total	FeO^T
GM-07a	OL	GM_07a_4_TMTE_4_6	0.10	8.87	0.75	51.21	0.04	0.00	37.40	1.73	0.24	0.00	100.58	83.48
GM-07a	OL	GM_07a_4_TMTE_5_2	0.11	8.66	0.77	51.66	0.05	0.00	36.88	1.85	0.22	0.02	100.65	83.37
GM-07a	OL	GM_07a_4_TMTE_5_3	0.09	8.63	0.75	51.98	0.03	0.00	37.12	1.78	0.25	0.00	100.94	83.89
GM-07a	OL	GM_07a_4_TMTE_5_4	0.15	8.84	0.78	51.21	0.02	0.00	37.40	1.80	0.22	0.00	100.64	83.48
GM-07a	OL	GM_07a_4_TMTE_5_5	0.13	8.91	0.76	51.27	0.04	0.00	37.28	1.85	0.24	0.02	100.80	83.42
GM-07a	OL	GM_07a_4_TMTE_5_6	0.13	8.54	0.77	51.76	0.04	0.00	37.15	1.79	0.22	0.02	100.71	83.73
GM-07a	OL	GM_07a_4_TMTE_6_2	0.18	8.63	0.83	51.29	0.08	0.00	37.20	1.70	0.25	0.00	100.47	83.35
GM-07a	OL	GM_07a_4_TMTE_7_1	0.15	8.97	0.73	50.70	0.04	0.00	36.96	2.16	0.23	0.00	100.24	82.58
GM-07a	OL	GM_07a_4_TMTE_7_5	0.18	8.55	0.75	51.74	0.05	0.00	36.77	2.11	0.24	0.01	100.70	83.32
GM-07a	OL	GM_07a_4_TMTE_8_1	0.10	8.77	0.73	51.55	0.03	0.00	37.10	2.08	0.22	0.01	100.81	83.49
GM-07a	OL	GM_07a_4_TMTE_8_5	0.11	8.70	0.70	51.72	0.05	0.00	36.99	2.03	0.22	0.01	100.81	83.53
GM-07a	OL	GM_07a_4_TMTE_10_1	0.11	8.76	0.80	51.11	0.03	0.00	37.16	1.85	0.21	0.01	100.28	83.14
GM-07a	OL	GM_07a_4_TMTE_10_3	0.10	8.72	0.82	51.39	0.06	0.00	37.03	1.87	0.20	0.01	100.53	83.28
GM-07a	OL	GM_07a_4_TMTE_11_1	0.20	8.83	0.82	51.10	0.05	0.00	37.47	1.76	0.22	0.00	100.78	83.45
GM-07a	OL	GM_07a_4_TMTE_11_2	0.16	8.98	0.78	50.76	0.06	0.00	37.47	1.79	0.22	0.00	100.51	83.15
GM-07a	OL	GM_07a_4_TMTE_11_4	0.20	8.98	0.77	51.05	0.04	0.00	37.71	1.74	0.21	0.01	101.00	83.65
GM-07a	OL	GM_07a_4_TMTE_13_1	0.16	9.08	0.79	50.77	0.02	0.00	37.65	1.82	0.26	0.01	100.80	83.33
GM-07a	OL	GM_07a_4_TMTE_14_2	0.16	8.93	0.85	50.98	0.05	0.00	37.46	1.81	0.22	0.00	100.84	83.34
GM-07a	OL	GM_07a_4_TMTE_15_1	0.08	8.73	0.83	51.42	0.03	0.00	37.18	1.76	0.24	0.01	100.55	83.45
GM-07a	OL	GM_07a_4_TMTE_15_2	0.10	8.04	1.12	51.78	0.04	0.00	36.67	1.61	0.22	0.02	99.79	83.26
GM-07a	OL	GM_07a_4_TMTE_15_3	0.07	8.61	0.85	51.76	0.05	0.00	37.03	1.76	0.23	0.02	100.69	83.60
GM-07a	OL	GM_07a_4_TMTE_15_4	0.08	8.92	0.77	51.06	0.05	0.00	37.38	1.74	0.23	0.01	100.53	83.33
GM-07a	OL	GM_07a_4_TMTE_15_5	0.07	8.73	1.36	50.99	0.03	0.00	37.40	1.73	0.24	0.01	100.83	83.29
GM-07a	OL	GM_07a_1_TMTE_10_15	0.10	9.06	0.92	50.46	0.06	0.00	37.53	1.77	0.23	0.01	100.41	82.93
GM-16	YE	GM_16_1_TMTE_2_1	0.17	6.95	1.00	54.22	0.05	0.00	36.57	0.79	0.33	0.02	100.24	85.36
GM-16	YE	GM_16_1_TMTE_2_2	0.18	6.95	1.00	54.27	0.05	0.00	36.58	0.82	0.32	0.00	100.29	85.41
GM-16	YE	GM_16_1_TMTE_2_4	0.17	6.77	1.05	54.48	0.02	0.00	36.35	0.77	0.34	0.01	100.09	85.37
GM-16	YE	GM_16_1_TMTE_2_5	0.13	6.38	1.04	55.53	0.04	0.00	36.10	0.73	0.30	0.00	100.43	86.07
GM-16	YE	GM_16_1_TMTE_2_6	0.16	6.66	0.99	55.18	0.04	0.00	36.39	0.73	0.32	0.01	100.63	86.04
GM-16	YE	GM_16_1_TMTE_2_7	0.18	6.81	1.00	54.75	0.05	0.00	36.52	0.72	0.33	0.01	100.53	85.78
GM-16	YE	GM_16_1_TMTE_2_9	0.20	7.35	1.02	53.59	0.04	0.00	36.93	0.79	0.33	0.00	100.48	85.16
GM-16	YE	GM_16_1_TMTE_2_10	0.19	7.31	1.00	53.64	0.05	0.00	36.91	0.76	0.32	0.00	100.42	85.18
GM-16	YE	GM_16_1_TMTE_2_11	0.15	6.22	1.00	55.59	0.04	0.00	35.89	0.70	0.32	0.01	100.10	85.91

Table 3: (continued)

Sample	Eruptive Unit	Analysis	SiO_2	TiO_2	Al_2O_3	Fe_2O_3	V_2O_3	Cr_2O_3	FeO	MnO	MgO	CaO	Total	FeO^T
GM-16	YE	GM_16_1_TMTE_2_12	0.17	7.00	1.03	54.49	0.03	0.00	36.70	0.75	0.32	0.01	100.71	85.73
GM-16	YE	GM_16_1_TMTE_2_14	0.17	7.09	1.03	54.05	0.03	0.00	36.67	0.78	0.33	0.00	100.36	85.30
GM-16	YE	GM_16_1_TMTE_2_15	0.18	6.81	1.12	54.29	0.01	0.00	36.39	0.74	0.31	0.01	100.04	85.24
GM-16	YE	GM_16_1_TMTE_2_16	0.17	7.18	1.05	53.70	0.02	0.00	36.59	0.75	0.35	0.01	100.05	84.91
GM-16	YE	GM_16_1_TMTE_2_17	0.19	6.38	1.03	55.15	0.04	0.00	36.19	0.71	0.31	0.02	100.15	85.81
GM-16	YE	GM_16_1_TMTE_2_18	0.18	7.02	1.01	54.18	0.04	0.00	36.62	0.77	0.34	0.00	100.33	85.38
GM-16	YE	GM_16_1_TMTE_2_19	0.20	7.07	1.00	54.32	0.03	0.00	36.72	0.76	0.34	0.02	100.63	85.60
GM-16	YE	GM_16_1_TMTE_2_20	0.20	7.08	1.00	54.01	0.05	0.00	36.62	0.79	0.34	0.01	100.25	85.22
GM-16	YE	GM_16_1_TMTE_2_21	0.17	6.50	1.10	54.79	0.05	0.00	36.18	0.70	0.34	0.01	99.95	85.48
GM-16	YE	GM_16_1_TMTE_2_22	0.15	6.64	1.02	54.70	0.06	0.00	36.10	0.74	0.30	0.01	99.95	85.32
GM-16	YE	GM_16_1_TMTE_2_23	0.16	6.79	0.97	54.76	0.04	0.00	36.58	0.72	0.30	0.01	100.48	85.85
GM-16	YE	GM_16_1_TMTE_2_24	0.17	7.02	1.06	54.05	0.03	0.00	36.64	0.74	0.32	0.01	100.28	85.27
GM-16	YE	GM_16_1_TMTE_2_25	0.14	7.22	0.95	53.79	0.07	0.00	36.82	0.77	0.32	0.02	100.27	85.23
GM-16	YE	GM_16_1_TMTE_2_26	0.19	7.44	0.96	53.54	0.05	0.00	37.01	0.84	0.33	0.00	100.58	85.19
GM-16	YE	GM_16_1_TMTE_2_27	0.16	7.40	0.99	53.57	0.04	0.00	36.97	0.79	0.32	0.01	100.41	85.18
GM-16	YE	GM_16_1_TMTE_2_28	0.20	7.18	1.02	53.87	0.06	0.00	36.81	0.77	0.33	0.00	100.49	85.29
GM-16	YE	GM_16_1_TMTE_2_29	0.18	7.09	1.01	54.27	0.04	0.00	36.80	0.76	0.34	0.00	100.65	85.64
GM-16	YE	GM_16_1_TMTE_2_30	0.18	7.33	1.04	53.58	0.05	0.00	37.04	0.78	0.32	0.00	100.42	85.25
GM-16	YE	GM_16_1_TMTE_2_33	0.18	6.35	0.99	55.46	0.04	0.00	36.04	0.71	0.27	0.02	100.28	85.95
GM-16	YE	GM_16_1_TMTE_2_34	0.18	6.95	1.01	54.34	0.06	0.00	36.60	0.80	0.34	0.01	100.46	85.50
GM-10	YO	GM_10_TMTE_2-1	0.13	7.68	1.18	52.10	0.05	0.00	36.91	0.86	0.28	0.00	99.33	83.79
GM-10	YO	GM_10_TMTE_2-2	0.14	7.68	1.17	52.20	0.04	0.00	36.82	0.87	0.30	0.01	99.44	83.80
GM-10	YO	GM_10_TMTE_2-3	0.09	7.70	0.91	52.50	0.05	0.00	36.59	0.96	0.30	0.02	99.31	83.83
GM-10	YO	GM_10_TMTE_2-4	0.08	7.75	0.95	52.79	0.04	0.00	36.97	0.92	0.30	0.00	99.95	84.48
GM-10	YO	GM_10_TMTE_2-5	0.11	7.57	0.96	52.87	0.05	0.00	36.64	0.91	0.32	0.01	99.63	84.21
GM-10	YO	GM_10_TMTE_2-6	0.10	7.58	0.97	52.70	0.06	0.00	36.77	0.88	0.31	0.01	99.51	84.19
GM-10	YO	GM_10_TMTE_2-7	0.15	7.39	1.19	52.66	0.05	0.00	36.47	0.92	0.30	0.02	99.34	83.85
GM-10	YO	GM_10_TMTE_2-8	0.08	7.15	0.99	53.75	0.04	0.00	36.37	0.85	0.30	0.01	99.76	84.73
GM-10	YO	GM_10_TMTE_2-9	0.10	7.26	0.97	53.54	0.05	0.00	36.27	0.94	0.31	0.03	99.68	84.45
GM-10	YO	GM_10_TMTE_2-10	0.11	7.41	0.95	53.22	0.04	0.00	36.65	0.87	0.30	0.00	99.72	84.54
GM-10	YO	GM_10_TMTE_2-11	0.13	7.46	0.95	52.89	0.06	0.00	36.66	0.88	0.31	0.01	99.56	84.26
GM-10	YO	GM_10_TMTE_2-12	0.12	7.40	0.99	53.21	0.04	0.00	36.62	0.90	0.30	0.01	99.78	84.50
GM-10	YO	GM_10_TMTE_4_1	0.16	8.10	0.96	51.72	0.05	0.00	37.34	0.90	0.30	0.00	99.70	83.88

Table 3: (continued)

Sample	Eruptive Unit	Analysis	SiO_2	TiO_2	Al_2O_3	Fe_2O_3	V_2O_3	Cr_2O_3	FeO	MnO	MgO	CaO	Total	FeO^T
GM-10	YO	GM_10_TMTE_4_3	0.19	7.91	0.96	52.01	0.04	0.00	37.11	0.89	0.30	0.01	99.62	83.90
GM-10	YO	GM_10_TMTE_4_4	0.17	7.95	0.96	52.03	0.05	0.00	36.98	0.89	0.31	0.04	99.58	83.80
GM-10	YO	GM_10_TMTE_4_5	0.20	7.90	0.95	51.84	0.05	0.00	37.10	0.89	0.33	0.02	99.45	83.75
GM-10	YO	GM_10_TMTE_4_7	0.17	7.98	0.98	51.55	0.04	0.00	36.95	0.97	0.32	0.00	99.18	83.33
GM-10	YO	GM_10_TMTE_4_8	0.14	8.10	0.97	51.82	0.03	0.00	37.33	0.91	0.32	0.01	99.77	83.96
GM-10	YO	GM_10_TMTE_4_9	0.17	8.17	0.91	51.56	0.03	0.00	37.31	0.97	0.30	0.00	99.63	83.71
GM-10	YO	GM_10_TMTE_4_10	0.14	7.68	1.00	52.30	0.04	0.00	36.79	0.89	0.32	0.01	99.31	83.85
GM-10	YO	GM_10_TMTE_4_11	0.15	7.36	0.95	52.78	0.04	0.00	36.52	0.83	0.31	0.01	99.10	84.02
GM-10	YO	GM_10_TMTE_4_12	0.14	7.31	0.97	52.95	0.04	0.00	36.59	0.81	0.27	0.01	99.27	84.24
GM-10	YO	GM_10_TMTE_6-6	0.18	7.31	0.96	53.46	0.04	0.00	36.69	0.89	0.29	0.01	100.04	84.80
GM-10	YO	GM_10_TMTE_6-8	0.20	7.42	0.99	52.92	0.03	0.00	36.90	0.88	0.29	0.02	99.77	84.53
GM-10	YO	GM_10_TMTE_6-12	0.20	7.36	0.92	53.46	0.04	0.00	36.76	0.85	0.29	0.03	100.11	84.86
GM-10	YO	GM_10_TMTE_7-3	0.17	7.91	0.92	52.25	0.05	0.00	37.21	0.88	0.28	0.01	99.85	84.22
GM-10	YO	GM_10_TMTE_7-5	0.16	7.73	0.95	52.55	0.05	0.00	37.03	0.92	0.28	0.01	99.82	84.32
GM-10	YO	GM_10_TMTE_7-6	0.19	7.83	0.98	52.15	0.03	0.00	37.05	0.85	0.30	0.01	99.60	83.98
GM-10	YO	GM_10_TMTE_7-7	0.17	7.62	0.99	52.77	0.06	0.00	36.89	0.88	0.28	0.02	99.87	84.37
GM-10	YO	GM_10_TMTE_7-8	0.20	7.86	1.00	52.01	0.05	0.00	37.06	0.92	0.28	0.02	99.57	83.86
GM-10	YO	GM_10_TMTE_7-9	0.20	7.99	0.96	51.70	0.05	0.00	37.16	0.90	0.32	0.00	99.48	83.68
GM-10	YO	GM_10_TMTE_7-10	0.18	7.87	1.00	52.01	0.05	0.00	37.17	0.90	0.29	0.02	99.70	83.97
GM-10	YO	GM_10_TMTE_8-4	0.19	7.99	0.98	51.97	0.03	0.00	37.20	0.95	0.30	0.01	99.81	83.97
GM-10	YO	GM_10_TMTE_9-4	0.19	7.34	0.97	53.30	0.06	0.00	36.84	0.87	0.30	0.01	100.05	84.81
GM-10	YO	GM_10_TMTE_9-11	0.17	7.40	0.95	53.25	0.04	0.00	36.78	0.83	0.28	0.01	99.90	84.70
GM-10	YO	GM_10_TMTE_9-16	0.19	7.56	1.00	52.94	0.04	0.00	36.99	0.86	0.31	0.00	100.07	84.63
GM-10	YO	GM_10_TMTE_9-17	0.19	7.54	0.95	52.98	0.05	0.00	36.88	0.89	0.30	0.00	100.00	84.55
GM-10	YO	GM_10_TMTE_10-1	0.11	7.62	0.95	52.87	0.04	0.00	36.68	1.00	0.31	0.01	99.75	84.25
GM-10	YO	GM_10_TMTE_10-3	0.13	7.12	0.94	53.87	0.05	0.00	36.31	1.00	0.30	0.00	99.93	84.78
GM-10	YO	GM_10_TMTE_10-4	0.13	7.62	0.95	52.80	0.05	0.00	36.69	1.02	0.31	0.01	99.77	84.19
GM-10	YO	GM_10_TMTE_10-5	0.13	7.64	0.97	52.74	0.05	0.00	36.75	1.04	0.31	0.01	99.82	84.20
GM-10	YO	GM_10_TMTE_10-6	0.18	7.64	1.02	52.26	0.06	0.00	36.63	0.98	0.32	0.01	99.37	83.66
GM-10	YO	GM_10_TMTE_10-7	0.13	7.85	0.93	52.38	0.05	0.00	36.95	1.04	0.32	0.01	99.82	84.09
GM-10	YO	GM_10_TMTE_10-8	0.14	7.85	0.92	52.35	0.04	0.00	36.95	0.99	0.32	0.01	99.80	84.06
GM-10	YO	GM_10_TMTE_10-9	0.13	7.66	0.94	52.82	0.04	0.00	36.79	1.02	0.32	0.01	99.90	84.32
GM-10	YO	GM_10_TMTE_10-10	0.16	7.54	0.89	53.16	0.02	0.00	36.71	1.02	0.33	0.00	100.05	84.54

Table 3: (continued)

Sample	Eruptive Unit	Analysis	SiO_2	TiO_2	Al_2O_3	Fe_2O_3	V_2O_3	Cr_2O_3	FeO	MnO	MgO	CaO	Total	FeO^T
GM-10	YO	GM_10_TMTE_10-12	0.16	7.24	0.90	53.90	0.03	0.00	36.51	0.99	0.28	0.02	100.25	85.01
GM-10	YO	GM_10_TMTE_10-13	0.16	7.26	1.04	52.99	0.04	0.00	36.29	1.00	0.30	0.01	99.27	83.98
GM-10	YO	GM_10_TMTE_10-14	0.16	7.35	0.94	52.77	0.06	0.00	36.36	1.02	0.31	0.01	99.14	83.84
GM-10	YO	GM_10_TMTE_10-15	0.17	7.46	0.99	52.86	0.05	0.00	36.47	1.04	0.31	0.01	99.56	84.04
GM-10	YO	GM_10_TMTE_11-3	0.20	7.84	0.97	51.87	0.03	0.00	37.03	0.88	0.29	0.00	99.29	83.71
GM-10	YO	GM_10_TMTE_12-1	0.13	7.49	1.00	52.87	0.03	0.00	36.75	0.89	0.31	0.01	99.63	84.33
GM-10	YO	GM_10_TMTE_12-2	0.14	7.55	0.98	53.17	0.04	0.00	36.94	0.94	0.29	0.01	100.24	84.79
GM-10	YO	GM_10_TMTE_12-3	0.16	7.59	0.94	52.83	0.06	0.00	36.85	0.91	0.31	0.01	99.89	84.38
GM-10	YO	GM_10_TMTE_12-4	0.14	7.54	0.94	52.84	0.05	0.00	36.90	0.87	0.30	0.02	99.74	84.45
GM-10	YO	GM_10_TMTE_12-5	0.15	7.29	1.08	53.22	0.03	0.00	36.58	0.88	0.29	0.00	99.75	84.47
GM-10	YO	GM_10_TMTE_12-6	0.15	7.24	1.02	53.32	0.04	0.00	36.67	0.81	0.27	0.00	99.69	84.66
GM-10	YO	GM_10_TMTE_12-8	0.15	7.51	0.99	53.21	0.04	0.00	36.96	0.92	0.30	0.02	100.28	84.84
GM-10	YO	GM_10_TMTE_12-9	0.13	7.22	0.96	53.70	0.05	0.00	36.57	0.83	0.29	0.02	99.92	84.90
GM-10	YO	GM_10_TMTE_12-10	0.17	7.20	0.99	53.42	0.05	0.00	36.56	0.86	0.29	0.01	99.69	84.63
GM-10	YO	GM_10_TMTE_12-11	0.11	7.95	0.92	52.23	0.04	0.00	37.21	0.89	0.29	0.01	99.81	84.21
GM-10	YO	GM_10_TMTE_12-14	0.13	8.54	0.96	51.22	0.06	0.00	37.69	0.95	0.32	0.01	100.06	83.78
GM-10	YO	GM_10_TMTE_12-15	0.14	8.51	0.94	51.14	0.05	0.00	37.71	0.90	0.32	0.01	99.92	83.73
GM-10	YO	GM_10_TMTE_12-16	0.12	8.32	0.96	51.61	0.08	0.00	37.64	0.92	0.32	0.02	100.11	84.08
GM-10	YO	GM_10_TMTE_12-17	0.15	8.24	0.93	51.33	0.07	0.00	37.32	0.93	0.29	0.00	99.46	83.51
GM-10	YO	GM_10_TMTE_14-2	0.10	7.87	0.90	52.42	0.04	0.00	36.91	0.96	0.32	0.01	99.74	84.08
GM-10	YO	GM_10_TMTE_14-3	0.12	7.97	0.96	52.32	0.04	0.00	37.20	0.93	0.32	0.01	100.04	84.28
GM-10	YO	GM_10_TMTE_14-4	0.14	7.89	1.03	52.27	0.05	0.00	37.13	0.95	0.34	0.02	99.97	84.16
GM-10	YO	GM_10_TMTE_14-5	0.11	7.72	0.99	52.44	0.04	0.00	36.76	0.93	0.32	0.01	99.49	83.95
GM-10	YO	GM_10_TMTE_14-6	0.14	7.46	1.01	52.84	0.05	0.00	36.57	0.90	0.31	0.01	99.44	84.12
GM-10	YO	GM_10_TMTE_14-7	0.13	7.69	0.98	52.80	0.04	0.00	36.92	0.96	0.33	0.01	100.02	84.43
GM-10	YO	GM_10_TMTE_14-8	0.18	7.37	1.16	52.44	0.05	0.00	36.47	0.90	0.32	0.00	99.09	83.66
GM-10	YO	GM_10_TMTE_14-9	0.19	7.18	0.98	53.31	0.04	0.00	36.40	0.88	0.30	0.01	99.49	84.37
GM-10	YO	GM_10_TMTE_14-11	0.14	7.57	1.07	52.24	0.02	0.00	36.56	0.94	0.32	0.00	99.04	83.56
GM-10	YO	GM_10_TMTE_14-12	0.15	7.47	1.25	52.42	0.02	0.00	36.50	0.94	0.31	0.02	99.26	83.67
GM-10	YO	GM_10_TMTE_14-13	0.14	7.48	1.06	52.95	0.03	0.00	36.59	0.97	0.35	0.01	99.73	84.25
GM-10	YO	GM_10_TMTE_14-14	0.13	7.20	1.04	53.10	0.05	0.00	36.45	0.86	0.27	0.01	99.27	84.24
GM-10	YO	GM_10_TMTE_14-15	0.18	8.02	0.96	51.73	0.03	0.00	37.17	0.93	0.32	0.00	99.50	83.72
GM-10	YO	GM_10_TMTE_14-16	0.11	7.67	0.99	52.67	0.05	0.00	36.75	0.98	0.31	0.00	99.73	84.15

Table 3: (continued)

Sample	Eruptive Unit	Analysis	SiO_2	TiO_2	Al_2O_3	Fe_2O_3	V_2O_3	Cr_2O_3	FeO	MnO	MgO	CaO	Total	FeO^T
GM-10	YO	GM_10_TMTE_14-17	0.11	7.47	0.95	53.03	0.06	0.00	36.60	0.86	0.32	0.01	99.63	84.32
GM-10	YO	GM_10_TMTE_14-18	0.10	7.89	0.93	52.54	0.03	0.00	36.97	0.92	0.34	0.01	99.94	84.25
GM-10	YO	GM_10_TMTE_14-19	0.14	7.82	1.06	52.08	0.07	0.00	36.90	0.96	0.32	0.01	99.58	83.76
GM-10	YO	GM_10_TMTE_14-20	0.11	7.77	1.08	52.15	0.06	0.00	36.75	0.93	0.32	0.02	99.36	83.68
GM-10	YO	GM_10_TMTE_15-1	0.20	8.38	0.98	51.15	0.04	0.00	37.65	0.94	0.31	0.00	99.79	83.68
GM-10	YO	GM_10_TMTE_15-2	0.16	8.35	0.95	51.15	0.05	0.00	37.49	0.92	0.35	0.01	99.59	83.52
GM-10	YO	GM_10_TMTE_15-3	0.16	8.19	1.02	51.43	0.04	0.00	37.24	0.87	0.34	0.01	99.52	83.52
GM-10	YO	GM_10_TMTE_15-4	0.19	8.00	1.00	51.71	0.04	0.00	37.22	0.89	0.33	0.01	99.56	83.75
GM-10	YO	GM_10_TMTE_15-5	0.20	7.94	0.99	51.83	0.05	0.00	37.01	0.97	0.31	0.01	99.54	83.65
GM-10	YO	GM_10_TMTE_15-6	0.20	7.85	0.95	52.01	0.05	0.00	37.11	0.90	0.32	0.01	99.52	83.91
GM-10	YO	GM_10_TMTE_15-8	0.19	7.65	0.96	52.33	0.07	0.00	36.82	0.93	0.32	0.00	99.42	83.91
GM-10	YO	GM_10_TMTE_15-9	0.19	7.73	0.97	52.33	0.06	0.00	36.97	0.90	0.32	0.01	99.68	84.06
GM-10	YO	GM_10_TMTE_15-10	0.19	7.71	0.95	52.46	0.06	0.00	36.96	0.89	0.32	0.00	99.76	84.17
GM-10	YO	GM_10_TMTE_15-11	0.19	7.72	0.97	52.22	0.03	0.00	36.91	0.89	0.30	0.01	99.42	83.90
GM-10	YO	GM_10_TMTE_16-1	0.11	8.26	0.94	51.31	0.02	0.00	37.20	0.93	0.30	0.00	99.30	83.37
GM-10	YO	GM_10_TMTE_16-2	0.13	8.06	0.96	51.63	0.04	0.00	36.99	0.90	0.33	0.01	99.24	83.45
GM-10	YO	GM_10_TMTE_16-3	0.11	7.77	0.92	52.07	0.05	0.00	36.79	0.90	0.29	0.01	99.07	83.64
GM-10	YO	GM_10_TMTE_16-4	0.13	7.42	1.00	52.94	0.03	0.00	36.52	0.88	0.31	0.00	99.46	84.16
GM-10	YO	GM_10_TMTE_16-5	0.14	7.47	0.96	52.97	0.06	0.00	36.83	0.84	0.30	0.02	99.78	84.49
GM-10	YO	GM_10_TMTE_16-6	0.10	6.90	1.00	53.62	0.05	0.00	36.03	0.84	0.29	0.01	99.00	84.27
GM-10	YO	GM_10_TMTE_16-7	0.07	7.51	0.97	52.96	0.05	0.00	36.71	0.87	0.29	0.01	99.62	84.36
GM-10	YO	GM_10_TMTE_16-8	0.13	7.26	0.95	53.48	0.04	0.00	36.67	0.84	0.29	0.01	99.82	84.80
GM-10	YO	GM_10_TMTE_17-1	0.10	8.08	0.92	51.44	0.04	0.00	37.09	0.88	0.29	0.01	99.01	83.38
GM-10	YO	GM_10_TMTE_17-2	0.11	7.95	0.95	51.91	0.04	0.00	37.04	0.87	0.32	0.01	99.38	83.76
GM-10	YO	GM_10_TMTE_17-3	0.10	7.95	1.00	52.19	0.04	0.00	36.76	0.89	0.28	0.00	99.18	83.72
GM-10	YO	GM_10_TMTE_17-4	0.09	7.95	0.96	52.24	0.06	0.00	36.70	0.89	0.29	0.00	99.14	83.71
GM-10	YO	GM_10_TMTE_17-5	0.13	7.95	0.96	52.25	0.06	0.00	36.79	0.88	0.29	0.01	99.22	83.80
GM-10	YO	GM_10_TMTE_17-6	0.11	7.95	1.01	51.63	0.05	0.00	36.67	0.88	0.30	0.01	98.69	83.13
GM-10	YO	GM_10_TMTE_17-7	0.10	7.95	1.00	52.47	0.05	0.00	36.52	0.88	0.29	0.00	98.98	83.73
GM-10	YO	GM_10_TMTE_17-8	0.08	7.95	0.93	50.54	0.05	0.00	37.50	0.93	0.33	0.02	99.28	82.98